The Potential of Renal Proximal Tubule Cells for Disease Modeling and Therapeutic Interventions

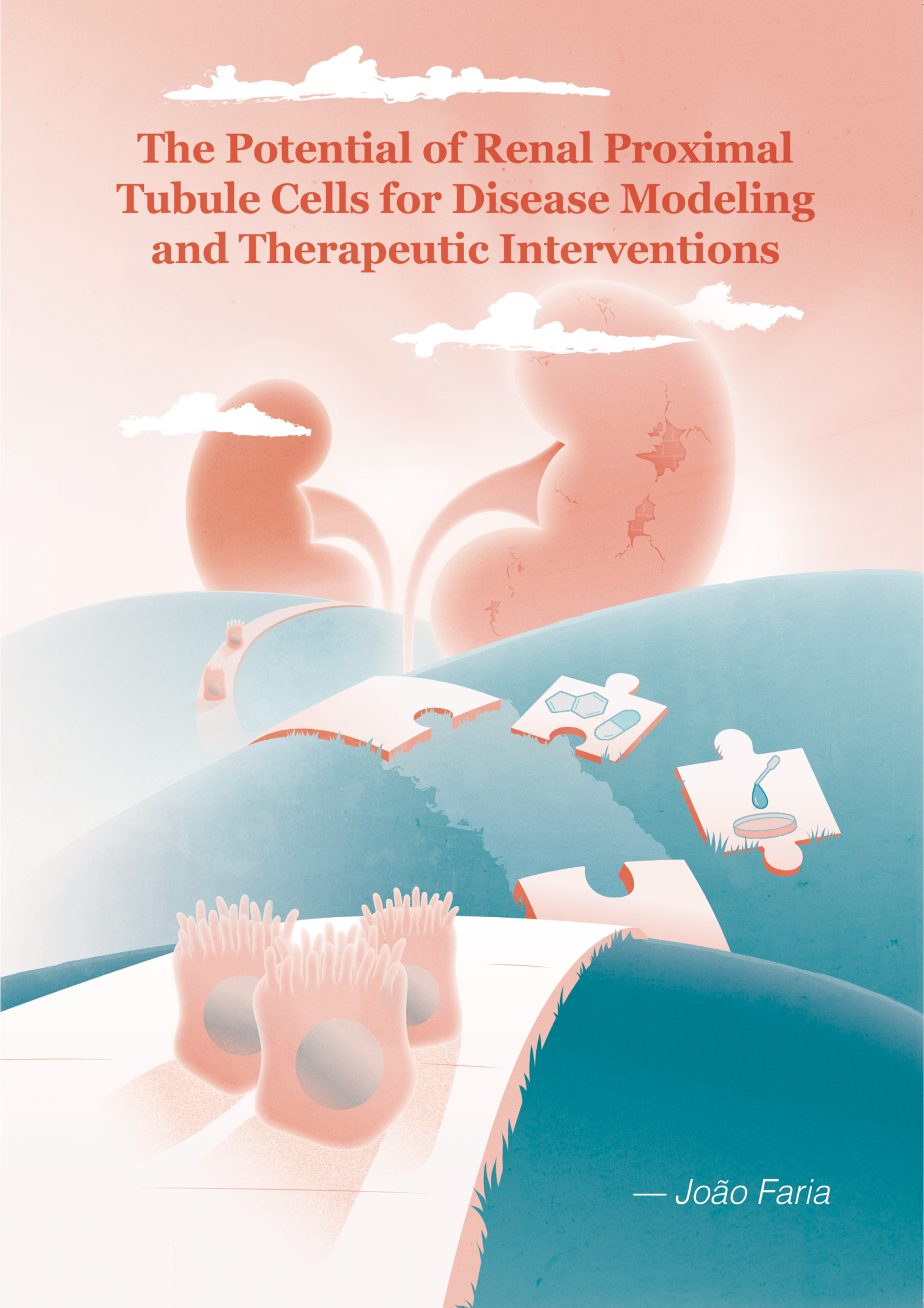

— João Faria

The Potential of Renal Proximal Tubule Cells for Disease Modeling and Therapeutic Interventions

João Faria

2024

Layout: João Faria
Cover design: Diogo Guerra (© Diogo Guerra. 2023)
Printed by: Ipskamp Printing
ISBN: 978-94-6473-376-1
DOI: https://doi.org/10.33540/2100

The research presented in this thesis was performed at the Division of Pharmacology, Utrecht Institute for Pharmaceutical Sciences, Faculty of Science, Utrecht University.

The research project was financially supported by funding from the European Union's Horizon 2020 research and innovation programme under the Marie Skłodowska-Curie Grant agreement no. 813839

The Potential of Renal Proximal Tubule Cells for Disease Modeling and Therapeutic Interventions

Het potentieel van proximale niertubulus cellen voor ziektemodellering en therapeutische interventies

(met een samenvatting in het Nederlands)

Proefschrift

ter verkrijging van de graad van doctor aan de
Universiteit Utrecht
op gezag van de
rector magnificus, prof. dr. H.R.B.M. Kummeling,
ingevolge het besluit van het college voor promoties
in het openbaar te verdedigen op

maandag 5 februari 2024 des middags te 12.15 uur

door

João Pedro Ferreira Faria

geboren op 11 januari 1994
te Vizela, Portugal

Promotor:

Prof. dr. R. Masereeuw

Copromotor:

Dr. S. M. Mihăilă

Beoordelingscommissie:

Prof. dr. R. Goldschmeding

Prof. dr. M. Griffin

Prof. dr. P. Murray

Prof. dr. S.W.C. van Mil

Dr. M. Hoogduin

TABLE OF CONTENTS

CHAPTER 1

General Introduction and Thesis Outline

1. Chronic Kidney Disease

Chronic kidney disease (CKD) is a progressive illness affecting >10% of the global population [1], for which diabetes mellitus and hypertension are among the most important risk factors [2, 3]. Up to date, there is no cure for CKD and its diagnosis relies on assessing kidney function, which may not always be accurate. Regardless of its cause, CKD is marked by a continuous and irreversible decline in nephron function due to alterations in, amongst others, cell metabolism, increased oxidative stress and inflammation, ultimately leading to the development of fibrosis [4]. As CKD advances, patients eventually reach a state of kidney failure requiring replacement therapies, such as organ transplantation. However, the shortage of available organs poses a significant challenge to patient survival. When a suitable organ is unavailable, kidney replacement therapies, such as dialysis, become the alternative option, particularly for patients who are not eligible for transplantation [5]. Given the limitations in both CKD diagnosis and management, the primary clinical challenge is to identify potential biomarkers for early disease detection and for developing effective therapies to target CKD.

2. The Proximal Tubule in Chronic Kidney Disease

The human kidney is composed of approximately one million nephrons that are responsible for filtering blood and maintaining electrolyte homeostasis by reabsorbing essential nutrients and excreting drugs and metabolic waste products from the bloodstream (**Figure 1**). These functions are carried out by the glomerulus, that acts as a filter, and tubular subunits, responsible for active and passive solute and water transport, present in each nephron (**Figure 1B**) [6]. Among the tubular subunits, the proximal tubule (PT) holds a crucial role in overall kidney function through its capacity to reabsorb nutrients, to secrete waste products and perform endocrine regulation (**Figure 1C-D**). Transporters responsible for secretion and reabsorption require energy provided by the large mitochondrial density in the PT. This renders the PT also highly susceptible to ischemic, metabolic, and toxin-related injuries [7]. Dysfunction of the PT can lead to disruptions in overall kidney function, a condition known as Fanconi's syndrome [8], characterized by the presence of glucosuria [9], tubular acidosis [10], and aminoaciduria [11].

The PT facilitates the active removal of retained solutes and medications from the bloodstream into the tubular lumen through the concerted action of uptake transporters and efflux pumps. The primary transporters involved in this cellular uptake include those of the organic anion and cation systems. The former includes the basolateral organic anion transporters (OAT1/3), as well as apically expressed breast cancer resistance protein (BCRP) and multidrug resistance-associated proteins 2 and 4 (MRP2/4). The latter includes the

basolateral organic cation transporter 2 (OCT2), and the apical multidrug and toxin extrusion 1 and 2k (MATE1/2k), and P-glycoprotein (P-gp) (**Figure 1C**) [7, 12]. Moreover, this secretory function is influenced by the competitive process between medications and circulating solutes, which can lead to an accumulation of harmful solutes as a result of tubular dysfunction, and can then progress to kidney failure and CKD [12]. Additionally, the PT is the major source of microsomal enzymes which may play a crucial role in the biotransformation of both xenobiotics and endogenous compounds, such as ß-lyase, hence contributing to nephrotoxicity [13].

In addition to its secretory function, the PT is responsible for reabsorbing glucose from the filtrate, as well as bicarbonate, amino acids and small peptides. This process is mediated by sodium-coupled cotransporters, which utilize the Na^+K^+-ATPase pump to facilitate the movement of solutes. Notably, the apical sodium-glucose cotransporters (SGLTs) are responsible for transporting glucose into the epithelium, and glucose transporters (GLUTs) facilitate its transport towards the plasma (**Figure 1D**) [14]. In addition to its transport and metabolism functions, the PT is also involved in the production and regulation of calcitriol (vitamin D) [15]. Taken together, the above-mentioned features make the PT a perfect target for disease modeling and drug screening aimed at treating CKD.

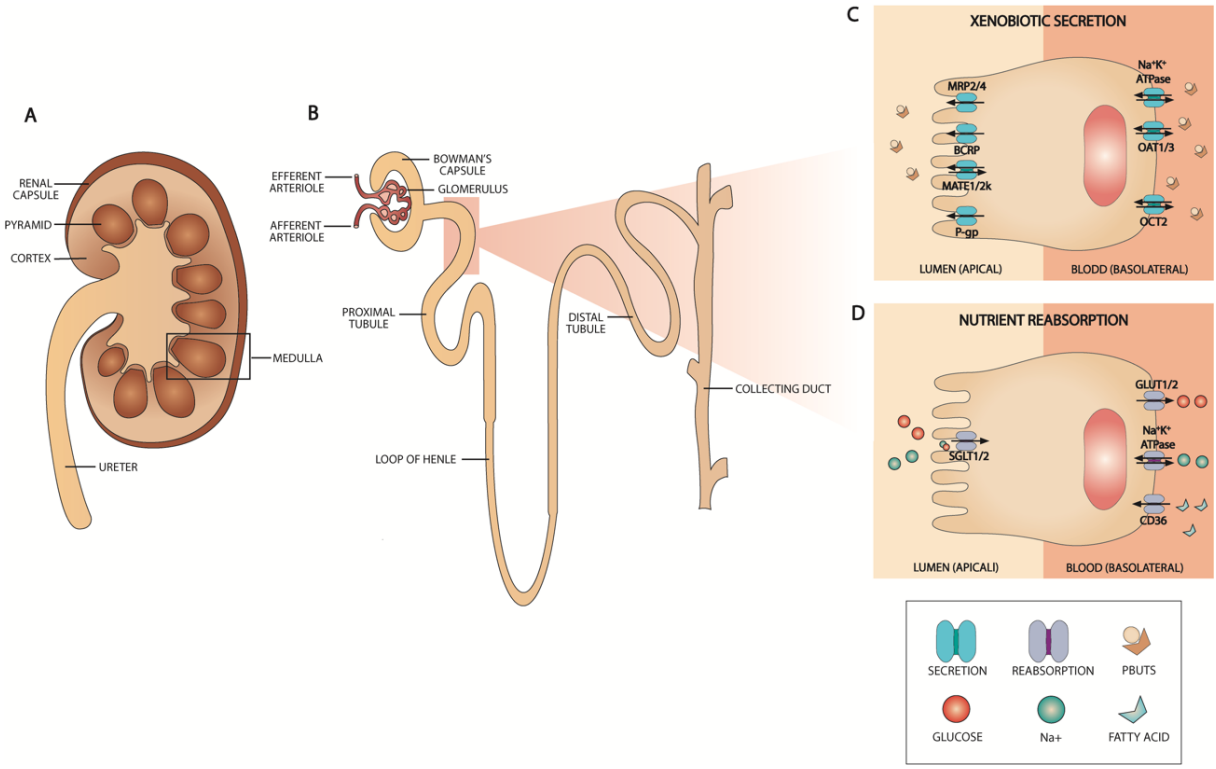

Figure 1. **Anatomical view of the kidney and schematic representation of some transport functions in proximal tubule.** (**A**) The kidney, (**B**) the nephron consisting of interconnected structures. The glomerulus enclosed by the Bowman's capsule, the proximal tubule, the loop of Henle, and the distal tubule, ending in the collecting duct system. (**C**, **D**) transport mechanisms in proximal tubule epithelial cells.

3. Modeling Kidney Diseases, *In Vivo*

Many kidney-related diseases have their origin or manifestations in the PT. To delve into these nephropathies and discover potential therapeutic targets and disease-specific biomarkers, various animal models have been employed. Among these models, rodents are most often used due to their smaller size, lower cost and accessibility, and possibility to genetically manipulate [16]. Often applied acute kidney injury (AKI) models include ischemia-reperfusion injury (IRI), also employed for kidney transplant studies, and drug/toxin-induced AKI. Additionally, often applied CKD models include diabetic kidney disease (DKD) and hypertensive nephropathy, among others [17].

The IRI model is commonly replicated by unilateral or bilateral clamping of renal arteries and veins in rodents. However, the outcome can differ depending on animal species and strains, and different surgical factors, including anesthetic agents used, clamping times and temperature. These variables can impact the overall severity of AKI observed in this model, and achieving a more severe phenotype is challenging as it coincides with a high mortality risk [18-20]. The PT is particularly vulnerable to damage in IRI, because of the high metabolic capacity and large number of mitochondria present in the cells making them sensitive to oxygen fluctuations in the ischemic microenvironment. During IRI, nutrient delivery to the PT is also impaired and its limited capacity to undergo anaerobic metabolism to compensate for the energy demands leads to cellular stress and damage, ultimately contributing to the development of AKI [21-23].

Drug/toxicant-induced AKI primarily affects the PT by using its transport system, leading to the accumulation of toxic compounds within tubular cells and causing oxidative stress and/or inflammation [24]. A number of drugs have frequently been associated with drug-induced AKI, such as chemotherapeutics (*e.g.*, cisplatin), antivirals (*e.g.*, tenofovir) and antibacterial agents (*e.g.*, gentamicin, vancomycin), and iron chelators (*e.g.*, deferasirox) [7, 25]. Moreover, the PT plays a crucial role in secreting endogenous organic retention solutes, also known as uremic toxins, that are not freely filtered by the glomerulus due to high protein binding (protein-bound uremic toxins, PBUTs; **Figure 1C**). This is especially detrimental in patients undergoing dialysis who already have a compromised kidney function. The accumulation of these uremic toxins is associated with increased risk of comorbidities, such as cardiovascular disease [26].

DKD remains the leading cause of end-stage kidney disease (ESKD), however, very few effective treatments are available [27]. The main challenge in DKD preclinical drug discovery is developing accurate models that replicate its intricate multigenic and environmental origin in human. Available animal models can only capture the early stages of DKD or replicate

specific pathological pathways [28-30]. Hyperglycemia, a common risk for DKD, highlights the importance of the PT in disease progression since the PT is responsible for glucose reabsorption. This process is energy demanding, relying on oxygen consumption, thus stressing the role of oxygen metabolism abnormalities, such as hypoxia, in the development and progression of DKD in addition to hyperglycemia [31]. Furthermore, a metabolic switch towards glycolysis in response to hypoxia, leads to abnormal lipid metabolism and lipid accumulation in PT [32]. Moreover, increased advanced glycation, the non-enzymatic reaction between glucose and albumin, is another factor that might contribute to diabetic kidney fibrosis [33]. Given the imbalanced glucose transport observed in DKD, therapeutic approaches targeting the main transporter involved in glucose reabsorption, SGLT2, have been explored. Through the inhibition of SGLT2, glucotoxicity is reduced, which in turns aids in the protection of the PT's integrity and function [34, 35].

The limitations of current animal models, along with their poor predictive capacity for clinical trials highlight the need for better approaches to study kidney function, preclinically. *In vitro* models offer a controlled and reproducible environment for studying specific aspects of PT function and pathologies, which can complement the findings from animal models.

4. Modeling Kidney Diseases, *In Vitro*

To date, researchers have successfully developed and employed several PT *in vitro* models to study the underlying mechanism of various kidney-related diseases. Adopting the most suitable model is crucial since certain models fail to fully replicate certain aspects, such as the native PT's transporter system, which can hinder disease modeling. While primary cells retain the phenotypic features of the native PT, they have a limited lifespan and tend to dedifferentiate over time. On the contrary, human cell lines, once established, generally display greater stability compared to primary cells and have been extensively used in *in vitro* nephrotoxicity studies [36], but may have undergone modifications upon culturing. For example, the human renal proximal tubule cell line, immortalized using the human telomerase reverse transcriptase (RPTEC/TERT1) [37] and the human conditionally immortalized proximal tubule epithelial cell (ciPTECs) line [38], represent suitable *in vitro* models for investigating drug/toxin-induced kidney injury due to several important aspects, including 1) their proximity to *in vivo* characteristics of the native PT, 2) their stable and reproducible phenotype derived from the immortalization processes, and 3) expression of several drug transporters and metabolic enzymes that play essential roles in drug handling. Moreover, the HK-2 cell line [39] is commonly employed for mechanistic kidney disease studies, such as DKD due to the expression of glucose transporters and other relevant transporters involved in

its pathology. For a comprehensive comparison of these and other cell lines and their advantages and disadvantages for the study of kidney-related diseases, a detailed review is available elsewhere [7, 40]. Additionally, the use of human induced-pluripotent stem cells (iPSCs) allows for their direct differentiation into different kidney cell types. IPSC technology permits to generate *in vitro* disease models by mimicking kidney development and generating three-dimensional (3D) structures, known as organoids. These iPSC-derived organoids contain most of the nephron segments [41]. Additionally, genome-editing technologies like CRISPR/Cas9, can be employed to model diseases, or even resort to patient-derived cells [42]. However, a limitation of this approach is that the resulting iPSC-derived organoids mainly resemble embryonic kidneys rather than fully mature ones [41]. To overcome this, kidney organoids derived from adult stem cells have been explored, either obtained from kidney biopsies or urine samples, and form in 3D the so-called tubuloids. These tubuloids carry the same genetic and perhaps epigenetic background of the donor [43, 44], therefore offering opportunity for the development of personalized medicine. Unlike iPSC-derived organoids, tubuloids mainly represent the tubular epithelium and lack the presence of other specialized nephron segments [43]. Nonetheless, both these organoid models lack vasculature and innervation. In addition, genome-editing protocols for tubuloids have not yet been established.

While the previous cell models have elucidated several cell biological and biomolecular mechanisms behind disease states, the use of dynamic culture conditions can more closely resemble kidney cell's physiological conditions. For this, kidney-on-chip models make use of physiological parameters, such as flow and shear stress, to capture functional features of the nephron, and organ-organ interactions. In more detail, this device will require a chamber, with one or two micrometric channels enclosed by a permeable interface to allow diffusion. The inlets/outlets will be connected to a perfusion system to recirculate the medium for further analysis [45, 46]. The majority of kidney-on-chip models focus on the PT, due to its secretion and reabsorption functions crucial for kidney homeostasis. Furthermore, some of these kidney-on-chip models have been employed for drug efficacy and toxicity testing [47, 48].

Nonetheless, considering the individual limitations of each *in vitro* model, researchers have then to decide on how to best mimic the disease *in vitro*. This may involve exposing cells to known drugs or solutes that initiate a cascade of effects, reflecting the *in vivo* situation. Despite these considerations, establishing an in vitro disease model requires the integration of cell-based assays. These assays must target specific disease processes without interference of other cellular responses as well as ensure reliable and reproducible results for translational studies.

5. Regenerative Nephrology

Regenerative nephrology is a field that focuses on repairing, replacing and/or regenerating the kidney, and includes various approaches (**Figure 2**) as discussed in the next paragraphs.

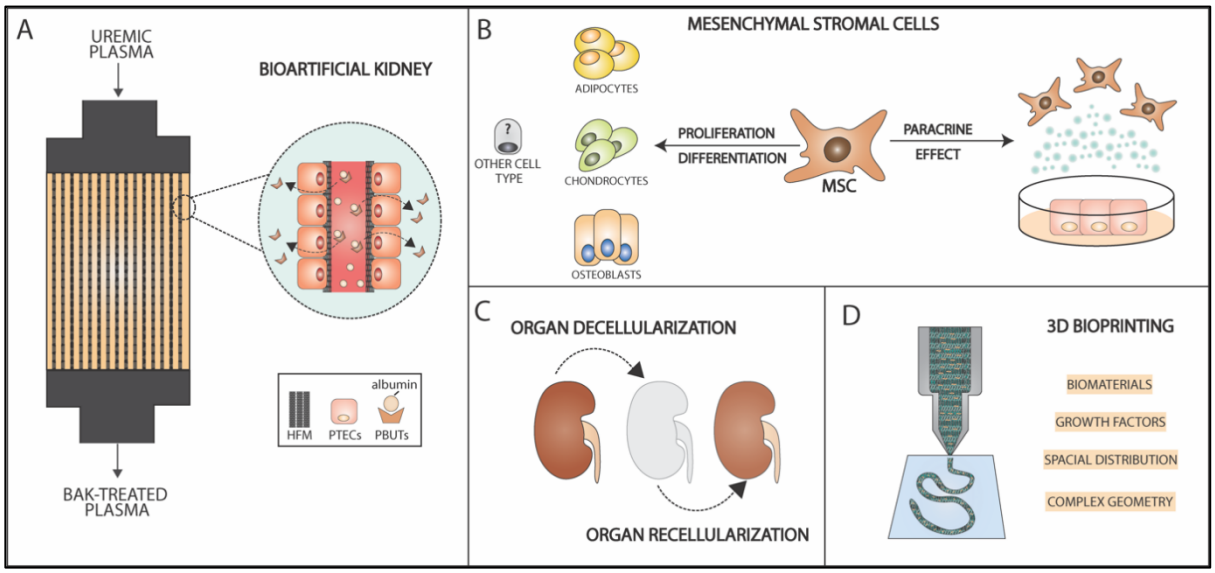

Figure 2. Schematic overview of current regenerative nephrology strategies that encompass either a functional replacement (A), stem cell therapy (B) or tissue engineering for transplantation (C-D). (**A**) Bioartificial kidney, composed of hollow fiber membranes (HFM) covered with proximal tubule epithelial cells (PTECs), capable of active secretion of protein-bound uremic toxins (PBUTs). The BAK is designed to complement current dialysis therapies by improving the clearance of PBUTs. (**B**) Mesenchymal stromal cells (MSCs) can proliferate and differentiate, under inductive stimuli, into adipocytes, chondrocytes, and osteoblasts, as well as other cell types, that can replace damaged cells. Additionally, through the release of paracrine factors, including cytokines, growth factors, and extracellular vesicles, offers a therapeutic approach to treat kidney diseases. (**C**) whole kidney decellularization allows for the preservation of the organ's macro- and micro-architecture that can be repopulated with another cell source, and (**D**) biofabrication using 3D printing of kidney constructs.

5.1. Developing Bioartificial Kidneys

The development of a bioartificial kidney (BAK), a device containing semipermeable (hollow fiber) membranes covered with PT cells (**Figure 2A**), is aimed at complementing conventional dialysis therapy currently lacking the capacity to remove PBUTs. Several groups, including ours, have delved in the design, optimization and up-scaling of such device [49-53]. Notably, we have demonstrated proof-of-concept in a BAK prototype, in which conditionally immortalized proximal tubule epithelial cells (ciPTECs) were seeded. Our BAK prototype possesses several key features of the PT, such as 1) its capacity to secrete PBUTs through

the interplay between apical and basolateral transporters [49, 54], 2) ability to reabsorb albumin [55], 3) activate the precursor of vitamin D [56], and, most importantly, 4) safety in use, as ciPTECs did not show an alloimmunogenic [57], tumorigenic and/or oncogenic potential both *in vitro* and *in vivo* [58]. However, despite these promising features and overall progress in the field, the clinical implementation of a BAK remains elusive.

5.2. Utilizing the Regenerative Properties of Mesenchymal Stromal Cells

The kidney's regenerative capacity is limited, and the ability to generate new nephrons after injury remains a challenging pursuit. To overcome these limitations, researchers are actively seeking ways to promote *in situ* regeneration and to develop transplantable kidney tissue, both aiming at restoring the injured tissue and its function.

In the field of regenerative nephrology, cell-based therapies, specifically mesenchymal stromal cell (MSC) therapy (**Figure 2B**), have shown great potential. MSCs possess immunomodulatory and anti-inflammatory properties, and they can promote tubular cell turnover in both preclinical and clinical models of several nephropathies [59, 60]. Notably, the therapeutic effect of MSCs is attributed to their secretome, consisting of cytokines, growth factors, and extracellular vesicles, rather than the cells themselves. In rodents, these cells are often entrapped in the lung capillaries [61, 62], which is not reported for humans [63, 64], highlighting their great potential for regenerative medicine approaches in clinics. MSCs can be isolated from different sources, including bone marrow, adipose tissue, and umbilical cords, each offering distinct advantages. However, several challenges remain, including determining the most suitable cell source for specific applications, standardizing the manufacturing process to ensure consistent culture conditions and cellular homogeneity across cell batches, and, most importantly, understanding the exact mechanism of action to support the design of the best therapeutical approach [65].

5.3. Employing Bioengineering Approaches to Generate Whole Kidneys or Tubular Structures

As an alternative to kidney transplants, bioengineering kidneys or tubular structures hold great promise. Whole kidneys regeneration can be achieved through the process of organ decellularization revealing an extracellular matrix that allows for repopulation with (patient-derived) cells and organogenesis (**Figure 2C**) [66]. Feasibility of decellularization has been shown using human kidneys, large animals (*e.g.*, porcine models), and rodent kidneys [66, 67]. Regardless of the source for the biological scaffold, the main challenge of scaffold recellularization lies in engineering an organ that is suitable for transplantation, in particular

the kidney which comprises over 26 different cell types [68]. Additionally, it is important that during the decellularization process the extracellular matrix and vasculature remain intact as these are key to support cell adhesion and nutrient delivery upon perfusion. Despite several attempts to develop whole kidneys using this approach, successfully repopulating the vasculature and epithelial compartment remains unattainable, hindering its potential as a solution for organ shortage [66, 67].

Furthermore, various 3D bioprinting techniques have been employed to create kidney constructs resembling the organ structure and function (**Figure 2D**). Lewis *et al.* were among the pioneers in successfully using bioprinting techniques to create a fully epithelialized PT exhibiting several morphological and functional features of the native PT [69]. The same group also showcased 3D bioprinting of a two-channel model comprised of a tubular and vascular compartment, demonstrating the interplay between these two compartments by mimicking renal reabsorption [70]. Both of these approaches were successfully employed by culturing primary cells and immortalized cell lines within the bioprinted channels, however their recent work using kidney organoids highlighted superior physiological resemblance, thus proving stem cells to be a better cell source for tissue engineering [71]. Despite the significant progress in utilizing biofabrication techniques to create functional kidney constructs, the intricate nature of the kidney's structure and function continues to pose hurdles.

Altogether, regenerative nephrology approaches hold promising potential for treating kidney diseases and restoring kidney function.

6. Thesis Aim and Outline

The aim of this thesis was to develop a series of *in vitro* models resembling the key phenotypical and molecular features of the native PT and to apply those in studying CKD progression, mimicking interventions and to potentially identify therapeutic targets. This thesis sought to address not only the overall impact of disease mediators on kidney health, but also the precise contributions and responses of the PT in disease progression.

Chapter 2 offers a comprehensive overview of drug-induced nephrotoxicity models, ranging from traditional 2D models to advanced (3D) *in vitro* models, while highlighting their individual contributions to advances in the field. Moreover, we compared the different *in vitro* models based on their levels of complexity and physiological relevance, while stressing which key features should be included in the development of new and more physiologically relevant *in vitro* models. Additionally, we provided an overview of the toxicity/injury biomarkers available, and compared these to the gold standard in clinics. We explored the necessity of validating these biomarkers for assessing disease progression and regeneration.

In **Chapter 3**, we focused on evaluating the role of OAT1 in facilitating the uptake of commonly prescribed drugs in CKD management and PBUTS. We hypothesized that since PBUTs and CKD drugs are both substrates for OAT1, their combination could potentially hamper residual kidney function by competing for uptake. To investigate this, we initially assessed the effect of either PBUTs or CKD drugs on OAT1 activity through the uptake of fluorescein as fluorescent OAT1 substrate. Subsequently, in a similar setting, we evaluated the combined exposure of PBUTs and CKD drugs. Our aim was to understand whether drugs would compromise the uptake (and subsequent excretion) of PBUTs through competition for OAT1.

In **Chapter 4**, we investigated the cytocompatibility of dialysis fluid (DF) for BAK applications. Our primary goal was to ensure that DF would not hinder the primary function of the BAK, which is the clearance of PBUTs. To achieve this, we conducted a series of experiments using conventional *in vitro* models aiming at assessing DF's effect on cell viability markers and monolayer integrity. Additionally, we conducted transepithelial transport studies using bioengineered kidney tubules, which represent the functional unit of the BAK, to determine whether DF would interfere with PBUTs clearance. This chapter aimed to ensure that DF would not compromise the effectiveness of the BAK in clearing PBUTs, ensuring their clinical suitability and safety.

In **Chapter 5**, we focused on the development of a novel *in vitro* model for the study of ischemia-reperfusion injury (IRI) by suppressing mitochondrial respiration and glycolysis under hypoxia. We assessed various parameters of mitochondrial health, including metabolic activity, mitochondrial mass, mitochondrial membrane potential, bioenergetics, and the cell metabolome. Upon characterization of the injury, and having in mind that IRI lacks effective therapies, we evaluated the therapeutic effect of mesenchymal stromal cell secretome from different sources (bone marrow, adipose tissue, and umbilical cord) in mitigating the damage observed in mitochondrial dysfunction and overall cell bioenergetics.

In **Chapter 6**, we delved into the pathophysiology of diabetic proximal tubulopathy, highlighting the key events driving disease progression. Furthermore, we explored the essential features required for an ideal PT *in vitro* model, while also discussing the pros and cons of the mo st commonly used PT *in vitro* models. In addition, we provided a comprehensive overview of the therapeutic potential of SGLT2 inhibitors in mitigating the detrimental effects of diabetic proximal tubulopathy. This included detailing their individual transporter affinities, associated benefits and side effects, and presenting evidence of their efficacy in the *in vitro* models covered in the chapter.

In **Chapter 7**, we assessed whether the most common used cell line for the study of DKD, the HK-2 cell line, is capable of replicating the phenotypic and molecular changes observed for the disease *in vivo*. To achieve this, we combined the effects of high glucose and hypoxia, known to better replicate the diabetic milieu, with two other diabetic mediators, namely palmitic acid or glycated albumin, both involved in disease progression. For this, we assessed how this combined effect could impact mitochondrial health, a critical aspect in DKD pathogenesis. Additionally, we evaluated the therapeutic effect of empagliflozin, an SGLT2 inhibitor, in mitigating the release of kidney injury markers.

Finally, **Chapter 8** provides a summary and general discussion of the findings in this thesis, as well as future perspectives in the field to help circumventing the drawbacks found.

REFERENCES

1. C. P. Kovesdy. Epidemiology of chronic kidney disease: an update 2022. Kidney Int Suppl (2011) 2022;12(1):7-11

2. O. Z. Ameer. Hypertension in chronic kidney disease: What lies behind the scene. Front Pharmacol 2022;13:949260

3. I. H. de Boer, K. Khunti, T. Sadusky*, et al.* Diabetes management in chronic kidney disease: a consensus report by the American Diabetes Association (ADA) and Kidney Disease: Improving Global Outcomes (KDIGO). Kidney Int 2022;102(5):974-989

4. M. Ruiz-Ortega, S. Rayego-Mateos, S. Lamas*, et al.* Targeting the progression of chronic kidney disease. Nat Rev Nephrol 2020;16(5):269-288

5. T. K. Chen, D. H. Knicely and M. E. Grams. Chronic Kidney Disease Diagnosis and Management: A Review. JAMA 2019;322(13):1294-1304

6. E. Bello-Reuss and L. Reuss. Homeostatic and Excretory Functions of the Kidney. In: S. Klahr, ed. *The Kidney and Body Fluids in Health and Disease*. Springer US: Boston, MA; 1983, 35-63.

7. J. Faria, S. Ahmed, K. G. F. Gerritsen*, et al.* Kidney-based in vitro models for drug-induced toxicity testing. Arch Toxicol 2019;93(12):3397-3418

8. M. Lemaire. Novel Fanconi renotubular syndromes provide insights in proximal tubule pathophysiology. Am J Physiol Renal Physiol 2021;320(2):F145-F160

9. M. Ahmad, I. Abramovich, B. Agranovich*, et al.* Kidney Proximal Tubule GLUT2-More than Meets the Eye. Cells 2022;12(1)

10. S. K. Haque, G. Ariceta and D. Batlle. Proximal renal tubular acidosis: a not so rare disorder of multiple etiologies. Nephrol Dial Transplant 2012;27(12):4273-4287

11. S. M. Malakauskas, H. Quan, T. A. Fields*, et al.* Aminoaciduria and altered renal expression of luminal amino acid transporters in mice lacking novel gene collectrin. Am J Physiol Renal Physiol 2007;292(2):F533-544

12. K. Wang and B. Kestenbaum. Proximal Tubular Secretory Clearance: A Neglected Partner of Kidney Function. Clin J Am Soc Nephrol 2018;13(8):1291-1296

13. S. Liu, Y. Yao, S. Lu*, et al.* The role of renal proximal tubule P450 enzymes in chloroform-induced nephrotoxicity: utility of renal specific P450 reductase knockout mouse models. Toxicol Appl Pharmacol 2013;272(1):230-237

14. C. Ghezzi, D. D. F. Loo and E. M. Wright. Physiology of renal glucose handling via SGLT1, SGLT2 and GLUT2. Diabetologia 2018;61(10):2087-2097

15. D. Santoro, D. Caccamo, S. Lucisano*, et al.* Interplay of vitamin D, erythropoiesis, and the renin-angiotensin system. Biomed Res Int 2015;2015:145828

16. G. J. Becker and T. D. Hewitson. Animal models of chronic kidney disease: useful but not perfect. Nephrol Dial Transplant 2013;28(10):2432-2438

17. A. Hosszu, T. Kaucsar, E. Seeliger*, et al.* Animal Models of Renal Pathophysiology and Disease. Methods Mol Biol 2021;2216:27-44

18. Z. Guan, G. Gobe, D. Willgoss*, et al.* Renal endothelial dysfunction and impaired autoregulation after ischemia-reperfusion injury result from excess nitric oxide. Am J Physiol Renal Physiol 2006;291(3):F619-628

19. Q. Wei and Z. Dong. Mouse model of ischemic acute kidney injury: technical notes and tricks. Am J Physiol Renal Physiol 2012;303(11):F1487-1494

20. N. I. Skrypnyk, R. C. Harris and M. P. de Caestecker. Ischemia-reperfusion model of acute kidney injury and post injury fibrosis in mice. J Vis Exp 2013(78)

21. A. M. Sheridan and J. V. Bonventre. Cell biology and molecular mechanisms of injury in ischemic acute renal failure. Curr Opin Nephrol Hypertens 2000;9(4):427-434

22. T. Kalogeris, C. P. Baines, M. Krenz*, et al.* Cell biology of ischemia/reperfusion injury. Int Rev Cell Mol Biol 2012;298:229-317

23. A. M. Hall and S. de Seigneux. Metabolic mechanisms of acute proximal tubular injury. Pflugers Arch 2022;474(8):813-827

24. N. Pannu. Drug-Induced AKI. In: J.-L. Vincent and J. B. Hall, eds. *Encyclopedia of Intensive Care Medicine*. Springer Berlin Heidelberg: Berlin, Heidelberg; 2012, 765-769.

25. E. Kwiatkowska, L. Domanski, V. Dziedziejko*, et al.* The Mechanism of Drug Nephrotoxicity and the Methods for Preventing Kidney Damage. Int J Mol Sci 2021;22(11)

26. J. H. Chen and C. K. Chiang. Uremic Toxins and Protein-Bound Therapeutics in AKI and CKD: Up-to-Date Evidence. Toxins (Basel) 2021;14(1)

27. M. C. Thomas, M. Brownlee, K. Susztak*, et al.* Diabetic kidney disease. Nat Rev Dis Primers 2015;1:15018

28. I. Nguyen, A. van Koppen and J. A. Joles. Animal Models of Diabetic Kidney Disease. In: J. J. Roelofs and L. Vogt, eds. *Diabetic Nephropathy: Pathophysiology and Clinical Aspects*. Springer International Publishing: Cham; 2019, 375-413.

29. F. E. Sembach, M. V. Ostergaard, N. Vrang*, et al.* Rodent models of diabetic kidney disease: human translatability and preclinical validity. Drug Discov Today 2021;26(1):200-217

30. A. Giralt-Lopez, M. Molina-Van den Bosch, A. Vergara*, et al.* Revisiting Experimental Models of Diabetic Nephropathy. Int J Mol Sci 2020;21(10)

31. V. Vallon. The proximal tubule in the pathophysiology of the diabetic kidney. Am J Physiol Regul Integr Comp Physiol 2011;300(5):R1009-1022

32. H. Wang, S. Zhang and J. Guo. Lipotoxic Proximal Tubular Injury: A Primary Event in Diabetic Kidney Disease. Front Med (Lausanne) 2021;8:751529

33. M. A. Gallicchio and L. A. Bach. Uptake of advanced glycation end products by proximal tubule epithelial cells via macropinocytosis. Biochim Biophys Acta 2013;1833(12):2922-2932

34. V. Vallon. Renoprotective Effects of SGLT2 Inhibitors. Heart Fail Clin 2022;18(4):539-549

35. V. Vallon. The mechanisms and therapeutic potential of SGLT2 inhibitors in diabetes mellitus. Annu Rev Med 2015;66:255-270

36. P. Jennings, C. KoppelstÄtter, J. Lechner*, et al.* Renal cell culture models: Contribution to the understanding of nephrotoxic mechanisms. In: M. E. De Broe, G. A. Porter, W. M. Bennett, et al., eds. *Clinical Nephrotoxins: Renal Injury from Drugs and Chemicals*. Springer US: Boston, MA; 2008, 223-249.

37. B. R. Simon-Friedt, M. J. Wilson, D. A. Blake*, et al.* The RPTEC/TERT1 Cell Line as an Improved Tool for In Vitro Nephrotoxicity Assessments. Biol Trace Elem Res 2015;166(1):66-71

38. T. T. Nieskens, J. G. Peters, M. J. Schreurs*, et al.* A Human Renal Proximal Tubule Cell Line with Stable Organic Anion Transporter 1 and 3 Expression Predictive for Antiviral-Induced Toxicity. AAPS J 2016;18(2):465-475

39. M. J. Ryan, G. Johnson, J. Kirk*, et al.* HK-2: an immortalized proximal tubule epithelial cell line from normal adult human kidney. Kidney Int 1994;45(1):48-57

40. J. Faria, K. G. F. Gerritsen, T. Q. Nguyen*, et al.* Diabetic proximal tubulopathy: Can we mimic the disease for in vitro screening of SGLT inhibitors? Eur J Pharmacol 2021;908:174378

41. M. Takasato, P. X. Er, H. S. Chiu*, et al.* Generation of kidney organoids from human pluripotent stem cells. Nat Protoc 2016;11(9):1681-1692

42. B. S. Freedman, C. R. Brooks, A. Q. Lam*, et al.* Modelling kidney disease with CRISPR-mutant kidney organoids derived from human pluripotent epiblast spheroids. Nat Commun 2015;6:8715

43. F. Schutgens, M. B. Rookmaaker, T. Margaritis*, et al.* Tubuloids derived from human adult kidney and urine for personalized disease modeling. Nat Biotechnol 2019;37(3):303-313

44. A. B. Nunez-Nescolarde, D. J. Nikolic-Paterson and A. N. Combes. Human Kidney Organoids and Tubuloids as Models of Complex Kidney Disease. The American Journal of Pathology 2022;192(5):738-749

45. A. van den Berg, C. L. Mummery, R. Passier*, et al.* Personalised organs-on-chips: functional testing for precision medicine. Lab Chip 2019;19(2):198-205

46. N. Ashammakhi, K. Wesseling-Perry, A. Hasan*, et al.* Kidney-on-a-chip: untapped opportunities. Kidney Int 2018;94(6):1073-1086

47. K. J. Jang, A. P. Mehr, G. A. Hamilton*, et al.* Human kidney proximal tubule-on-a-chip for drug transport and nephrotoxicity assessment. Integr Biol (Camb) 2013;5(9):1119-1129

48. T. T. G. Nieskens, O. Magnusson, P. Andersson*, et al.* Nephrotoxic antisense oligonucleotide SPC5001 induces kidney injury biomarkers in a proximal tubule-on-a-chip. Arch Toxicol 2021;95(6):2123-2136

49. J. Jansen, M. Fedecostante, M. J. Wilmer*, et al.* Bioengineered kidney tubules efficiently excrete uremic toxins. Sci Rep 2016;6:26715

50. N. V. Chevtchik, M. Fedecostante, J. Jansen*, et al.* Upscaling of a living membrane for bioartificial kidney device. Eur J Pharmacol 2016;790:28-35

51. D. L. Ramada, J. de Vries, J. Vollenbroek*, et al.* Portable, wearable and implantable artificial kidney systems: needs, opportunities and challenges. Nat Rev Nephrol 2023;19(8):481-490

52. H. D. Humes, S. M. MacKay, A. J. Funke*, et al.* Tissue engineering of a bioartificial renal tubule assist device: in vitro transport and metabolic characteristics. Kidney Int 1999;55(6):2502-2514

53. C. Ronco, A. Davenport and V. Gura. A wearable artificial kidney: dream or reality? Nat Clin Pract Nephrol 2008;4(11):604-605

54. J. Jansen, I. E. De Napoli, M. Fedecostante*, et al.* Human proximal tubule epithelial cells cultured on hollow fibers: living membranes that actively transport organic cations. Sci Rep 2015;5:16702

55. M. J. Wilmer, M. A. Saleem, R. Masereeuw*, et al.* Novel conditionally immortalized human proximal tubule cell line expressing functional influx and efflux transporters. Cell Tissue Res 2010;339(2):449-457

56. M. Mihajlovic, M. Fedecostante, M. J. Oost*, et al.* Role of Vitamin D in Maintaining Renal Epithelial Barrier Function in Uremic Conditions. Int J Mol Sci 2017;18(12)

57. M. Mihajlovic, L. P. van den Heuvel, J. G. Hoenderop*, et al.* Allostimulatory capacity of conditionally immortalized proximal tubule cell lines for bioartificial kidney application. Sci Rep 2017;7(1):7103

58. M. Mihajlovic, S. Hariri, K. C. G. Westphal*, et al.* Safety evaluation of conditionally immortalized cells for renal replacement therapy. Oncotarget 2019;10(51):5332-5348

59. I. C. S. Calcat, C. Sanz-Nogues and T. O'Brien. When Origin Matters: Properties of Mesenchymal Stromal Cells From Different Sources for Clinical Translation in Kidney Disease. Front Med (Lausanne) 2021;8:728496

60. A. J. Peired, A. Sisti and P. Romagnani. Mesenchymal Stem Cell-Based Therapy for Kidney Disease: A Review of Clinical Evidence. Stem Cells Int 2016;2016:4798639

61. U. M. Fischer, M. T. Harting, F. Jimenez*, et al.* Pulmonary passage is a major obstacle for intravenous stem cell delivery: the pulmonary first-pass effect. Stem Cells Dev 2009;18(5):683-692

62. C. H. Masterson, A. Tabuchi, G. Hogan*, et al.* Intra-vital imaging of mesenchymal stromal cell kinetics in the pulmonary vasculature during infection. Sci Rep 2021;11(1):5265

63. P. Erpicum, L. Weekers, O. Detry*, et al.* Infusion of third-party mesenchymal stromal cells after kidney transplantation: a phase I-II, open-label, clinical study. Kidney Int 2019;95(3):693-707

64. M. E. J. Reinders, K. E. Groeneweg, S. H. Hendriks*, et al.* Autologous bone marrow-derived mesenchymal stromal cell therapy with early tacrolimus withdrawal: The randomized prospective, single-center, open-label TRITON study. Am J Transplant 2021;21(9):3055-3065

65. I. C. S. Calcat, E. Rendra, E. Scaccia*, et al.* Harmonised culture procedures minimise but do not eliminate mesenchymal stromal cell donor and tissue variability in a decentralised multicentre manufacturing approach. Stem Cell Res Ther 2023;14(1):120

66. M. J. A. de Haan, F. M. R. Witjas, M. A. Engelse*, et al.* Have we hit a wall with whole kidney decellularization and recellularization: A review. Current Opinion in Biomedical Engineering 2021;20:100335

67. A. C. Destefani, G. M. Sirtoli and B. V. Nogueira. Advances in the Knowledge about Kidney Decellularization and Repopulation. Front Bioeng Biotechnol 2017;5:34

68. Q. Al-Awqati and J. A. Oliver. Stem cells in the kidney. Kidney Int 2002;61(2):387-395

69. K. A. Homan, D. B. Kolesky, M. A. Skylar-Scott*, et al.* Bioprinting of 3D Convoluted Renal Proximal Tubules on Perfusable Chips. Sci Rep 2016;6:34845

70. N. Y. C. Lin, K. A. Homan, S. S. Robinson*, et al.* Renal reabsorption in 3D vascularized proximal tubule models. Proc Natl Acad Sci U S A 2019;116(12):5399-5404

71. J. O. Aceves, S. Heja, K. Kobayashi*, et al.* 3D proximal tubule-on-chip model derived from kidney organoids with improved drug uptake. Sci Rep 2022;12(1):14997

CHAPTER 2

Kidney-Based *In Vitro* Models for Drug-Induced Toxicity Testing

João Faria[1*], Sabbir Ahmed[1*], Karin G.F. Gerritsen[2], Silvia M. Mihăilă[1], Rosalinde Masereeuw[1]

[1] Division of Pharmacology, Department of Pharmaceutical Sciences, Utrecht Institute for Pharmaceutical Sciences, Utrecht University, Universiteitsweg 99, 3584 CG, Utrecht, The Netherlands

[2] Department of Nephrology and Hypertension, University Medical Center, Utrecht, The Netherlands

[*]These authors contributed equally

Published in Arch Toxicol. 2019;93(12):3397-3418

ABSTRACT

The kidney is frequently involved in adverse effects caused by exposure to foreign compounds, including drugs. An early prediction of those effects is crucial for allowing novel, safe, drugs entering the market. Yet, in current pharmacotherapy, drug-induced nephrotoxicity accounts for up to 25% of the reported serious adverse effects, of which one-third is attributed to antimicrobials use. Adverse drug effects can be due to direct toxicity, for instance as a result of kidney-specific determinants, or indirectly by *e.g.*, vascular effects or crystals deposition. Currently used *in vitro* assays do not adequately predict *in vivo* observed effects, predominantly due to an inadequate preservation of the organs' microenvironment in the models applied. The kidney is highly complex, composed of a filter unit and a tubular segment, together containing over twenty different cell types. The tubular epithelium is highly polarized, and the maintenance of this polarity is critical for optimal functioning and response to environmental signals. Cell polarity is dependent on communication between cells, which includes paracrine and autocrine signals, as well as biomechanic and chemotactic processes. These processes all influence kidney cell proliferation, migration and differentiation. For drug disposition studies, this microenvironment is essential for prediction of toxic responses. This review provides an overview of drug-induced injuries to the kidney, details on relevant and translational biomarkers, and advances in 3D cultures of human renal cells, including organoids and kidney-on-a-chip platforms.

KEYWORDS: Nephrotoxicity; Drug-induced kidney injury; *In vitro* models; Biomarkers.

1. INTRODUCTION

The kidneys play an essential role in preserving homeostasis of the body's internal environment, including regulation of water, electrolyte, nitrogen and acid-base balances. They also control the red blood cell production and blood pressure [1]. Impaired renal function is commonly observed in clinical practice and is often associated with use of drugs. One third of all drugs and drug candidates are excreted unchanged from the body by the kidneys, and drug-induced nephrotoxicity accounts for 20% of all episodes that lead to acute kidney failure [2].

Human kidneys contain around one million nephrons. A nephron is composed of different subunits and includes the glomerulus, proximal tubule, loop of Henle, distal tubule, and the collecting duct [3] (**Figure 1**). All subunits contribute to the excretory function of the kidney in three steps: glomerular filtration, tubular reabsorption, and tubular secretion [4]. During glomerular filtration (**Figure 2**), blood plasma is filtered in the glomerulus, a bundle of porous capillaries lined by a membrane and specialized epithelial cells, that allows solutes and waste, including drugs and their metabolites, and water to pass through while ensuring bigger substances, such as blood cells and proteins, remain in the circulatory system [5]. Protein-bound molecules, including drugs, are eliminated by proximal tubular secretion via a well-coordinated process of uptake into the tubular cells at the blood-facing basolateral site and secretion into the tubular lumen. Tubular reabsorption begins as soon as the filtrate enters the lumen of the proximal tubule and involves the reabsorption of organic nutrients, such as glucose, and hormonal-regulated reabsorption of ions coupled with passive water reabsorption. Megalin and cubilin receptors at the apical membrane are responsible for endocytosis-mediated reuptake of filtered low molecular weight proteins, such as β2-microglobulin [6]. As the filtrate travels along the nephron, some drugs, hydrogen ions, and ammonia are secreted into the collecting tubule [7].

Even though the main function of the kidney is to excrete waste products from the bloodstream, it is important to mention that the kidney is also a major endocrine organ. Five very important hormones/enzymes are produced by the kidney, *viz*. 1,25-dihydroxyvitamin D3, erythropoietin, renin, Klotho, and kallikrein [8, 9]. Calcitriol, 1,25-dihydroxyvitamin D3, is activated in the proximal tubule and acts in the reabsorption of calcium, but it is also involved in bone health and in the regulation of parathyroid function [10]. Erythropoietin is produced by peritubular capillary endothelial cells in the proximal tubule, and acts by stimulating the production of red blood cells in the bone marrow [11].

Renin is secreted by granular cells of the juxtaglomerular apparatus. This enzyme, also known as angiotensinogenase is the key factor of the renin-angiotensin system (RAS) that

lead to the production of the potent vasoconstrictor angiotensin controlling blood pressure [12]. Klotho is synthesized and secreted by the distal tubule. Similar to calcitriol, Klotho is involved in the calcium and phosphate homeostasis [13]. Kallikrein of the renal kallikrein-kinin system is found in the distal tubule, and is involved in the regulation of blood pressure [14].

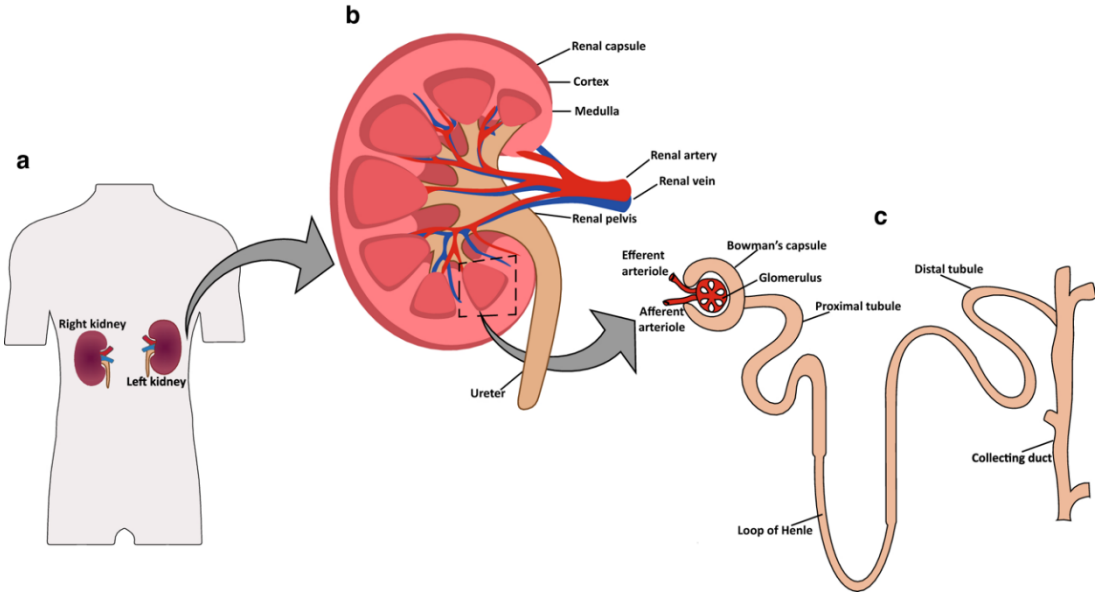

Figure 1. Human kidney anatomy. (**a**) External view, (**b**) Internal view, and (**c**) its functional unit nephron.

Due to the complexity of the kidney, as an organ containing specialized structures and multiple cell types, it becomes quite difficult to find a reliable model system to study the effects or toxicity of drugs and their metabolites on this organ. In this review, detailed information on drug induced kidney injury mechanisms and available *in vitro* models to predict this with relevant translational biomarkers will be discussed, with an emphasis on novel developments in the field of microphysiological systems that meet the requirements of the 3Rs (replacement, reduction, refinement) of animal experiments for drug safety screenings.

2. Subphenotypes in Kidney Injury

2.1. Drug-Induced Kidney Injury

Exposure to various drugs or drug candidates for therapeutic or diagnostic purposes (**Figure 3**) could possibly lead to toxicity in the kidney, resulting in damage of the tubules, interstitium, glomerulus or renal microvasculature, and consequently in various clinical manifestations (**Table 1**) [15]. About 36% of nephrotoxicity incidence has been attributed to antimicrobials (*e.g.*, aminoglycosides). While in most cases, the drug-induced kidney injury is reversible upon cease of treatment some medications could lead to chronic dysfunction such as papillary

necrosis, tubulointerstitial nephritis or prolonged proteinuria [16]. Nephrotoxicity of most drugs is more severe in patients already suffering from kidney disease [17].

2.2. Kidneys Can Experience Both Structural Damage and Loss of Function

Acute kidney injury (AKI) is characterized by an increase in blood levels of waste solutes, such as urea and creatinine, and often oliguria and electrolyte disorders. AKI can be classified into three categories: prerenal, intrinsic and postrenal [18]. In prerenal AKI, the kidney may function normally, but there is a decrease in either intravascular volume or arterial pressure, which results in a reduced glomerular filtration rate (GFR) [19]. RAS inhibitors such as angiotensin-converting enzyme inhibitors and angiotensin receptor blockers can also lead to prerenal AKI, as it causes dilation of the efferent arteriole which contributes to reduced intraglomerular pressure [20]. Further, nonsteroidal anti-inflammatory drugs (NSAIDs) are known to decrease the GFR by changing the balance of vasodilatory/vasoconstrictive agents in the renal microcirculation [21]. The most common type of intrinsic AKI is acute tubular necrosis, which is usually caused by ischemia or toxic injury [22]. Postrenal AKI occurs when there is an obstruction of urinary flow that can lead to impaired renal blood flow and inflammatory processes, seen for example in urate and oxalate imbalances [18].

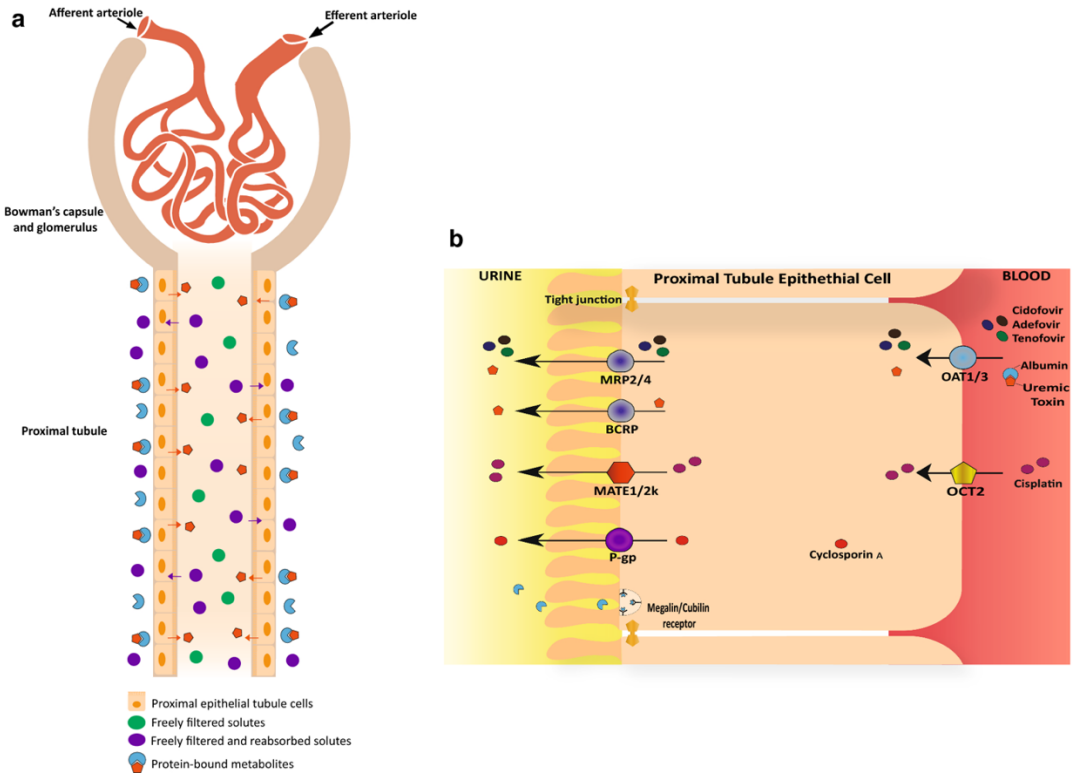

Figure 2. The renal proximal tubule. (**a**) Blood plasma solutes and proteins pass through the glomerular filter. Organic and inorganic solutes (in green) are freely filtered by the glomerulus. Some solutes, such as glucose and amino acids (in purple), are reabsorbed completely by the proximal tubule epithelial cells and transferred back to the systemic circulation. Protein-bound metabolites (in orange) are actively secreted by the proximal tubule epithelial cells. (**b**) Drug transporters involved in nephrotoxicity. The organic anion transporters OAT1 (*SLC22A6*) and OAT3 (*SLC22A8*) are involved in the uptake of known antiviral agents, such as cidofovir, adefovir and tenofovir which will then be secreted by MRP2 (*ABCC2*) and MRP4 (*ABCC4*) located at the apical side of the membrane. The chemoterapeutic agent cisplatin is imported by OCT2 (*SLC22A2*) and exported via MATE1 (*SLC47A1*) and MATE2-k (*SLC47A2*). P-gp (*ABCB1*) is involved in the secretion of the immunosuppressant cyclosporin A. Uremic toxins, such as Indoxyl sulfate and kynurenic acid are uptaken via OAT1 and excreted by MRP2/4 and BCRP (*ABCG2*).

When these changes become persistent both in structure and function, AKI may progress to chronic kidney disease (CKD), and when not properly treated, it can lead to end-stage kidney disease. The GFR is used to categorize CKD in five distinct stages, along with the presence or absence of proteinuria [23].

Nephrotoxicants, including chemotherapeutics, drugs of abuse, antimicrobials, radiocontrast agents, environmental pollutants and natural substances, can induce kidney injury via similar mechanisms. Renal cell death can be mediated by drug transporters that

determine the selectivity for the tubular cell, mitochondrial damage and drug metabolism [24] . The reabsorption of solutes by the kidneys is a task that demands a large consumption of energy. The proximal tubule is the nephron's segment that is the most susceptible to toxic effects due to its role in absorption and secretion, both requiring high rates of oxidative metabolism. For this reason, mitochondrial damage will lead to a reduction in ATP production that in turn will increase oxidative stress, disrupt cell volume, ion concentrations, and apoptosis or, in severe cases necrosis, thus compromising renal function [25]. Renal transporters may facilitate drugs to enter the tubular cells, sometimes followed by metabolism leading to their bioactivation [26]. These transporters belong to two large families: the solute carrier family (SLC) and the adenosine triphosphate (ATP)-binding cassette (ABC) transporter family. Uptake of organic anions (**Figure 2**) is mediated by the organic anion transporters 1 (OAT1; *SLC22A6*) and 3 (OAT3; *SLC22A8*) and their removal from the cell via breast cancer resistance protein (BCRP; *ABCG2*), multidrug resistance protein 2 (MRP2; *ABCC2*) and 4 (MRP4; *ABCC4*) [27-29]. Organic cations (**Figure 2**) are transported into tubular cells predominantly via the basolateral organic cation transporter 2 (OCT2; *SLC22A2*) and then excreted into the tubular lumen via multidrug and toxin extrusion protein 1 (MATE1; *SLC47A1*) and 2-k (MATE2-k; *SLC47A2*) and P-glycoprotein (P-gp; *ABCB1*). Although most drugs are metabolized by the liver, some nephrotoxicants are known to be dependent on kidney metabolism as this organ also expresses Phase I (CYPs) and Phase II (GSTs) enzymes [30].

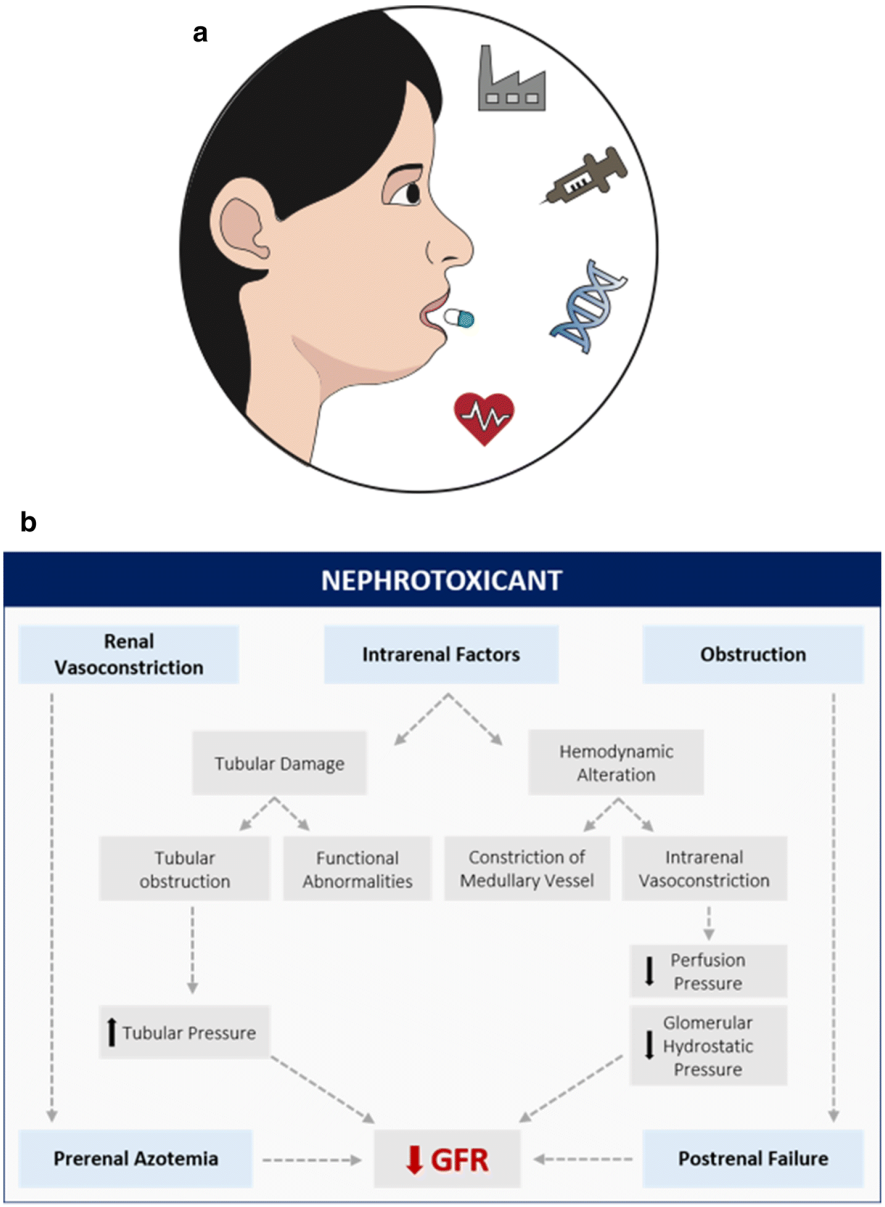

Figure 3. Risk of drugs to affect kidney function. (**a**). The human body is subjected to a variety of nephrotoxicants, including chemotherapeutics, drugs of abuse, antimicrobials, environmental pollutants and natural substances, which can induce kidney injury via several mechanisms. (**b**). These nephrotoxicants can lead to acute kidney injury (AKI). AKI is characterized by gradual loss of kidney function that, when not properly treated, can lead to irreversible kidney failure. Renal vasoconstriction, intrarenal factors, and obstruction are some of the effects of the nephrotoxicants on the kidney, which will lead to a decrease in the glomerular filtration rate (GFR). An estimation of the GFR is widely used in clinic as an indicator of kidney function.

2.3. Vascular Injury

Several immunosuppressive agents such as cyclosporin, tacrolimus and muromonab-CD3 may cause renal vascular injury by damaging primary endothelium that induces platelet aggregation and consumption. Such an effect is also associated with antiplatelet agents, for instance, ticlopidine and clopidogrel, and chemotherapeutic agents (*e.g.*, mitomycin C and gemcitabine; **Table 1**) [16]. The narrow arteries of the kidney including glomerular capillaries, interlobular and arcuate arteries can be clogged by arterial cholesterol plaques following administration of thrombolytic agents (*e.g.*, streptokinase) and anticoagulants (*e.g.*, warfarin). This can result in ischemia, infarction, necrosis and inflammation of the surrounding interstitium, often also affecting tubular cells leading to acute tubular necrosis (ATN; **Table 1**) [31].

2.4. Tubular Injury

Proximal tubule cells absorb and concentrate compounds from the glomerular filtrate as well as from the systemic circulation, and are prone to be affected by nephrotoxic drugs. These drugs can cause tubular toxicity by various mechanisms such as oxidative stress, diminishing mitochondrial function, restricting tubular transport processes and generating oxidative stress [32]. Drugs such as antimicrobials, chemotherapeutics, radiocontrast agents, immunosuppressives and bisphosphonates are associated with tubular injury. These xenobiotics disrupt tubular cell polarity which, along with the expression of apical and basolateral transporters, is crucial for tubular cell function. This leads to the dislocation of apical and basolateral transporters (*e.g.*, Na^+K^+-ATPase) resulting in a leaky epithelium. Furthermore, subsequent increase in intracellular calcium disrupts ion homeostasis, leading to cell death [33].

2.5. Inflammation

Induction of inflammatory responses in the glomerulus, renal tubular cells and the surrounding interstitium is another mechanism of drug-induced nephrotoxicity that can lead to fibrosis and renal scarring [2]. An immune-mediated inflammatory condition, glomerulonephritis, has been reported to be induced by several medications such as Penicillin and NSAIDs (**Table 1**) and is associated with proteinuria [34]. Drugs including lithium, penicillin and NSAIDs are found to cause such inflammatory condition (**Table 1**).

Table 1. **Commonly used nephrotoxic drugs and associated toxicities.**

Therapeutic Class	Drugs	Toxic events	References
Anticoagulants	Warfarin, heparin	Renal tissue ischemia Necrosis Infarction	[35]
Anticonvulsant	Phenytoin	Acute interstitial nephritis Diabetes insipidus	[36]
Antidepressant	Amitriptyline	Rhabdomyolysis	[37]
	Lithium	Chronic interstitial nephritis Glomerulonephritis Rhabdomyolysis	[37, 38]
Antifungal agent	Amphotericin B	ATN Renal tubular acidosis (RTA) Electrolyte imbalance Urinary concentration defects	[39]
Antihistamine	Diphenhydramine, doxylamine	Rhabdomyolysis	[37]
Antihypertensive	Hydralazine, minoxidil	Prerenal azotemia	[40]
	Angiotensin-converting enzyme inhibitors, angiotensin II receptor blockers	Renal artery stenosis Volume depletion	[41]
Antimicrobials	Aminoglycosides	Hypomagnesemia Nonoliguric ATN Chronic tubulointerstitial nephritis Fanconi syndrome	[42]
	Vancomycin	Acute tubular necrosis Tubular damage	[43, 44]
	Ciprofloxacin	AIN Crystalluria	[45]
	Penicillin	Glomerulonephritis	[2]
	Cephalosporin	Acute interstitial nephritis	[2]
Antiplatelet	Ticlopidine, clopidogrel and quinine	Ahrombotic microangiopathy Renal vascular injury	[46]
Antiretroviral agents	Cidofovir, adefovir	Proximal tubule damage	[47]
	Tenofovir	ATN Proximal tubulopathy	[48, 49]
	Indinavir	Tubular crystallization Nephrolithiasis	[47]
	Atazanavir	AIN	[50]
Antiviral	Valaciclovir	Thrombotic microangiopathy Renal vascular injury	[51]
	Acyclovir	Tubular crystallization	[52]
	Foscarnet	Crystal deposition Electrolyte abnormalities	[53]
Bisphosphonates	Bisphosphonate zoledronate	Deranged Na^+K^+-ATPase Loss of brush border Apoptosis	[54]
Calcineurin inhibitor	Tacrolimus	Tubular vacuolization	[55]

Therapeutic Class	Drugs	Toxic events	References
	Cyclosporin	Renal vasoconstriction Tubular atrophy	
Chemotherapeutic agent	Cisplatin	Proximal tubular necrosis Tubular cell deletion	[56]
	Nedaplatin	Lysosomal hyperplasia Necrosis and hyperplasia of renal papilla and collecting duct	[57]
	Mitomycin C	Thrombotic microangiopathy Renal vascular injury	[58]
	Ifosfamide	Proximal tubular dysfunction Fanconi-like syndrome	[59]
	Methotrexate (MTX)	Tubular cristallization ATN	[60]
	Pemetrexed	ATN Nephrogenic diabetes insipidus (NDI) RTA	[61]
Contraceptive	Estrogen containing	Hemolytic uremic syndrome	[16]
Diuretics	Thiazides, loop, Potassium-sparing	Prerenal azotemia	[2]
Immunomodulatory	Intravenous Immunoglobulin (IVIG)	Osmotic nephrosis	[62]
Immunosuppressive	Ciclosporin	Decreased glomerulus filtration rate	[63]
	Ciclosporin, tacrolimus and muromonab-CD3	Thrombotic microangiopathy Renal vascular injury	[64]
Narcotic analgesic	Cocaine, heroin, methadone	Rhabdomyolysis	[65, 66]
Non-narcotic analgesic	Aspirin, acetaminophen	Chronic Interstitial nephritis	[67]
	Nonsteroidal anti-inflammatory drugs	Glomerulonephritis Acute interstitial nephritis Chronic interstitial nephritis Prerenal azotemia Acute papillary necrosis Membranous nephropathy	[2, 68]
Osmotic agents	Mannitol, dextran	Isometric vacuolization Swelling of proximal tubule	[16]
Thrombolytic agents	Streptokinase and tissue-plasminogen activator	Renal tissue ischemia Necrosis Infarction	[69]

It can also be a complication of lithium, although less well known than its tubulotoxic effects. Another inflammatory condition, acute interstitial nephritis (AIN), occurs as adverse reaction to several drugs that are assumed to induce an immune response by binding to the antigens in the kidney. Medications such as antimicrobials, phenytoin, proton pump inhibitors, allopurinol, lithium and antivirals have been implicated in this condition [70].

2.6. Crystal Nephropathy

Various drugs and their derivatives may lead to precipitation of crystals within the distal tubular lumen because of their insolubility in urine, thereby restricting urine flow and triggering a cellular reaction in the interstitium. Renal insufficiency and intravascular volume depletion increase the risk of crystal nephropathy. Concentration of the drug in the urine and urinary pH may influence the precipitation of crystals and volume repletion and adjustment of urinary pH, improving solubility, may be of benefit. Medications associated with crystal nephropathy include antivirals and antimicrobials as mentioned in **Table 1** [71].

2.7. Patient-Specific Risk Factors

Some patients are more susceptible to develop drug-induced nephrotoxicity. Volume depletion increases the risk by changing the drug concentration to a toxic level. Hypoalbuminemia, commonly observed in cirrhotic patients, increases the risk of unwanted drug overdose by elevating the serum concentration of the unbound drug fractions [72]. Both elderly and neonates possess a particular risk for drug-induced nephrotoxicity. Comorbid conditions and administration of multiple nephrotoxic drugs carry a significant burden to elderly patients, while premature delivery predisposes neonates to develop kidney function impairment [73]. In addition, individual genetic makeup, responsible for variable metabolic pathways and related drug sensitivity, can also influence the vulnerability of kidneys to nephrotoxicants. Polymorphisms in genes encoding enzymes that are involved in drugs' metabolism and elimination processes may increase the risk of nephrotoxicity. For instance, polymorphism of cytosolic glutathione-S-transferase (GST) enzyme elevates the risk for cisplatin-induced nephrotoxicity since this enzyme can, to a certain extent, detoxify reactive molecules [74]. A systematic review on inter-individual differences in cisplatin-induced nephrotoxicity has recently pointed towards three genes (*SLC22A2*, and two DNA repair genes) that determine sensitivity, suggesting patient specific dose optimization can be applied according to the genetic makeup. This approach could possibly reduce cisplatin toxicity [75].

2.8. Kidney Failure Due to Remote Organ Damage

Several risk factors such as genetics, obesity, diabetes, cardiovascular disease, and age can increase the chances of an individual to develop kidney disease, or when already diagnosed it can gradually drive the progression of the disease [76]. It is important to note that renal dysfunction can also be affected by the performance of distinct organs, such as the heart, lung and liver. As the kidneys receive ~25% of the cardiac output, a condition known as cardiorenal syndrome (CRS) can manifest when either the heart or the kidneys fail [77]. Considering that some segments of the nephron are highly sensitive to oxygen variations, if the lung is injured it can cause severe hypoxemia which in time can reduce renal blood flow, contributing to renal impairment as well [78]. Patients suffering from cirrhosis can develop hepatorenal syndrome (HRS), which can lead to damage and degeneration of the kidney. If the hepatic metabolism is compromised, a downregulation of cytochrome P450 (CYP) enzymes activity can lead to an accumulation of nephrotoxic drugs in the systemic circulation, resulting in kidney injury [79].

3. Biomarkers for Drug-Induced Kidney Injury

Creatinine and urea have long been considered as the “gold standard” to identify drug-induced nephrotoxicity and to detect renal dysfunction. However, various limitations of these two biomarkers, including low sensitivity and specificity, delayed rise in plasma because of functional reserve, and extrarenal clearance, demand for novel renal biomarkers to early detect and monitor drug-induced nephrotoxicity with high specificity and sensitivity. To address this, new potential markers are continuously being developed and qualified, resulting in a substantial increase of biomarker research [80]. Until now several biomarkers have been identified, as enlisted in **Table 2**. A biomarker qualification data submission released by the Predictive Safety Testing Consortium (PSTC) in 2009 included urinary kidney injury molecule-1 (KIM-1), urinary trefoil factor 3 (TFF-3), urinary beta-2 microglobulin (B2M), urinary cystatin C (CysC), urinary albumin (uALB), urinary total protein (uTP) and urinary clusterin (CLU) as emerging biomarkers to study xenobiotic-induced kidney injury in rat [81].

Table *2*. Overview of renal toxicity biomarker.

Nephron	Biomarker	Species	Indicator	Limitation	Biomarker type	References
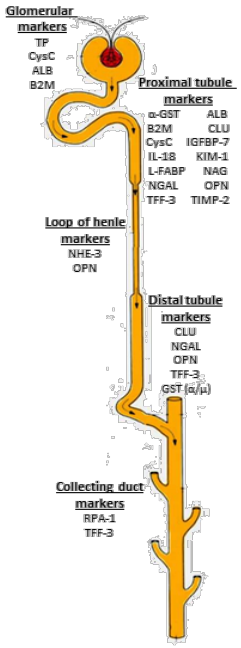	Kidney Injury molecule-1 (KIM-1)	Humans, rats, and mice	Proximal tubular damage	Not suitable as early marker and not specific	Injury	[82-84]
	Trefoil factor 3 (TFF3)		Humans and rats		Functional	[85, 86]
	N-acetyl-β-D-glucosamininidase (NAG)	Humans and rats	Proximal tubular damage	Inhibited by endogenous urea, no specificity	Leakage and functional	[82, 83]
	α-Glutathione S-Transferase (α-GST)	Humans and rats	Proximal tubular damage		Leakage	[87, 88]
	ɣ-Glutamyl Transferase (GGT)	Humans and rats	Proximal tubular damage			[82, 89]
	alkaline phosphatase (ALP)	Humans and rats	Proximal tubular damage			[85, 89]
	Clusterin (CLU)	Humans, rats, and dogs	Proximal tubular damage	Clinical data is not extensively available	Injury	[90]
	IL-18	Humans and mice	Proximal tubular damage	Not specific and lower sensitivity	Injury	[72]
	Insulin-like Growth factor-Binding Protein 7 (IGFBP-7)	Humans	Proximal tubular damage	Less accuracy	Injury	[91]
	Tissue Inhibitor of Metalloproteinases-2 (TIMP-2)	Humans	Proximal tubular damage	Less accuracy	Injury	[91]
	Heme oxygenase-1 (HO-1)	Humans and mice	Proximal tubular damage		Injury	[92]

Na^+/H^+ exchanger isoform 3 protein (NHE-3)	Humans	Proximal tubular damage		Injury	[93]
Albumin (ALB or uALB)	Humans and rats	Proximal tubular and glomerular dysfunction		Functional	[83]
Retinol Binding Protein (RBP)	Humans	Proximal tubular and glomerular dysfunction	Less specificity and limited detection	Functional	[83]
β2-Microglobulin (B2M)	Humans and rodents	Proximal tubular damage and glomerular damage	Less specificity and instability at acidic pH in urine	Functional	[85]
Serum creatinine (SCr)	Humans and rats	Change in GFR	Poor sensitivity and specificity and poor accuracy	Functional	[89]
Matrix metalloproteinase 9 (MMP-9)	Humans	Glomerular injury	Less sensitive for case-control study	Injury	[94]
Cysteine-rich 6 (Cyr61)	Humans	Glomerular injury	Disappear quickly in urine	injury	[95]
π-Glutathione S-Transferase (π-GST)	Humans and rats	Distal tubular damage			[89]
Urinary total protein (TP or uTP)	Humans and rats	Glomerular and tubular dysfunction		Functional	[80, 83]
Serum cystatin C (serum Cys C)	Humans and rats	Change in GFR and tubular dysfunction	Unreliable marker of GFR when proteinuria is present	Functional	[96]
Neutrophil Gelatinase-Associated Lipocalin (NGAL)	Humans, mice and rats	Proximal tubular damage and distal tubular damage	Affected by interference factors	Injury	[97]

Liver type- Fatty Acid Binding Protein (L-FABP)	Humans	Proximal tubular damage and distal tubular damage.	Not well established for contrast induced AKI	Functional	[98, 99]
Renal papillary antigen-1 (RPA-1)	Rats	Papillary necrosis			[100]
Osteoactivin	Humans and rodents	Tubular damage		Injury	[101]
Osteopontin (OPN)	Humans and rats	Tubular damage		Injury	[102]
Midkine (MK)	Humans	Tubular damage			[103]
miRNA	Humans and rats	Vascular damage		Injury	[104]
Netrin-1	Humans and mice	Early renal damage		Functional	[105]
Fetuin-A	Humans and mice	Autosomal dominant polycystic kidney disease (ADPKD)	Limited clinical application	Functional	[106]
Monocyte chemotactic protein 1 (MCP-1)	Humans	Ischemia–reperfusion injury (IRI), schistosomal nephropathy		Injury	[107, 108]

Later in 2014, with the support of Food and Drug Administration (FDA) and European Medicines Agency (EMA), the PSTC included neutrophil gelatinase-associated lipocalin (NGAL) and osteopontin (OPN) for further evaluation as emerging biomarkers [81].

KIM-1, a sensitive and specific damage marker of proximal tubule epithelial cells, can cleave and move into the tubule lumens upon diverse primary and secondary renal damages. It is found up-regulated in CKD with renal fibrosis and is significantly elevated in early stages of AKI. It is considered an early marker for detection, progression and outcome of kidney diseases. However, increased KIM-1 may also play role in renal tubular epithelial cells regeneration after acute injury [80, 109]. One of the least studied, biologically qualified urinary markers is TFF3, which is reduced significantly in a time- and dose-dependent manner following proximal tubular damage. This small peptide hormone is also found to correlate with the severity of kidney lesions and is considered as a sensitive marker for AKI [110]. B2M is a low molecular weight protein filtered completely and reabsorbed almost completely by the proximal tubule. Therefore, a significant increase of B2M is observed in urine following a minor impairment in tubular uptake. Thus, urine B2M is considered as a potential indicator of impaired function during drug-induced nephrotoxicity. In addition, glomerular injury can also elevate urinary excretion of B2M and it has therefore been qualified as glomerular injury marker as well in rodents [111]. Contrary to the conventional renal function biomarkers, CysC exhibits high sensitivity and specificity in monitoring acute and chronic renal impairments. Determination of CysC levels can be used to diagnose early-stages of renal dysfunction and to monitor functional alterations over time. This biomarker is considered a better diagnostic tool for preclinical renal disease and is found to be a more accurate detector of early-stage diabetic nephropathy [112]. Its plasma level is used as glomerular marker for GFR and the urine level as functional marker of proximal tubule since it is a low molecular weight protein that needs to be reabsorbed by megalin. Urinary albumin (uALB) has been considered a well-established diagnostic and prognostic marker to study the extent of glomerular injury in CKD. Because of its specificity to intrinsic causes such as rhabdomyolysis and ischemia-reperfusion, it remains unchanged in prerenal and postrenal events of AKI [113].

Another early marker of renal damage is urinary clusterin (CLU), which is a heterodimeric glycoprotein that contributes to cellular interaction, lipid transport and initiation of apoptosis during renal damage. Like KIM-1, expression of CLU is significantly elevated in dedifferentiated tubular cells during AKI but also in polycystic kidney disease, nephrectomy and renal cell carcinoma [114]. This marker has been found as a promising indicator of tubulointerstitial renal lesions and able to predict end-stage kidney disease (ESKD) [90], and also helps in triaging of patients with delayed graft function in less than 4 hours after

transplantation [115]. A lysosomal enzyme of proximal tubule, N-acetyl-β-glucosaminidase (NAG), is a persistent, sensitive, quantitative and robust biomarker of proximal tubular injury. It has been found elevated following kidney diseases such as AKI, diabetic nephropathy and chronic glomerular diseases [82]. Some other enzymes such as GST, γ-glutamyltransferase (GGT) and alkaline phosphatase (ALP), released from proximal and distal tubule cells into urine relate to early damage. In AKIs, two subtypes of GST, α and π, are released from proximal and distal tubule respectively allowing distinguishing between the two segments when affected [87]. As GGT and ALP increase during damage in the brush border, elevated levels of these enzymes were associated with complicated pyelonephritis and renal impairment [116].

4. Models for Nephrotoxicity Screening

4.1. Conventional In Vitro Models

Until recently, researchers were left with only two options: *in vitro* cultures of primary human cells or the use of animal models, both having limitations. Primary cells are used as they mimic the physiological state of cells *in vivo* most closely; however, these cells have a limited growth capacity and tend to lose their phenotype over time (**Table 3**). Despite these limitations, primary renal cells still remain a reliable option to study basic renal cellular functions and the effects of nephrotoxicants thereon. To overcome the difficulty in culturing primary cells, immortalized cells can be used because of their capacity to grow and divide indefinitely. The disadvantages of these cells include the immortalization procedure that by itself may result in some changes that, overtime, can alter the functions and characteristics of cells [117]. Animal models are used as they can fill the gap that *in vitro* models often have, *viz.* the lack of physiological resemblance. However, the use of animal models is expensive, requires a lot of time and expertise, has low throughput potential, poses ethical issues, but most importantly, these models often do not correlate to human systems [118].

Being the proximal tubule a major target for many nephrotoxicants, it is logical that cell-based *in vitro* models that seek to resemble this segment of the nephron should be characterized by the expression of important markers, including *SLC22A6* (OAT1), *SLC22A8* (OAT3), *SLC22A2* (OCT2) on the basolateral membrane and *ABCB1* (P-gp), *SLC47A1* (MATE1), *SLC47A2* (MATE2), *ABCC2* (MRP2), *ABCC4* (MRP4), *ABCG2* (BCRP) and the endocytosis receptors megalin and cubilin on the apical membrane [117] (**Figure 2**). Although often applied, the immortalized HK-2 cell line lacks the expression of OAT1, OAT3, OCT2, MRP2, and BCRP, and may be not a representative model to study nephrotoxicity [119].

Two important immortalized cell lines have been extensively used for nephrotoxicity

screening: RPTEC/TERT1 and ciPTEC. The RPTEC/TERT1 cell line was immortalized using the human telomerase reverse transcriptase (hTERT) [120] whereas ciPTEC lines, obtained either from urine or kidney tissue were transfected using hTERT and a temperature-sensitive mutant of SV large T antigen (SV40T), allowing these cells to proliferate at 33 ºC and mature at 37 ºC [121, 122] (**Table 3**). These cell lines surpass HK-2 cells by expressing all relevant markers cited above; however, OAT function was only attained after lentiviral transduction [123]. Using the same immortalization procedure in the ciPTEC line, a podocyte cell line (CIHP) was generated. As these cells maintain the filtration barrier of the glomeruli, it is expected that they will also be targets of nephrotoxicants that can ultimately lead to nephrotic syndrome, although no data is as of yet available on drug effects in this cell line [124].

Toxicity assays mainly focus on measuring cell death; however renal toxicity can also be manifested by changes in cell polarity, membrane integrity, and mitochondrial function. With this in mind, Sjögren *et al.* developed a machine learning model that allowed screening of 62 drugs in which ciPTEC-OAT1 cell line was used to predict their nephrotoxicity based on multiple parameters [125]. Similarly, Secker *et al.* made use of the RPTEC/TERT1 cell line to evaluate transepithelial transports in a small set of known nephrotoxic and non-nephrotoxic drugs demonstrating that further evaluation of functional parameters, including transepithelial electrical resistance (TEER), reabsorption and secretion of solutes is essential to understand the nephrotoxicity mechanisms of drugs and predict the *in vivo* implication in regard to kidney performance [126].

4.2. Advanced In Vitro Models

To bypass the limitations of 2D cultures, advanced *in vitro* culture systems have been developed, including the use of 3D organized structures, known as organoids, and kidney microphysiological systems (MPS) that can recreate fluidic characteristics found *in vivo* (**Figure 4**). Organoids can be cultured from different sources of stem cells, including embryonic stem cells (ESC), induced pluripotent stem cells (iPSC), and adult stem cells. Due to ethical concerns regarding the culture of embryonic stem cells, iPSCs and adult stem cells are preferred. Using human iPSC cells (**Table 3**), it was possible to generate kidney organoids that contained cell types from different nephron segments; however, the generated cells are not fully mature [127]. To overcome this problem, Chuva *et al.* developed a 2-step protocol in which kidney organoids were transplanted into a chick chorioallantoic membrane to provide a vascularized environment that is necessary for the further maturation of the organoids [128]. Examples of other 3D culture systems include RPTEC/TERT1 and Nki-2 cells that, when cultured in Matrigel or Matrigel mixed with collagen I, respectively, were able to further mature

and form tubular structures as seen *in vivo*. Both models showed increased sensitivity to known nephrotoxic drugs when compared to 2D cultures [129, 130].

Table *3. In vitro* models for toxicity screening.

	Species	Characteristics	Pros	Cons	References
Primary					
RPTEC	Human	**Morphology** Cuboidal with a characteristic pattern of swirled cells; **Markers** Complete expression of transporters and metabolic enzymes **Function** Active transepithelial transport function Polarized tight monolayer formation	Preserve genetic and phenotypic aspects of the tissue of origin Easy to isolate Compatible with high-throughput screening and advanced imaging techniques	Cell sourcing problems Inter-donor variability Functional changes during passages Low lifespan Low predictivity	[132, 134]
HRMC (mesangium)	Human	**Markers** Fibronectin, Thy-1, smooth muscle actin Study IgA Nephropathy			[134, 135]
HRCEpiC (renal cortical)	Human	**Markers** Cytokeratin 18,19, vimentin **Function** Production of IL-8 Inflammation (IL-2Ra and MHC II)			[136, 137]
aProximate™	Human, Rat, Mouse	**Morphology** RPTEC **Makers** MDR1, MRP2/4, BCRP, OCTN1/2, OAT1/2/3/4, OCT2/3, OATP4C1 **Function** Net secretion of substrates Calcein efflux via MRP2 BCRP and MDR1 activity (Hoechst 33342 dye)			[119, 138]
Kidney Slices	Human, Rat, Mice, Dog	Retain the multicellular, structural, and functional features		Damage from cutting Heterogenous population	[139-141]
Isolated Perfused Kidney	Rat, Mouse	Tubulovascular integrity		Short lifespan Lower levels of filtration rate and ion reabsorption Not suitable for routine studies	[142]

Primary					
Isolated Perfused Nephrons	Rat, Rabbit	Knowledge on location of enzyme systems, metabolic pathways, and distribution of receptors		Not suitable for routine studies	[143]
Immortalized Cell Lines					
RPTEC/TERT1	Human	**Morphology** Functional tight junctions, dome formation, microvilli and primary cilium **Markers** Aminopeptidase-N, E-cadherin, MRP2, MRP4, OAT4, MDR1, MATE1, OCTN2, OCT3 **Function** Response to PTH treatment by increased cAMP levels; Gamma glutamyl-transferase activity; Megalin/cubilin transport system		Absence of OAT1 and OAT3 anion importers	[121, 144-146]
ciPTEC	Human	**Morphology** Formation of tight juntions, **Markers** Aminopeptidase N, Pgp, AQP1, dpp-IV, MRP2/4, OCT2, OAT1, OAT3, BCRP, MATE1/2, CaSR, Megalin/Cubilin receptors **Function** ALP activity, Albumin endocytosis, sodium-dependent phosphate uptake, OCT2 and P-gp activity, UGT activity	Enhanced proliferative capacity Differences in morphology and function Possible inclusion of ECM Compatible with high-throughput screening and advanced imaging techniques Cost-effective	Absence of SGLT2	[121-123]
HK-2	Human	**Morphology** Cuboidal morphology, contact inhibition, dome formation, and microvilli **Markers** Vimentin, cytokeratin, α3β1 integrin, leucine aminopeptidase, fibronectin, MCT1, MDR1, OATP4C1 **Function** Gluconeogenesis, and Na^+-dependent glucose uptake; GGT and alkaline phosphatase activity; Increased cAMP levels in response to PTH; Synthesis and secretion of plasma proteins		Does not represent a good model for the study of key renal uptake transporters Low predictivity	[129, 147-149]

Immortalized Cell Lines					
Nki-2	Human	Epithelial and proximal tubule phenotype **Markers** E-Cadherin, CK8/18/19, GGT1, OAT1, OAT4 **Function** Production of cAMP in response to PTH, ADH GGT and LAP activity Absorption of glucose in the presence of NaCl		Limited data available	[129]
CIHP-1	Human	**Morphology** Foot processes, and slit-diafragm-like structures **Markers** Synaptopodin, nestin, CD2AP, nephrin, podocin, WT1, podocalyxin, P-Cadherin, α, β,γ-catenin		Limited data available	[124]
Stem cell-derived					
ESC/iPSC	Human	**Markers** N-Cadherin, KSP-CAD, AQP1/2/3, Megalin/Cubilin, GLUT1, OCT2, MDR1, GGT, OAT1/3, PODXL, UMOD **Function** Citrin uptake by OAT1/3 (inhibited by probenecid)	Easy to isolate (iPSC) Possible inclusion of ECM Study molecular mechanisms of diseases Enables personalized medicine	Ethical issues (ESC) Low sensitivity Extensive protocol	[150-153]
Organoids	Human	**Markers** PODXL, WT1, LTL, E-Cadherin, UMOD, SIX2, PAX2, JAG1 **Function** Transport of fluorescent compounds (lucifer yellow, rhodamine-conjugated dextran, fluorescein methotrexate)	Inclusion of ECM Heterogenous population Epithelial cell polarization Enables personalized medicine	Heterogenous population Difficult access to apical compartment Batch-to-batch variability of matrigel	[127, 154, 155]
Others					
Kidney-on-a-chip	Human	Resemble kidney proximal tubules (Tubular conformation and active transepithelial transport)	Increased physiological relevance (3D structures, ECM, multiple compartments) Exposure to fluid flow and sheer stress Suitable for studying transepithelial transport	Prototype Require external tube and pump connection Made of materials that absorb hydrophobic compounds Not suitable for routine studies	[156-160]

Others					
Bioartificial Kidney Tubules	Human	**Morphology and Markers** ciPTEC **Function** Polarized secretion of immune modulators (upon LPS stimulation) Transport of organic anions and cations Reabsorption of albumin Diffusion of FITC-Inulin	Inclusion of ECM Epithelial cell polarization Suitable for studying transepithelial transport Exposure to fluid flow and sheer stress	Only basolateral perfusion Low high throughput Not suitable for routine studies	[161-163]
Decellularized Kidney	Rat	**Recellularization** ciPTEC **Markers** ZO-1, AQP1, CLDN-2, OCT2, MATE-1, MATE-2K, OAT1, MRP4, P-gp, BCRP, GLUT1, OATP4C1 **Function** OCT2 activity (ASP^+)	Native scaffold Improved cell function	Homogenous cell population No fluid shear stress included	[164]

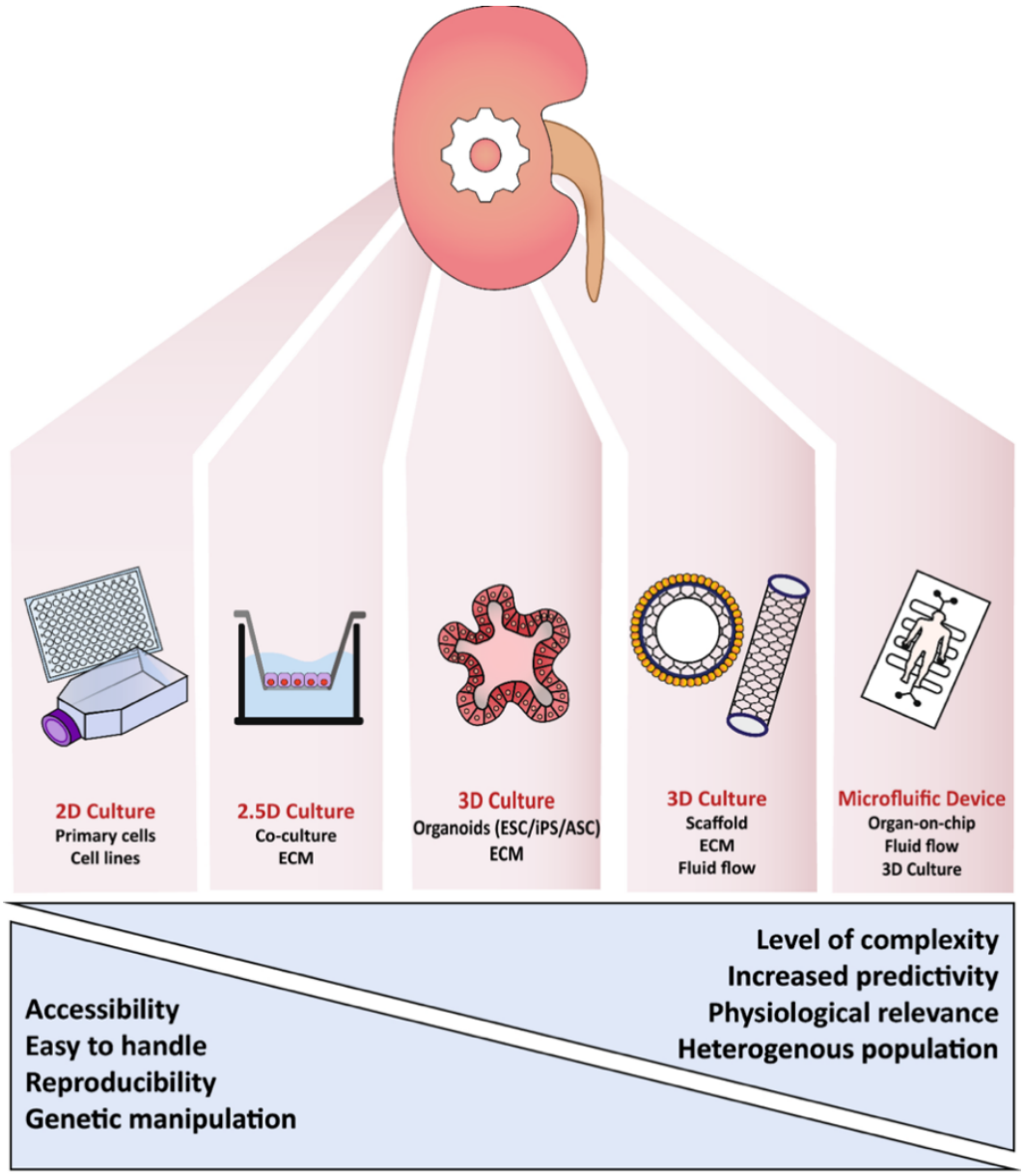

Figure 4. Schematic figure of the different *in vitro* models developed for use in nephrotoxicity screenings.

In line with these 3D culture systems, a bioengineered kidney tubule was developed that mimics the physiological geometry of the nephron segment. Briefly, ciPTEC-OAT1 cells were seeded onto polyethersulfone (PES) hollow fiber membranes (HFM; **Table 3**), previously double-coated with 3,4-dihydroxyl-L-phenylalanine (L-DOPA) and collagen IV. Using this system, the excretion of protein-bound uremic toxins and reabsorption of albumin were shown under perfusion conditions, thus mimicking the *in vivo* situation [161, 162], and allowing revealing a remote sensing and signaling pathway to balance microbial metabolite levels in the human body [165]. Further, attenuation of uremic toxin-induced damage by vitamin D

activated by the bioengineered kidney tubules was demonstrated [166]. The use of decellularized kidneys (**Table 3**) can also be a suitable platform for studying drug-induced nephrotoxicity. Fedecostante *et al.* decellularized surplus rat kidneys using sodium dodecyl sulfate (SDS) and recellularized these with ciPTEC-OAT1. An increased sensitivity to cisplatin, tenofovir and cyclosporin A was shown for this model as compared to the 2D system [167].

For further improvement of these *in vitro* models, implementation of fluid flow and vasculature is crucial, not only to increase maturation of the kidney cells but also to provide an environment that more closely resembles the *in vivo* situation. Flow in tubular lumens varies between 0.2-2.0 dyne/cm² [168] and triggers mechanosensitive pathways via microvilli, primary cilia and the glycocalyx, all expressed at the tubular apical membrane [169]. Advances in microelectromechanical systems (MEMs) allowed researchers to apply microfluidics in cell and tissue cultures that resulted in the so-called organ-on-a-chip (**Table 3**). Vriend *et al.* demonstrated that culturing ciPTEC-OAT1 in an OrganoPlate, a 3D platform consisting of 96 chips that provides fluid shear stress by placing the plate on a rocker platform, it was possible to create a high-throughput screening method compatible with advanced imaging techniques [170]. Following a similar approach, Schutgens *et al.* developed a new microfluidic *in vitro* system using kidney tubular epithelial organoids, or "tubuloids", derived from adult stem cells. The generated tubuloids showed active transepithelial transport function and were used to model several diseases, including BK virus, Wilms tumor, and cystic fibrosis, showing the great potential of this culture system for disease modeling and the possibility to use it for drug screening [160].

A lack of vascularization could potentially be overcome by the use of a 3D-print chip that combines hPSC-derived kidney organoids co-cultured with glomerular microvascular endothelial cells (GMECs) in a gelatin-fibrin ECM, as recently reported [171, 172]. The researchers showed an improved maturation of the kidney organoids when cultured under flow and in the presence of vascularization. Later, the same microfluidic platform was used to study active reabsorption of solutes between proximal tubule epithelial cells and vascular epithelium, and for the study of hyperglycemic conditions.

As mentioned before, the kidney also interacts with and reacts on remote organs. The liver and the kidney are two very complex organs that together lead to the metabolism and excretion of drugs, respectively. To predict biotransformation (liver) and elimination (kidney) in humans is a rather difficult task to achieve using normal 2D cultures [173]; however, the combination of these two complex organs in an organ-on-a-chip platform made it possible to study the toxic effects of aristolochic acid I, a well-known nephrotoxicant that requires first hepatic bioactivation [174]. **Table 3** summarizes the different *in vitro* models discussed to

study drug-induced nephrotoxicity. Together, the findings suggest that the development and use of advanced *in vitro* kidney models are important improvements in renal drug safety assessment.

4.3. Perspectives in In Vitro Models' Development

Renal clearance is an important route of drug elimination from the bloodstream, mainly facilitated by the proximal tubule, which renders proximal tubule epithelial cells prone to drug-induced kidney injury. Mimicking the *in vivo* environment by including extracellular matrix (ECM) components, three-dimensional (3D) architectural features, a heterogeneous cellular composition and incorporating fluid shear stress in an *in vitro* kidney model could improve prediction of injury after drug exposures. These features need to be taken into consideration when trying to develop new *in vitro* models. The complex renal ECM, recently reviewed in [175], is in constant remodeling, especially in the transition of healthy to disease state, such as fibrosis. As fibrosis affect the different compartments of the kidney, a comprehensive analysis of the renal ECM is crucial to study the pathophysiology of the disease and its specific biomarkers [176]. As stated before, shear stress triggers mechanosensitive pathways via microvilli, cilia, and the glycocalyx. Understanding how these structures coordinate with each other in response to flow will broaden our knowledge and help identify new molecular targets of diseases [169]. Combining these features in a 3D model that includes tubule curvature [177] will allow for a better cell polarization and enhanced expression of cell markers.

Currently, in pre-clinical safety assessment studies only a limited number of drug candidates (2-8%) are being rejected because of nephrotoxicity [178, 179]. A survey among pharmaceutical companies showed that the majority of drug candidates displaying nephrotoxicity in clinical trials did not show nephrotoxicity in pre-clinical trials [180]. It is thus apparent that the currently used strategies to predict drug-induced injury warrant strong improvements. Immortalized cell lines, like ciPTEC, represent a steady and reproducible cell source for *in vitro* models, but are derived from one single donor and show significant changes in cell function and morphology compared to primary cells [181]. Baseline levels of injury marker KIM-1 were 20-fold higher in immortalized cells compared to primary cells [182]. In addition, immortalized cell lines often show chromosomal instability, as demonstrated for ciPTEC-OAT1 without affecting cell function or posing a tumorigenic risk [183], and represent a homogenous population instead of a genetic diverse population. Therefore, new sources for kidney cells emerged in the past decade. Stem cell-derived tubular cells can be obtained from multiple donors and may have potential for studying nephrotoxicity in a heterogeneous population [184]. Well-defined protocols to establish kidney organoids of renal tubular

epithelial cells from induced pluripotent stem cells (iPSCs) derived from fibroblasts are now available [127, 155, 185-187]. In these cultures, typical proximal tubule cell characteristics have been demonstrated, such as albumin uptake, expression of tight junction proteins, expression of OAT1, microvilli and apical and basolateral membrane polarization. In addition, cytotoxicity was demonstrated using cisplatin [127, 155, 185-187], gentamicin [155, 186, 187], tacrolimus [187] and adriamycin [188]. As earlier stated, kidney tubuloids grown from adult stem cells (ASCs) are another promising approach as they allow for long-term culturing and better maturation without losing chromosomal stability [160].

To model kidney diseases, direct pathogen exposure and genome editing have been applied, depending on the cause of disease. Effects of Shiga toxin 2, a cytotoxic protein causing hemolytic-uremic syndrome (HUS), was studied in a 3D model of renal cortical epithelial cells [189]. And polycystic kidney disease was studied via CRISPR-Cas9 genome editing of PC-1 and -2 in iPSCs-derived kidney organoids [155, 185]. Personalized medicine allows for studying disease progression and testing treatment options in a tailor-made fashion via obtaining tissue from kidney disease patients. ASCs-derived tubuloids from Wilms tumors elucidated an important role for SIX2, a kidney development marker [160, 190]. Furthermore, tubuloids obtained via urine from a cystic fibrosis patients were used to assess treatment efficacy and circumvented the use of an invasive method to obtain patient material [160]. Furthermore, the dynamic process of kidney stone formation was studied in HK-2 cells cultured in a microfluidic device, which allowed real-time monitoring of calcium phosphate deposition in the lumen [191].

Improving predictability of *in vitro* models fits also in the scope of the 3Rs (replacement, reduction, refinement) of animal experiments. This could reduce costs of the pre-clinical and clinical phases of drug development by filtering out the harmful compounds. But, more importantly, it also meets the societal demands to reduce the number of animals in drug development. Drug regulatory authorities, such as FDA and EMA, support the use of physiologically-based pharmacokinetic (PBPK) modeling as a tool to facilitate the process of drug development. *In vitro* to *in vivo* extrapolation (IVIVE) can be coupled with PBPK modeling as a way to predict the *in vivo* pharmacokinetic characteristics of a new drug based on *in vitro* studies. *In vitro* studies can provide information regarding drug-enzyme and drug-transporter interactions; However, the full understanding of the absorption, distribution, metabolism, and excretion (ADME) processes is not feasible. By extrapolating complex scenarios observed *in vitro* while having in mind that intrinsic and extrinsic factors can alter the kinetic values, one can identify optimal dosing regimens for individual patients [192, 193].

5. CONCLUSIONS

Nephrotoxicity is associated with significant mortality and morbidity. Undoubtedly, drug-induced nephrotoxicity is a major cause of renal impairments and a potential impediment to the research and development of drugs, requiring more reliable and early diagnosis in order to avoid potentially fatal chronic conditions. To date, there is no ideal kidney-based *in vitro* model for the study of nephrotoxicity; however, we are moving towards more advanced *in vitro* culture systems that offer great promise for the assessment of drug toxicity. These new models include several characteristics that are important for the successful toxicologic read-out of drug candidates, including 3D architectural features, ECM components, fluid flow and multiple cell types combined. Despite the promising advances of these models, appropriate toxicity endpoints and sensitive translational biomarkers are yet to be identified. Current efforts remain as “bench-work” and do not reach the “bed-side”. Therefore, there is a pressing need to systematically combine *in vitro*, *in vivo* and clinical inspections to develop a panel of safety biomarkers that can effectively and reliably diagnose and monitor renal function, damage and recovery.

CONFLICT OF INTEREST

The authors declare no conflicts of interest with the contents of this article.

ACKNOWLEDGEMENTS

This study has received funding from the European Union’s Horizon 2020 research and innovation programme under the Marie Skłodowska-Curie grant agreement No 813839.

REFERENCES

1. E. Bello-Reuss and L. Reuss. Homeostatic and Excretory Functions of the Kidney. *The Kidney and Body Fluids in Health and Disease*. Boston, MA: Springer US; 1983, 35-63.

2. C. A. Naughton. Drug-induced nephrotoxicity. American family physician 2008;78:743-750

3. C. J. Lote. Essential Anatomy of the Kidney. *Principles of Renal Physiology*. New York, NY: Springer New York; 2012, 21-32.

4. B. M. Koeppen and B. A. Stanton. Renal physiology. 2013:240

5. M. J. Holechek. Glomerular filtration: an overview. Nephrology nursing journal : journal of the American Nephrology Nurses' Association 2003;30:285-290; quiz 291-282

6. M. L. Eshbach and O. A. Weisz. Receptor-Mediated Endocytosis in the Proximal Tubule. Annual Review of Physiology 2017;79(1):425-448

7. J. Feher. Tubular Reabsorption and Secretion. Quantitative Human Physiology 2017:719-729

8. M. R. Haussler, G. K. Whitfield, C. A. Haussler*, et al.* 1,25-Dihydroxyvitamin D and Klotho: A Tale of Two Renal Hormones Coming of Age. Vitamins & Hormones 2016;100:165-230

9. K. Shimamoto and O. Iimura. Physiological role of renal kallikrein-kinin system in human. Advances in experimental medicine and biology 1989;247A:87-96

10. R. Kumar, P. J. Tebben and J. R. Thompson. Vitamin D and the kidney. Archives of biochemistry and biophysics 2012;523:77-86

11. Y. H. Ohana, T. Liron, S. Prutchi-Sagiv*, et al.* Erythropoietin. Handbook of Biologically Active Peptides 2013:1619-1626

12. M. L. S. S. Lopez and R. A. Gomez. The renin phenotype: roles and regulation in the kidney. Current opinion in nephrology and hypertension 2010;19:366-371

13. J.-H. Kim, K.-H. Hwang, K.-S. Park*, et al.* Biological Role of Anti-aging Protein Klotho. Journal of lifestyle medicine 2015;5:1-6

14. M. Kakoki and O. Smithies. The kallikrein–kinin system in health and in diseases of the kidney. Kidney international 2009;75:1019

15. J. Małyszko, K. Kozłowska, L. Kozłowski*, et al.* Nephrotoxicity of anticancer treatment. Nephrology Dialysis Transplantation 2016;32(6):924-936

16. D. Choudhury and Z. Ahmed. Drug-associated renal dysfunction and injury. Nat Clin Pract Nephrol 2006;2(2):80-91

17. B. A. Vervaet, P. C. D'Haese and A. Verhulst. Environmental toxin-induced acute kidney injury. Clinical kidney journal 2017;10:747-758

18. K. Makris and L. Spanou. Acute Kidney Injury: Definition, Pathophysiology and Clinical Phenotypes. The Clinical Biochemist Reviews 2016;37:85

19. E. Macedo and R. L. Mehta. Prerenal Failure: From Old Concepts to New Paradigms. Current opinion in critical care 2009;15:467

20. G. Navis, H. J. Faber, D. de Zeeuw*, et al.* ACE Inhibitors and the Kidney. Drug Safety 1996;15:200-211

21. M. Dixit, T. Doan, R. Kirschner*, et al.* Significant Acute Kidney Injury Due to Non-steroidal Anti-inflammatory Drugs: Inpatient Setting. Pharmaceuticals (Basel, Switzerland) 2010;3:1279-1285

22. D. P. Basile, M. D. Anderson and T. A. Sutton. Pathophysiology of acute kidney injury. Comprehensive Physiology 2012;2:1303-1353

23. R. Kipp and P. S. Kellerman. Chronic Kidney Disease. Pathophysiology of Kidney Disease and Hypertension 2009:145-157

24. L. M. A. Barnett and B. S. Cummings. Nephrotoxicity and renal pathophysiology: A contemporary perspective. Toxicological Sciences 2018;164:379-390
25. A. Eirin, A. Lerman and L. O. Lerman. The Emerging Role of Mitochondrial Targeting in Kidney Disease. Handbook of experimental pharmacology 2017;240:229-250
26. Y. Liang, S. Li and L. Chen. The physiological role of drug transporters. Protein & Cell 2015;6:334
27. S. K. Nigam, W. Wu, K. T. Bush*, et al.* Handling of Drugs, Metabolites, and Uremic Toxins by Kidney Proximal Tubule Drug Transporters. Clinical Journal of the American Society of Nephrology 2015;10(11):2039-2049
28. S. K. Nigam. The SLC22 Transporter Family: A Paradigm for the Impact of Drug Transporters on Metabolic Pathways, Signaling, and Disease. Annual Review of Pharmacology and Toxicology 2018;58(1):663-687
29. K. M. Giacomini, S. M. Huang, D. J. Tweedie*, et al.* Membrane transporters in drug development. Nat.Rev.Drug Discov. 2010;9(3):215-236
30. M. W. Anders. Metabolism of drugs by the kidney. Kidney International 1980;18:636-647
31. W. A. Hitti and J. Anderson. Cholesterol emboli-induced renal failure and gastric ulcer after thrombolytic therapy. South Med J 2005;98(2):235-237
32. M. A. Perazella. Drug-induced nephropathy: an update. Expert Opin Drug Saf 2005;4(4):689-706
33. N. Lameire, W. Van Biesen and R. Vanholder. Acute renal failure. Lancet 2005;365(9457):417-430
34. K. S. Frazier and L. A. Obert. Drug-induced Glomerulonephritis: The Spectre of Biotherapeutic and Antisense Oligonucleotide Immune Activation in the Kidney. Toxicol Pathol 2018;46(8):904-917
35. S. V. Brodsky. Anticoagulants and acute kidney injury: clinical and pathology considerations. Kidney research and clinical practice 2014;33(4):174-180
36. F. Ghane Shahrbaf and F. Assadi. Drug-induced renal disorders. Journal of renal injury prevention 2015;4(3):57-60
37. T. J. Coco and A. E. Klasner. Drug-induced rhabdomyolysis. Curr Opin Pediatr 2004;16(2):206-210
38. A. N. Azab, A. Shnaider, Y. Osher*, et al.* Lithium nephrotoxicity. International journal of bipolar disorders 2015;3(1):28-28
39. G. Deray. Amphotericin B nephrotoxicity. J Antimicrob Chemother 2002;49 Suppl 1:37-41
40. P. Ejaz, K. Bhojani and V. R. Joshi. NSAIDs and kidney. J Assoc Physicians India 2004;52:632-640
41. B. F. Palmer. Renal dysfunction complicating the treatment of hypertension. N Engl J Med 2002;347(16):1256-1261
42. J. M. Lopez-Novoa, Y. Quiros, L. Vicente*, et al.* New insights into the mechanism of aminoglycoside nephrotoxicity: an integrative point of view. Kidney International 2011;79(1):33-45
43. N. L. Htike, J. Santoro, B. Gilbert*, et al.* Biopsy-proven vancomycin-associated interstitial nephritis and acute tubular necrosis. Clin Exp Nephrol 2012;16(2):320-324
44. Y. Liu, Y. Yin, X. Z. Liu*, et al.* Retrospective Analysis of Vancomycin Nephrotoxicity in Elderly Chinese Patients. Pharmacology 2015;95(5-6):279-284
45. S. T. Bird, M. Etminan, J. M. Brophy*, et al.* Risk of acute kidney injury associated with the use of fluoroquinolones. Cmaj 2013;185(10):E475-482
46. P. J. Medina, J. M. Sipols and J. N. George. Drug-associated thrombotic thrombocytopenic purpura-hemolytic uremic syndrome. Curr Opin Hematol 2001;8(5):286-293

47. R. Kalyesubula and M. A. Perazella. Nephrotoxicity of HAART. AIDS Res Treat 2011;2011:562790
48. B. Fernandez-Fernandez, A. Montoya-Ferrer, A. B. Sanz*, et al.* Tenofovir nephrotoxicity: 2011 update. AIDS research and treatment 2011;2011:354908-354908
49. A. Jafari, H. Khalili and S. Dashti-Khavidaki. Tenofovir-induced nephrotoxicity: incidence, mechanism, risk factors, prognosis and proposed agents for prevention. Eur J Clin Pharmacol 2014;70(9):1029-1040
50. M. Hara, A. Suganuma, N. Yanagisawa*, et al.* Atazanavir nephrotoxicity. Clinical kidney journal 2015;8(2):137-142
51. H. Izzedine, V. Launay-Vacher and G. Deray. Antiviral drug-induced nephrotoxicity. Am J Kidney Dis 2005;45(5):804-817
52. C. Yildiz, Y. Ozsurekci, S. Gucer*, et al.* Acute kidney injury due to acyclovir. CEN case reports 2013;2(1):38-40
53. V. Frochot, D. Bazin, E. Letavernier*, et al.* Nephrotoxicity induced by drugs: The case of foscarnet and atazanavir—A SEM and μFTIR investigation. Comptes Rendus Chimie 2016;19(11):1565-1572
54. G. S. Markowitz, P. L. Fine, J. I. Stack*, et al.* Toxic acute tubular necrosis following treatment with zoledronate (Zometa). Kidney Int 2003;64(1):281-289
55. M. Naesens, D. R. J. Kuypers and M. Sarwal. Calcineurin Inhibitor Nephrotoxicity. Clinical Journal of the American Society of Nephrology 2009;4(2)
56. R. P. Miller, R. K. Tadagavadi, G. Ramesh*, et al.* Mechanisms of Cisplatin nephrotoxicity. Toxins 2010;2(11):2490-2518
57. T. Uehara, J. Yamate, M. Torii*, et al.* Comparative nephrotoxicity of Cisplatin and nedaplatin: mechanisms and histopathological characteristics. Journal of toxicologic pathology 2011;24(2):87-94
58. N. Lameire. Nephrotoxicity of recent anti-cancer agents. Clinical kidney journal 2014;7(1):11-22
59. I. Nissim, O. Horyn, Y. Daikhin*, et al.* Ifosfamide-induced nephrotoxicity: mechanism and prevention. Cancer Res 2006;66(15):7824-7831
60. B. C. Widemann and P. C. Adamson. Understanding and managing methotrexate nephrotoxicity. Oncologist 2006;11(6):694-703
61. Y. Zajjari, M. Azizi, Y. Sbitti*, et al.* Nephrotoxicity in a Patient Treated with Pemetrexed. Indian journal of nephrology 2017;27(3):243-244
62. J. B. Levy and C. D. Pusey. Nephrotoxicity of intravenous immunoglobulin. Qjm 2000;93(11):751-755
63. A. Busauschina, P. Schnuelle and F. J. van der Woude. Cyclosporine nephrotoxicity. Transplant Proc 2004;36(2 Suppl):229s-233s
64. A. J. Olyaei, A. M. de Mattos and W. M. Bennett. Nephrotoxicity of immunosuppressive drugs: new insight and preventive strategies. Curr Opin Crit Care 2001;7(6):384-389
65. S. Alinejad, K. Ghaemi, M. Abdollahi*, et al.* Nephrotoxicity of methadone: a systematic review. SpringerPlus 2016;5(1):2087-2087
66. B. McCann, R. Hunter and J. McCann. Cocaine/heroin induced rhabdomyolysis and ventricular fibrillation. Emergency Medicine Journal 2002;19(3):264
67. K. Sampathkumar, A. Rajiv and D. Sampathkumar. Analgesic Nephropathy—A Painful Progression. 2016;9:CMU.S13179
68. G. N. C. Lucas, A. C. C. Leitão, R. L. Alencar*, et al.* Pathophysiological aspects of nephropathy caused by non-steroidal anti-inflammatory drugs %J Brazilian Journal of Nephrology. 2019;41:124-130

69. A. A. Eddy and A. B. Fogo. Plasminogen Activator Inhibitor-1 in Chronic Kidney Disease: Evidence and Mechanisms of Action. 2006;17(11):2999-3012
70. J. Rossert. Drug-induced acute interstitial nephritis. Kidney Int 2001;60(2):804-817
71. G. S. Markowitz and M. A. Perazella. Drug-induced renal failure: a focus on tubulointerstitial disease. Clin Chim Acta 2005;351(1-2):31-47
72. G. S. Pazhayattil and A. C. Shirali. Drug-induced impairment of renal function. International journal of nephrology and renovascular disease 2014;7:457-468
73. L. Patzer. Nephrotoxicity as a cause of acute kidney injury in children. Pediatric Nephrology 2008;23(12):2159-2173
74. W. P. Petros, P. J. Hopkins, S. Spruill*, et al.* Associations between drug metabolism genotype, chemotherapy pharmacokinetics, and overall survival in patients with breast cancer. J Clin Oncol 2005;23(25):6117-6125
75. Z. Zazuli, L. S. Otten, B. I. Drögemöller*, et al.* Outcome Definition Influences the Relationship Between Genetic Polymorphisms of ERCC1, ERCC2, SLC22A2 and Cisplatin Nephrotoxicity in Adult Testicular Cancer Patients. Genes 2019;10(5):364
76. R. Kazancioğlu. Risk factors for chronic kidney disease: an update. Kidney International Supplements 2013;3:368
77. C. Ronco, M. Cicoira and P. A. McCullough. Cardiorenal Syndrome Type 1: Pathophysiological Crosstalk Leading to Combined Heart and Kidney Dysfunction in the Setting of Acutely Decompensated Heart Failure. Journal of the American College of Cardiology 2012;60:1031-1042
78. R. K. Basu and D. S. Wheeler. Kidney-lung cross-talk and acute kidney injury. Pediatric nephrology (Berlin, Germany) 2013;28:2239-2248
79. K. Lane, J. J. Dixon, I. A. M. Macphee*, et al.* Renohepatic crosstalk: does acute kidney injury cause liver dysfunction? Nephrol Dial Transplant 2013;28:1634-1647
80. H. G. Xie, S. K. Wang, C. C. Cao*, et al.* Qualified kidney biomarkers and their potential significance in drug safety evaluation and prediction. Pharmacol Ther 2013;137(1):100-107
81. F. Dieterle, F. Sistare, F. Goodsaid*, et al.* Renal biomarker qualification submission: a dialog between the FDA-EMEA and Predictive Safety Testing Consortium. Nat Biotechnol 2010;28(5):455-462
82. V. S. Vaidya, M. A. Ferguson and J. V. Bonventre. Biomarkers of acute kidney injury. Annual review of pharmacology and toxicology 2008;48:463-493
83. K. Vlasakova, Z. Erdos, S. P. Troth*, et al.* Evaluation of the relative performance of 12 urinary biomarkers for renal safety across 22 rat sensitivity and specificity studies. Toxicol Sci 2014;138(1):3-20
84. V. S. Vaidya, S. S. Waikar, M. A. Ferguson*, et al.* Urinary biomarkers for sensitive and specific detection of acute kidney injury in humans. Clin Transl Sci 2008;1(3):200-208
85. A. B. Chapman, O. Devuyst, K.-U. Eckardt*, et al.* Autosomal-dominant polycystic kidney disease (ADPKD): executive summary from a Kidney Disease: Improving Global Outcomes (KDIGO) Controversies Conference. Kidney international 2015;88(1):17-27
86. L. Xiao, Y.-P. Liu, C.-X. Xiao*, et al.* Serum TFF3 may be a pharamcodynamic marker of responses to chemotherapy in gastrointestinal cancers. BMC clinical pathology 2014;14:26-26
87. J. J. Wang, N. H. Chi, T. M. Huang*, et al.* Urinary biomarkers predict advanced acute kidney injury after cardiovascular surgery. Crit Care 2018;22(1):108
88. C. M. Walshe, F. Odejayi, S. Ng*, et al.* Urinary glutathione S-transferase as an early marker for renal dysfunction in patients admitted to intensive care with sepsis. Crit Care Resusc 2009;11(3):204-209

89. M. Andreucci, T. Faga, A. Pisani*, et al.* The ischemic/nephrotoxic acute kidney injury and the use of renal biomarkers in clinical practice. European Journal of Internal Medicine 2017;39:1-8

90. C.-Y. Wu, H.-Y. Yang, H.-P. Chien*, et al.* Urinary clusterin—a novel urinary biomarker associated with pediatric lupus renal histopathologic features and renal survival. Pediatric Nephrology 2018;33(7):1189-1198

91. H. M. Jia, L. F. Huang, Y. Zheng*, et al.* Diagnostic value of urinary tissue inhibitor of metalloproteinase-2 and insulin-like growth factor binding protein 7 for acute kidney injury: a meta-analysis. Crit Care 2017;21(1):77

92. E. J. Weber, J. Himmelfarb and E. J. Kelly. Concise review: Current and emerging biomarkers of nephrotoxicity. Current Opinion in Toxicology 2017;4:16-21

93. D. du Cheyron, C. Daubin, J. Poggioli*, et al.* Urinary measurement of Na+/H+ exchanger isoform 3 (NHE3) protein as new marker of tubule injury in critically ill patients with ARF. Am J Kidney Dis 2003;42(3):497-506

94. W. K. Han, S. S. Waikar, A. Johnson*, et al.* Urinary biomarkers in the early diagnosis of acute kidney injury. Kidney Int 2008;73(7):863-869

95. K. Sawai, M. Mukoyama, K. Mori*, et al.* Expression of CCN1 (CYR61) in developing, normal, and diseased human kidney. Am J Physiol Renal Physiol 2007;293(4):F1363-1372

96. J. S. Ozer, F. Dieterle, S. Troth*, et al.* A panel of urinary biomarkers to monitor reversibility of renal injury and a serum marker with improved potential to assess renal function. Nat Biotechnol 2010;28(5):486-494

97. D. Bolignano, V. Donato, G. Coppolino*, et al.* Neutrophil gelatinase-associated lipocalin (NGAL) as a marker of kidney damage. Am J Kidney Dis 2008;52(3):595-605

98. K. Manabe, H. Kamihata, M. Motohiro*, et al.* Urinary liver-type fatty acid-binding protein level as a predictive biomarker of contrast-induced acute kidney injury. Eur J Clin Invest 2012;42(5):557-563

99. A. Kamijo, T. Sugaya, A. Hikawa*, et al.* Urinary liver-type fatty acid binding protein as a useful biomarker in chronic kidney disease. Mol Cell Biochem 2006;284(1-2):175-182

100. S. A. Price, D. Davies, R. Rowlinson*, et al.* Characterization of renal papillary antigen 1 (RPA-1), a biomarker of renal papillary necrosis. Toxicol Pathol 2010;38(3):346-358

101. M. V. Pahl, N. D. Vaziri, J. Yuan*, et al.* Upregulation of monocyte/macrophage HGFIN (Gpnmb/Osteoactivin) expression in end-stage renal disease. Clin J Am Soc Nephrol 2010;5(1):56-61

102. Y. Xie, M. Sakatsume, S. Nishi*, et al.* Expression, roles, receptors, and regulation of osteopontin in the kidney. Kidney Int 2001;60(5):1645-1657

103. H. Hayashi, W. Sato, T. Kosugi*, et al.* Efficacy of urinary midkine as a biomarker in patients with acute kidney injury. Clin Exp Nephrol 2017;21(4):597-607

104. Y. Liu, B. Liu, Y. Liu*, et al.* MicroRNA expression profile by next-generation sequencing in a novel rat model of contrast-induced acute kidney injury. Ann Transl Med 2019;7(8):178

105. W. B. Reeves, O. Kwon and G. Ramesh. Netrin-1 and kidney injury. II. Netrin-1 is an early biomarker of acute kidney injury. Am J Physiol Renal Physiol 2008;294(4):F731-738

106. N. Piazzon, F. Bernet, L. Guihard*, et al.* Urine Fetuin-A is a biomarker of autosomal dominant polycystic kidney disease progression. J Transl Med 2015;13:103

107. X. Liu, Y. Guan, S. Xu*, et al.* Early Predictors of Acute Kidney Injury: A Narrative Review. Kidney Blood Press Res 2016;41(5):680-700

108. A. L. Hanemann, A. B. Liborio, E. F. Daher*, et al.* Monocyte chemotactic protein-1 (MCP-1) in patients with chronic schistosomiasis mansoni: evidences of subclinical renal inflammation. PLoS

One 2013;8(11):e80421

109. C. Yin and N. Wang. Kidney injury molecule-1 in kidney disease. Ren Fail 2016;38(10):1567-1573

110. Y. Yu, H. Jin, D. Holder*, et al.* Urinary biomarkers trefoil factor 3 and albumin enable early detection of kidney tubular injury. Nat Biotechnol 2010;28(5):470-477

111. F. Dieterle, E. Perentes, A. Cordier*, et al.* Urinary clusterin, cystatin C, beta2-microglobulin and total protein as markers to detect drug-induced kidney injury. Nat Biotechnol 2010;28(5):463-469

112. A. Onopiuk, A. Tokarzewicz and E. Gorodkiewicz. Cystatin C: a kidney function biomarker. Adv Clin Chem 2015;68:57-69

113. S. Bolisetty and A. Agarwal. Urine albumin as a biomarker in acute kidney injury. Am J Physiol Renal Physiol 2011;300(3):F626-627

114. S. Hidaka, B. Kranzlin, N. Gretz*, et al.* Urinary clusterin levels in the rat correlate with the severity of tubular damage and may help to differentiate between glomerular and tubular injuries. Cell Tissue Res 2002;310(3):289-296

115. T. J. Pianta, P. W. Peake, J. W. Pickering*, et al.* Clusterin in kidney transplantation: novel biomarkers versus serum creatinine for early prediction of delayed graft function. Transplantation 2015;99(1):171-179

116. C. Han, Y.-K. Lee, H. C. Park*, et al.* Serum alkaline phosphatase and γ-glutamyl transferase in acute pyelonephritis. Kidney research and clinical practice 2019;38(2):205-211

117. P. Bajaj, S. K. Chowdhury, R. Yucha*, et al.* Emerging Kidney Models to Investigate Metabolism, Transport, and Toxicity of Drugs and Xenobiotics. 2018(1521-009X (Electronic))

118. F. Barré-Sinoussi and X. Montagutelli. Animal models are essential to biological research: issues and perspectives. Future science OA 2015;1(4):FSO63-FSO63

119. S. E. Jenkinson, G. W. Chung, L. E. van*, et al.* The limitations of renal epithelial cell line HK-2 as a model of drug transporter expression and function in the proximal tubule. Pflugers Arch. 2012;464(6):601-611

120. B. R. Simon-Friedt, M. J. Wilson, D. A. Blake*, et al.* The RPTEC/TERT1 Cell Line as an Improved Tool for In Vitro Nephrotoxicity Assessments. Biological Trace Element Research 2015;166:66-71

121. J. Jansen, C. M. S. Schophuizen, M. J. Wilmer*, et al.* A morphological and functional comparison of proximal tubule cell lines established from human urine and kidney tissue. Experimental Cell Research 2014;323(1):87-99

122. M. J. Wilmer, M. A. Saleem, R. Masereeuw*, et al.* Novel conditionally immortalized human proximal tubule cell line expressing functional influx and efflux transporters. Cell and Tissue Research 2010;339:449-457

123. T. T. G. Nieskens, J. G. P. Peters, M. J. Schreurs*, et al.* A Human Renal Proximal Tubule Cell Line with Stable Organic Anion Transporter 1 and 3 Expression Predictive for Antiviral-Induced Toxicity. The AAPS Journal 2016;18:465-475

124. T. Sakairi, Y. Abe, H. Kajiyama*, et al.* Conditionally immortalized human podocyte cell lines established from urine. American Journal of Physiology - Renal Physiology 2010;298:F557

125. A.-K. Sjögren, K. Breitholtz, E. Ahlberg*, et al.* A novel multi-parametric high content screening assay in ciPTEC-OAT1 to predict drug-induced nephrotoxicity during drug discovery. Archives of Toxicology 2018;92:3175-3190

126. P. F. Secker, N. Schlichenmaier, M. Beilmann*, et al.* Functional transepithelial transport measurements to detect nephrotoxicity in vitro using the RPTEC/TERT1 cell line. Archives of

Toxicology 2019:1-14

127. M. Takasato, P. X. Er, H. S. Chiu*, et al.* Kidney organoids from human iPS cells contain multiple lineages and model human nephrogenesis. Nature 2015;526:564-568

128. S. M. Chuva de Sousa Lopes. Accelerating maturation of kidney organoids. Nature Materials 2019;18(4):303-304

129. T. Desrochers, L. Suter-Dick, A. Roth, et al. Bioengineered 3D Human Kidney Tissue, a Platform for the Determination of Nephrotoxicity, Placed Published: 2013.

130. P. F. Secker, L. Luks, N. Schlichenmaier*, et al.* RPTEC/TERT1 cells form highly differentiated tubules when cultured in a 3D matrix. 2017(1868-596X (Print))

131. K. M. Stray, R. A. Bam, G. Birkus*, et al.* Evaluation of the Effect of Cobicistat on the In Vitro Renal Transport and Cytotoxicity Potential of Tenofovir. Antimicrobial Agents and Chemotherapy 2013;57(10):4982

132. R. Uetake, T. Sakurai, A. Kamiyoshi*, et al.* Adrenomedullin-RAMP2 System Suppresses ER Stress-Induced Tubule Cell Death and Is Involved in Kidney Protection. PLOS ONE 2014;9(2):e87667

133. P. C. Breda, T. Wiech, C. Meyer-Schwesinger*, et al.* Renal proximal tubular epithelial cells exert immunomodulatory function by driving inflammatory CD4+ T cell responses. American Journal of Physiology-Renal Physiology 2019;317(1):F77-F89

134. A. Rodriguez-Barbero, B. L'azou, J. Cambar*, et al.* Potential use of isolated glomeruli and cultured mesangial cells as in vitro models to assess nephrotoxicity. In: *Cell Biology and Toxicology*. *2000*: Abstract 16, p. 145-153.

135. Y. Liang, J. Zhang, Y. Zhou*, et al.* Proliferation and Cytokine Production of Human Mesangial Cells Stimulated by Secretory IgA Isolated from Patients with IgA Nephropathy. Cellular Physiology and Biochemistry 2015;36(5):1793-1808

136. R. L. Schmouder, R. M. Strieter, R. C. Wiggins*, et al.* In vitro and in vivo interleukin-8 production in human renal cortical epithelia. In: *Kidney International*. *1992*: Abstract 41, p. 98.

137. E. J. Lee, H. W. Song Sa Fau - Mun, K. H. Mun Hw Fau - Yoo*, et al.* Blockade of interleukin-8 receptor signalling inhibits cyst development in vitro, via suppression of cell proliferation in autosomal polycystic kidney disease. 2014(1440-1797 (Electronic))

138. C. D. Brown, R. Sayer, A. S. Windass*, et al.* Characterisation of human tubular cell monolayers as a model of proximal tubular xenobiotic handling. Toxicol.Appl.Pharmacol. 2008;233(3):428-438

139. K. Kowalkowski, M. Klapczynski, E. Blomme*, et al.* Evaluating In Vitro Canine Kidney Slices as a Renal Toxicity Model Using Nephrotoxic Agents Cisplatin and Cadmium Chloride. The FASEB Journal 2017;31:819.818-819.818

140. R. De Kanter, P. Olinga, M. H. De Jager*, et al.* Organ slices as an in vitro test system for drug metabolism in human liver, lung and kidney. Toxicol In Vitro 1999;13(4-5):737-744

141. H. Arakawa, I. Washio, N. Matsuoka*, et al.* Usefulness of kidney slices for functional analysis of apical reabsorptive transporters. Scientific Reports 2017;7:12814

142. T. Georgiev, R. Iliev, S. Mihailova*, et al.* THE ISOLATED PERFUSED KIDNEY MODELS - CERTAIN ASPECTS. Trakia Journal of Sciences 2011;9(3):82-87

143. J. A. Schafer, L. Watkins Ml Fau - Li, P. Li L Fau - Herter*, et al.* A simplified method for isolation of large numbers of defined nephron segments. American Journal of Physiology-Renal Physiology 1997;273(4):F650-F657

144. L. Aschauer, A. Limonciel, A. Wilmes*, et al.* Application of RPTEC/TERT1 cells for investigation of repeat dose nephrotoxicity: A transcriptomic study. Toxicology in Vitro 2015;30:106-116

145. M. Wieser, G. Stadler, P. Jennings*, et al.* hTERT alone immortalizes epithelial cells of renal proximal tubules without changing their functional characteristics. Am J Physiol Renal Physiol 2008;295(5):F1365-1375

146. A. Wilmes, C. Bielow, C. Ranninger*, et al.* Mechanism of cisplatin proximal tubule toxicity revealed by integrating transcriptomics, proteomics, metabolomics and biokinetics. Toxicology in Vitro 2015;30:117-127

147. M. J. Ryan, G. Johnson, J. Kiiu*, et al.* HK-2: An immortalized proximal tubule epithelial cell line from normal adult human kidney. In: *Kidney International*. *1994*: Abstract 45, p. 48-57.

148. K.-W. Zhao, E. J. B. Murray and S. S. Murray. HK2 Proximal Tubule Epithelial Cells Synthesize and Secrete Plasma Proteins Predominantly Through the Apical Surface. Journal of Cellular Biochemistry 2017;118:924-933

149. R. A. Murphy, R. M. Stafford, B. A. Petrasovits*, et al.* Establishment of HK-2 Cells as a Relevant Model to Study Tenofovir-Induced Cytotoxicity. International journal of molecular sciences 2017;18

150. A. Q. Lam, B. S. Freedman, R. Morizane*, et al.* Rapid and efficient differentiation of human pluripotent stem cells into intermediate mesoderm that forms tubules expressing kidney proximal tubular markers. Journal of the American Society of Nephrology : JASN 2014;25:1211-1225

151. S.-I. Mae, A. Shono, F. Shiota*, et al.* Monitoring and robust induction of nephrogenic intermediate mesoderm from human pluripotent stem cells. Nature communications 2013;4:1367

152. K. Kandasamy, J. K. C. Chuah, R. Su*, et al.* Prediction of drug-induced nephrotoxicity and injury mechanisms with human induced pluripotent stem cell-derived cells and machine learning methods. Scientific reports 2015;5:12337

153. M. Takasato, P. X. Er, M. Becroft*, et al.* Directing human embryonic stem cell differentiation towards a renal lineage generates a self-organizing kidney. Nature Cell Biology 2014;16:118-126

154. Y. Xia, I. Sancho-Martinez, E. Nivet*, et al.* The generation of kidney organoids by differentiation of human pluripotent cells to ureteric bud progenitor–like cells. Nature Protocols 2014;9:2693-2704

155. B. S. Freedman, C. R. Brooks, A. Q. Lam*, et al.* Modelling kidney disease with CRISPR-mutant kidney organoids derived from human pluripotent epiblast spheroids. Nature Communications 2015;6:8715

156. K. J. Jang, A. P. Mehr, G. A. Hamilton*, et al.* Human kidney proximal tubule-on-a-chip for drug transport and nephrotoxicity assessment. Integrative Biology (United Kingdom) 2013

157. M. J. Wilmer, C. P. Ng, H. L. Lanz*, et al.* Kidney-on-a-Chip Technology for Drug-Induced Nephrotoxicity Screening. Trends in biotechnology 2016;34:156-170

158. E. J. Weber, A. Chapron, B. D. Chapron*, et al.* Development of a microphysiological model of human kidney proximal tubule function. Kidney International 2016;90(3):627-637

159. J. Lee and S. Kim. Kidney-on-a-Chip: A New Technology for Predicting Drug Efficacy, Interactions, and Drug-induced Nephrotoxicity. Current Drug Metabolism 2018;19:577-583

160. F. Schutgens, M. B. Rookmaaker, T. Margaritis*, et al.* Tubuloids derived from human adult kidney and urine for personalized disease modeling. Nature Biotechnology 2019;37:303-313

161. J. Jansen, I. E. De Napoli, M. Fedecostante*, et al.* Human proximal tubule epithelial cells cultured on hollow fibers: living membranes that actively transport organic cations. Scientific Reports 2015;5:16702

162. J. Jansen, M. Fedecostante, M. J. Wilmer*, et al.* Bioengineered kidney tubules efficiently excrete uremic toxins. Scientific Reports 2016;6:26715

163. N. V. Chevtchik, M. Mihajlovic, M. Fedecostante*, et al.* A bioartificial kidney device with polarized secretion of immune modulators. Journal of Tissue Engineering and Regenerative Medicine 2018;12:1670-1678

164. M. Fedecostante, K. G. C. Westphal, M. F. Buono*, et al.* Recellularized Native Kidney Scaffolds as a Novel Tool in Nephrotoxicity Screening. Drug Metab Dispos 2018;46(9):1338-1350

165. J. Jansen, K. Jansen, E. Neven*, et al.* Remote sensing and signaling in kidney proximal tubules stimulates gut microbiome-derived organic anion secretion. Proc Natl Acad Sci U S A 2019

166. M. Mihajlovic, M. Fedecostante, M. J. Oost*, et al.* Role of Vitamin D in Maintaining Renal Epithelial Barrier Function in Uremic Conditions. International journal of molecular sciences 2017;18(12):2531

167. M. Fedecostante, O. G. Onciu, K. G. C. Westphal*, et al.* Towards a bioengineered kidney: recellularization strategies for decellularized native kidney scaffolds. The International Journal of Artificial Organs 2017;40:150-158

168. Z. Cai, J. Xin, D. M. Pollock*, et al.* Shear stress-mediated NO production in inner medullary collecting duct cells. American Journal of Physiology-Renal Physiology 2000;279(2):F270-F274

169. V. Raghavan and O. A. Weisz. Discerning the role of mechanosensors in regulating proximal tubule function. American Journal of Physiology-Renal Physiology 2016;310(1):F1-F5

170. J. Vriend, T. T. G. Nieskens, M. K. Vormann*, et al.* Screening of Drug-Transporter Interactions in a 3D Microfluidic Renal Proximal Tubule on a Chip. The AAPS Journal 2018;20:87

171. K. A. Homan, D. B. Kolesky, M. A. Skylar-Scott*, et al.* Bioprinting of 3D Convoluted Renal Proximal Tubules on Perfusable Chips. Scientific Reports 2016

172. K. A. Homan, N. Gupta, K. T. Kroll*, et al.* Flow-enhanced vascularization and maturation of kidney organoids in vitro. Nature Methods 2019;16(3):255-262

173. S. Y. Chang, E. J. Weber, K. V. Ness*, et al.* Liver and Kidney on Chips: Microphysiological Models to Understand Transporter Function. Clinical pharmacology and therapeutics 2016;100(5):464-478

174. S.-Y. Chang, E. J. Weber, V. S. Sidorenko*, et al.* Human liver-kidney model elucidates the mechanisms of aristolochic acid nephrotoxicity. JCI insight 2017;2(22):e95978

175. A. M. van Genderen, J. Jansen, C. Cheng*, et al.* Renal Tubular- and Vascular Basement Membranes and their Mimicry in Engineering Vascularized Kidney Tubules. Adv Healthc Mater 2018;7(19):e1800529

176. R. D. Bülow and P. Boor. Extracellular Matrix in Kidney Fibrosis: More Than Just a Scaffold. Journal of Histochemistry & Cytochemistry 2019:0022155419849388

177. S.-M. Yu, J. M. Oh, J. Lee*, et al.* Substrate curvature affects the shape, orientation, and polarization of renal epithelial cells. Acta Biomaterialia 2018;77:311-321

178. F. P. Guengerich. Mechanisms of drug toxicity and relevance to pharmaceutical development. Drug metabolism and pharmacokinetics 2011;26(1):3-14

179. D. Cook, D. Brown, R. Alexander*, et al.* Lessons learned from the fate of AstraZeneca's drug pipeline: a five-dimensional framework. Nature Reviews Drug Discovery 2014;13:419

180. S. P. Troth, F. Simutis, G. S. Friedman*, et al.* Kidney Safety Assessment: Current Practices in Drug Development. Seminars in Nephrology 2019;39(2):120-131

181. A. Astashkina, B. Mann and D. W. Grainger. A critical evaluation of in vitro cell culture models for high-throughput drug screening and toxicity. Pharmacology & Therapeutics 2012;134(1):82-106

182. C. Sakolish, E. J. Weber, E. J. Kelly*, et al.* Technology Transfer of the Microphysiological Systems: A Case Study of the Human Proximal Tubule Tissue Chip. Scientific Reports

2018;8(1):14882

183. M. Mihajlovic, S. Hariri, K. C. G. Westphal*, et al.* Safety evaluation of conditionally immortalized cells for renal replacement therapy. Oncotarget 2019;10(51):5332-5348

184. A. Wnorowski, H. Yang and J. C. Wu. Progress, obstacles, and limitations in the use of stem cells in organ-on-a-chip models. Advanced Drug Delivery Reviews 2018

185. S. M. Czerniecki, N. M. Cruz, J. L. Harder*, et al.* High-Throughput Screening Enhances Kidney Organoid Differentiation from Human Pluripotent Stem Cells and Enables Automated Multidimensional Phenotyping. Cell Stem Cell 2018;22(6):929-940.e924

186. R. Morizane, A. Q. Lam, B. S. Freedman*, et al.* Nephron organoids derived from human pluripotent stem cells model kidney development and injury. Nature Biotechnology 2015;33:1193

187. Michael M. Kaminski, J. Tosic, C. Kresbach*, et al.* Direct reprogramming of fibroblasts into renal tubular epithelial cells by defined transcription factors. Nature Cell Biology 2016;18:1269

188. S. V. Kumar, P. X. Er, K. T. Lawlor*, et al.* Kidney micro-organoids in suspension culture as a scalable source of human pluripotent stem cell-derived kidney cells. Development (Cambridge, England) 2019;146(5):dev172361

189. T. M. DesRochers, E. P. Kimmerling, D. M. Jandhyala*, et al.* Effects of Shiga toxin type 2 on a bioengineered three-dimensional model of human renal tissue. Infection and immunity 2015;83(1):28-38

190. A. Kobayashi, M. T. Valerius, J. W. Mugford*, et al.* Six2 Defines and Regulates a Multipotent Self-Renewing Nephron Progenitor Population throughout Mammalian Kidney Development. Cell Stem Cell 2008;3(2):169-181

191. Z. Wei, P. K. Amponsah, M. Al-Shatti*, et al.* Engineering of polarized tubular structures in a microfluidic device to study calcium phosphate stone formation. Lab on a chip 2012;12(20):4037-4040

192. A. Rostami-Hodjegan. Physiologically Based Pharmacokinetics Joined With In Vitro–In Vivo Extrapolation of ADME: A Marriage Under the Arch of Systems Pharmacology. Clinical Pharmacology & Therapeutics 2012;92(1):50-61

193. P. Zhao, L. Zhang, J. Grillo*, et al.* Applications of Physiologically Based Pharmacokinetic (PBPK) Modeling and Simulation During Regulatory Review. 2011;89(2):259-267

CHAPTER 3

Drugs Commonly Applied to Kidney Patients May Compromise Renal Tubular Uremic Toxins Excretion

Silvia M. Mihăilă[1], **João Faria**[1], Maurice F. J. Stefens[1], Dimitrios Stamatialis[2], Marianne C. Verhaar[3], Karin G.F. Gerritsen[3], Rosalinde Masereeuw[1]

[1] Division of Pharmacology, Utrecht Institute for Pharmaceutical Sciences, Utrecht University, 3854 CG Utrecht, The Netherlands

[2] (Bio)artificial Organs, Department of Biomaterials Science and Technology, University of Twente, 7522 LW Enschede, The Netherlands

[3] Department of Nephrology and Hypertension, University Medical Center Utrecht, 3582 CX Utrecht, The Netherlands

Published in Toxins. 2020;12(6):391

ABSTRACT

In chronic kidney disease (CKD), the secretion of uremic toxins is compromised leading to their accumulation in blood, which contributes to uremic complications, in particular cardiovascular disease. Organic anion transporters (OATs) are involved in the tubular secretion of protein-bound uremic toxins (PBUTs). However, OATs also handle a wide range of drugs, including those used for treatment of cardiovascular complications and their interaction with PBUTs is unknown. The aim of this study was to investigate the interaction between commonly prescribed drugs in CKD and endogenous PBUTs with respect to OAT1-mediated uptake. We exposed a unique conditionally immortalized proximal tubule cell line (ciPTEC) equipped with OAT1 to a panel of selected drugs, including angiotensin-converting enzyme inhibitors (ACEIs: captopril, enalaprilate, lisinopril), angiotensin receptor blockers (ARBs: losartan and valsartan), furosemide and statins (pravastatin and simvastatin), and evaluated the drug-interactions using an OAT1-mediated fluorescein assay. We show that selected ARBs and furosemide significantly reduced fluorescein uptake, with the highest potency for ARBs. This was exaggerated in presence of some PBUTs. Selected ACEIs and statins had either no or a slight effect at supratherapeutic concentrations on OAT1-mediated fluorescein uptake. In conclusion, we demonstrate that PBUTs may compete with co-administrated drugs commonly used in CKD management for renal OAT1 mediated secretion, thus potentially compromising the residual renal function.

KEYWORDS: protein-bound uremic toxins; chronic kidney disease management; drug-toxin interaction, OAT1-mediated transport

1. INTRODUCTION

Chronic kidney disease (CKD) is a worldwide public health problem associated with considerable prevalence of comorbidities, impaired quality of life and premature mortality [1]. In patients with advanced CKD, uremic solutes accumulate due to impaired renal clearance [2]. Many of them are considered uremic toxins (UTs) and are believed to contribute to the uremic syndrome, a generalized organ dysfunction occurring in CKD [3-9]. In particular, protein-bound uremic toxins (PBUTs) were shown to exert toxic effects or disrupt key signaling and metabolic pathways, including those controlled by a complex network of solute carrier (SLC) and ATP-binding cassette (ABC) transporters and drug-metabolizing enzymes (DMEs), many of which are critical for drug absorption, distribution, metabolism and elimination (ADME) [10, 11]. As CKD progresses, drug-metabolite interactions involving transporters can become more deleterious, potentially contributing to new and increased drug toxicities [7, 12-15].

CKD patients are routinely treated with many drugs that require transporters and DMEs for their disposition [11, 16]. The daily medication burden in kidney patients is one of the highest reported to date in any chronic disease state [17], and drugs are prescribed mainly at alleviating the metabolic, endocrine and cardiovascular complications in renal insufficiency [18-21]. Antihypertensive drugs (*e.g.*, renin-angiotensin-aldosterone system inhibitors, such as angiotensin-converting enzyme inhibitors (ACEIs) or angiotensin receptor blockers (ARBs), and diuretics) and cholesterol-lowering drugs (*e.g.*, statins) are frequently prescribed medications for cardiovascular risk management in the CKD population [20, 22-28].With drug-drug interactions occurring even in patients without renal impairment, such interactions are likely more prevalent in CKD owing to the presence of high levels of uremic solutes that also compete with the administered drugs and with each other for transporters and DMEs [7].

In renal tissue, the key mediators of transepithelial transport of many endogenous metabolites are the organic anion transporters (OATs), which play a central role in the cellular uptake of uremic retention solutes as a first step in their excretion [11, 29, 30]. Amongst the OATs, OAT1 (*SLC22A6*) and OAT3 (*SLC22A8*) are abundantly expressed at the basolateral membrane of proximal tubule cells, and appear to be the most important transporters involved in the renal uptake of endogenous metabolites, including PBUTs (*e.g.*, indoxyl sulfate, p-cresylsulfate, kynurenic acid, etc.), with OAT1 dominating over OAT3 with respect to PBUT uptake [10, 29, 31, 32], drugs (probenecid, methotrexate, adefovir, indomethacin) and other exogeneous toxins [33]. The interactions between PBUTs and commonly prescribed drugs are currently unknown.

The aim of this study was to investigate the pharmacokinetic interactions between commonly prescribed drugs in CKD management (ACEIs, ARBs, statins and furosemide) and

PBUTs with respect to OAT1-mediated uptake in an *in vitro* setting. First, the inhibitory potency of the selected PBUTs and drugs on OAT1 activity was evaluated. For this, we exposed a human conditionally immortalized proximal tubule cells line (ciPTEC) expressing OAT1 (ciPTEC-OAT1) previously developed and characterized [34-37], to variable concentrations of PBUTs or drugs and evaluated fluorescein uptake, a known substrate for OAT1 [38]. Subsequently, we explored the effect of PBUTs presence, at concentrations similar to those in plasma of CKD patients, on the drug profiles, again, by studying OAT1-mediated fluorescein uptake.

2. MATERIALS AND METHODS

2.1. Chemicals

A brief overview of the uremic toxins used within the study (indoxyl sulfate, indoxyl-β-D-glucoronide, indole-3-acetic acid, kynurenic acid, L-kynurenine, hippuric acid, *p*-cresylsulfate, *p*-cresylglucuronide) and tested drugs (ACEIs, ARBs, statins, furosemide and cimetidine) is available in Supplementary Materials section (**Supplementary Table S1** and **Supplementary Table S3**, respectively). Chemicals were purchased from Sigma-Aldrich (Zwijndrecht, The Netherlands) unless stated otherwise. The uremic toxins *p*-cresylsulfate and *p*-cresylglucuronide were synthesized by the Institute for Molecules and Materials, Radboud University, Nijmegen, The Netherlands, as described earlier [37].

2.2. Cell Cultures

Conditionally immortalized proximal tubule epithelial cells overexpressing the organic anion transporter 1 (ciPTEC-OAT1) were cultured as described by Nieskens *et al.* [36]. Briefly, cells were cultured up to maximum 60 passages in Dulbecco's Modified Eagle Medium/Nutrient Mixture F-12 (1:1 DMEM/F-12) (Gibco, Life Technologies, Paisley, UK) supplemented with 10% fetal calf serum (FCS) (Greiner Bio-One, Alphen aan den Rijn, The Netherlands), 5µg/mL insulin, 5µg/mL transferin, 5µg/mL selenium, 35ng/mL hydrocortisone, 10 ng/mL epidermal growth factor and 40pg/mL tri-iodothyronine to form a complete culture medium, without addition of antibiotics. Cells were cultured at 33°C and 5% (*v*/*v*) CO_2 to allow expansion and prior to the experiments seeded at a density of 63,000 cells/cm^2. Subsequently, cells were grown 24h at 33°C, 5% (*v*/*v*) CO_2 to allow adhesion and proliferation, then cultured for 7 days at 37°C, 5% (*v*/*v*) CO_2 for differentiation and maturation, refreshing the medium every other day. The temperature shift ensured the maturation of cells into fully differentiated epithelial cells able to form confluent monolayers.

2.3. Fluorescein Inhibition Assay

The potency of a panel of several commonly prescribed drugs in the CKD management to inhibit OAT1-mediated fluorescein uptake was investigated in ciPTEC-OAT1 mature monolayers using an inhibition assay, as previously described by Nieskens *et al.* [36]. CiPTEC-OAT1 cultured in 96-well plates were co-incubated with fluorescein (1 μM, unless otherwise stated) and the selected drugs (**Supplementary Table S3**) at different concentrations (nM-mM) prepared in Krebs-Henseleit Buffer supplemented with 10 mM HEPES (KHH buffer, pH 7.4) for 10min at 37°C. To confirm the activity of OAT1, probenecid (500 μM in KHH) was simultaneously incubated with fluorescein. Uptake arrest was performed

by washing with ice-cold HBSS (Life Technologies Europe BV), and then the cells were lysed by 100μL 0.1M NaOH for 10min, at room temperature and under mild shaking. Intracellular fluorescence was detected using the Fluoroskan Ascent FL microplate reader, at excitation wavelength of 490nm and emission wavelength of 518nm. Background values were subtracted and normalized arbitrary fluorescence unit (AFU) data were converted into percentage (%). Incubation with fluorescein alone was assigned as 100% uptake. The reduction in fluorescein uptake in the presence of the inhibitor (drugs) was normalized to fluorescein uptake without the inhibitor.

2.4. Co-Exposure of CiPTEC-OAT1 to Selected PBUTs and Drugs

To confirm the ability of the ciPTEC-OAT1 to handle uremic toxins, cells were co-incubated with fluorescein and PBUTs (indoxyl sulfate, IS 110μM; kynurenic acid, KA 1μM; p-cresylsulfate, PCS 125μM), following the procedure described above. In order to replicate the uremic condition present in CKD patients, a specific mixture of eight known anionic PBUTs (**Supplementary Table S1**), predominantly derived from endogenous metabolism pathways and food digestion in the gut, was used at concentrations corresponding to those found in patients. The inhibition of OAT1-mediated fluorescein uptake during the co-exposure to drugs (variable concentrations) and PBUTs (fixed concentration) was determined by the percentage reduction of fluorescein uptake in the cells. Additionally, concentration-dependent mediated fluorescein uptake (concentration range= 0-3μM) in the presence of PBUTs (IS, KA, pCS and UTox) was studied.

2.5. Data Analysis

All data are expressed as mean ± standard deviation (SD) of at least three separate experiments. Inhibition data were fitted according to one-site total binding saturation curve using non-linear regression analysis ((inhibitor) *vs*. response - variable slope) and Vmax values were calculated according to Michaelis-Menten kinetics using non-linear regression analysis. Statistical analysis was performed using one-way ANOVA analysis followed by Tukey's multiple comparison test (OAT1-mediated inhibition uptake of fluorescein in the presence of PBUTs, reference values = arbitrary units of fluorescence when cells are exposure to fluorescein 1μM = 100%) or two-way ANOVA analysis followed by Dunnett's Multiple Comparison test (drug-toxins inhibition of OAT1-mediated fluorescein uptake, reference values= fluorescein percentage in the presence of toxin alone) with GraphPad Prism version 8.4 (La Jolla, CA, USA). All experiments were performed four times.

3. RESULTS

3.1. Protein Bound Uremic Toxins Reduce OAT1-Mediated Uptake at Clinically Relevant Concentrations

First, the effect of PBUTs on OAT1-mediated uptake of fluorescein by ciPTEC-OAT1 was evaluated. Fluorescein, an OAT1 model substrate, was used to evaluate the transporter activity as described earlier [36]. To confirm the OAT1 specificity of fluorescein uptake, we have co-incubated fluorescein with probenecid, a well-known OAT1 inhibitor [39, 40], which resulted in a fluorescein uptake of 24.9 ± 3.2% of the fluorescein alone values. This confirms the stable OAT1 activity on our cell line, as shown in previous studies [36]. Next, the decrease in fluorescein uptake in the presence of PBUTs was evaluated and was considered to occur via competition for the transporter (**Figure 1A**). The selection of the uremic toxins in the UTox mixture was based on their reported proximal tubule-mediated urinary secretion profile and association with CKD progression [36, 41, 42]. Indoxyl sulfate (IS), kynurenic acid (KA) and p-cresylsulfate (PCS) reduced fluorescein uptake at clinically relevant concentrations (*viz.* 110 μM, 1 μM and 125 μM, respectively). The concomitant exposure to a mixture of eight uremic toxins (UTox; for composition see **Supplementary Table S1**), further reduced fluorescein uptake (**Figure 1B**, to 34.4 ± 8.3%, $p<0.0001$ when compared to control).

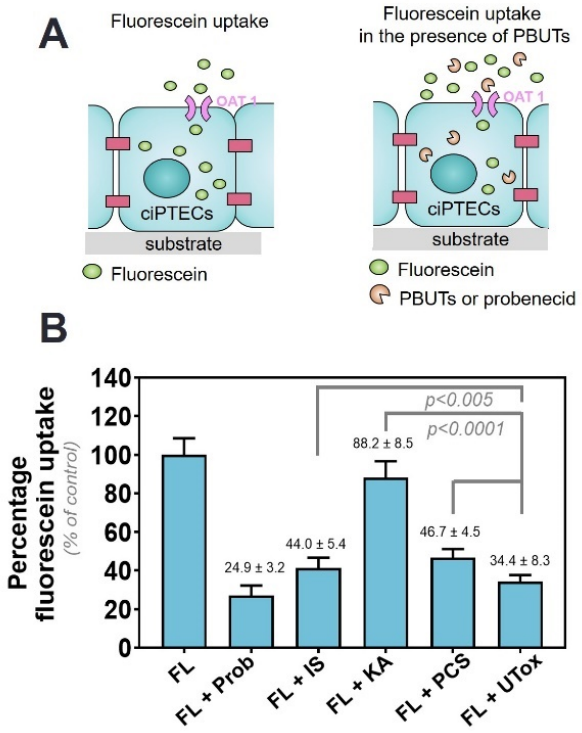

Figure 1. Organic anion transporter (OAT)1-mediated uptake of fluorescein (FL) in the presence of protein-bund uremic toxins (PBUTs). (**A**) Schematic representation of the experiment. To evaluate the potency of the transporter, fluorescein was incubated with matured ciPTECs. Fluorescein uptake was then quantified and assigned as 100% uptake. Secondly, fluorescein was incubated together with either probenecid, a known inhibitor of OAT1 activity, or individual PBUTs (IS = indoxyl sulfate, KA = kynurenic acid, PCS = p-cresylsulfate) and UTox (a mix of 8 PBUTs at concentrations found in uremic serum). (**B**) The intracellular accumulation of fluorescein was measured. Data are shown as mean ± SD of four independent experiments, performed in triplicate. P<0.005 and p<0.0001 using one-way ANOVA analysis followed by a Tukey's multiple comparison test.

The reduction of fluorescein uptake in the presence of probenecid (500 μM) was in agreement with our previous findings [36]. Additionally, the transport kinetics of OAT1-mediated fluorescein uptake was investigated by studying the concentration-dependent uptake of the substrate in the presence of selected uremic toxins. The fluorescein uptake by ciPTEC-OAT1 followed Michaelis-Menten kinetics from which kinetic parameters (Km and Vmax values) were determined (**Supplementary Figure S1** and **Supplementary Table S2**).

3.2. Commonly Prescribed Drugs in CKD Management Reduce OAT1-Mediated Uptake

To evaluate the role of OAT1 in the disposition of commonly prescribed drugs in CKD management, a panel of nine drugs selected based on their use within our hospital (ACEIs: captopril, enalaprilate and lisinopril; ARBs: losartan and valsartan; statins: pravastatin and

simvastatin and diuretics: furosemide, **Supplementary Table S3**) was selected. Cimetidine (a histamine H2 receptor antagonist**,** H2RA) and a model drug for inhibition of the organic cation transport (OCT2, *SLC22A2*) was used to reflect the non-inhibition of OAT1 [43].

A concentration-dependent reduction of fluorescein uptake was observed for all drugs (**Figure 2**), with the most potent interactions found for ARBs and furosemide (approx. 50% reduction in fluorescein uptake at the highest therapeutic concentration) and statins (approx. 20% reduction in fluorescein uptake at the highest therapeutic concentration), while for ACEIs and cimetidine either no effect was measured or a decrease was observed only at the highest concentrations tested beyond the therapeutic range (**Table 1**). Notably, at the highest concentrations of the ARBs and furosemide, the reduction in fluorescein uptake reached values similar to those obtained for probenecid, suggesting a (nearly) complete inhibition of the transporter. In the case of statins, at the highest concentration, the reduction in fluorescein was modest, an indication of partial inhibition of the transporter's activity. Thus, our data suggest that the selected ARBs, statins and furosemide act as transport inhibitors of OAT1-mediated uptake.

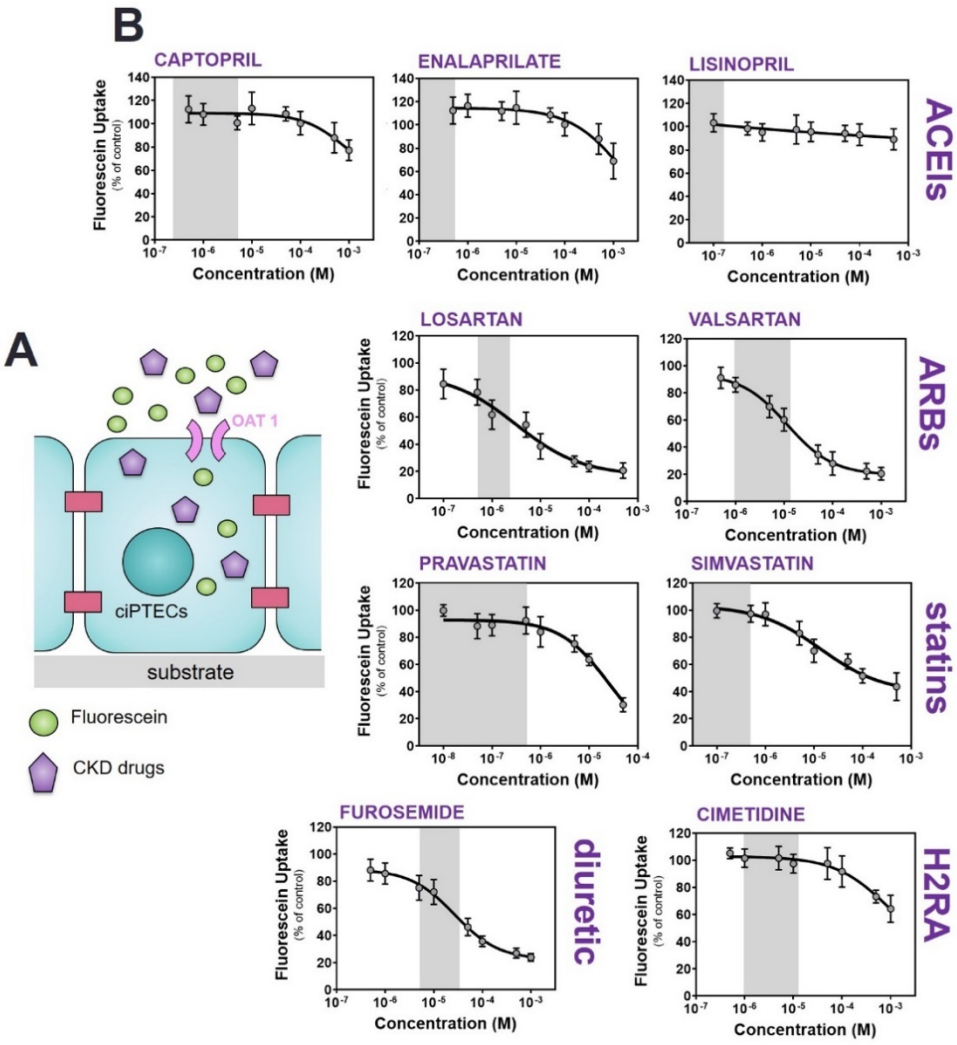

Figure 2. Inhibition of OAT1-mediated fluorescein uptake by a panel of drugs commonly used in CKD management. (**A**) Schematic representation of the co-incubation of fluorescein with variable concentration of drugs. (**B**) Fluorescein uptake (1μM) by ciPTEC-OAT1 in the presence of drugs (ACEIs: captopril, enalaprilate and lisinopril; ARBs: losartan and valsartan; statins: pravastatin and simvastatin; diuretics: furosemide). relative to the uptake of fluorescein without drugs (=100%). The histamine H2 receptor antagonist (H2RA): cimetidine) was used as a reference of no inhibitory effect on OAT1-mediated fluorescein. All data are expressed as mean ± SD of four independent experiments. Grey regions indicate the therapeutic window of the respective drug

Table 1. Inhibitory potencies of selected drugs on fluorescein uptake in ciPTEC-OAT1.

Drug	IC_{50} (μM)[a]	R square[b]	Therapeutic concentrations (μM) [44]
ACEIs			
Captopril	2022 ± 465	0.5557	0.2-5
Enalaprilate	1853 ± 370	0.6753	0.04-0.4
Lisinopril	-	0.1671	0.01-0.16
ARBs			
Losartan	3.1 ± 0.7	0.8713	0.5-1.5
Valsartan	11.5 ± 3.5	0.9374	2-14
DIURETICS			
Furosemide	28.1 ± 9.1	0.9301	6-30
STATINS			
Pravastatin	13.8 ± 8.5	0.8757	0.08-0.3 [45] 0.43 [46, 47]
Simvastatin	21.3 ± 3.8	0.8613	0.006-0.014[44] 0.55 [46, 47]
H2RA			
Cimetidine	887.6 ± 198.4	0.7441	1-16

[a]Data are expressed as mean ± SD. [b]Curves were obtained after non-linear regression analysis. **Abbreviations: ACEIs**, angiotensin-converting enzyme inhibitors; **ARBs**, angiotensin receptor blockers; **H2RA**, histamine H_2 receptor antagonists.

3.3. Commonly Prescribed Drugs in CKD in Combination with PBUTs Further Reduce OAT1-Mediated Uptake

Next, a dual competitive inhibition experiment with drugs and PBUTs on OAT1-mediated fluorescein uptake was performed, leaving out the ACEIs and cimetidine because of their supra pharmacological, clinically irrelevant interactions. To this end, mature monolayers of ciPTEC-OAT1 were co-incubated with the selected drugs at variable concentrations (as inhibitor 1) and PBUTs (IS, KA, PCS, UTox as inhibitor 2) at uremic concentrations, together with fluorescein.

In the presence of PBUTs the inhibitory effect of the drugs on fluorescein uptake was maintained with a clear dose-response relationship. The IC_{50} values were affected by the presence of PBUTs as shown in **Table 2**. In the case of drug-IS co-incubation, fluorescein uptake was considerably reduced in the presence of IS at low drug concentrations as compared to incubation of the drug alone, suggesting a strong inhibition of the transporter

primarily determined by IS. For the ARBs, fluorescein uptake showed an immediate progressive decrease with increasing drug concentrations already at low, therapeutic concentrations, while for furosemide and statins this decrease appeared only when co-incubation was performed at higher drug concentrations (**Figure 3**). In all cases, the maximum percentage reduction was in the same range as that of probenecid, suggesting a complete inhibition of the transporter.

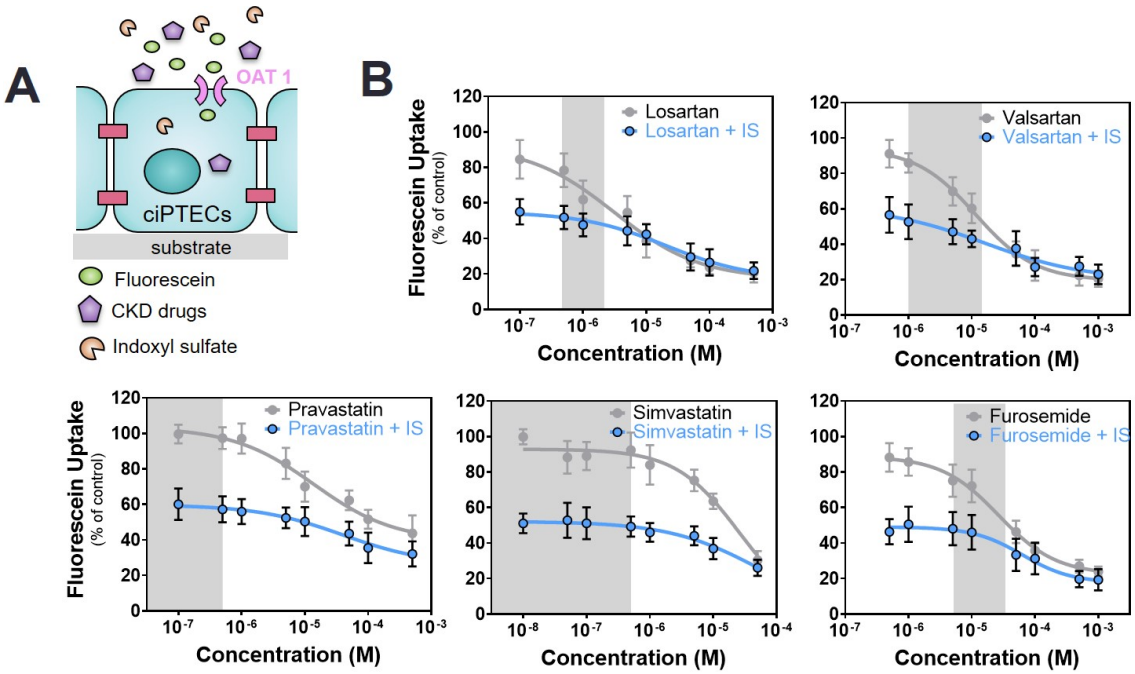

Figure 3. Combined interaction of drugs and indoxyl sulfate (IS) on OAT1-mediated fluorescein uptake. (**A**) Schematic representation of the co-incubation of fluorescein with variable concentrations of drugs and fixed concentration of IS (blue line). (**B**) The drug alone (grey line) shows a concentration-dependent inhibitory effect. Co-incubation with IS (110 μM, blue line) results in a further decrease of fluorescein uptake. All data are expressed as mean ± SD of four independent experiments. Curves were obtained after non-linear regression analysis. The reference value for the drug alone is fluorescein without the drug (100%), while for the co-incubation with IS the reference value is fluorescein in the presence of IS without the drug (44.0 ± 5.4%). Grey regions indicate the therapeutic window of the respective drug.

Table 2. OAT1 mediated fluorescein uptake: IC50 (μM) in the absence (-) and presence (+) of individual uremic toxins (IS, KA and PCS).

Drug / Toxin	-	+ IS 110μM	+ KA 1μM	+ PCS 125μM
		ARBs		
Losartan	8.6 ± 2.5	13.9 ± 5.9 [b]	28.2 ± 2.7 [a]	15.97 ± 3.9 [a]
Valsartan	11.5 ± 3.5	16.1 ± 3.6 [b]	46.9 ± 4.6 [a]	17.9 ± 3.8 [b]
		STATINS		
Pravastatin	13.8 ± 8.35	40.9 ± 9.2 [a]	243.0 ± 45.8 [a]	19.1± 3.2 [a]
Simvastatin	21.3 ± 3.8	71.8 ± 27.3 [a]	28.4 ± 10.1 [b]	32.8 ± 7.6 [a]
		DIURETICS		
Furosemide	28.1 ± 9.1	44.7 ± 12.4 [a]	24.8 ± 6.2 [b]	60.2 ± 1.0 [a]

[a] significant increase when compared with IC_{50} values of corresponding drug alone, [b] no significant change when compared with IC_{50} values of corresponding drug alone. **Abbreviations: IS**, indoxyl sulfate; **KA**, kynurenic acid; **PCS**, p-cresylsulfate; **ARBs**, angiotensin receptor blockers.

With KA alone, only a slight reduction in fluorescein uptake was noticed. In co-incubation with drugs, the inhibitory potencies of the drugs were not aggravated (**Figure 4; Table 2**). In the case of ARBs, the co-incubation with KA resulted in an increase in fluorescein uptake when compared to drug alone.

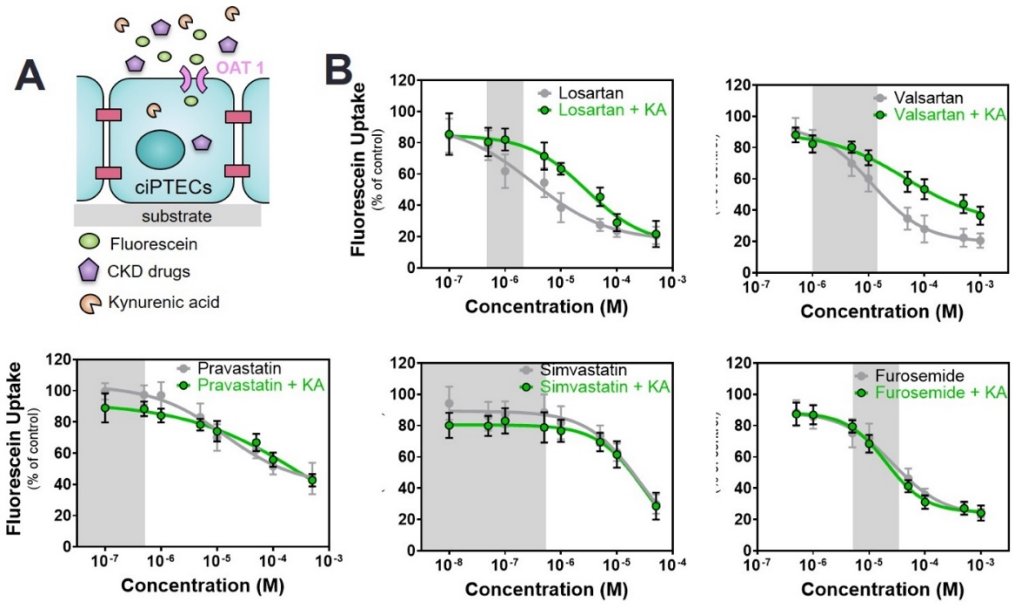

Figure 4. Combined interaction of drugs and kynurenic acid (KA) on OAT1-mediated fluorescein uptake. (**A**) Schematic representation of the co-incubation of fluorescein with variable concentrations of drugs and fixed concentration of KA. (**B**) The drug alone (grey line) shows a concentration-dependent inhibitory effect, that is not affected by the presence of KA (1 μM, green line) in the case of furosemide and statins. For ARBs, the inhibitory effect of the drugs is diminished in the presence of KA. All data are expressed as mean ± SD of four independent experiments. Curves were obtained after non-linear regression analysis. The reference value for the drug alone is fluorescein without the drug (100%), while for the co-incubation with KA the reference value is fluorescein in the presence of KA without the drug (88.2 ± 8.5). Grey regions indicate the therapeutic window of the respective drug.

With PCS, fluorescein uptake was strongly inhibited in the absence of drugs confirming the role of OAT1 in handling PCS [48]. During co-incubations with variable drug concentrations, a further reduction was noticed (**Figure 5; Table 2**), similar to IS. Again, in the case of furosemide and ARBs, the additional reduction in fluorescein uptake was observed at concentrations within the therapeutic range of the drugs.

The exposure to the mixture of PBUTs (UTox) resulted in a strong reduction of fluorescein uptake (34.4 ± 8.3%). With the addition of drugs, a further decrease was observed at the lowest concentration of each drug (with values comparable to probenecid), with a more pronounced effect for losartan and valsartan. This drop remained stable with the increase of the drug concentration (**Supplementary Figure S2, Supplementary Table S4)**.

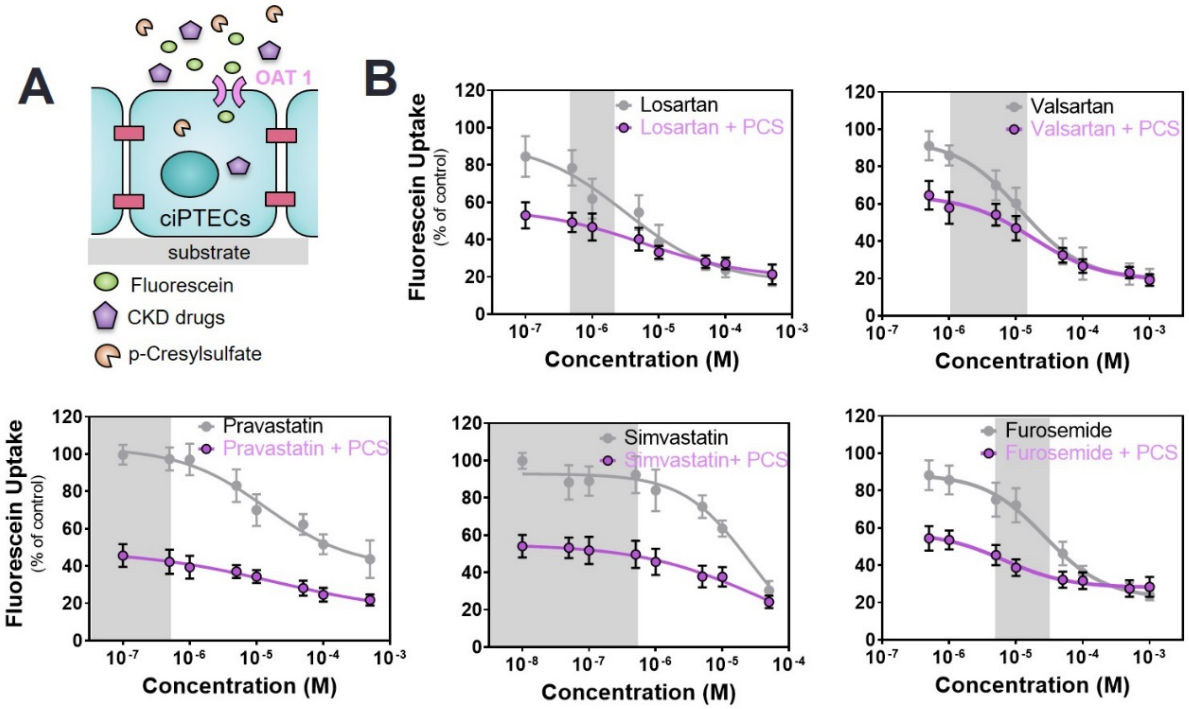

Figure 5. Combined interaction between drugs and p-cresylsulfate (PCS) on OAT1-mediated fluorescein uptake. (**A**) Schematic representation of the co-incubation of fluorescein with variable concentrations of drugs and fixed concentration of PCS. (**B**) The drug alone (grey line) shows a concentration-dependent inhibition effect. During the co-incubation of cells with variable drug concentrations and a fixed concentration of PCS (125 μM, purple line), the concentration-dependent inhibition trend is maintained. All data are expressed as mean ± SD of four independent experiment. Curves were obtained after non-linear regression analysis. The reference value for the drug alone (grey line) is fluorescein without the drug (100%), while for the co-incubation with PCS (purple line) the reference value is fluorescein in the presence of PCS without the drug (46.7 ± 4.5%). Grey regions indicate the therapeutic window of the respective drug.

4. DISCUSSION

Our major findings are that PBUTs may directly interact with drugs commonly prescribed in CKD management for OAT1-mediated renal transport, at concentrations found in uremic serum. These interactions could exert widespread and unpredictable effects in CKD patients that already have a high burden of co-existing diseases, poor health-related quality of life and are prescribed many medications [16, 17]. CKD patients use multiple drugs, in particular for CKD related complications such as hypertension, CVD and lipid disorders. There is a high variability in pharmacokinetics in CKD patients, which can be partly explained by drug-drug interactions (DDIs) resulting from this polypharmacy [49-51]. In addition, as CKD progresses and uremic toxins accumulate, drug-metabolite interactions involving transporters can become more prevalent and more deleterious, potentially contributing to new and/or increased drug toxicities [7]. Although not all drugs tested show a high renal clearance profile (**Supplementary Table S6**), we consider the findings still clinically relevant. In CKD, pharmacokinetics can be severely altered not only due to renal dysfunction but also affecting drug absorption and metabolism [52]. In addition, DDIs can take place on protein binding.

The potential interaction of drugs and metabolites with the renal organic ion secretion system (OAT1 and OAT3, organic cation transporter 2 (OCT2), and multidrug and toxin extrusion (MATE)) has been acknowledged by the US Food and Drug Administration (FDA). They released regulatory guidelines to study the contribution of (renal) transporters in disposition of new pharmaceutical entities to identify and understand potential DDIs and (drug-induced) nephrotoxicity including evaluation of interaction with the transporters *in vitro* [53]. Noteworthy, drugs for which the kidney is not the main route of excretion (losartan, valsartan, simvastatin), but have an inhibitory effect towards OATs, could contribute to the reduction of PBUTs clearance, and thus, to the progression of the disease. For this purpose, human models with a high predictive capacity for renal drug handling are being used [54-56]. The human-derived proximal tubule epithelial cell model, ciPTEC-OAT1, developed by us [34-37], was shown to be a robust *in vitro* model to study drug interactions. We here demonstrate the potency of commonly prescribed drugs in the management of CKD comorbidities (ACEIs, ARBs, statins and diuretics) [24, 27, 57, 58] to inhibit basolateral OAT1-mediated uptake of fluorescein at clinically relevant concentrations.

The potential involvement of OAT1 in the handling of the drugs tested had been previously reported [56], but not in the context of uremia. Sato *et al.* [58] reported comparable IC_{50} values for losartan and valsartan (12 μM and 16 μM, respectively; compared with 8.6 ± 2.5 μM and 11.5 ± 3.5 μM reported here), based on uptake of uric acid by OAT1-expressing Flp-HEK293 cells. For statins, exposure to our *in vitro* cell model revealed higher affinities

towards OAT1 than those reported in literature (pravastatin: 23.2 ± 8.3 μM vs. 408 ± 55 μM reported by Taketa *et al*. [47] and simvastatin: 21.3 ± 3.8 μM vs. 73.7 ± 6.6 μM reported in the same study). However, these experiments were performed in OAT1-expressing muscle cells and not in renal proximal tubule cells. With regard to ACEIs, we show that human OAT1 is inhibited by captopril and enalaprilate (albeit at high concentrations with no therapeutic relevance), but not by lisinopril, similar as reported for mouse Oat1 [59, 60]. Therefore, we did not continue with further evaluation of these drugs in combination with uremic toxins. Further, previous studies performed by our group showed a strong inhibitory potential of furosemide, in contrast with the slight effect of cimetidine, but in line with the data here presented [36]. Noteworthy, some of the tested drugs were reported to interact with OAT3 as well [56, 58].

The accumulation of PBUTs due to decreased renal excretion and gut dysbiosis is associated with several comorbidities and altered drug metabolism [61-63], thus further contributing to the progression of renal disease. Here, three PBUTs (IS, KA and PCS) were selected for drug-interaction studies using the ciPTEC-OAT1 model, as it was previously reported that these toxins interact with OAT1 and have been associated with CKD progression and its related complications [37, 48, 64, 65]. Competitive inhibition of drug transporters and the concomitant alteration in pharmacokinetics, may result from elevated levels of multiple retention solutes within the serum [29, 63]. To reflect this complexity, we also prepared a mixture of the most relevant PBUTs (UTox), at uremic concentrations taken from the EUTox Uremic Solutes Database [http://www.uremic-toxins.org/DataBase.html]. Of note, the variability of PBUTs levels among individuals is large [66], thus the PBUTs concentrations of the UTox were chosen within the average levels. While confirming the inhibitory potential of the individual toxins (IS, KA, PCS), we showed a significantly stronger inhibition when cells were exposed to the UTox, but not enough to reach the inhibitory potential of probenecid, which we consider as reference inhibitor of OAT1. When co-incubating with selected drugs, a further decrease in fluorescein uptake was observed, reaching similar levels as those obtained with probenecid, suggesting a complete saturation of the transporter *via* competitive inhibition.

The simultaneous incubation of individual toxins at uremic concentrations (IS-110 μM, KA-1 μM and PCS-125 μM) with the selected drugs resulted in a significant alteration of the inhibition potential of drugs on OAT1-mediated fluorescein uptake, when compared to the toxins alone. This indicates that the transporter is susceptible to modifications of the microenvironmental composition. In the case of IS- and PCS-drug co-incubation, at the lowest concentration of the drugs tested, the inhibitory potential was similar to that of toxin alone, suggesting that the competitive inhibition was mainly toxin-dominated. With increasing drug concentrations, which in case of furosemide, losartan and valsartan was still within their

therapeutic window, a significant inhibition occurred, which is further evidence of OAT1-mediated handling of the drugs, concomitant with the PBUTs (**Supplementary Table S5**). Of note, the concentrations of IS and PCS were higher than their IC_{50} values (IS IC_{50} = 25 ± 4 μM and PCS IC_{50} = 79± 14 μM) reported for the ciPTEC-OAT1 system [37]. KA on the other hand was studied here at a concentration lower than its reported IC_{50} (IC_{50} = 6 ± 1 μM) [37], which explains the slight reduction in fluorescein uptake.

For KA-ARBs co-incubation, the inhibitory potential was lower than when the cells were exposed to the drug alone, despite the increase in drug concentration, an indication that KA compromises the uptake of ARBs in favor of fluorescein, suggesting that the toxin acts as a negative allosteric modulator, an effect previously documented for *α*7 nicotinic receptors [67]. Such effect was not observed for furosemide and statins, for which the drug-KA curves overlapped with those of the drugs alone.

This study has some limitations that should be addressed in future research. First, PBUTs in plasma are highly bound to plasma proteins (90-95% for IS [68] and PCS and 70% for KA [69]) and their renal excretion depends largely on active tubular secretion, which shifts the binding and powers the active secretion of the free fraction. The same holds true for the drugs tested in our study (**Supplementary Table S6**). Thus, future research will be needed to elucidate the contribution of protein binding in drug-toxins interactions with the transporters. Recently, we have demonstrated that protein binding positively affects the renal tubular clearance of uremic toxins (IS and KA) using the ciPTEC-OAT1 model [37, 70]. As demonstrated by others, the binding capacity of albumin is diminished in CKD patients, most likely due to posttranslational modifications of albumin sites which could contribute to less efficient transport of uremic toxins by the renal tubular excretory machinery [70-72], thus resulting in further elevated plasma levels and their well-known consequences. Moreover, studies have revealed that interactions between drugs and uremic toxins could result in altered protein binding affinities [73-76].

Second, our study design relied on the use of flat monolayers of ciPTEC-OAT1. Herein, the intracellular accumulation of fluorescein was used as a measure of OAT1 activity. With the uptake transporters at the basolateral site, the proximal tubule cells possess a series of renal efflux transporters in the apical membrane responsible for the excretion of endo- and xenobiotics into the pro-urine. Although this 2D configuration cannot replicate the basolateral and apical compartments and does not sustain the monolayer polarization, it allows for high throughput screening of multiple drugs, toxins and their combination. A 3D configuration would permit the exposure of drugs and toxins at the basolateral side, with excretion at the apical side, as previously shown by us [37]. However, such systems are labor and time consuming

and difficult to standardize [55].

Kidney failure not only alters the renal excretion processes, but also the non-renal disposition of drugs that are extensively metabolized by the liver. Their pharmacokinetics is often unpredictable, possibly due to alterations in the expression and activity of extra-renal DMEs and transporters. Uremic toxins interfere with transcriptional activation and directly inhibit the activity of many members of the cytochrome P450 enzyme (CYP) family and SLC and ABC drug transporters. Recent evidence suggests that PBUTs can alter the hepatocyte mitochondrial function and the bile acid transport and synthesis [77]. Therefore, drug-PBUTs interactions in relation to drug handling by hepatocytes is primordial.

To summarize, the results of this study indicate a potential interaction of commonly prescribed drugs in CKD and PBUTs secretion, thus bringing another layer of complexity in the management of CKD. Our results show that the drug-toxins interactions with transporters lead to altered and heterogeneous uptake patterns, based on their affinity for the transporters within a uremic microenvironment. The immediate effect of these interactions could result in potential inhibition of uremic toxins or drug excretion, thus leading to their accumulation within the blood and systemic toxicity. Finally, this study contributes to the further advancement in understanding drug-toxins interaction and alterations in drug pharmacokinetics that aid in appropriate dose adjustment in CKD patients.

AUTHOR CONTRIBUTIONS

Conceptualization, **S.M.M.**, **R.M.** and **K.G.F.G.**; Methodology, **S.M.M.** and **M.F.S.**; Formal analysis, **S.M.M.** and **M.F.S.**; Data curation, **S.M.M.**, **J.F.** and **M.F.S.**; Data interpretation, **S.M.M.**, **R.M.** and **K.G.F.G.**; Writing—original draft preparation, **S.M.M.**; Writing—review and editing, **S.M.M.**, **D.S.**, **M.C.V.**, **K.G.F.G.**, and **R.M**.; Supervision, **K.G.F.G** and **R.M.**; Funding acquisition, **D.S.**, **M.C.V**, **K.G.F.G.**, and **R.M.**

FUNDING

This research was funded by the Strategic Agency of the University of Twente, University of Utrecht and University Medical Center Utrecht and the “European Uremic Toxin working group” (EUTox) of the “European Society for Artificial Organs” (ESAO) endorsed by the “European Renal Association-European Dialysis Transplantation Association” (ERA-EDTA), of which D.S and R.M. are members. J.F. received funding from the European Union’s Horizon 2020 research and innovation programme under the Marie Skłodowska-Curie grant agreement No 813839. M.C.V. and R.M. kindly acknowledge support by RegMed XB (REGenerative MEDicine crossing Borders) powered by Top Sector Life Sciences & Health (Health~Holland).

ACKNOWLEDGEMENTS

The authors acknowledge the valuable support of Katja Jansen and Anne Metje van Genderen for the interpretation of the concentration-dependent inhibition curves.

CONFLICTS OF INTEREST

The authors declare no conflict of interest.

SUPPLEMENTARY MATERIALS

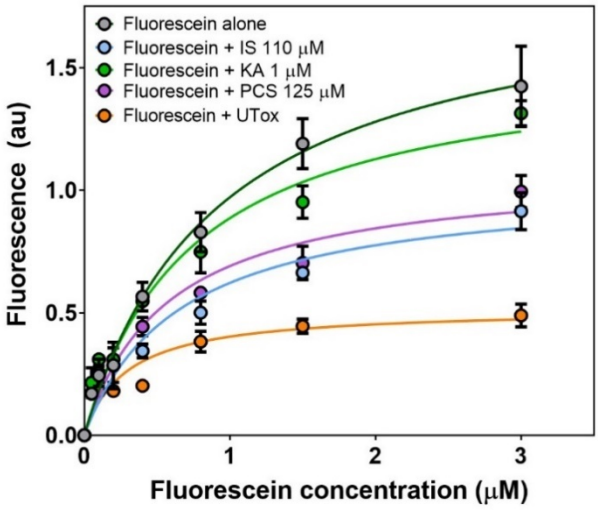

Supplementary Figure S1. Concentration-dependent OAT1-mediated uptake of fluorescein (0-3*μ*M) after 10 min incubation in ciPTEC-OAT1 in the presence of selected uremic toxins. The curves (n=3) were fitted according to a Michaelis-Menten model.

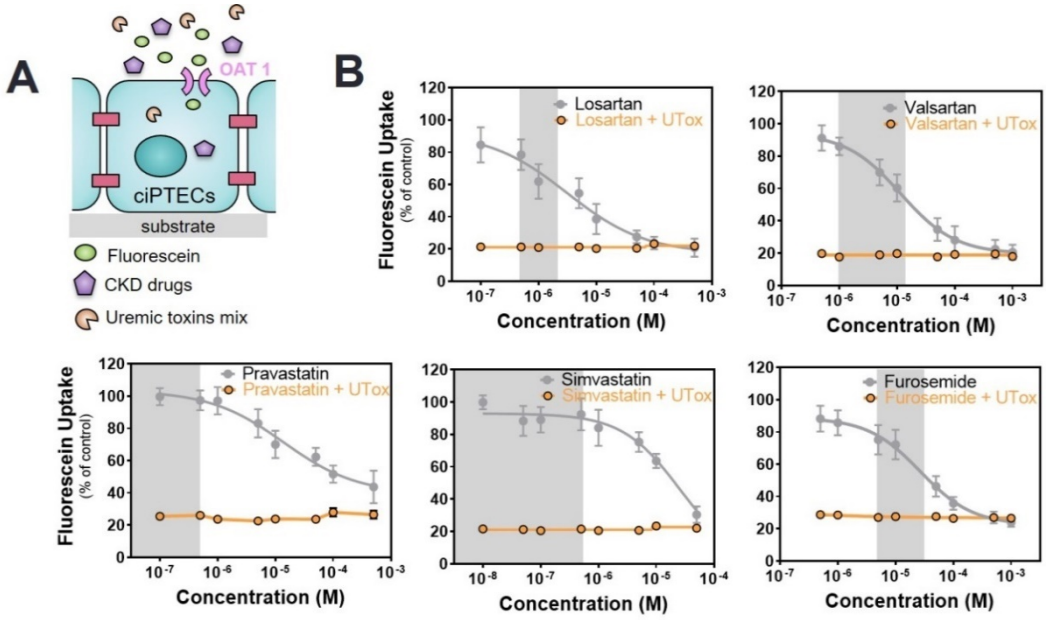

Supplementary Figure S2. **Interaction between drugs and uremic toxins mix (UTox) to inhibit OAT1-mediated fluorescein uptake.** (**A**) Schematic representation of the co-incubation of fluorescein with variable concentrations of drugs and UTox. (**B**) The drug alone (grey line) shows a concentration-dependent inhibition effect. The incubation with UTox alone results in a strong inhibitory effect, which is maintained during co-incubation with selected drugs (orange line). Grey regions indicate the therapeutic window of the respective drug.

Supplementary Table S1. Concentrations of PBUTs used in the present study (individual and in UTox). Concentrations are adapted from EUToX Uremic Solutes Database (http://www.uremic-toxins.org/DataBase.html) and Jansen *et al.* [37]

Compound	Concentration (μM)		
		Individual	
Indoxyl sulfate		110	
Kynurenic acid		1	
p-Cresylsulfate		125	
Uremic toxin mix (UTox)	**Uremic concentration (μM)**		**IC_{50} (μM) [37]**
Indoxyl sulfate	173.5 ± 121.9	100	25 ± 4
Indoxyl-β-D-glucoronide	9.4 ± 9.4	10	492 ± 68
Indole-3-acetic acid	11.4 ± 2.3	10	19 ± 2
Kynurenic acid	0.8 ± 0.4	1	6 ± 1
L-Kynurenine	3.3 ± 0.9	5	65 ± 8
Hippuric acid	608.4 ± 362.8	300	5 ± 1
p-Cresylglucuronide	30.1 ± 6.7	40	2650 ± 922
p-Cresylsulfate	122.2 ± 90.3	125	79 ± 14

Supplementary Table S2. Michaelis-Menten parameters for concentration-dependent OAT1-mediated fluorescein (FL) uptake in ciPTEC-OAT1 in the presence of selected uremic toxins.

Compound	Compound concentration (μM)	K_m (μM)	V_{max} (au)	R square
FL alone	0-3	0.93 ± 0.09	1.87 ± 0.07	0.971
FL + IS	110	0.66 ± 0.10	1.03 ± 0.06	0.907
FL + KA	1	0.75 ± 0.08	1.55 ± 0.67	0.954
FL + pCS	125	0.57 ± 0.07	1.09 ± 0.49	0.938
FL + UTox	mix	0.29 ± 0.03	0.52 ± 0.03	0.852

Supplementary Table S3. Panel of selected drugs tested for their inhibitory effect over the fluorescein OAT1-mediated uptake in ciPTEC-OAT1: characteristics and range of concentrations used within the study.

Drug	Molecular weight (g/mol)	Catalog number (Sigma)	Stock concentration	Solvent	Range of concentrations
ACEIs					
Captopril	217	C4042	100mM	MilliQ	500nM-mM
Enalaprilate	384	E9658	10mM	MilliQ	500nM-1mM
Lisinopril	441	L0702000	50mM	MilliQ	100nM-500μM
ARBs					
Valsartan	435	SML0142	10mM	DMSO	50 nM-1mM
Losartan	422	Y0001062	50mM	DMSO	100nM-500μM
STATINS					
Simvastatin	418	S6196	5mM	DMSO	10nM-50μM
Pravastatin	446	P4498	50mM	MilliQ	100nM-500μM
DIURETICS					
Furosemide	330	F4381	100mM	DMSO	500nM-1mM
H2RA					
Cimetidine	252	C4522	150mM	MilliQ	500nM-1mM

Abbreviations: ACEIs, angiotensin-converting enzyme inhibitors; **ARBs**, angiotensin receptor blockers; **H2RA**, histamine H_2 receptor antagonists.

Supplementary Table S4. Overview of the percentage (%) reduction of fluorescein uptake in the presence of UTox and drugs (at the lowest concentration).

Toxin	Percentage (%) fluorescein uptake at the lowest drug concentration					
	No Drug	ARBs		STATINS		DIURETICS
	Reference	Losartan	Valsartan	Pravastatin	Simvastatin	Furosemide
UTox	34.4 ± 8.3	23.5 ± 3.5	24.7 ± 4.5	27.8 ± 2.6	25.7 ± 2.9	28.7 ± 3.2

Abbreviations: UTox, uremic toxin mix; **ARBs**, angiotensin receptor blockers.

Supplementary Table S5. Physicochemical determinants of human renal clearance of tested drugs.

Drug	Total CL (mL/min/kg) [78]	Renal CL (mL/min/kg) [78]	Renal clearance (% of total CL)	Protein binding (%) (www.drugbank.ca)	$T_{1/2}$ (h) [44]
ACEIs					
Captopril	12	12	100	25-30	1-2
Enalaprilate	1.6	1.6	100	50	8-11
Lisinopril	1.2	1.2	100	negligible	12
ARBs					
Losartan	8.2	0.9	11	99	1.5-2
Valsartan	0.49	0.14	29	94-97	6-9
DIURETICS					
Furosemide	2.4	1.7	71	95-99	1-3
STATINS					
Pravastatin	14	6.3	45	60	1-2.5 [45]
Simvastatin	-	-	13	95	2
H2RA					
Cimetidine	8.1	7.9	97	20	1.5-4

Abbreviations: CL, clearance; **ARBs**, angiotensin receptor blockers; **H2RA**, histamine H_2 receptor antagonists.

Supplementary Table S6. Overview of the lowest drug concentrations at which a statistically significant decrease ($p<0.05$) of the percentage (%) of fluorescein uptake was observed.

	Drug concentration (μM)					
	No Drug	ARBs		STATINS		DIURETICS
PBUTs	**% FL uptake** *reference values*	**Losartan**	**Valsartan**	**Pravastatin**	**Simvastatin**	**Furosemide**
IS	44.0 ± 5.4	1*	5*	5	5	50
KA	88.2 ± 8.5	5	10*	5	10	5*
PCS	46.7 ± 4.5	1*	1*	1*	1*	5*

*Indicates concentrations that fall in the therapeutic concentration range. **Abbreviations: FL**, fluorescein; **PBUTs**, protein-bound uremic toxins; **IS**, indoxyl sulfate; **KA**, kynurenic acid; **PCS**, p-cresylsulfate; **ARBs**, angiotensin receptor blockers.

REFERENCES

1. M. T. James, B. R. Hemmelgarn and M. Tonelli. Early recognition and prevention of chronic kidney disease. Lancet 2010;375(9722):1296-1309

2. C. Ronco, M. Haapio, A. A. House*, et al.* Cardiorenal syndrome. J Am Coll Cardiol 2008;52(19):1527-1539

3. H. Fujii, S. Goto and M. Fukagawa. Role of Uremic Toxins for Kidney, Cardiovascular, and Bone Dysfunction. Toxins (Basel) 2018;10(5)

4. R. Vanholder, R. De Smet and N. Lameire. Protein-bound uremic solutes: the forgotten toxins. Kidney Int Suppl 2001;78:S266-270

5. S. Liabeuf, T. B. Drueke and Z. A. Massy. Protein-bound uremic toxins: new insight from clinical studies. Toxins (Basel) 2011;3(7):911-919

6. S. Ito and M. Yoshida. Protein-bound uremic toxins: new culprits of cardiovascular events in chronic kidney disease patients. Toxins (Basel) 2014;6(2):665-678

7. A. J. Prokopienko and T. D. Nolin. Microbiota-derived uremic retention solutes: perpetrators of altered nonrenal drug clearance in kidney disease. Expert Rev Clin Pharmacol 2018;11(1):71-82

8. W. C. Liu, C. C. Wu, P. S. Lim*, et al.* Effect of uremic toxin-indoxyl sulfate on the skeletal system. Clin Chim Acta 2018;484:197-206

9. Y. T. Lin, P. H. Wu, S. S. Liang*, et al.* Protein-bound uremic toxins are associated with cognitive function among patients undergoing maintenance hemodialysis. Sci Rep 2019;9(1):20388

10. S. K. Nigam, W. Wu, K. T. Bush*, et al.* Handling of Drugs, Metabolites, and Uremic Toxins by Kidney Proximal Tubule Drug Transporters. Clin J Am Soc Nephrol 2015;10(11):2039-2049

11. J. Jansen, J. Jankowski, P. R. Gajjala*, et al.* Disposition and clinical implications of protein-bound uremic toxins. Clin Sci (Lond) 2017;131(14):1631-1647

12. R. Vanholder, E. Schepers, A. Pletinck*, et al.* The uremic toxicity of indoxyl sulfate and p-cresyl sulfate: a systematic review. J Am Soc Nephrol 2014;25(9):1897-1907

13. M. Murray and F. Zhou. Trafficking and other regulatory mechanisms for organic anion transporting polypeptides and organic anion transporters that modulate cellular drug and xenobiotic influx and that are dysregulated in disease. Br J Pharmacol 2017;174(13):1908-1924

14. D. Xu and G. You. Loops and layers of post-translational modifications of drug transporters. Adv Drug Deliv Rev 2017;116:37-44

15. T. Sato, H. Yamaguchi, T. Kogawa*, et al.* Organic anion transporting polypeptides 1B1 and 1B3 play an important role in uremic toxin handling and drug-uremic toxin interactions in the liver. J Pharm Pharm Sci 2014;17(4):475-484

16. H. J. Manley, C. G. Garvin, D. K. Drayer*, et al.* Medication prescribing patterns in ambulatory haemodialysis patients: comparisons of USRDS to a large not-for-profit dialysis provider. Nephrol Dial Transplant 2004;19(7):1842-1848

17. Y. W. Chiu, I. Teitelbaum, M. Misra*, et al.* Pill burden, adherence, hyperphosphatemia, and quality of life in maintenance dialysis patients. Clin J Am Soc Nephrol 2009;4(6):1089-1096

18. K. Zandi-Nejad and B. M. Brenner. Strategies to retard the progression of chronic kidney disease. Med Clin North Am 2005;89(3):489-509

19. R. Kazancioglu. Risk factors for chronic kidney disease: an update. Kidney Int Suppl (2011) 2013;3(4):368-371

20. S. Said and G. T. Hernandez. The link between chronic kidney disease and cardiovascular disease. J Nephropathol 2014;3(3):99-104

21. A. K. Bello, M. Alrukhaimi, G. E. Ashuntantang*, et al.* Complications of chronic kidney disease: current state, knowledge gaps, and strategy for action. Kidney Int Suppl (2011) 2017;7(2):122-129
22. A. S. Go, G. M. Chertow, D. Fan*, et al.* Chronic kidney disease and the risks of death, cardiovascular events, and hospitalization. N Engl J Med 2004;351(13):1296-1305
23. D. S. Keith, G. A. Nichols, C. M. Gullion*, et al.* Longitudinal follow-up and outcomes among a population with chronic kidney disease in a large managed care organization. Arch Intern Med 2004;164(6):659-663
24. E. Ku, C. E. McCulloch, E. Vittinghoff*, et al.* Use of Antihypertensive Agents and Association With Risk of Adverse Outcomes in Chronic Kidney Disease: Focus on Angiotensin-Converting Enzyme Inhibitors and Angiotensin Receptor Blockers. J Am Heart Assoc 2018;7(19):e009992
25. M. R. Weir, J. I. Lakkis, B. Jaar*, et al.* Use of Renin-Angiotensin System Blockade in Advanced CKD: An NKF-KDOQI Controversies Report. Am J Kidney Dis 2018;72(6):873-884
26. X. Xie, Y. Liu, V. Perkovic*, et al.* Renin-Angiotensin System Inhibitors and Kidney and Cardiovascular Outcomes in Patients With CKD: A Bayesian Network Meta-analysis of Randomized Clinical Trials. Am J Kidney Dis 2016;67(5):728-741
27. S. D. Navaneethan, F. Pansini and G. F. Strippoli. Statins in patients with chronic kidney disease: evidence from systematic reviews and randomized clinical trials. PLoS Med 2006;3(5):e123
28. V. Tsimihodimos, Z. Mitrogianni and M. Elisaf. Dyslipidemia associated with chronic kidney disease. Open Cardiovasc Med J 2011;5:41-48
29. R. Masereeuw, H. A. Mutsaers, T. Toyohara*, et al.* The kidney and uremic toxin removal: glomerulus or tubule? Semin Nephrol 2014;34(2):191-208
30. S. K. Nigam, K. T. Bush, G. Martovetsky*, et al.* The organic anion transporter (OAT) family: a systems biology perspective. Physiol Rev 2015;95(1):83-123
31. T. Deguchi, H. Kusuhara, A. Takadate*, et al.* Characterization of uremic toxin transport by organic anion transporters in the kidney. Kidney Int 2004;65(1):162-174
32. W. Wu, K. T. Bush and S. K. Nigam. Key Role for the Organic Anion Transporters, OAT1 and OAT3, in the in vivo Handling of Uremic Toxins and Solutes. Sci Rep 2017;7(1):4939
33. S. K. Nigam and K. T. Bush. Uraemic syndrome of chronic kidney disease: altered remote sensing and signalling. Nat Rev Nephrol 2019;15(5):301-316
34. J. Jansen, C. M. Schophuizen, M. J. Wilmer*, et al.* A morphological and functional comparison of proximal tubule cell lines established from human urine and kidney tissue. Exp Cell Res 2014;323(1):87-99
35. M. J. Wilmer, M. A. Saleem, R. Masereeuw*, et al.* Novel conditionally immortalized human proximal tubule cell line expressing functional influx and efflux transporters. Cell Tissue Res 2010;339(2):449-457
36. T. T. Nieskens, J. G. Peters, M. J. Schreurs*, et al.* A Human Renal Proximal Tubule Cell Line with Stable Organic Anion Transporter 1 and 3 Expression Predictive for Antiviral-Induced Toxicity. AAPS J 2016;18(2):465-475
37. J. Jansen, M. Fedecostante, M. J. Wilmer*, et al.* Bioengineered kidney tubules efficiently excrete uremic toxins. Sci Rep 2016;6:26715
38. D. M. Truong, G. Kaler, A. Khandelwal*, et al.* Multi-level analysis of organic anion transporters 1, 3, and 6 reveals major differences in structural determinants of antiviral discrimination. J Biol Chem 2008;283(13):8654-8663
39. S. A. Lacy, M. J. Hitchcock, W. A. Lee*, et al.* Effect of oral probenecid coadministration on the chronic toxicity and pharmacokinetics of intravenous cidofovir in cynomolgus monkeys. Toxicol Sci 1998;44(2):97-106

40. B. M. Tune, K. Y. Wu and R. L. Kempson. Inhibition of transport and prevention of toxicity of cephaloridine in the kidney. Dose-responsiveness of the rabbit and the guinea pig to probenecid. J Pharmacol Exp Ther 1977;202(2):466-471
41. R. Vanholder, R. De Smet, G. Glorieux*, et al.* Review on uremic toxins: classification, concentration, and interindividual variability. Kidney Int 2003;63(5):1934-1943
42. F. Duranton, G. Cohen, R. De Smet*, et al.* Normal and pathologic concentrations of uremic toxins. J Am Soc Nephrol 2012;23(7):1258-1270
43. H. Ehrsson and I. Wallin. Cimetidine as an organic cation transporter antagonist. Am J Pathol 2010;177(3):1573-1574; author reply 1574
44. M. Schulz, S. Iwersen-Bergmann, H. Andresen*, et al.* Therapeutic and toxic blood concentrations of nearly 1,000 drugs and other xenobiotics. Crit Care 2012;16(4):R136
45. R. Siekmeier, W. Gross and W. März. Determination of pravastatin by high performance liquid chromatography. Int J Clin Pharmacol Ther 2000;38(9):419-425
46. K. S. Patrick. Goodman and Gilman's The Pharmacological Basis of Therapeutics. 10th Edition Edited by J. G. Hardman, L. E. Limbird, and A. G. Gilman. McGraw Hill, New York. 2001. xxvii + 2148 pp. 21 × 26 cm. ISBN 0-07-1354469-7. $125.00. Journal of Medicinal Chemistry 2002;45(6):1392-1393
47. M. Takeda, R. Noshiro, M. L. Onozato*, et al.* Evidence for a role of human organic anion transporters in the muscular side effects of HMG-CoA reductase inhibitors. Eur J Pharmacol 2004;483(2-3):133-138
48. Y. Miyamoto, H. Watanabe, T. Noguchi*, et al.* Organic anion transporters play an important role in the uptake of p-cresyl sulfate, a uremic toxin, in the kidney. Nephrol Dial Transplant 2011;26(8):2498-2502
49. M. L. Tan, K. Yoshida, P. Zhao*, et al.* Effect of Chronic Kidney Disease on Nonrenal Elimination Pathways: A Systematic Assessment of CYP1A2, CYP2C8, CYP2C9, CYP2C19, and OATP. Clin Pharmacol Ther 2018;103(5):854-867
50. A. Saleem, I. Masood and T. M. Khan. Clinical relevancy and determinants of potential drug-drug interactions in chronic kidney disease patients: results from a retrospective analysis. Integr Pharm Res Pract 2017;6:71-77
51. K. Rowland Yeo, M. Aarabi, M. Jamei*, et al.* Modeling and predicting drug pharmacokinetics in patients with renal impairment. Expert Rev Clin Pharmacol 2011;4(2):261-274
52. R. K. Verbeeck and F. T. Musuamba. Pharmacokinetics and dosage adjustment in patients with renal dysfunction. Eur J Clin Pharmacol 2009;65(8):757-773
53. F. U.S. Department of Health and Human Services, Center for Drug Evaluation and Research (CDER). Clinical Drug Interaction Studies — Study Design, Data Analysis, and Clinical Implications Guidance for Industry. http://www.fda.gov/Drugs/GuidanceComplianceRegulatoryInformation/Guidances/default.htm. 2017(Center for Drug Evaluation and Research)
54. K. M. Giacomini and S. M. Huang. Transporters in drug development and clinical pharmacology. Clin Pharmacol Ther 2013;94(1):3-9
55. J. Y. Soo, J. Jansen, R. Masereeuw*, et al.* Advances in predictive in vitro models of drug-induced nephrotoxicity. Nat Rev Nephrol 2018;14(6):378-393
56. G. Burckhardt. Drug transport by Organic Anion Transporters (OATs). Pharmacol Ther 2012;136(1):106-130
57. D. A. Sica. Diuretic use in renal disease. Nat Rev Nephrol 2011;8(2):100-109

58. M. Sato, T. Iwanaga, H. Mamada*, et al.* Involvement of uric acid transporters in alteration of serum uric acid level by angiotensin II receptor blockers. Pharm Res 2008;25(3):639-646
59. K. Kuze, P. Graves, A. Leahy*, et al.* Heterologous expression and functional characterization of a mouse renal organic anion transporter in mammalian cells. J Biol Chem 1999;274(3):1519-1524
60. M. Sugawara, T. Mochizuki, Y. Takekuma*, et al.* Structure-affinity relationship in the interactions of human organic anion transporter 1 with caffeine, theophylline, theobromine and their metabolites. Biochim Biophys Acta 2005;1714(2):85-92
61. M. Reyes and L. Z. Benet. Effects of uremic toxins on transport and metabolism of different biopharmaceutics drug disposition classification system xenobiotics. J Pharm Sci 2011;100(9):3831-3842
62. H. A. Mutsaers, M. J. Wilmer, D. Reijnders*, et al.* Uremic toxins inhibit renal metabolic capacity through interference with glucuronidation and mitochondrial respiration. Biochim Biophys Acta 2013;1832(1):142-150
63. H. Sun, L. Frassetto and L. Z. Benet. Effects of renal failure on drug transport and metabolism. Pharmacol Ther 2006;109(1-2):1-11
64. A. Enomoto, M. Takeda, K. Taki*, et al.* Interactions of human organic anion as well as cation transporters with indoxyl sulfate. Eur J Pharmacol 2003;466(1-2):13-20
65. Y. Uwai, H. Honjo and K. Iwamoto. Interaction and transport of kynurenic acid via human organic anion transporters hOAT1 and hOAT3. Pharmacol Res 2012;65(2):254-260
66. S. Eloot, W. Van Biesen, S. Roels*, et al.* Spontaneous variability of pre-dialysis concentrations of uremic toxins over time in stable hemodialysis patients. PLoS One 2017;12(10):e0186010
67. C. Hilmas, E. F. Pereira, M. Alkondon*, et al.* The brain metabolite kynurenic acid inhibits alpha7 nicotinic receptor activity and increases non-alpha7 nicotinic receptor expression: physiopathological implications. J Neurosci 2001;21(19):7463-7473
68. L. Viaene, P. Annaert, H. de Loor*, et al.* Albumin is the main plasma binding protein for indoxyl sulfate and p-cresyl sulfate. Biopharm Drug Dispos 2013;34(3):165-175
69. N. Fabresse, I. Uteem, E. Lamy*, et al.* Quantification of free and protein bound uremic toxins in human serum by LC-MS/MS: Comparison of rapid equilibrium dialysis and ultrafiltration. Clin Chim Acta 2020;507:228-235
70. T. K. van der Made, M. Fedecostante, D. Scotcher*, et al.* Quantitative Translation of Microfluidic Transporter in Vitro Data to in Vivo Reveals Impaired Albumin-Facilitated Indoxyl Sulfate Secretion in Chronic Kidney Disease. Mol Pharm 2019;16(11):4551-4562
71. O. Deltombe, W. Van Biesen, G. Glorieux*, et al.* Exploring Protein Binding of Uremic Toxins in Patients with Different Stages of Chronic Kidney Disease and during Hemodialysis. Toxins (Basel) 2015;7(10):3933-3946
72. M. Rueth, H. D. Lemke, C. Preisinger*, et al.* Guanidinylations of albumin decreased binding capacity of hydrophobic metabolites. Acta Physiol (Oxf) 2015;215(1):13-23
73. N. Takamura, T. Maruyama and M. Otagiri. Effects of uremic toxins and fatty acids on serum protein binding of furosemide: possible mechanism of the binding defect in uremia. Clin Chem 1997;43(12):2274-2280
74. G. Mingrone, R. De Smet, A. V. Greco*, et al.* Serum uremic toxins from patients with chronic renal failure displace the binding of L-tryptophan to human serum albumin. Clin Chim Acta 1997;260(1):27-34
75. N. Florens, D. Yi, L. Juillard*, et al.* Using binding competitors of albumin to promote the removal of protein-bound uremic toxins in hemodialysis: Hope or pipe dream? Biochimie 2018;144:1-8

76. T. Santana Machado, C. Cerini and S. Burtey. Emerging Roles of Aryl Hydrocarbon Receptors in the Altered Clearance of Drugs during Chronic Kidney Disease. Toxins (Basel) 2019;11(4)
77. K. M. Weigand, T. J. J. Schirris, M. Houweling*, et al.* Uremic solutes modulate hepatic bile acid handling and induce mitochondrial toxicity. Toxicol In Vitro 2019;56:52-61
78. M. V. Varma, B. Feng, R. S. Obach*, et al.* Physicochemical determinants of human renal clearance. J Med Chem 2009;52(15):4844-4852

CHAPTER 4

Bioengineered Kidney Tubules Efficiently Clear Uremic Toxins in Experimental Dialysis Conditions

João Faria[1], Sabbir Ahmed[1], Dimitrius Stamatialis[2], Marianne C. Verhaar[3], Rosalinde Masereeuw[1], Karin G.F. Gerritsen[3], Silvia M. Mihăilă[1]

[1] Division of Pharmacology, Utrecht Institute for Pharmaceutical Sciences, Utrecht University, 3584 CG Utrecht, The Netherlands

[2] Advanced Organ Bioengineering and Therapeutics, Faculty of Science and Technology, Technical Medical Centre, University of Twente, 7522 NB Enschede, The Netherlands

[3] Department of Nephrology and Hypertension, University Medical Center, 3508 GA Utrecht, The Netherlands

Published in Int J Mol Sci. 2023;24(15):12435

ABSTRACT

Patients with end-stage kidney disease (ESKD) suffer from high levels of protein-bound uremic toxins (PBUTs) that contribute to various comorbidities. Conventional dialysis methods are ineffective in removing these PBUTs. A potential solution could be offered by a bioartificial kidney (BAK) composed of porous membranes covered by proximal tubule epithelial cells (PTEC) that actively secrete PBUTs. However, BAK development is currently being hampered by a lack of knowledge regarding the cytocompatibility of dialysis fluid (DF) that comes in contact with the PTECs. Here, we conducted a comprehensive functional assessment of DF on human conditionally immortalized PTEC (ciPTECs) cultured as monolayers in well plates, on Transwell® inserts, or on hollow fiber membranes (HFM) that form functional units of a BAK. We evaluated cell viability markers, monolayer integrity and PBUT clearance. Our results show that exposure to DF did not affect ciPTECs viability, membrane integrity, or function. Seven anionic PBUTs were efficiently cleared from the perfusion fluid containing a PBUTs cocktail or uremic plasma, which were enhanced in the presence of albumin. Overall, our findings support that DF is cytocompatible and does not compromise PTEC function, paving the way for further advancements in BAK development and its potential clinical application.

KEYWORDS: bioartificial kidney, dialysis fluid, uremic plasma, uremic toxins, proximal tubule epithelial cells**.**

1. INTRODUCTION

Chronic kidney disease (CKD) is a progressive condition characterized by the deterioration of kidney function, ultimately leading to end-stage kidney disease (ESKD). As kidney function declines, endogenous metabolites that are normally cleared by the kidney accumulate in the plasma of CKD patients. These metabolites are referred to as uremic retention solutes, and their accumulation can lead to cellular dysfunction, inflammation, and oxidative stress [1], all of which are associated with CKD-related comorbidities such as cardiovascular disease, secondary immunodeficiency and neurologic manifestations, and to progression of CKD itself [2]. Uremic retention solutes are classified based on their physicochemical properties and dialytic removal patterns [2]. Among these uremic retention solutes, protein-bound uremic toxins (PBUTs) are of particular concern, as they have a strong binding affinity towards plasma proteins, in particular albumin, and are not effectively removed by conventional dialysis methods [3].

To address the challenge of enhancing PBUTs clearance, we drew inspiration from the natural process of PBUTs elimination within the kidneys. Proximal tubule epithelial cells (PTECs) in the kidney express key membrane transporters, the organic anion transporters (OATs), which are responsible for the secretion of anionic PBUTs from the blood into urine [4]. OAT1 (*SLC22A6*) and its homolog OAT3 (*SLC22A*8) are the most important transporters involved in the uptake and excretion of a variety of endogenous metabolites, including PBUTs, but also drugs administered to patients, with OAT1 having a higher capacity in handling the smaller compounds [4-6]. Incorporating an active secretory compartment composed of PTECs into the development of a bioartificial kidney (BAK) device would facilitate the efficient removal of PBUTs. Previously, we designed a BAK using porous hollow fiber membranes (HFMs) covered with a monolayer of conditionally immortalized proximal tubule cells (ciPTECs) on the outer surface [7]. In this configuration, the cells demonstrated the expression and function of the basolateral OAT1 and an effective removal of the PBUTs kynurenic acid (KA) and indoxyl sulfate (IS) [7].

To ensure the clinical suitability of the BAK, it is of paramount importance to determine whether these bioengineered tubules can effectively secrete PBUTs under conditions mimicking their intended use, *viz.* as an extracorporeal device connected in series with a conventional hemodialysis filter. In this setup, blood is pumped through the dialyzer (hemofilter or BAK), while dialysis fluid (DF) is perfused on the other side of the membranes, as described by Ramada *et. al* [8]. DF is an essential component in standard dialysis, as it facilitates the purification process and enables the removal of harmful substances from the body [9]. Given the direct exposure of cells to DF, it is essential to assess its effects on cellular homeostasis.

Therefore, the aim of this study was to evaluate the function of bioengineered kidney tubules under experimental dialysis conditions resembling those encountered in the intended application of BAK. Specifically, we examined cell viability markers following DF exposure, assessed the effects of DF in combination with healthy and uremic plasma (HP and UP, respectively) at the 'blood side' on monolayer integrity using a Transwell® system, and investigated the potential of bioengineered kidney tubules for PBUTs clearance during exposure to DF. We perfused these tubules with UP at the basal side and DF at apical side to simulate experimental dialysis conditions in patients with ESKD.

2. MATERIALS AND METHODS

2.1. Reagents

DF was freshly prepared by adding sodium hydrogen carbonate (Fresenius, Zeist, The Netherlands) to acid concentrate for bicarbonate dialysis (MTN, Neubrandenburg, Germany) followed by a dilution in demi water. The final composition of DF is provided in **Supplementary Table S1.** The DF was used within 24 h of preparation. The concentration of a panel of 7 PBUTs (indoxyl sulfate, indoxyl-β-D-glucuronide, indole-3-acetic acid, kynurenic acid, L-kynurenine, hippuric acid, *p*-cresylsulfate, *p*-cresylglucuronide), healthy and uremic plasma, HP and UP, used within this study is available in **Supplementary Table S2**. Chemicals were purchased from Sigma-Aldrich (Zwijndrecht, The Netherlands) unless stated otherwise. Of note, human serum albumin (A9511, Sigma Aldrich; HSA) used in this study was not further purified, hence minor impurities (e.g, fatty acids) could still be in its composition. Additionally, we confirmed that 1mM HSA/ Krebs-Henseleit Buffer supplemented with 10 mM HEPES (KHH buffer, pH 7.4) and used in **Section *4.5***.'s tubules did not contain considerable amounts of the PBUTs tested.

Flat type 2F iv hydrophilic polyethersulfone micro membranes (microPES, thickness 100 µm, max pore size 0.5 µm) and microPES type TF10 hollow fiber capillary membranes (wall thickness 100 µm, inner diameter 300 µm, max pore size 0.5 µm) were obtained from 3M GmbH (Wuppertal, Germany). HP and UP were obtained from the donor mini-bank of Utrecht University Medical Center (The Netherlands), with informed consent and donor anonymity ensured by internal protocols.

2.2. CiPTECs-OAT1

Conditionally immortalized proximal tubule epithelial cells overexpressing the organic anion transporter 1 (ciPTECs-OAT1) were cultured as reported previously [7]. Briefly, cells were cultured up to 60 passages in Dulbecco's Modified Eagle Medium/Nutrient Mixture F-12 (1:1 DMEM/F-12) (Gibco, Life Technologies, Paisley, UK) supplemented with 10% fetal calf serum (FCS) (Greiner Bio-One, Alphen aan den Rijn, The Netherlands), 5 µg/mL insulin, 5 µg/mL transferrin, 5 µg/mL selenium, 35 ng/mL hydrocortisone, 10 ng/mL epidermal growth factor and 40 pg/mL tri-iodothyronine, or complete culture medium. Cells were cultured at 33°C and 5% (*v*/*v*) CO_2 to allow expansion.

2.3. Evaluation of the Effects of DF on Flat Cultures of CiPTECs-OAT1

2.3.1. 2D Exposure of Cells to DF

CiPTEC-OAT1 cells were seeded at a density of 63,000 cells/cm2 in 96-well plates. Subsequently, cells were grown 24h at 33 °C, 5% (v/v) CO_2 to allow adhesion and proliferation, then transferred to 37 °C, 5% (v/v) CO_2 where they were cultured for 7 days to allow for differentiation and maturation, refreshing the medium every other day. The temperature shift ensured the maturation of cells into fully differentiated epithelial cells able to form confluent monolayers. After this period, the cells were carefully washed with Hank's balanced salt solution (HBSS, Life Technologies Europe BV, Roskilde, Denmark) and subsequently incubated to 100 µL of DF/ well for up to 240 min (the standard dialysis time). At selected time points, several assays that reflect the viability and functional performance of the cells were performed, as described below.

2.3.2. Cell Viability Assay

Cell viability was measured using PrestoBlue® cell viability reagent (Life Technologies). After exposure to DF, the cells were rinsed once with HBSS and incubated with 100 µL/ well PrestoBlue® cell viability reagent (diluted 1:10 in complete culture medium), in the dark. After 1 h incubation at 37 °C, 5% (v/v) CO_2, 80 µL were transferred from each well into a separate 96-well plate. The fluorescence was measured using a GloMax® Discover microplate reader (Promega, Wisconsin, United States), at an excitation wavelength of 530 nm and emission wavelength of 590 nm. Data were corrected for the background, normalized to untreated cells, and presented as relative percentage (%) of viability of untreated cells.

2.3.3. Intracellular Reactive Oxygen Species (ROS) Detection

Intracellular ROS generation was measured by means of cell permeant fluorogenic substrate 2′,7′-dichlorofluorescein diacetate (H2DCFDA). Briefly, cells were washed once with HBSS, immediately loaded with H2DCFDA (50 µM in serum-free medium) and incubated at 37 °C, 5% (v/v) CO_2, in the dark for 45 min. Afterwards, cells were washed with complete culture medium and exposed to DF for several periods of time, up to 240 min at 37 °C, 5% (v/v) CO_2, in the dark. H_2O_2 (500 μM) was used as a positive control. Following the incubation, cells were washed twice with HBSS and lysed using 0.1 M NaOH for 10 min. Finally, fluorescence was measured at an excitation wavelength of 490 nm and emission wavelength of 520 nm, in a GloMax® Navigator microplate reader (Promega, Wisconsin, United States). Measured

fluorescence values were corrected for the fluorescence of the blank sample (untreated lysed cells) and used to calculate relative ROS production, using untreated cells as control.

2.3.4. Lactate Dehydrogenase (LDH) Activity

The evaluation of cell membrane integrity upon exposure to DF was evaluated by measuring the extracellular LDH activity. LDH is an intracellular enzyme which catalysis NADH lactate to pyruvate. LDH is released into the supernatant from the cytosol upon cell damage. Briefly, upon exposure to DF, samples were collected on ice. LDH activity was measured using the Cytotoxicity Detection KitPLUS (Roche, Germany), following the manufacturer's protocol. Briefly, 50 µL of cell supernantant was added to a 96-well plate. In addition, a calibration curve using a NADH (1.25 mM) standard was prepared. Assay buffer was added to a final volume of 50 µL per well and then a master reaction mix was added per well (1:1, v/v). After 10 min, absorbance was measured at 450 nm in a GloMax® Navigator microplate reader (Promega, Wisconsin, United States), and every 10 min until absorbance measured in a sample was higher than the highest level of NADH in the calibration curve (12.5 nmol/well). Extracellular LDH activity was expressed as percentage (%) of the positive control at the corresponding time point. Triton X-100 (Merck, Darmstadt, Germany) at 0.5% (v/v) was used as positive control and untreated cells as negative control.

2.3.5. IL-6 and IL-8 Release

The release of IL-6 and IL-8 upon exposure to DF was measured using the Enzyme-Linked Immunosorbent Assay (ELISA). Cell culture supernatants were collected after 240 min of exposure. Afterwards, cell culture supernatants were centrifuged for 10 min, 240× g, 4 °C, and stored at –20 °C until analysis. DuoSet® ELISA Development Systems kits (IL-6 and IL-8, R&D Systems, Abingdon, UK) were used to quantify the cytokines levels in supernatants following manufacturer’s instructions. The optical density was determined using a GloMax® Navigator microplate reader (Promega, Wisconsin, United States) set to 450 nm. Untreated cells, cultured in serum-free medium, were used as negative controls, while exposure to lipopolysaccharide (LPS, Escherichia coli 0127: B8, 10 µg/mL) was used as positive control for the release of IL-6 and IL-8 [10].

2.3.6. OAT1-Mediated Fluorescein Uptake

To evaluate the effect of the DF on OAT1 activity, we performed an OAT1-mediated fluorescein uptake assay. Upon exposure to DF, ciPTECs-OAT1 were carefully washed with

HBSS and then incubated with fluorescein (1 µM) prepared in KHH buffer for 10 min at 37 °C. To confirm the activity of OAT1, probenecid (500 µM in KHH) was simultaneously incubated with fluorescein. Uptake arrest was performed by washing the monolayers with ice-cold HBSS, and then the cells were lysed by 100 µL 0.1 M NaOH for 10 min, at room temperature (RT) and under mild shaking. Intracellular fluorescence was detected using a GloMax® Navigator microplate reader (Promega, Wisconsin, United States), at excitation wavelength of 490 nm and emission wavelength of 520 nm. Untreated cells were used as positive control. Data is represented as percentage (%) of positive control.

2.4. Combinatorial Effect of DF and Plasma on CiPTECs-OAT1 Seeded onto Transwell® Inserts

2.4.1. CiPTECs-OAT1 Culture on Adapted Transwell® Inserts

To address the basal exposure to plasma and the apical exposure to DF, we have cultured ciPTECs-OAT1 cells on an adapted Transwell® (Corning Costar, NY, USA) system in which the membranes have been replaced with a flat microPES membrane with the same characteristics (porosity, pore size and thickness) as those of the HFM used for dialysis. For this purpose, round-shaped pieces of the microPES membranes (diameter 12 mm, surface growth area 1.12 cm^2) were cut from the flat sheets, mounted on empty Transwell® membrane support systems using custom-made sealing rings [11], sterilized with 0.2 % (v/v) solution of peracetic acid (Sigma Aldrich, Zwijndrecht, the Netherlands) in 4 % (v/v) ethanol for 1 h, and then extensively rinsed with HBSS. Afterwards, to ensure cell attachment and growth, a double coating was applied on the membranes based on previously reported protocol [11].

First, the membranes were incubated with sterile 2 mg/mL L-DOPA (L-3,4-dihydroxyphenylalanine, Sigma Aldrich, Zwijndrecht, the Netherlands) prepared in 10 mM Tris buffer (pH 8.5) at 37 °C for 4 h. The second coating consisted of 25 µg/mL solution of collagen IV (Sigma Aldrich, Zwijndrecht, the Netherlands), for 1 h at 37 °C. Following the coating procedure, microPES membranes were washed in HBSS and used further for cell seeding. ciPTECs-OAT1 were seeded on double-coated membranes, in the apical compartment of the Transwell® system, at 90,000 cells/cm^2.

2.4.2. Exposure to Plasma and Assessment of Monolayer Permeability

After initial proliferation at 33 °C for 3 days, and 7 days maturation at 37 °C, the apical compartment was loaded with 500 µL DF, while the basal compartment was loaded with 1 mL HP or UP and incubated for 240 min. Cultures with complete culture medium on both apical

and basal sides were used as controls. Following the incubation period, the monolayer permeability was assessed by quantifying diffusion of fluorescein isothiocyanate-inulin (FITC-inulin, Sigma Aldrich, Zwijndrecht, the Netherlands) (0.1 mg/mL in Krebs-Henseleit (KH) buffer (Sigma Aldrich, Zwijndrecht, the Netherlands) supplemented with 10 mM HEPES (Acros Organics, New Jersey, USA) from basolateral to apical compartment for 30 min at 37 °C, under gentile shaking. Coated and non-coated membranes without cells were used as controls. Fluorescence was measured at excitation wavelength of 490 nm and emission wavelength of 520 nm, by means of fluorescent plate microplate reader (Promega, Wisconsin, United States). Measured fluorescence values were used to calculate inulin-FITC concentration in apical compartment of all samples.

2.4.3. Immunocytochemistry

After the evaluation of the membrane permeability, the cells were washed with HBSS twice, fixed with 4% (w/v) paraformaldehyde in PBS for 20 min, then washed three times with 0.1% (v/v) Tween (Sigma Aldrich, Zwijndrecht, the Netherlands) solution in PBS and permeabilized with 0.3% (v/v) Triton x100 (Merck, Darmstadt, Germany) solution for 10 min. After another three washing steps with 0.1% (v/v) Tween-PBS, cells were exposed to a blocking solution ((2% (*v/v*) FCS, 2% (*w/v*) bovine serum albumin (BSA), 0.1% (*v/v*) Tween-20 in HBSS) for 30 min, followed by the incubation with Phalloidin-iFluor 594 (1:1000 in blocking solution) (Abcam, Netherlands) for 1 h at RT to stain for actin filaments. Finally, membranes were mounted on glass slides using ProLong Gold antifade reagent containing DAPI (Life Technologies, Eugene, OR, USA) and cells were imaged using confocal microscope (Leica TCS SP8 X, Leica Microsystems CMS GmbH, Wetzlar, Germany) and analyzed using Leica Application Suite X software 1.4.4 (Leica Microsystems CMS GmbH). The cell coverage was assessed using ImageJ analysis and reported as percentage (%) of coverage of phalloidin staining from the total imaged area.

2.5. Assessment of Transepithelial Transport of PBUTs on Bioengineered Kidney Tubules

2.5.1. Culture of CiPTECs-OAT1-Seeded HFM, Perfusion with Plasma and PBUTs Quantification

To assess the transepithelial transport of PBUTs from the basal compartment into the apical side, containing DF, we employed a perfusion setup consisting of HFM coated, seeded and cultured with ciPTEC-OAT1, previously described by Jansen *et al.* [7]. In this system, HFMs

measuring 1.5 cm in length, seeded with mature ciPTEC-OAT1, were loaded into a custom-made perfusion system. The apical compartment was filled with 300 µL DF. Using a perfusion pump, the HFMs were continuously perfused (6mL/ h) at the basolateral side with KHH (with and without supplementation with 1mM HSA) spiked with seven representative PBUTs at concentrations found in CKD patients (**Supplementary Table 2**) for 30 min, at RT, after which the total volume of the apical compartment was collected. In a similar fashion, the fibers were perfused with either HP or UP, respectively. Before perfusion, both HP and UP were passed through a 40 µm strainer to remove protein clumps that could obstruct the fibers. The albumin concentration in UP was found to be 0.70mM.

Total PBUTs concentrations (free + protein-bound) in the DF compartment were analyzed using a LC-MS/MS method [10, 12]. Their transepithelial clearance was calculated according to equation 1:

$$\text{Transepithelial clearance} = (U \times V) / (P \times T \times A) \quad (1)$$

where U=apical concentration (µmol/L); V= volume in the apical compartment (ml); P= basolateral concentration (µmol/L); T = time (min); A = outer surface area (cm^2).

Using the same LC-MS/MS, we have also confirmed that the 1mM HSA/KHH did not contain considerable amounts of the PBUTs studied.

2.5.2. Assessment of Monolayer Integrity Following Perfusion with Plasma

To assess the (maintenance of) monolayer integrity after the perfusion with plasma, we conducted an evaluation of FITC-inulin leakage in the apical compartment. The exposed fibers were perfused once again, this time with FITC-inulin (0.1mg/mL) in KHH for 10min. Subsequently, we measured FITC-inulin leakage in the apical compartment, as described above. The data were reported as percentage of leakage compared with the positive control. Fibers without cells were used as positive control for leakage and represented as 100% leakage.

2.5.3. Evaluation of Albumin Leakage

To investigate potential protein leakage during perfusion with plasma while exposed with DF at the apical side, a similar setup was prepared to evaluate the leakage of HSA from the basal side into the apical side. We collected the entire apical volume at specific time points and replenished it with fresh DF. Protein content was determined using the Bradford assay (BCA Protein Assay Kit, ThermoFischer) following the manufacturer's instructions. Based on the

perfusion rate, we calculated the total amount (mg) of HSA perfused through the fibers for the experimental period.

2.6. Statistical Analysis

The data and graphs were analyzed and plotted using the GraphPad Prism version 9.5.2 (GraphPad Software, Inc., San Diego, CA, USA). Quantitative data are reported as mean ± standard deviation (SD). The statistical test and replicates are indicated in the figure legends. A p-value < 0.05 was considered statistically significant.

3. RESULTS

3.1. Exposure of CiPTECs to DF in 2D Leads to Minor Alteration in Cell Viability Markers

To investigate whether DF affects cell homeostasis, ciPTECs overexpressing OAT1 (ciPTECs-OAT1) were exposed to DF (see **Supplementary Table S1** for composition) or medium (control) for up to 240 min, the standard time of a dialysis session (**Figure 1A**)**.** After 30 min of exposure to DF, the cell viability decreased slightly. This descending pattern was maintained over time reaching 80 ± 4% of control (**Figure 1B**), which is the threshold of any intervention to be considered as non-cytotoxic [13]. Furthermore, the release of LDH, a marker of plasma membrane damage, increased during the first 60 min, but remained stable for the remainder of the exposure time **(Figure 1C).** This was accompanied by an increase of intracellular ROS production, an indicator of oxidative stress (**Figure 1D**). The release of IL-6 and IL-8 was not affected (**Figure 1E-F**), suggesting that exposure to DF does not elicit an inflammatory response. We next investigated the activity of OAT1, the key transporter involved in the secretion of PBUTs, through the uptake of fluorescein as substrate [14]. We found that the OAT1-mediated uptake capacity slightly decreased over time, in line with the decrease in cell viability. Overall, these findings suggest that exposure of ciPTECs-OAT1 to DF for 4 h does not warrant concerns in terms of viability and functionality.

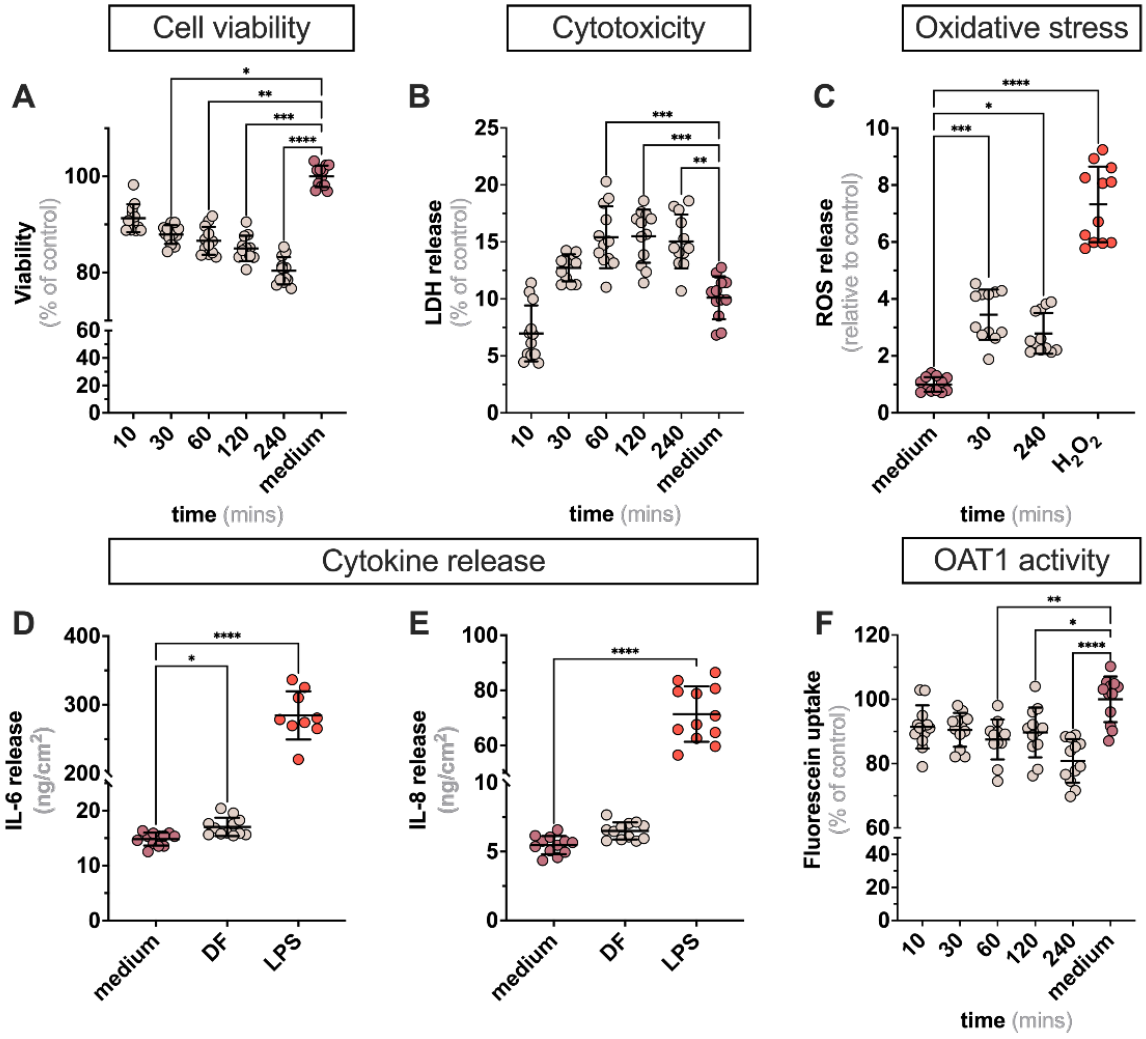

Figure 1. Characterization of ciPTECs upon exposure to DF. To assess the effect of DF on cell behavior, measurements of cell viability (**A**), cytotoxicity (**B**), oxidative stress (**C),** cytokine release (**D,E**), and OAT1 activity (**F**) were performed on ciPTECs-OAT1. H_2O_2 (500 μM) and LPS (1 µg/mL) were used as positive controls to oxidative stress and cytokine release, respectively. Data are shown as mean ± SD of four replicates from four independent experiments. * p< 0.01, ** p< 0.01, *** p< 0.005 and ****p< 0.0001 using one-way ANOVA analysis followed by Tukey's multiple comparisons test.

3.2. CiPTECs-OAT1 Cultured on Flat Membranes Show Minor Changes in Barrier Integrity upon Exposure to DF (Apically) and Plasma (Basolaterally)

Next, we investigated the effect on monolayer integrity of simultaneous exposure for 4 hours to plasma at the basal side and DF at the apical side of the cell-covered membranes. Staining for the cytoskeleton (phalloidin) allowed to visualize the coverage of the cell monolayer on the porous surface (**Figure 2A**). Cells cultured with medium in both apical and basal compartments displayed a full coverage of the membrane (**Figure 2A-B**). With the addition of DF to the apical side, the coverage percentage slightly decreased (**Figure 2B**). This trend

became more evident when HP or UP, respectively, were added to the basal side, with small cell-free areas emerging in the monolayer (**Figure 2A-B**). Furthermore, the observed gaps in the monolayer did not result in fluid flow through the gaps. We then analyzed the barrier properties of cell-seeded membranes under the same conditions, by applying FITC-inulin, a commonly used tracer to assess monolayer integrity, at the basal side (**Figure 2C**). Despite the loss in cell coverage under apical exposure to DF (**Figure 2B**), the barrier properties were not affected, as the leakage of FITC-inulin at the apical side was not enhanced in the aforementioned conditions (**Figure 2C**).

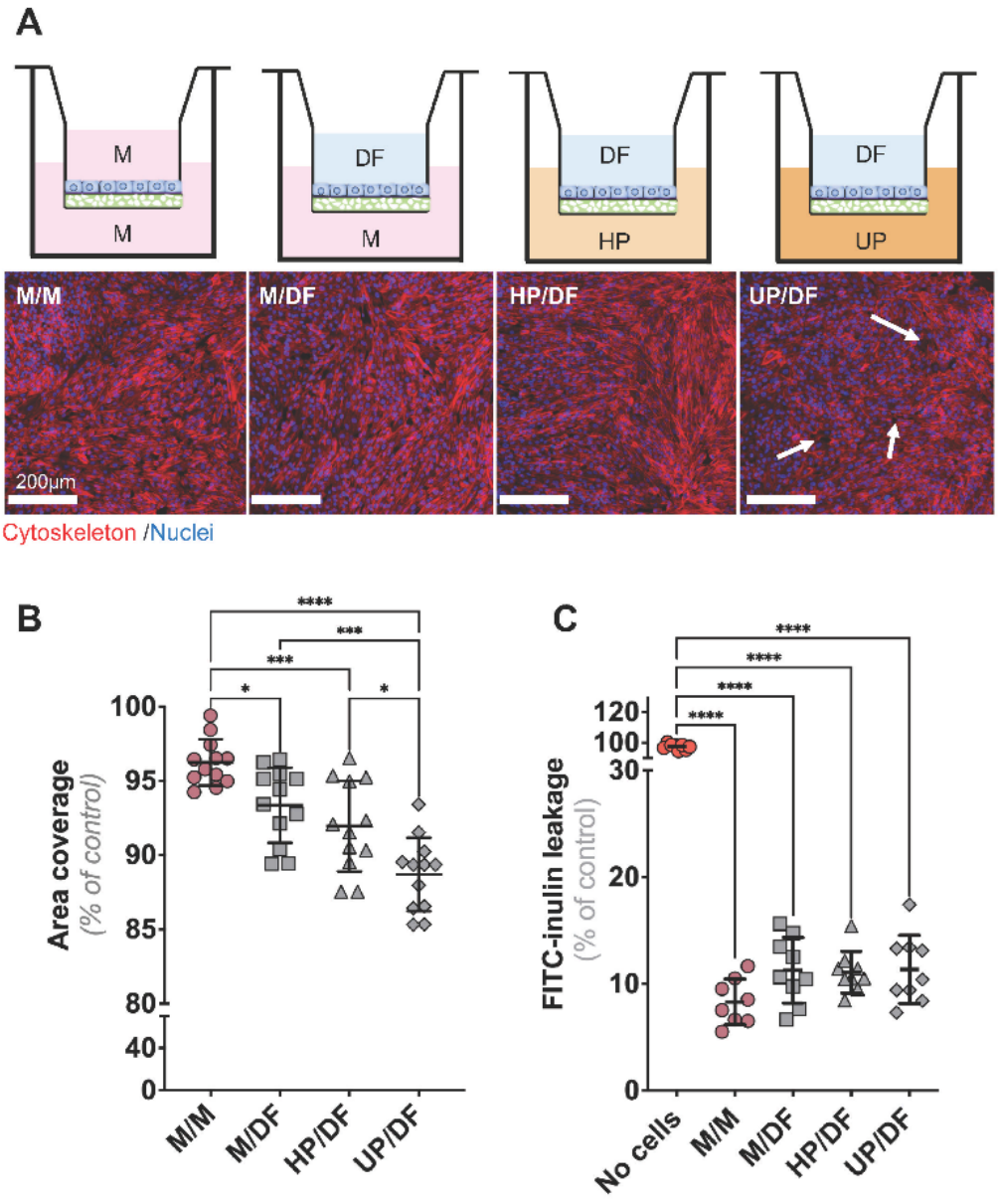

Figure 2. Evaluation of the monolayer integrity in flat membranes exposed to DF and plasma. (**A**) F-actin filaments (in red) and nuclei (in blue) were stained with phalloidin and DAPI, respectively, to assess damage in the cell monolayer for different experimental settings, as depicted by the schematics. White arrows indicate monolayer derangements. (**B**) Measurement of cell surface coverage in the

different experimental settings. (**C**) Monolayer permeability was evaluated by the leakage of FITC-inulin from basal to apical compartment. Data are shown as mean ± SD of four replicates from three independent experiments. * p< 0.01, *** p< 0.005 and ****p< 0.0001 using one-way ANOVA analysis followed by Tukey's multiple comparisons test. **Abbreviations: M**, medium; **DF**, dialysis fluid; **HP**, healthy plasma; **UP**, uremic plasma.

3.3. CiPTECs-Seeded HFMs Effectively Secreted PBUTs when Exposed to Plasma

We previously developed bioengineered kidney tubules using an HFM system as functional units for a BAK in which the cells are seeded on the outer surface of a double-coated fiber [15]. To replicate the intended use, we perfused the lumen of the ciPTECs-seeded HFMs with perfusates containing PBUTs for 30 min by using a custom-made flow system (**Figure 3A)**. The addition of DF at the apical compartment did not affect the barrier performance of the cell monolayers, as determined by FITC-inulin leakage, regardless of the perfusates composition (**Figure 3B**). To confirm the barrier function towards albumin, we collected samples from the apical compartment after basolateral perfusion with a buffer-containing human serum albumin (HSA; 1 mM) at specific time points. During the first 10 min of perfusion, only 1% albumin was lost, which was maintained during the rest of the experiment (**Figure 3C**). These findings not only support active albumin reabsorption, but also show that our monolayer prevents substantial protein loss under physiological conditions.

We next evaluated the efficacy of the bioengineered kidney tubules to actively remove PBUTs (**Figure 3D**). Transepithelial transport, from basal to apical side, was determined for seven PBUTs and quantified using LC-MS/MS to calculate their clearance rates. Notably, we built upon our previous knowledge on PBUT clearance, in a probenecid-sensitive manner [15-17]. However, in the current study, we do not include this control to emphasize the pivotal role of our bioengineered kidney tubules in effectively removing PBUTs. All PBUTs tested were detected at the apical side in either PBUT or PBUT+HSA basolateral perfusions. While the first perfusate displayed comparable clearance rates for all UTs, the presence of HSA led to a significant increase in clearance rates, especially for kynurenic acid (KA), kynurenine (Kyn), and indoxyl sulfate (IS) (**Figure 3D**). In addition, as a proof-of concept, we investigated the transepithelial clearance of the same PBUTs in an experimental model that best reflects the use of the BAK system by perfusing with patient derived-UP with known PBUTs concentrations (**Supplementary Table S2**) and apical exposure to DF (**Figure 3D**). Except for indole-3 acetic acid (IAA), perfusing kidney tubules with UP resulted in lower transepithelial clearance rates than perfusing with PBUTs, despite the presence of HSA (**Figure 3E**). **Table 1** summarizes the comparisons of the different perfusion settings and their respective clearance rates.

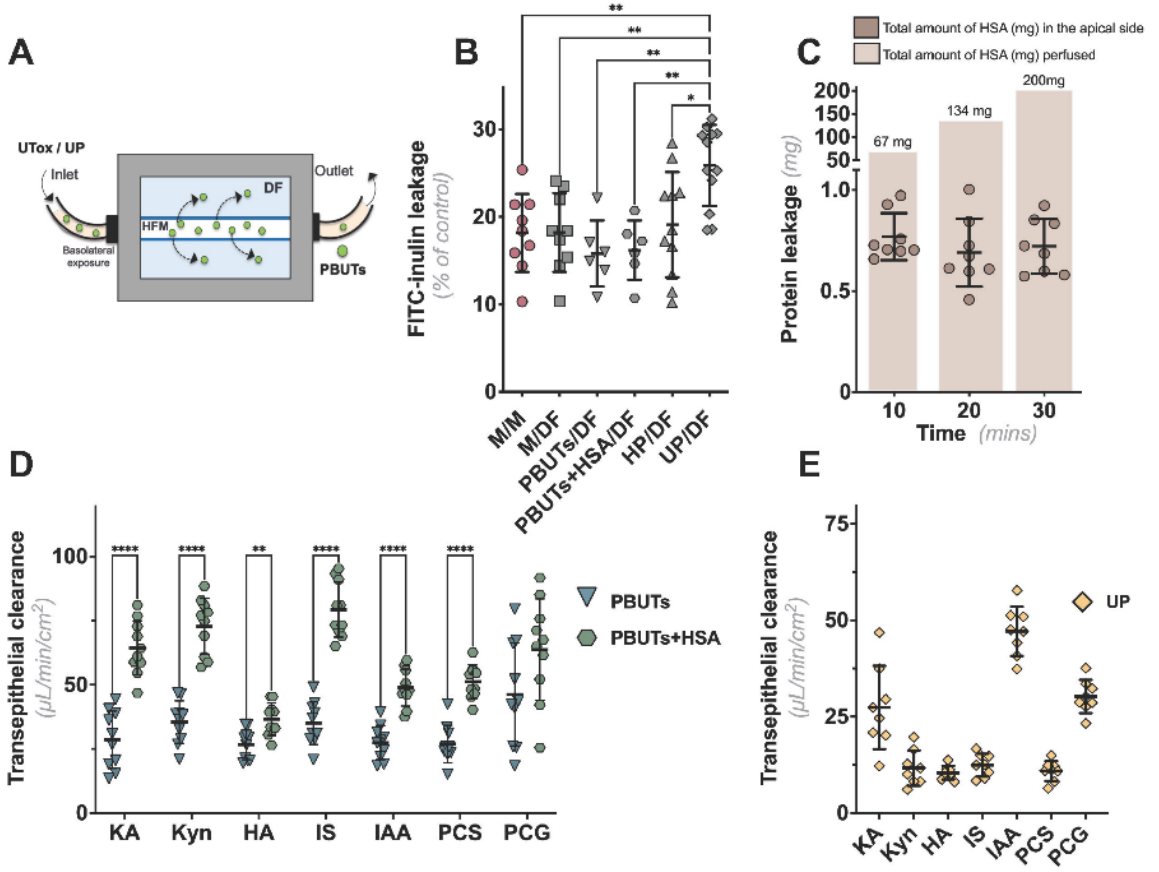

Figure 3. Evaluation of the monolayer integrity in HFM upon exposure to DF and UP. (**A**) Schematic representation of the BAK prototype. (**B**) Upon cell maturation, cells were perfused with either medium, PBUTs, PBUTs with HSA (PBUTs + HSA), HP, or UP for 30 min, followed by a 10 min perfusion with FITC-Inulin to evaluate monolayer integrity. (**C**) Quantification of total HSA leakage at the apical side. In brown blocks is the total amount of HSA (mg) perfused (6mL/h) through the fibers at the corresponding time points. (**D**) Transepithelial clearance of PBUTs during the perfusion of the fibers with either PBUTs alone, with HSA 1 mM, or (**E**) UP. Data are shown as mean ± SD of four replicates from three independent experiments. * p< 0.01, ** p< 0.01, and ****p< 0.0001 using (**A**) one-way ANOVA analysis followed by Tukey's multiple comparison tests or (**D**) multiple Mann-Whitney tests. **Abbreviations**: **M**, medium; **DF**, dialysis fluid; **HP**, healthy plasma; **UP**, uremic plasma; **KA**, kynurenic acid; **Kyn**, kynurenine; **HA**, hippuric acid; **IS**, indoxyl sulfate; **IAA**, indole-3 acetic acid; **PCS**, p-cresyl sulfate; **PCG**, p-cresyl glucuronide.

Table 1. Clearance rate of the individual PBUTs obtained after perfusion with either PBUTs, PBUTs containing 1mM HSA, or UP.[1]

PBUTs	Clearance rate (µl/min/cm²) Mean ± SD		
	PBUT	PBUT+HSA	UP
Kynurenic acid	29 ± 11	64 ± 11 (****)	27 ± 11
Kynurenine	38 ± 8	73 ± 11 (****)	12 ± 5
Hippuric acid	27 ± 6	37 ± 6 (**)	10 ± 2
Indoxyl sulfate	35 ± 8	79 ± 11 (****)	12 ± 3
Indole-3 acetic acid	27 ± 7	49 ± 7 (****)	47 ± 6
p-cresyl sulfate	27 ± 7	51 ± 7 (****)	11 ± 3
p-cresyl glucuronide	46 ± 20	64 ± 20	30 ± 4

[1]Clearance values are presented as mean ± SD. ** p< 0.01, and ****p< 0.0001 (Multiple Mann-Whitney tests, using PBUTs values as controls).

4. DISCUSSION

The development of a BAK as a viable addition to traditional dialysis therapies for ESKD patients is an ongoing research endeavor. A key component of such device is a "living membrane" that consists of a PTEC monolayer on a porous membrane that allows transport of molecules from one side to the other. Previous BAK research has focused on determining its feasibility, safety, effectiveness, and design optimization [18-20]. While these characteristics are important for clinical translation, there is still a lack of information regarding the cytocompatibility of DF, a solution that will be in direct contact with the BAK-containing cells. To address this, we conducted a study in which PTECs, highly appealing for BAK-like applications, were cultured on porous membranes and exposed to DF at the apical side and plasma at the basal side, a representation of the setup envisioned for BAK. Our findings demonstrate acceptable viability and active transepithelial PBUT clearance when PTEC monolayers were exposed to DF.

In our study, we initially assessed a panel of cell viability parameters by exposing ciPTECs to DF for a period of up to 4 hours, the standard duration of a dialysis session. We observed that exposure to DF did not induce cytotoxicity or inflammation in flat cultures. However, we noted a minor decrease in cell viability and OAT1 activity, suggesting minimal damage or environmental changes that could compromise its function. We did observe an initial increase in ROS production likely due to an acute response to DF, which subsided over time. This could be caused by a lack of nutrients or adverse effects to DF components, such as acetate whose concentration in DF is higher than what cells would encounter in cell culture medium [21-23].

Instead of DF, the use of culture medium during HD could be considered to provide a more stable environment for the cells, thus supporting its viability and function [24]. However, this coincides with increased treatment costs and is more challenging to control for batch-to-batch variation in some of the components of culture medium. Addition of specific components to DF, such as amino acids and growth factors, could prove to be more beneficial for BAK applications. Still, considering the limited magnitude of the adverse effects within the allowable range, we conclude that DF can be used in close contact with cells for the duration of a dialysis session without causing significant problems.

Another key parameter investigated in our study was the combined effect of DF and plasma on the integrity of the PTEC monolayer, thereby mimicking the BAK application setting. Exposure to both DF and UP resulted in minor disruption of the monolayer, most likely due to a modulation of the tight junctions [25]. This may be due to both the nutrient-deprived nature of DF and the complex composition of UP, which contains many other toxins and drugs prescribed to ESKD patients. The combination of these factors creates a more toxic environment for the cells, resulting in the observed changes in monolayer integrity. Additionally, the possible presence of shed cells due to exposure to DF could have also played a role in the observed changes. Furthermore, PBUTs found in UP have been shown to negatively impact cell function and phenotype [26], stimulate inflammatory pathways [10], and affect tight junctions [25], thus potentially compromising the barrier function and BAK efficacy.

To create a model relevant to BAK setup, we employed the HFMs-based system. As already reported for the 2D model, the barrier function was maintained when the bioengineered tubules were concomitantly exposed to PBUTs (alone or with HSA) and DF. Additionally, we evaluated the efficacy of the HFM-based BAK model in removing PBUTs. Our data revealed that all tested PBUTs demonstrated a higher transepithelial clearance in the presence of HSA, pointing towards the potential role of albumin as a facilitator of transporter activity, an observation noted earlier for transport in kidney [7, 27], but also liver [28, 29]. When exposed to UP, with a more complex composition in terms of uremic compounds load, including PBUTs repertoire, ciPTECs were still able to remove PBUTs, however the clearance rate was lower compared to experimentally controlled uremic conditions. This discrepancy is in line with the complex composition of UP which can interfere with the overall cell capacity to clear these PBUTs. Additionally, the initial PBUTs concentrations in the experimental uremic conditions, chosen to reflect the average PBUTs concentrations reported in ESKD (https://database.uremic-toxins.org, accessed on 28 March 2023 and [10]), are different that those we identified in the UP that we have used in this study. Furthermore, since we measured the total concentration of PBUTs (both free and protein-bound), we cannot attribute the

differences in clearance rates to partitioning between water and albumin. Instead, the variations in clearance rates are likely influenced by the individual characteristics of the PBUTs, such as initial concentration, protein binding properties [30], and OAT1 affinity [4]. In future studies, the partitioning between water and albumin should be addressed in order to provide more accurate interpretation of the results. Nonetheless, while our model demonstrates the ability to remove PBUTs, the actual clearance capacity and effectiveness might vary per patient. Moreover, in future studies, several uremic plasma batches, with a known profile of PBUTs and medication load should be tested.

Dialysis patients are often prescribed drugs that have been shown to compete with transporter function for PBUTs [16]. These patients do not share the same medical history and their residual kidney function, a determinant in toxin clearance, differs among them [31]. Furthermore, the PBUTs studied here are all OAT1 substrates while UP may also contain additional UTs [32, 33] and other molecules that may impact transporter activity and contribute to the patients' clinical deterioration. Of note, Jansen *et al.* demonstrated that, in short exposure, IS can specifically enhance the expression and function of OAT1 in ciPTECs through a complex, receptor-mediated process [34]. This was explained as a coordinated function through sensing increased levels and stimulating this PBUT's clearance, adhering to the remote sensing and signaling theory [35]. Subsequently, enhancing PBUTs clearance through a preconditioning approach, thereby activating signaling pathways such as the remote-sensing one, could allow for a reduction of the BAK size. Of note, complete removal of PBUTs can also lead to adverse effects as these are also involved in metabolic processes [36].

Another important factor to consider is protein leakage which compromises patients' prognosis. During dialysis, albumin loss is influenced by the type of dialysis membrane and different HD modalities. Notably, high-cut off HD membranes, which are known for their high efficiency in solute removal in dialysis and similar to those used in this study, have been reported to result in albumin loss that ranges from 6-9g/4-5 treatment [37]. Despite this, the acceptable limit of albumin loss for a potential BAK device has yet to be determined as this will differ among BAK's design and patients with different medical records. In the present study, only 1% of albumin was lost during the 30 min of perfusion. This loss in protein may be due to active reabsorption by the cells, as previously reported [7], or albumin adsorption to the system [38, 39]. Nevertheless, our results support that the cell monolayer in BAK prevents substantial protein loss under physiological conditions.

While this study has several notable strengths, it also has some limitations. First, the lack of an apical, unidirectional flow during cell culture and dialysis may have influenced proximal

tubule performance. Nonetheless, our current perfusion setup offers a simpler approach to culture cells on fibers and load them into the perfusion chambers. Compared to more complex microfluidic devices, our setup allows us to generate more robust, reliable and reproducible data. The addition of fluid shear stress has been reported to support the proximal tubule's phenotype by improving cell maturation, polarization, and transport functions [40, 41]. This improvement could potentially lead to better removal of uremic retention solutes and shorter dialysis time. Future studies will be directed towards studying bi-directional flow, which requires a novel microfluidic design and its optimization. Second, only one flow rate was applied in the functional studies, which was carefully selected based on our previous study [42], building upon prior work [43]. However, it is important to acknowledge that different flow rates should be explored in future studies, as they could potentially impact the clearance capacity [44, 45]. To achieve a more accurate representation of physiological conditions, both basal (inner) and apical (outer) flow rates should be fine-tuned and coordinated effectively. By ensuring optimal flow conditions, we can better mimic physiological conditions, and ensure an optimal cell behavior and respective transport function. This is of particular importance since toxin clearance can be affected by the flow rate of the blood/plasma and DF near the membrane surface, which will require further optimization to avoid toxin accumulation, thus reducing its clearance [46]. Subsequently, enhancing PBUT clearance could lead to a reduction of the BAK size, enabling the development of portable or even wearable versions of the device. Third, perfusion times of only 30 min were evaluated and experiments with longer durations should be tested to have a thorough understanding of the tubule's capability. Furthermore, extending perfusion time will also require an optimization of the device itself, as continuous perfusions are prone to air bubble entrapment, leakage and potential cell detachment [47, 48]. Nonetheless, prolonged exposure to DF might compromise cell homeostasis although we found 4h exposure to be within the accepted limits.

In conclusion, the findings from this study demonstrate that the use of DF does not have a detrimental impact on PTECs' viability or their ability to secrete PBUTs. Furthermore, the maintained barrier function and clearance capacity of the bioengineered kidney tubules as functional unit of BAK provides a solid base and paves the way to its further development. This includes upscaling of the current model by including multiple fibers and other features above mentioned, and its preclinical validation. Altogether, our model serves as a valuable tool for investigating novel dialysis strategies.

AUTHOR CONTRIBUTIONS

Conceptualization, **S.M.M.**, **R.M.**, **K.G.F.G** and **D.S.**; methodology, **J.F**, **S.A** and **S.M. M**.; **J.F** and **S.M.M.** writing—original draft preparation, **J.F**, **S.A**, **D.S.**, **M.C.V.**, **R.M.**, **K.G.F.G.** and **S.M.M.** writing—review and editing. All authors have read and agreed to the published version of the manuscript.

FUNDING

This study has received funding from the Strategic Alliance of the University of Twente, University of Utrecht and University Medical Center Utrecht, the European Union's Horizon 2020 research and innovation programme under the Marie Skłodowska-Curie grant agreement No 813839 and the European Union's Horizon EIC Pathfinder Open programme under grant agreement No 101099092 (KIDNEW).

INFORMED CONSENT STATEMENT

Not applicable.

DATA AVAILABILITY STATEMENT

The data underlying this article will be shared upon reasonable request to the corresponding author

CONFLICTS OF INTEREST

R.M. is co-inventor of the cell line ciPTEC-OAT1, for which the patent is held by Radboud University Nijmegen, the Netherlands. Cells were used under conditions of a non-commercial MTA.

SUPPLEMENTARY MATERIALS

Supplementary Table S1. Dialysis fluid and culture medium solute concentrations.

Solute	DF concentration (mmol/L)	Culture medium Concentration (mmol/L)
Na^+	130	121.6
K^+	3.00	4.16
Mg^{2+}	0.50	0.71
Ca^{2+}	1.50	1.05
Cl^-	110	126.1
CH_3COO^-	3.00	0
HCO_3^-	32.0	29.0
Glucose	5.55	17.5

Supplementary Table S2. PBUTs concentrations in healthy individuals, kidney disease patients and as applied within the PBUTs cocktail[1] and in uremic plasma (UP) in this study, with their individual protein binding[2].

PBUTs	Healthy conc. (µM) (Mean ± SD)	Uremic conc. (µM) (Mean ± SD)	PBUTs (µM)[1]	UP (µM)[2]	Protein binding (%)[3]	OAT1 affinity (uM)[4]
Indoxyl sulfate	2.3 ± 18.8	173.5 ± 121.9	100	68.0 ± 5.8	87-98	20.5
***p*-cresyl sulfate**	10.1 ± 12.2	122.2 ± 90.3	500	42.2 ± 2.5	95	232
***p*-cresyl glucuronide**	0.3 ± 0.2	30.1 ± 6.7	40	1.35 ± 0.10	12-13	-
Indol-3-acetic acid	2.9 ± 1.7	11.4 ± 2.3	3	5.28 ± 0.56	53-69	14.0
Hippuric acid	16.7 ± 11.2	608.4 ± 362.8	300	177.2 ± 11.4	39-41	23.5
Kynurenic acid	0.03 ± 0.01	0.8 ± 0.4	3	2.55 ± 0.20	95	5.1
L-kynurenine	1.9	3.3 ± 0.9	5	4.00 ± 0.42	67	-

[1]Concentrations reported on EUTox Uremic Solutes Database (https://database.uremic-toxins.org accessed on 28 March 2023) and Mihajlovic *et al.* [10]. [2]Albumin concentration in UP (HSA, 0.70 mM). [3]Protein binding values were reported in [30]. [4]OAT1 affinity constants were reported in [4].

REFERENCES

1. S. K. Nigam and K. T. Bush. Uraemic syndrome of chronic kidney disease: altered remote sensing and signalling. Nat Rev Nephrol 2019;15(5):301-316

2. M. H. Rosner, T. Reis, F. Husain-Syed*, et al.* Classification of Uremic Toxins and Their Role in Kidney Failure. Clin J Am Soc Nephrol 2021;16(12):1918-1928

3. R. Vanholder, R. De Smet, G. Glorieux*, et al.* Review on uremic toxins: classification, concentration, and interindividual variability. Kidney Int 2003;63(5):1934-1943

4. R. Masereeuw, H. A. Mutsaers, T. Toyohara*, et al.* The kidney and uremic toxin removal: glomerulus or tubule? Semin Nephrol 2014;34(2):191-208

5. W. Wu, K. T. Bush and S. K. Nigam. Key Role for the Organic Anion Transporters, OAT1 and OAT3, in the in vivo Handling of Uremic Toxins and Solutes. Sci Rep 2017;7(1):4939

6. S. K. Nigam, K. T. Bush, G. Martovetsky*, et al.* The organic anion transporter (OAT) family: a systems biology perspective. Physiol Rev 2015;95(1):83-123

7. T. T. Nieskens, J. G. Peters, M. J. Schreurs*, et al.* A Human Renal Proximal Tubule Cell Line with Stable Organic Anion Transporter 1 and 3 Expression Predictive for Antiviral-Induced Toxicity. AAPS J 2016;18(2):465-475

8. D. L. Ramada, J. de Vries, J. Vollenbroek*, et al.* Portable, wearable and implantable artificial kidney systems: needs, opportunities and challenges. Nat Rev Nephrol 2023:1-10

9. R. L. McGill and D. E. Weiner. Dialysate Composition for Hemodialysis: Changes and Changing Risk. Semin Dial 2017;30(2):112-120

10. M. Mihajlovic, M. M. Krebber, Y. Yang*, et al.* Protein-Bound Uremic Toxins Induce Reactive Oxygen Species-Dependent and Inflammasome-Mediated IL-1beta Production in Kidney Proximal Tubule Cells. Biomedicines 2021;9(10)

11. M. Mihajlovic, L. P. van den Heuvel, J. G. Hoenderop*, et al.* Allostimulatory capacity of conditionally immortalized proximal tubule cell lines for bioartificial kidney application. Sci Rep 2017;7(1):7103

12. H. A. Mutsaers, L. P. van den Heuvel, L. H. Ringens*, et al.* Uremic toxins inhibit transport by breast cancer resistance protein and multidrug resistance protein 4 at clinically relevant concentrations. PLoS One 2011;6(4):e18438

13. I. Iso. 10993–5: 2009 Biological evaluation of medical devices—part 5: tests for in vitro cytotoxicity. International Organization for Standardization, Geneva 2009:34

14. T. T. G. Nieskens, J. G. P. Peters, D. Dabaghie*, et al.* Expression of Organic Anion Transporter 1 or 3 in Human Kidney Proximal Tubule Cells Reduces Cisplatin Sensitivity. Drug Metab Dispos 2018;46(5):592-599

15. J. Jansen, M. Fedecostante, M. J. Wilmer*, et al.* Bioengineered kidney tubules efficiently excrete uremic toxins. Sci Rep 2016;6:26715

16. S. M. Mihaila, J. Faria, M. F. J. Stefens*, et al.* Drugs Commonly Applied to Kidney Patients May Compromise Renal Tubular Uremic Toxins Excretion. Toxins (Basel) 2020;12(6)

17. T. K. van der Made, M. Fedecostante, D. Scotcher*, et al.* Quantitative Translation of Microfluidic Transporter in Vitro Data to in Vivo Reveals Impaired Albumin-Facilitated Indoxyl Sulfate Secretion in Chronic Kidney Disease. Mol Pharm 2019;16(11):4551-4562

18. H. D. Humes, D. Buffington, A. J. Westover*, et al.* The bioartificial kidney: current status and future promise. Pediatr Nephrol 2014;29(3):343-351

19. R. Masereeuw and D. Stamatialis. Creating a bioartificial kidney. Int J Artif Organs 2017;40(7):323-327

20. M. K. van Gelder, S. M. Mihaila, J. Jansen*, et al.* From portable dialysis to a bioengineered kidney. Expert Rev Med Devices 2018;15(5):323-336

21. R. H. Richards, J. A. Dowling, H. J. Vreman*, et al.* Acetate levels in human plasma. Proc Clin Dial Transplant Forum 1976;6:73-79

22. E. Coll, R. Perez-Garcia, P. Rodriguez-Benitez*, et al.* [Clinical and analytical changes in hemodialysis without acetate]. Nefrologia 2007;27(6):742-748

23. R. A. Ward, R. L. Wathen, T. E. Williams*, et al.* Hemodialysate composition and intradialytic metabolic, acid-base and potassium changes. Kidney Int 1987;32(1):129-135

24. T. Yao and Y. Asayama. Animal-cell culture media: History, characteristics, and current issues. Reprod Med Biol 2017;16(2):99-117

25. N. D. Vaziri, N. Goshtasbi, J. Yuan*, et al.* Uremic plasma impairs barrier function and depletes the tight junction protein constituents of intestinal epithelium. Am J Nephrol 2012;36(5):438-443

26. Y. Yang, M. Mihajlovic, M. J. Janssen*, et al.* The Uremic Toxin Indoxyl Sulfate Accelerates Senescence in Kidney Proximal Tubule Cells. Toxins (Basel) 2023;15(4)

27. K. Besseghir, D. Mosig and F. Roch-Ramel. Facilitation by serum albumin of renal tubular secretion of organic anions. Am J Physiol 1989;256(3 Pt 2):F475-484

28. S. Miyauchi, S. J. Kim, W. Lee*, et al.* Consideration of albumin-mediated hepatic uptake for highly protein-bound anionic drugs: Bridging the gap of hepatic uptake clearance between in vitro and in vivo. Pharmacol Ther 2022;229:107938

29. P. Poulin and S. Haddad. Albumin and Uptake of Drugs in Cells: Additional Validation Exercises of a Recently Published Equation that Quantifies the Albumin-Facilitated Uptake Mechanism(s) in Physiologically Based Pharmacokinetic and Pharmacodynamic Modeling Research. J Pharm Sci 2015;104(12):4448-4458

30. M. K. van Gelder, I. R. Middel, R. W. M. Vernooij*, et al.* Protein-Bound Uremic Toxins in Hemodialysis Patients Relate to Residual Kidney Function, Are Not Influenced by Convective Transport, and Do Not Relate to Outcome. Toxins (Basel) 2020;12(4)

31. L. L. Ganesan, F. J. O'Brien, T. L. Sirich*, et al.* Association of Plasma Uremic Solute Levels with Residual Kidney Function in Children on Peritoneal Dialysis. Clin J Am Soc Nephrol 2021;16(10):1531-1538

32. S. K. Nigam, W. Wu, K. T. Bush*, et al.* Handling of Drugs, Metabolites, and Uremic Toxins by Kidney Proximal Tubule Drug Transporters. Clin J Am Soc Nephrol 2015;10(11):2039-2049

33. F. Duranton, G. Cohen, R. De Smet*, et al.* Normal and pathologic concentrations of uremic toxins. J Am Soc Nephrol 2012;23(7):1258-1270

34. J. Jansen, K. Jansen, E. Neven*, et al.* Remote sensing and signaling in kidney proximal tubules stimulates gut microbiome-derived organic anion secretion. Proc Natl Acad Sci U S A 2019;116(32):16105-16110

35. S. K. Nigam and J. C. Granados. OAT, OATP, and MRP Drug Transporters and the Remote Sensing and Signaling Theory. Annu Rev Pharmacol Toxicol 2023;63:637-660

36. R. Vanholder, S. K. Nigam, S. Burtey*, et al.* What If Not All Metabolites from the Uremic Toxin Generating Pathways Are Toxic? A Hypothesis. Toxins (Basel) 2022;14(3)

37. K. Kalantar-Zadeh, L. H. Ficociello, J. Bazzanella*, et al.* Slipping Through the Pores: Hypoalbuminemia and Albumin Loss During Hemodialysis. Int J Nephrol Renovasc Dis 2021;14:11-21

38. J. L. Brash, T. A. Horbett, R. A. Latour*, et al.* The blood compatibility challenge. Part 2: Protein adsorption phenomena governing blood reactivity. Acta Biomater 2019;94:11-24
39. H. Ji, H. Xu, L. Jin*, et al.* Surface engineering of low-fouling and hemocompatible polyethersulfone membranes via in-situ ring-opening reaction. Journal of Membrane Science 2019;581:373-382
40. E. J. Ross, E. R. Gordon, H. Sothers*, et al.* Three dimensional modeling of biologically relevant fluid shear stress in human renal tubule cells mimics in vivo transcriptional profiles. Sci Rep 2021;11(1):14053
41. J. Vriend, J. G. P. Peters, T. T. G. Nieskens*, et al.* Flow stimulates drug transport in a human kidney proximal tubule-on-a-chip independent of primary cilia. Biochim Biophys Acta Gen Subj 2020;1864(1):129433
42. J. Jansen, I. E. De Napoli, M. Fedecostante*, et al.* Human proximal tubule epithelial cells cultured on hollow fibers: living membranes that actively transport organic cations. Sci Rep 2015;5:16702
43. Z. Y. Oo, K. Kandasamy, F. Tasnim*, et al.* A novel design of bioartificial kidneys with improved cell performance and haemocompatibility. J Cell Mol Med 2013;17(4):497-507
44. Y. Shi, H. Tian, Y. Wang*, et al.* Improved Dialysis Removal of Protein-Bound Uraemic Toxins with a Combined Displacement and Adsorption Technique. Blood Purif 2022;51(6):548-558
45. T. L. Sirich, F. J. Luo, N. S. Plummer*, et al.* Selectively increasing the clearance of protein-bound uremic solutes. Nephrol Dial Transplant 2012;27(4):1574-1579
46. R. Refoyo, E. D. Skouras, N. V. Chevtchik*, et al.* Transport and reaction phenomena in multilayer membranes functioning as bioartificial kidney devices. Journal of Membrane Science 2018;565:61-71
47. C. M. Leung, P. de Haan, K. Ronaldson-Bouchard*, et al.* A guide to the organ-on-a-chip. Nature Reviews Methods Primers 2022;2(1):33
48. V. Silverio, S. Guha, A. Keiser*, et al.* Overcoming technological barriers in microfluidics: Leakage testing. Front Bioeng Biotechnol 2022;10:958582

CHAPTER 5

Mesenchymal Stromal Cells Secretome Restores Bioenergetic and Redox Homeostasis in Human Proximal Tubule Cells after Ischemic Injury

João Faria[1*], Sandra Calcat-i-Cervera[2*], Renata Skovronova[3*], Bonnie C. Broeksma[4], Alinda J. Berends[1], Esther A. Zaal[5], Benedetta Bussolati[3], Timothy O'Brien[2], Silvia M. Mihăilă[1], Rosalinde Masereeuw[1]

[1] Utrecht University, Department of Pharmaceutical Sciences, The Netherlands

[2] Regenerative Medicine Institute (REMEDI), CÚRAM, Biomedical Science Building, National University of Ireland, Galway, Ireland

[3] Department of Molecular Biotechnology and Health Sciences, University of Turin, 10126 Turin, Italy

[4] Danone Nutricia Research, Utrecht, The Netherlands

[5] Biomolecular Mass Spectrometry and Proteomics, Bijvoet Center for Biomolecular Research, Utrecht Institute of Pharmaceutical Sciences, Utrecht University, 3508 TB Utrecht, The Netherlands

*These authors contributed equally

Published in Stem Cell Res Ther 2023; 14, 353

ABSTRACT

Ischemia/reperfusion injury is the leading cause of acute kidney injury (AKI). The current standard of care focuses on supporting kidney function, stating the need for more efficient and targeted therapies to enhance repair. Mesenchymal stromal cells (MSCs) and their secretome, either as conditioned medium (CM) or extracellular vesicles (EVs), have emerged as promising options for regenerative therapy, however, their full potential in treating AKI remains unknown.

In this study, we employed an *in vitro* model of chemically-induced ischemia using antimycin A combined with 2-deoxy-D-glucose to induce ischemic injury in proximal tubule epithelial cells. Afterwards, we evaluated the effects of MSC secretome, CM or EVs obtained from adipose tissue, bone marrow, and umbilical cord, on ameliorating the detrimental effects of ischemia. To assess the damage and treatment outcomes, we analyzed cell morphology, mitochondrial health parameters (mitochondrial activity, ATP production, mass and membrane potential), and overall cell metabolism by metabolomics.

Our findings show that ischemic injury caused cytoskeletal changes confirmed by disruption of the F-actin network, energetic imbalance as revealed by a 50% decrease in the oxygen consumption rate, increased oxidative stress, mitochondrial dysfunction, and reduced cell metabolism. Upon treatment with MSC secretome, the morphological derangements were partly restored and ATP production increased by 40-50%, with umbilical cord-derived EVs being most effective. Furthermore, MSC treatment led to phenotype restoration as indicated by an increase in cell bioenergetics, including increased levels of glycolysis intermediates, as well as an accumulation of antioxidant metabolites.

Our *in vitro* model effectively replicated the *in vivo*-like morphological and molecular changes observed during ischemic injury. Additionally, treatment with MSC secretome ameliorated proximal tubule damage, highlighting its potential as a viable therapeutic option for targeting AKI.

KEYWORDS: Ischemia, proximal tubule, mesenchymal stromal cell, extracellular vesicles, metabolism

1. INTRODUCTION

Ischemia/reperfusion injury (IRI) is a leading cause of acute kidney injury (AKI) and can even result in kidney failure after transplantation. Current treatments mainly support or replace kidney function, with few effective strategies to prevent or treat ischemic AKI [1, 2]. During ischemia, the temporary restriction in blood flow to the kidney generates a local hypoxic environment, thereby decreasing ATP production and altering mitochondrial metabolism. When blood flow is restored, oxygen levels rapidly increase, mitochondrial oxidative phosphorylation and the production of reactive oxygen species (ROS) increase leading to oxidative stress and inflammation, which exacerbate further tissue damage [3, 4].

Within the kidney, proximal tubule epithelial cells (PTECs) are particularly susceptible to IRI given their high active metabolism, supported by abundant mitochondria present, dependence on aerobic oxidative phosphorylation [5] and limited ability to undergo anaerobic glycolysis [6]. Severe IRI can cause permanent tissue damage and functional impairment, therefore, it is important to understand the underlying mechanisms and develop therapeutic interventions.

In recent years, cell-based regenerative therapies have been explored in a wide range of nephropathies to facilitate tissue repair following kidney injury. In particular mesenchymal stromal cells (MSCs) have shown promise by promoting angiogenesis, tubular cell turnover, and modulation of immune response and inflammation in preclinical [7-9] and clinical research [10, 11]. Lately, it has been reported that MSCs also exert antioxidant properties that may enhance their cytoprotective effects in IRI, such as damping mitochondrial dysfunction [12] and increasing cell bioenergetics [13], ultimately reducing oxidative stress [12-16]. These such renoprotective mechanisms are suggested to be mediated through paracrine signaling, which involves cytokines, growth factors, and nucleic acids, often harbored in extracellular vesicles (EVs) [14-18]. However, the precise mechanism is still unknown, partially due to the inherent heterogeneity of the MSCs related to the various sources of origin [19-22]. Importantly, a comparison of efficiency between various MSCs to attenuate kidney damage after IRI remains to be explored.

To address this, we established an *in vitro* model to replicate the effects of ischemia on PTECs by suppressing mitochondrial respiration and glycolysis under hypoxia. We assessed various parameters of mitochondrial function, including metabolic activity, mitochondrial mass, mitochondrial membrane potential, metabolic profile, and cytoarchitecture as well as the cell metabolome. Afterwards, cells were treated with MSC secretome isolated from adipose tissue (A), bone marrow (B), and umbilical cord (U) to determine whether mitochondrial function and metabolic activity could be restored during the reperfusion phase.

2. MATERIALS AND METHODS

2.1. Cell Culture

2.1.1. CiPTEC-14.4

The ciPTEC-14.4 cell line (RRID: CVCL_W184) was purchased from Cell4Pharma (Oss, the Netherlands), obtained at passage 38 and cultured as reported previously [23]. Mycoplasma contamination was checked monthly and was found to be negative in all cells used. ciPTECs were used for experiments from passage numbers 42 to 50, during which robust and reproducible results were obtained in agreement with previous findings [24-26].

2.1.2. MSCs Culture

The MSCs, all human-derived, were obtained within the European Union's Horizon 2020 research and innovation collaborative network RenalToolBox (Grant Agreement 813839) and well-characterized [27]. A-MSCs from lipoaspirates were processed in Heidelberg (Germany) after obtaining informed consent (Mannheim Ethics Commission; vote number 2006-192NMA). B-MSCs provided by Galway (Ireland) (Galway University Hospital Clinical Research Ethics Committee; approval number 02/08) were purchased from Lonza (Basel, Switzerland), and U-MSCs with informed consent obtained in accordance with the Declaration of Helsinki were sourced from the NHS Blood and Transplant and transferred to the University of Liverpool (United Kingdom) (NHS Blood and Transplant, Cellular and Molecular Therapies; approval number: RTB21112019). MSCs were cultured as reported previously [27]. Briefly, A-MSCs were seeded at a density of 300 cells/cm^2, and B- and U-MSCs at 3,000 cells/cm^2 at 37 °C with 5% (v/v) CO_2, and cultured in basic growth medium (MEM-α media, Gibco, ThermoFisher Scientific), supplemented with 10% of fetal bovine serum (FBS, Gibco, ThermoFisher Scientifics, Cat-No. 10,270–106, Lot 42Q7096K) until reaching 80% confluency. A thorough characterization of all three MSC sources, including morphology, growth kinetics, differentiation capabilities, and immunophenotypic profiles, was recently published [27]. In the current study, all MSCs were cultured from passage numbers 3 to 6.

2.1.3. CM Collection

Upon reaching 80% confluency, MSCs were washed once with HBSS and incubated for 24h in serum-free MEM-α media. The supernatant was then collected and centrifuged for 5 min at 400 g to remove cell debris before being transferred to Amicon Ultra-15 centrifugal units (3

kDa molecular cutoff) (Millipore, UFC900324) for concentration at 3,000 g for 90 min at 4°C. Concentrated CM was then stored at –80°C until further use.

2.1.4. EV Isolation

EVs from MSCs were collected as reported previously [28]. Briefly, the supernatant was collected and centrifuged for 10 min at 300 g to remove cell debris, transferred into new tubes and centrifuged for 20 min at 3,000 g to discard apoptotic cells. The supernatant was then ultracentrifuged for 1 h at 10,000 g and 4°C, using the Beckman Coulter Optima L-100K Ultracentrifuge with the rotor type 70 Ti. At this speed, the subpopulation of 10k EVs (large EVs, LEVs) was collected. The supernatant was further ultracentrifuged for 1 h at 100,000 g and 4°C, to obtain the 100k EV (small EVs, SEVs) subpopulation. The EV pellet was resuspended in PBS supplemented with 0.1% DMSO and stored at -80°C until further use.

2.1.5. CiPTEC Ischemic Model

To mimic ischemia *in vitro*, ciPTECs were chemically exposed to 10 nM of antimycin A (AA, Sigma-Aldrich, A8674) and 20 mM of 2-deoxy-D-glucose (2DG, Sigma-Aldrich D6134), as previously described [29-32], for 24h in serum-free medium (SFM) at 37°C under normoxia (21% O_2). Additionally, to enhance the simulation of blood supply disruption which deprives cells of nutrients, we exposed these chemically-treated ciPTECs to a hypoxic environment (1% O2). The experimental groups were labelled as: sham, ciPTECs cultured in serum-containing medium; vehicle, ciPTECs cultured in SFM; and ischemia, ciPTECs exposed to AA and 2DG in SFM and under normoxia (21% O_2) or hypoxia (1% O_2).

Afterwards, ischemic cells were washed once with Hank's balanced salt solution (HBSS; Gibco, Life Technologies) to remove AA and 2DG before being treated with MSC secretome, either as conditioned medium (CM) or EVs (small, SEV; and large, LEV) [28] from each of the MSCs sources for an additional 24h at 37 °C. When collecting MSC bioproducts for both the secretome and the EVs, the generating MSCs were harvested and counted to calculate the cell-equivalent concentration of the secretome and EVs. This was used to enable the comparison of the effects exerted by both bioproducts under cell-equivalent doses. Based on previous studies reported in the literature [33, 34], we administered the amount of bioproduct equivalent obtained from 2 MSCs per each ciPTEC in SFM (ratio 2:1). This study incorporated three donors for each MSC type, and the average values from these three donors were employed for subsequent in-depth analysis.

To effectively assess the efficacy of MSC secretome in mitigating ischemic damage, we established a comparative analysis. On one hand, we exposed ischemic ciPTECs to MSC

secretome in SFM, to allow us the study of the specific effects of the secretome. On the other hand, we subjected ischemic ciPTECs to serum-containing medium, replicating the conditions in which blood flow is reintroduced post-ischemia (labelled as 'reperfusion' group). By comparing the effects of MSC secretome treatment under serum-free conditions with those in a reperfusion-like setting, we aimed to gain insights into the potential benefits of the secretome.

2.2. Injury and Treatment Assessment

The same readouts performed to assess the ischemic injury were repeated to determine MSC secretome therapeutic effect. All experiments were performed on 96-well plates (Greiner Bio-One, Frickenhausen, Germany), unless stated otherwise.

2.2.1. Cell Metabolic Activity

Cell metabolic activity was measured using PrestoBlue® reagent (ThermoFischer Scientific, A13262) [35]. ciPTECs were rinsed once with HBSS and incubated with PrestoBlue® (diluted 1:10 in SFM), in the dark. After 1 h of incubation at 37°C the fluorescence was measured using the GloMax® Discover microplate reader (Promega, Wisconsin, United States), at an excitation wavelength of 530 nm and emission wavelength of 590 nm.

2.2.2. ATP Production

ATP production was quantified using the CellTiter-Glo® 2.0 reagent (Promega, G9242) [36]. ciPTECs were incubated with 100 µl/well of reagent and the solutions were mixed on an orbital shaker for 2 min. The plates were incubated at room temperature for 10 min, and the luminescent signal was read using the GloMax® Discover microplate reader.

2.2.3. Intracellular ROS Production

The generation of intracellular ROS was measured using a cell permeant fluorogenic substrate, CM-H_2DCFDA (Invitrogen, C6827) [37]. ciPTECs were rinsed once with HBSS before being loaded with CM-H_2DCFDA (50 µM in SFM medium) and incubated at 37°C in the dark for 20 min. H_2O_2 (500 µM) was used as a positive control. Following the incubation period, cells were washed twice with HBSS and lysed for 10 min in 0.1 M NaOH. Lastly, fluorescence was measured at excitation/emission wavelengths of 492/518 nm, using the GloMax® Discover microplate reader.

2.2.4. Mitochondrial Mass

The mitochondrial mass was quantified using MitoTracker™ Orange CMTMRos (Invitrogen, M7510) [38]. ciPTECs were rinsed once with HBSS, loaded with MitoTracker Orange CMTMRos (200 nM in SFM), and incubated at 37°C in the dark for 30 min. Additionally, ciPTECs were counterstained with 1 µM Hoechst 33342 for nuclei detection. Afterwards, ciPTECs were washed with HBSS and fluorescence was measured using the GloMax® Discover microplate reader at excitation/emission wavelengths of 554/576 for MitoTracker™ Orange CMTMRos and 361/497 for Hoechst. Fluorescent values were corrected to account for background signals. Subsequently, the quantification of mitochondrial mass was executed by calculating the ratio of fluorescent values derived from MitoTracker™ Orange CMTMRos to those originating from Hoechst.

2.2.5. Mitochondrial Membrane Potential (Δψ)

The integrity of mitochondrial membrane potential (Δψ) was measured using JC-10 (Abcam, ab112134) [39]. ciPTECs were rinsed once with HBSS and incubated with 50 µl of JC-10 loading solution for 30 mins at 37 °C in the dark. Subsequently, 50 µl of assay buffer B was added to the plate and fluorescence was read at excitation/emission wavelengths of 490/525 and 540/590 for ratio analysis, using the GloMax® Discover microplate reader. In the assay, carbonyl cyanide 4-(trifluoromethoxy) phenylhydrazone (FCCP, 10 μM), a mitochondrial uncoupler, was used as a positive control for loss of Δψ.

2.2.6. Bioenergetic Profile

The oxygen consumption rate (OCR) and extracellular acidification rate (ECAR) were monitored in real-time using the Seahorse extracellular flux analyzer XF 96 (Agilent Technologies, USA). ciPTECs were seeded into a XF96 cell culture microplate (Seahorse Bioscience) at a density of 4,000 cells/well. Prior to starting the assay, cells were incubated in a non-CO_2 incubator at 37°C. Bioenergetic profiles were measured by serial injections of olygomycin (1 μM), FCCP (2 μM) and rotenone/antimycin A (Rot/AA, 0.5 μM respectively) with the Seahorse XF Cell Mito Stress Test [40]. At the end of the assay, cells were lysed in RIPA buffer (ThermoFisher Scientific, 89900) and the protein content per well was determined using the Pierce™ BCA Protein Assay Kit (ThermoFisher Scientific, 23227).

The OCR and ECAR values were normalized to the protein values and subsequently several mitochondrial-related parameters were extracted. Following the calculations described by Mookerjee and colleagues [41, 42], OCR and ECAR were converted to the same

units (pmol ATP/min/μg protein) and used to calculate net rates of ATP that can originate from between glycolysis ($J_{ATPglyc}$) and oxidative phospholylation (J_{ATPox}). J_{ATPox} can be further represented as ATP production due to the tricarboxylic acid cycle ($J_{ATPox\ TCA}$) and rate coupled to oxidative phosphorylation ($J_{ATPox\ coupled}$).

2.2.7. Immunofluorescence Analysis

For immunofluorescence procedures, ciPTECs were cultured in a 96-well black/*clear* bottom plates (ThermoFischer, 165305) [35]. At the end of the experimental protocol, cells were washed with HBSS and fixed in 4% paraformaldehyde (ThermoFisher Scientific) for 10 mins at room temperature (RT). After fixation, ciPTECs were permeabilized with 0.3% Triton X-100 in PBS and blocked in blocking buffer (2% FBS, 2% BSA, 0.1% Tween20 in PBS). Primary and secondary antibodies were incubated for 1h at RT, and samples were washed three times in 0.1% Tween in PBS for 5 mins. Nuclei were stained using 4',6-diamidino-2-phenylindole (DAPI) for 7 min, followed by three washing steps in 0.1% Tween in PBS for 5 mins. Immunofluorescence was conducted using confocal microscopy (Leica TCS SP8 X) and the software Leica Application Suite X. The antibodies are listed in **Supplementary Table S1**.

2.2.8. Metabolomics Analysis

LC-MS analysis was performed on a Q-Exactive HF mass spectrometer (Thermo Scientific) coupled to a Vanquish autosampler and pump (Thermo Scientific). Metabolites were separated using a Sequant ZIC-pHILIC column (2.1 x 150 mm, 5 µm, guard column 2.1 x 20 mm, 5 µm; Merck) with acetonitrile and eluent A (20 mM (NH4)2CO3, 0.1% NH4OH in ULC/MS grade water (Biosolve)). The gradient ran from 20% eluent to 60% eluent in 20 minutes, followed by a wash step at 80% and equilibration at 20%. The flow rate was set at 100 µl/min. The MS operated in polarity-switching mode with spray voltages of 4.5 kV and -3.5 kV. Metabolites were identified and quantified on the basis of exact mass within 5 ppm and further validated by concordance with retention times of standards and peak areas were normalized based on total signal [43]. Analysis was performed using TraceFinder software (Thermo Scientific), R and MetaboAnalyst software.

2.3. Statistical Analysis

Quantitative data are reported as mean ± standard deviation (SD). N indicates the number of biological replicates, and n the number of independent experiments. In fluorescence and luminescence-based assays, data were corrected for background, normalized to untreated cells, and presented as a fold-change to the control group. Statistical analyses were performed using GraphPad Prism version 9.2.0 (GraphPad Software, Inc., San Diego, CA, USA). The statistical test and replicates are indicated in the figure legends. A p-value < 0.05 was considered statistically significant.

3. RESULTS

3.1. Treatment with MSCs Secretome Restores Cell Morphology upon Ischemia Induced Damage

To model ischemia *in vitro*, cells were treated with antimycin A (AA) and 2-deoxyglucose (2DG) to inhibit mitochondrial respiration and glycolysis, respectively, under normoxia (N-ciPTECs) and hypoxia (H-ciPTECs) conditions (**Figure 1a**). N-ciPTECs were used as control conditions of the oxygen-deprived group. This injury treatment led to disruption of the F-actin network and a decrease in the number of nuclei per surface area, particularly in the hypoxic group (**Figure 1b**). H-ciPTECs increased collagen IV deposition when co-treated with TGF-β while this was not observed in the sham, vehicle and ischemic groups, confirming the efficacy of our model to mimic the progression to chronic kidney disease observed after AKI (**Supplementary Figure S1**). Treatment with MSC-secretome improved cell morphology in a qualitative analysis in N-ciPTECs as evidenced by cytoskeleton staining, regardless of the source of MSCs (**Figure 1c**). However, MSC therapy was less effective in H-ciPTECs, as observed by the presence of holes in the monolayers (**Figure 1c**).

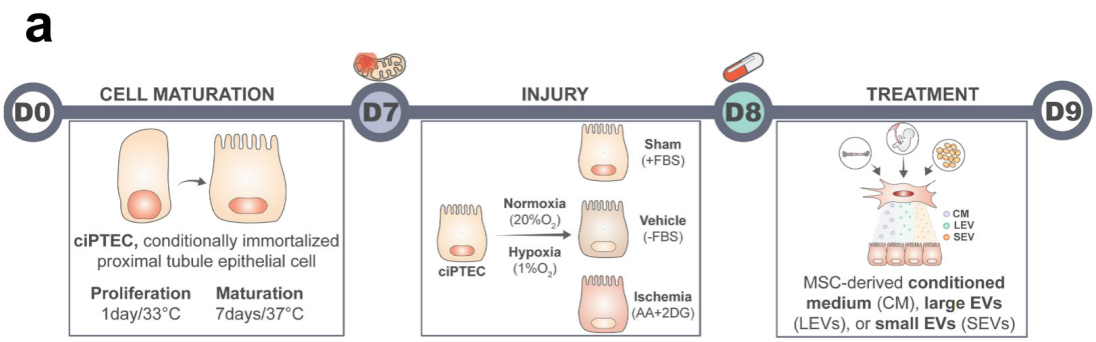
a
D0
CELL MATURATION
D7
INJURY
D8
TREATMENT
D9
ciPTEC, conditionally immortalized proximal tubule epithelial cell
Proliferation 1day/33°C
Maturation 7days/37°C
Sham (+FBS)
Normoxia (20%O2)
Vehicle (-FBS)
Hypoxia (1%O2)
ciPTEC
Ischemia (AA+2DG)
CM
LEV
SEV
MSC-derived conditioned medium (CM), large EVs (LEVs), or small EVs (SEVs)

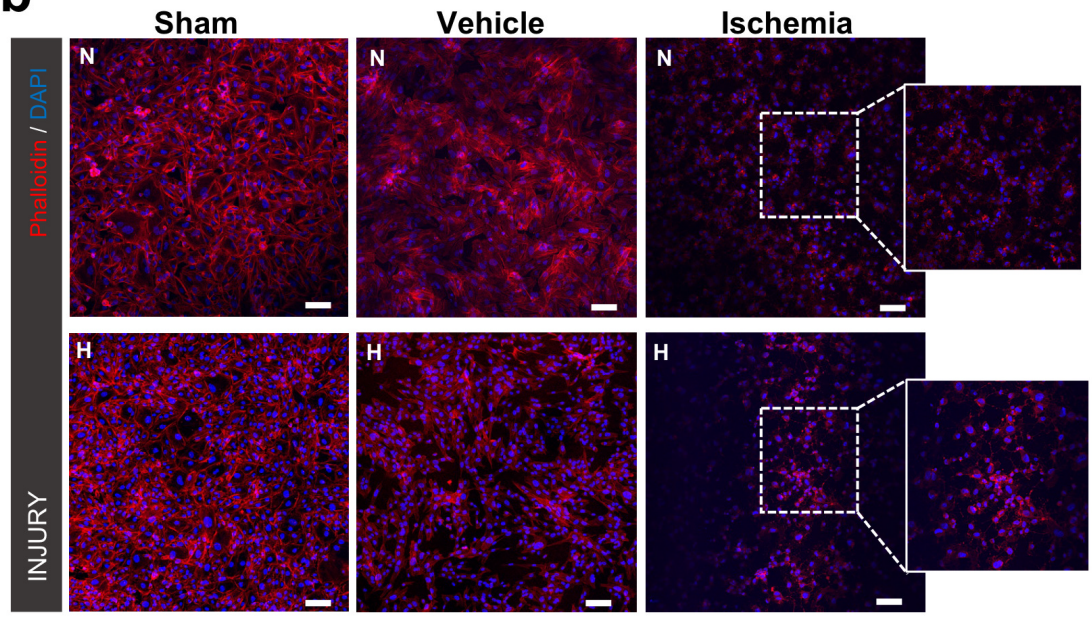
b
Sham
Vehicle
Ischemia
Phalloidin / DAPI
INJURY
N
H

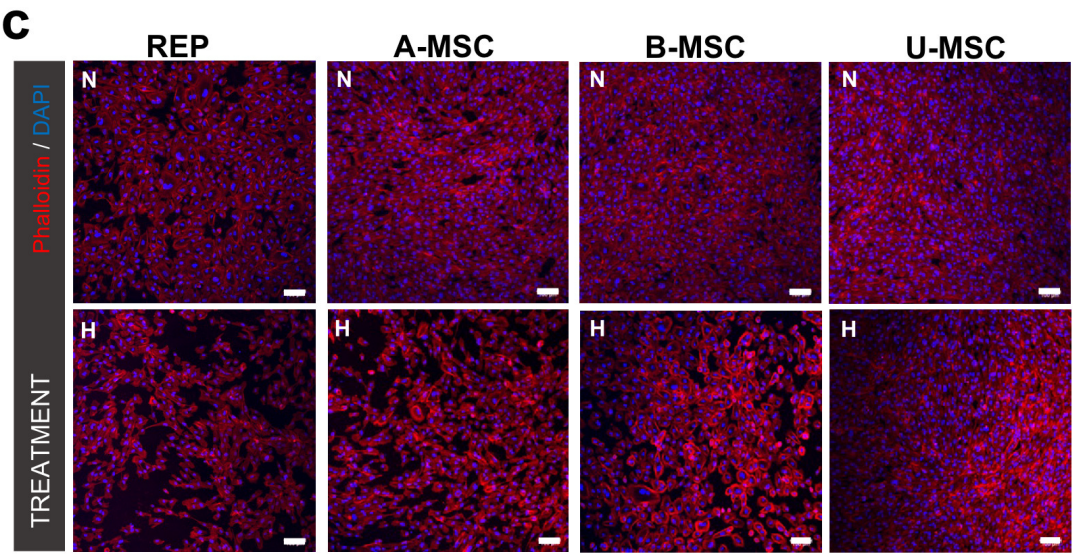
c
REP
A-MSC
B-MSC
U-MSC
Phalloidin / DAPI
TREATMENT
N
H

Figure 1. **Morphological rearrangements following *in vitro* ischemia and MSC treatment.** (**a**) Schematic overview of the protocol for inducing ischemia-like effects in human ciPTEC line. **Sham**: ciPTECs cultured in serum-containing medium; **Vehicle**: ciPTECs cultured in serum-free medium; **Ischemia**: ciPTECs cultured in serum-free medium containing antimycin AA (AA) and 2-deoxy-D-glucose (2DG) (**b**) Immunofluorescence of the cellular organization of ciPTECs cultured under normoxia (N) and hypoxia (H) conditions showed cytoskeleton derangements. (**c**) MSC-derived secretome partially reverted alterations in cell morphology. Representative images obtained using confocal microscopy showing: in blue: DAPI (nuclei staining), in red: Phalloidin (binds to F-actin filaments). Scale bar: 100μm. **Abbreviations: REP** - reperfusion; **A-/B-/U-MSC** – adipose-/bone marrow-/umbilical cord-derived mesenchymal stromal cells; **N**: normoxia; **H**: hypoxia.

3.2. Treatment with MSCs-Secretome Ameliorates Mitochondrial Dysfunction in Experimental Ischemia

During cellular ischemia and/or hypoxia, the cells experience metabolic and mitochondrial dysfunctions due to lack of nutrients and oxygen supply. In serum-deprived (vehicle) ciPTECs there was a decrease in metabolic activity (**Figure 2a)** and in ATP production (**Figure 2b)**, which was more pronounced in the ischemia group and under hypoxia. These changes were consistent with a reduction in mitochondrial mass (**Figure. 2c**) and a decreased mitochondrial membrane potential (Δψ) (**Figure 3a**). ROS production increased gradually over time in N-ciPTECs (**Supplementary Figure S2a**), while in H-ciPTECs ROS production increased but to a lesser extent (**Supplementary Figure S2b**), suggesting that the combination of chemically-induced ischemia and hypoxia may interfere with ROS generation.

During experimental reperfusion, B-CM treatment slightly increased the metabolic activity in ischemic N-ciPTECs and U-CM was somewhat effective in H-ciPTECs (**Figure 2d)**. The remaining treatments showed similar levels (**Figure 2g-j)**, indicating that MSC therapy can (partially) restore cellular metabolic activity. All MSC-derived treatments (CM, LEV, SEV) significantly increased ATP production in N-ciPTECs (**Figure 2e, h, k**), with U-LEV (**Figure 2h**) and B-SEV (**Figure 2k**) having stronger effects. Similarly, CM and LEVs treatment from all sources significantly increased ATP in H-ciPTECs (**Figure 2e, h**). Interestingly, CM and LEV treatment reduced mitochondrial mass (**Figure 2f, i**), whereas SEV treatment, regardless of the source, revealed similar mitochondrial mass levels in H-ciPTECs (**Figure 2l**). This suggests that the effects of different MSC-derived therapies on mitochondrial mass may vary. In N-ciPTECs, MSC treatment showed comparable levels of Δψ (**Figure 3a**). Distinctively, all MSC-derived treatments enhanced Δψ in H-ciPTECs compared with the no treatment control (**Figure 3b-d**). Overall, MSC-derived secretome can restore metabolic activity and increase ATP levels, critical for cell survival and injury resolution following reperfusion.

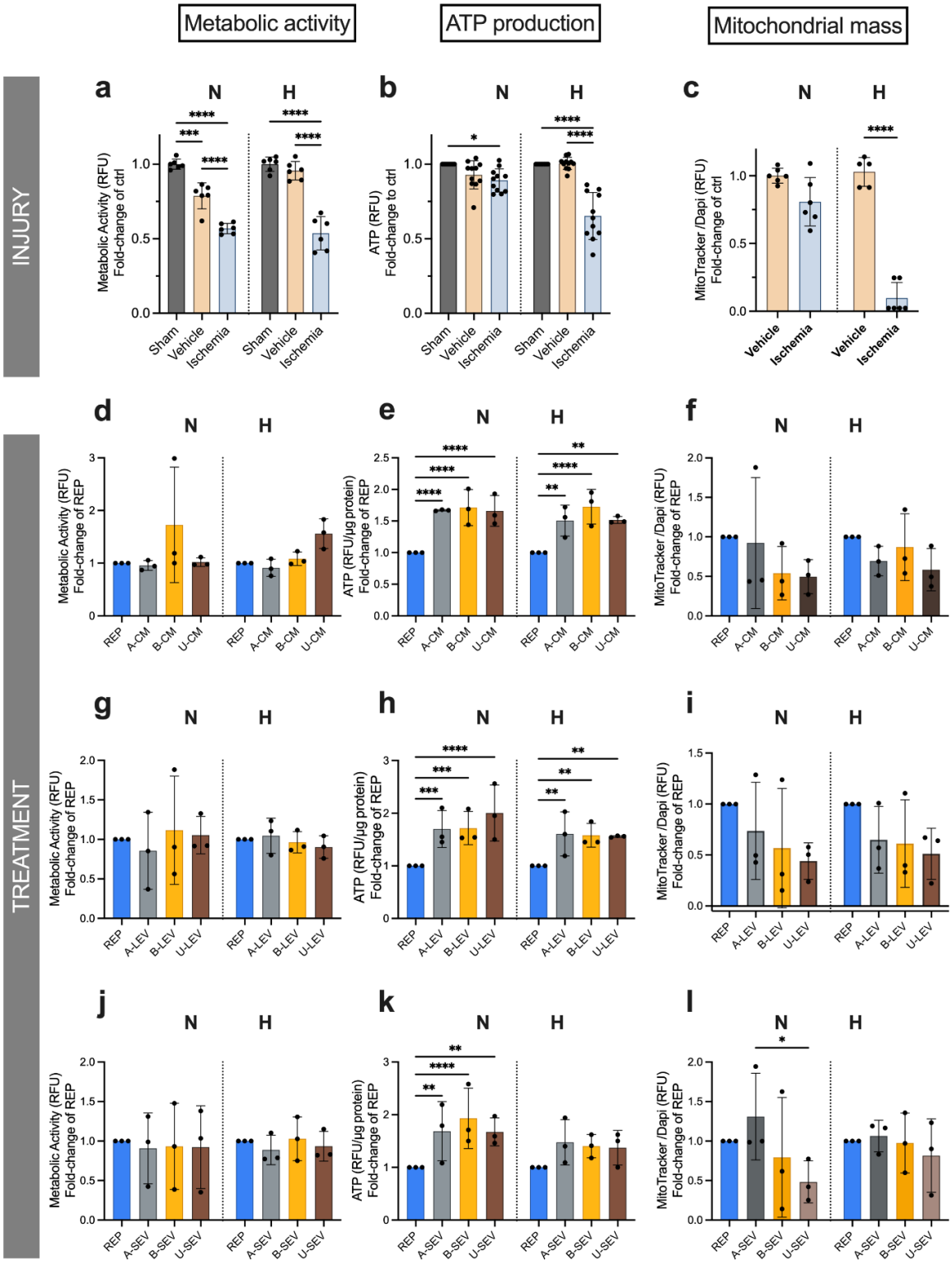

Figure 2. ***In vitro*** **characterization of metabolic and mitochondrial amelioration following MSC therapy.** To evaluate the level of metabolic dysfunction after ischemic injury we looked into metabolic activity (**a**), ATP production (**b**), and mitochondrial mass (**c**). Similarly, effects of the treatment with CM (**d-f**), LEV (**g-i**), and SEV (**j-l**). Data are shown as mean ± SD of three replicates from three independent experiments. One-way ANOVA statistical analysis performed (*p-value < 0.05; **p-value < 0.01; *** p-value <0.001; **** p-value < 0.0001).

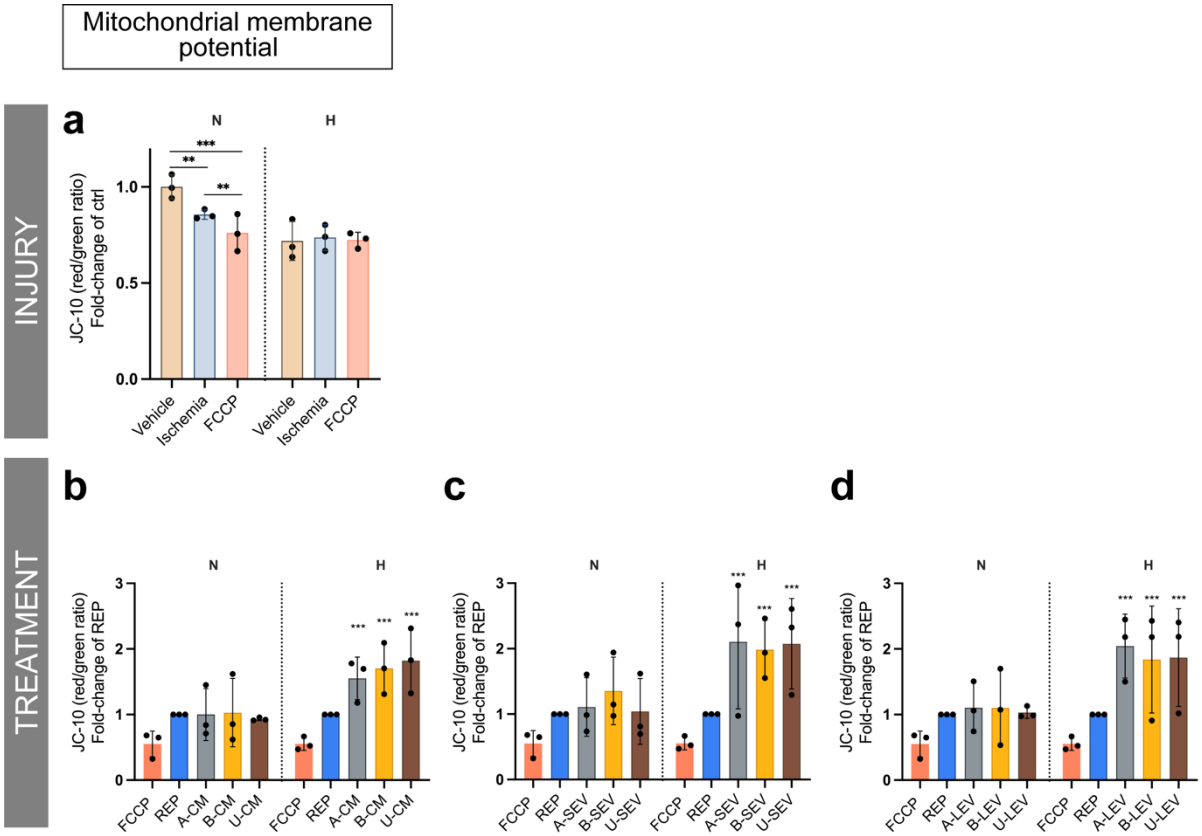

Figure 3. ***In vitro*** **characterization mitochondrial membrane potential following MSC therapy.** To evaluate the level of mitochondrial dysfunction after ischemic injury we looked into mitochondrial membrane potential levels following (**a**) injury. Similarly, effects of the treatment with CM (**b**), SEV (**c**), and LEV (**d**). Data are shown as mean ± SD of three replicates from three independent experiments. FCCP was used as a positive control for depolarized mitochondrion. One-way ANOVA statistical analysis performed (*p-value < 0.05; **p-value < 0.01; *** p-value <0.001; **** p-value < 0.0001).

3.3. MSC Therapy Rescues Energetic Phenotype by Increasing Glycolytic Rates in Ischemic Kidney Proximal Tubule Cells

Under ischemia, metabolic dysfunction is induced by alterations in the mitochondrial ETC resulting in diminished metabolic activity and ATP production. The bioenergetic status of the cells was affected, as evidence by reduced oxygen consumption rate (OCR) (**Figure 4a-b**) and extracellular acidification rate (ECAR) (**Figure 4c-d**) in both vehicle and ischemia groups.

Upon starvation and particularly during ischemia, cells showed a decline in their energetic space dimensions, which restricted metabolism that hampers cell survival and function (**Supplementary Figure S3a-b**). Similarly, basal and ATP-linked respiration were reduced in the vehicle and ischemia groups (**Figure 4e**), reflecting a decline in the cellular capacity to produce ATP via oxidative phosphorylation (OXPHOS). Hypoxic conditioning led to a more severe damage to the inner mitochondrial membranes (IMM) and/or the ETC, as

demonstrated by a decline in coupling efficiency and an increase in proton leak (**Figure 4e**). The spare respiratory capacity (SRC) is an important measure of cellular ability to respond to stress by increasing energy demand. We found that SRC was significantly increased in both vehicle and ischemic N-ciPTECs (**Figure 4f**). In H-ciPTECs, this effect was less prominent and occurred only in the vehicle group (**Figure 4f**).

Treatment with MSC-secretome rescued the bioenergetic status of N-ciPTECs (**Figure 5**) to a greater extent than in H-ciPTECs (**Fig. 6**). Specifically, in normoxia, A-CM and B-CM together with U-LEVs and A-SEVs yielded higher OCR and ECAR values than the reperfusion group (**Figure 5a-f**). Furthermore, A- and B-CM showed an increase in the energetic space (**Figure 5g**). U-LEVs generated a similar bioenergetic profile (**Figure 5h**), while MSC-SEVs generated a more restricted space (**Figure 5i**). The OCR-related parameters in CM-treated cells increased in basal and maximal respiration (**Supplementary Figure S4a**). Additionally, LEVs, and especially B-LEVs, increased the maximal respiration levels compared to the reperfusion treatment (**Supplementary Figure S4b**), while B-SEV showed no effect (**Supplementary Figure S4c**). All treatments, except for A-MSCs, showed a tendency to increase SRC and maintain similar levels of coupling efficiency, indicating a recovery in the ETC and/or IMM health status (**Supplementary Figure S4d-f**). In H-ciPTECs, all MSC treatments induced bioenergetics of oxygen consumption compared to the reperfusion group (**Figure 6a-c**), but only CM from all sources and B-SEVs increased the ECAR profile (**Figure 6d-f**). The energetic space of CM-treated ciPTECs occupied a larger space when compared to the reperfusion group, indicating the induction of an energetic phenotype (**Figure 6g-i**). Specifically, B- and U-CM treatments showed a tendency to increase basal levels of oxygen consumption and increased the maximal respiration levels achieved (**Supplementary Figure S4a**), similar to what was observed for B-SEVs (**Supplementary Figure S4c**). All treatments slightly increased SRC and lowered coupling efficiency rates (**Supplementary Figure S4d-f**). The vehicle and ischemia groups showed an increase in their glycolytic profile ($J_{ATPglyc}$) relative to the sham group (**Supplementary Figure S5a-b**), likely due to compensation for OXPHOS inhibition. Both in normoxia and hypoxia, the ischemia group exhibited a decrease in $J_{ATPox\ coupled}$ without changes in $J_{ATPox\ TCA}$ (**Supplementary Figure S5a-b**). Similarly, glycolysis remained to be the primary source of ATP following MSC treatment (**Supplementary Figure S5c-h**). In N-ciPTECs, both B- and U-EVs showed similar trends (**Supplementary Figure S5d-e**), while A-EVs induced distinct responses: A-LEV exhibited a trend of increased $J_{ATPox\ coupled}$, whereas A-SEV increased $J_{ATPglyc}$ compared to the reperfusion group (**Supplementary Figure S5e**). In contrast, in H-ciPTECs, CM treatment reduced $J_{ATPglyc}$ (**Supplementary Figure S5f**) while B- and U-treatments increased $J_{ATPox\ coupled}$ (**Supplementary Figure S5f-h**).

Further, LEVs showed similar percentages to the reperfusion group (**Supplementary Figure S5g**) and only B-SEVs increased $J_{ATPox\ coupled}$ (**Supplementary Figure S5h**).

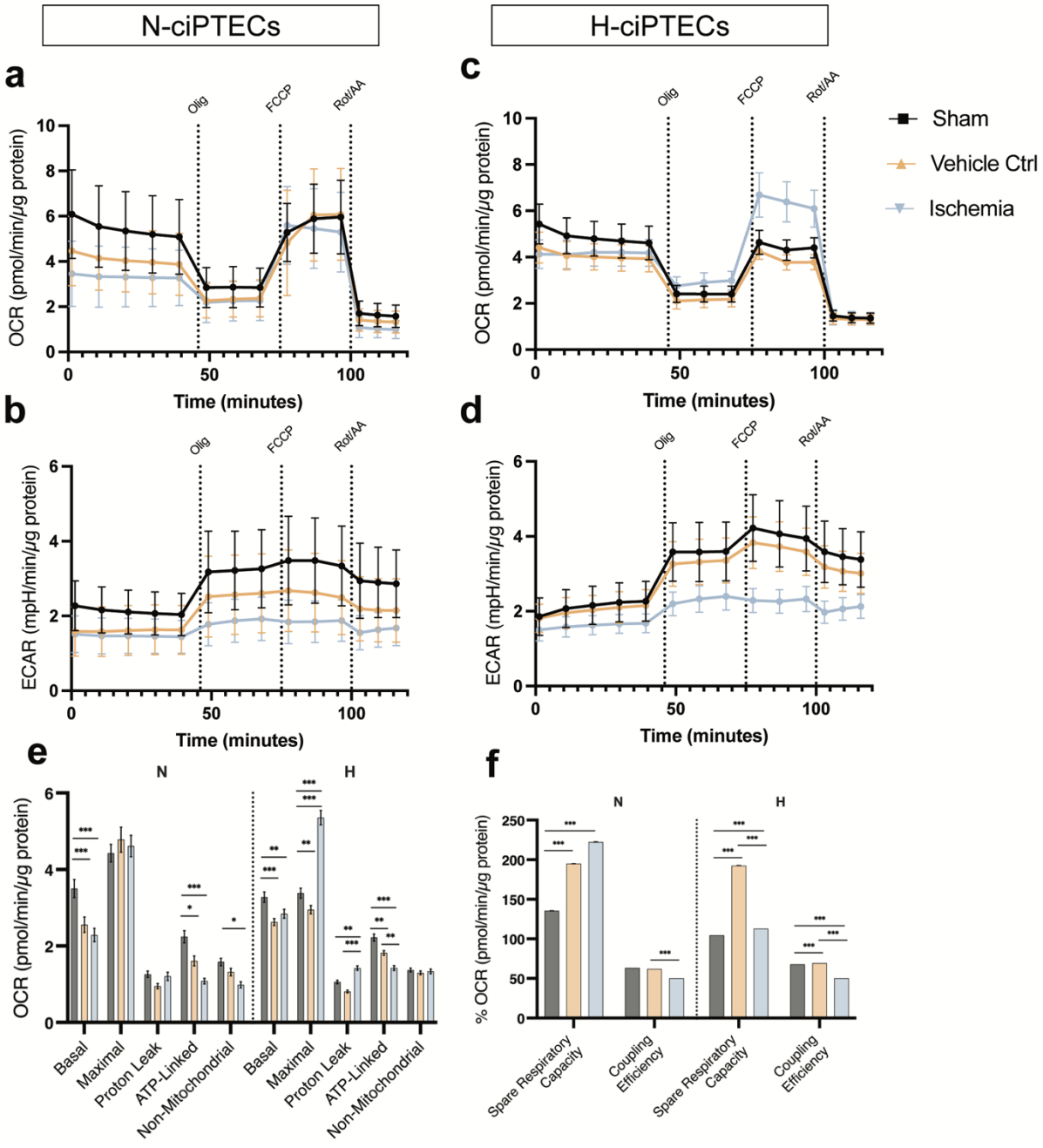

Figure 4. Bioenergetic profiles of ciPTECs after ischemia. (**a, c**) OCR and (**b, d**) and ECAR levels measured before and after injections of oligomycin, FCCP, and rotenone/antimycin A. Specific parameters derived from OCR levels from N- and H-ciPTECs (**e, f**) were plotted in bar graphs. Data are shown as mean ± SD of six replicates from three independent experiments. One-way ANOVA statistical analysis performed (*p-value < 0.05; **p-value < 0.01; *** p-value <0.001; **** p-value < 0.0001).

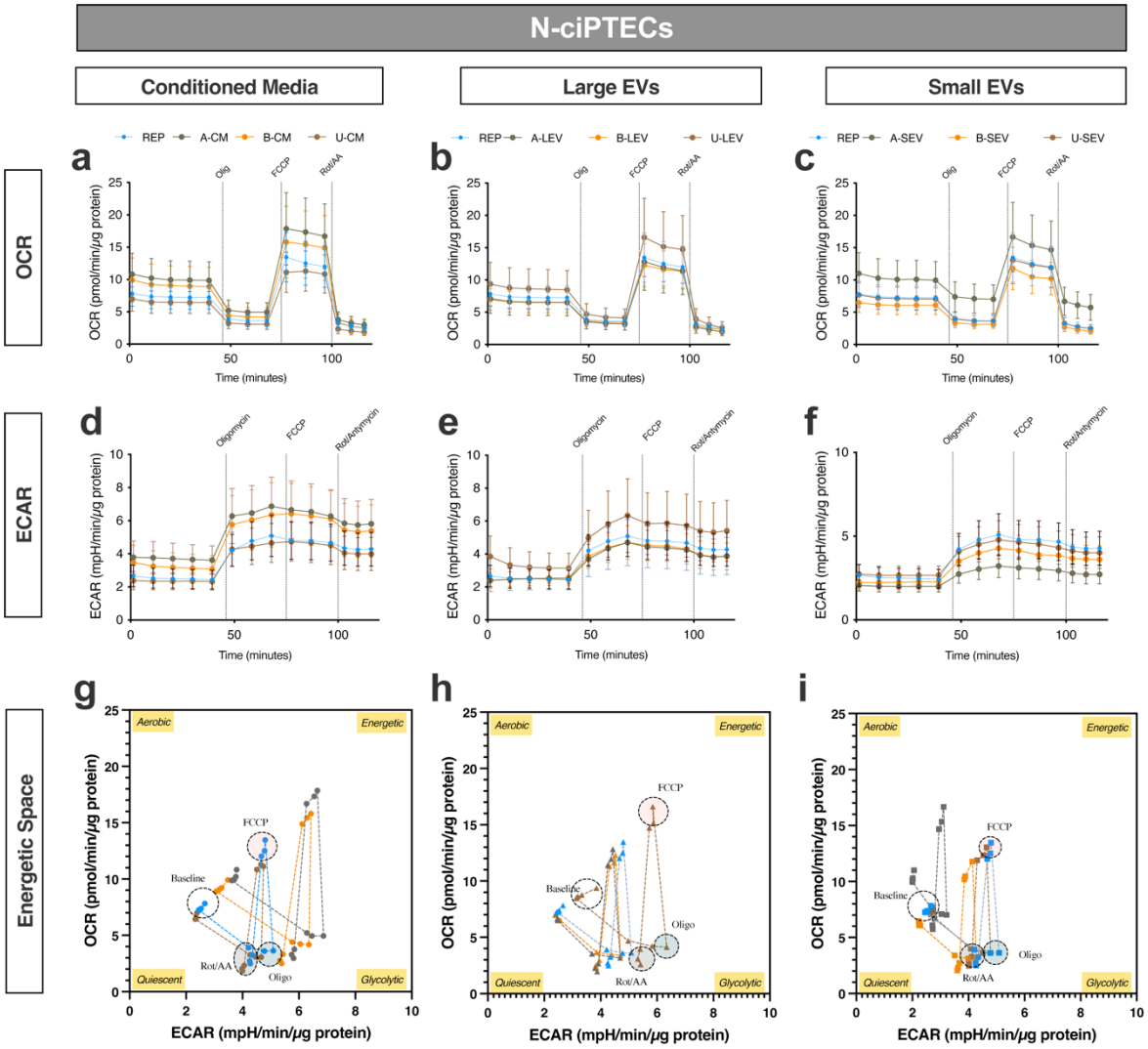

Figure 5. **Bioenergetic profile of ischemic N-ciPTECs upon MSC therapy.** OCR (**a-c**) and ECAR (**d-e**) levels were measured before and after injections of oligomycin, FCCP, and rotenone/antimycin A. Energetic space of MSC-treated ischemic ciPTECs (**g-i**). Data are shown as mean ± SD of 6 replicates of three independent experiments.

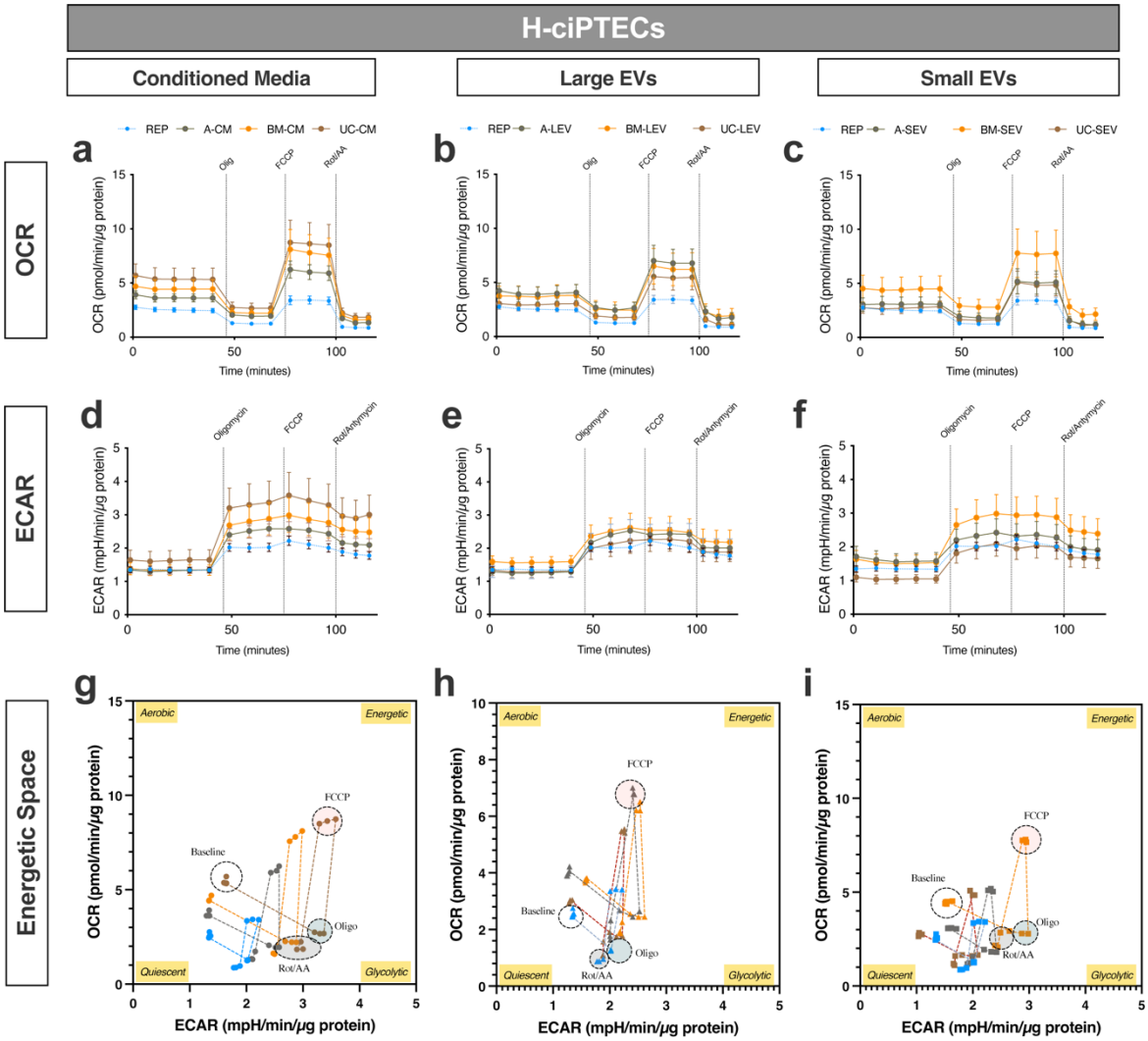

Figure 6. Bioenergetic profile of ischemic H-ciPTECs upon MSC therapy. OCR (**a-c**) and ECAR (**d-e**) levels were measured before and after injections of oligomycin, FCCP, and rotenone/antimycin A. Energetic space of MSC-treated ischemic ciPTECs (**g-i**). Data are shown as mean ± SD of 6 replicates of three independent experiments.

3.4. MSC Therapy Increases Glycolytic Activity of Ischemic CiPTECs and Reduces Oxidative Stress after Chemically-Induced Ischemia.

After ischemic injury, changes in fatty acid metabolism were characterized by an increased accumulation of long-chain acylcarnitines (LCAC), compounds required for the transfer of fatty acids in and out of mitochondria, whereas for the sham group the opposite was observed (**Figure 7a-b**). These findings can point to an altered catabolic capacity since fatty acids can be used to fuel the TCA cycle via β-oxidation. In addition, depletion of TCA cycle intermediates are in line with lower OXPHOS, indicating lower mitochondrial energy production with the exception of succinate (**Figure 7c-d**), which favors the development of a microenvironment for oxidative stress and apoptosis [44].

Ischemic cells had higher levels of upstream glycolytic intermediates, such as glucose 6-phosphate (G6P) and other hexose-phosphates (HexP), and phosphoenolpyruvate (PEP), which can be converted into pyruvate. Reduced downstream glycolytic metabolites in ischemic groups indicated the successful inhibition of glucose metabolism by 2DG (**Figure 7e-f**). Together with the reduced levels of TCA cycle intermediates, this confirms a lower energy metabolism. A metabolite set enrichment analysis was performed to investigate the molecular pathways altered in ischemic ciPTECs. Results showed that in N-ciPTECs (**Figure 7g**), the enriched metabolic pathways were beta-alanine metabolism, inositol phosphate metabolism, glycerolipid metabolism and fatty acid degradation, suggesting a priority for energy production and protection against cellular damage. In H-ciPTECs (**Figure 7h**), the enriched metabolic pathways were fatty acid degradation, glycerolipid metabolism, glycine, serine and threonine metabolism, with a priority for energy production and essential biomolecule synthesis.

Metabolomic analysis following experimental reperfusion indicated that A- and B-MSC secretome in ischemic N-ciPTECs elicited similar metabolic effects as the positive control. In contrast, U-MSC secretome clustered distinctly (**Figure 8a**). In ischemic H-ciPTECs, the reperfusion showed an heterogenous metabolic profile as multiple treatments were clustered together, while B-SEV, A-LEV and A-SEV clustered the furthest (**Figure 9a**). Considering the improvements observed in ATP content and the predominantly glycolytic phenotype of the cells, we investigated the metabolic changes associated with these pathways. In ischemic N-ciPTECs, U-MSC secretome, particularly U-LEV, showed the most prominent improvements in cellular bioenergetics, as evidenced by increased levels of glycolysis intermediates (**Figure 8b**), NADH and NADPH (**Figure 8c**), as well as a reduction in oxidized metabolites such as NAD+ and NADP+ (**Figure 8c**). Additionally, U-MSC secretome showed an increase in reduced and oxidated glutathione levels (**Figure 8c**), suggesting improved redox balance. In ischemic H-ciPTECs, U-SEV and U-LEV showed increased levels of glycolytic intermediates

(**Figure 9b**), indicating an upregulation of glycolysis, with U-SEV showing the highest increase in ATP (**Figure 9c**). On the other hand, B-CM, B-LEV, and U-CM treatments resulted in an increase in NADH, NADPH, GSSG, and glutathione (**Figure 9c**), indicating an accumulation of reducing equivalents, at a possible lower rate of consumption leading to a decrease in ATP (**Figure 9c**). Moreover, the metabolite set enrichment analysis demonstrated an enrichment of pentose phosphate pathway in either N-ciPTECs and H-ciPTECs (**Supplementary Figure S6**), which supports a potential antioxidant therapeutic effect.

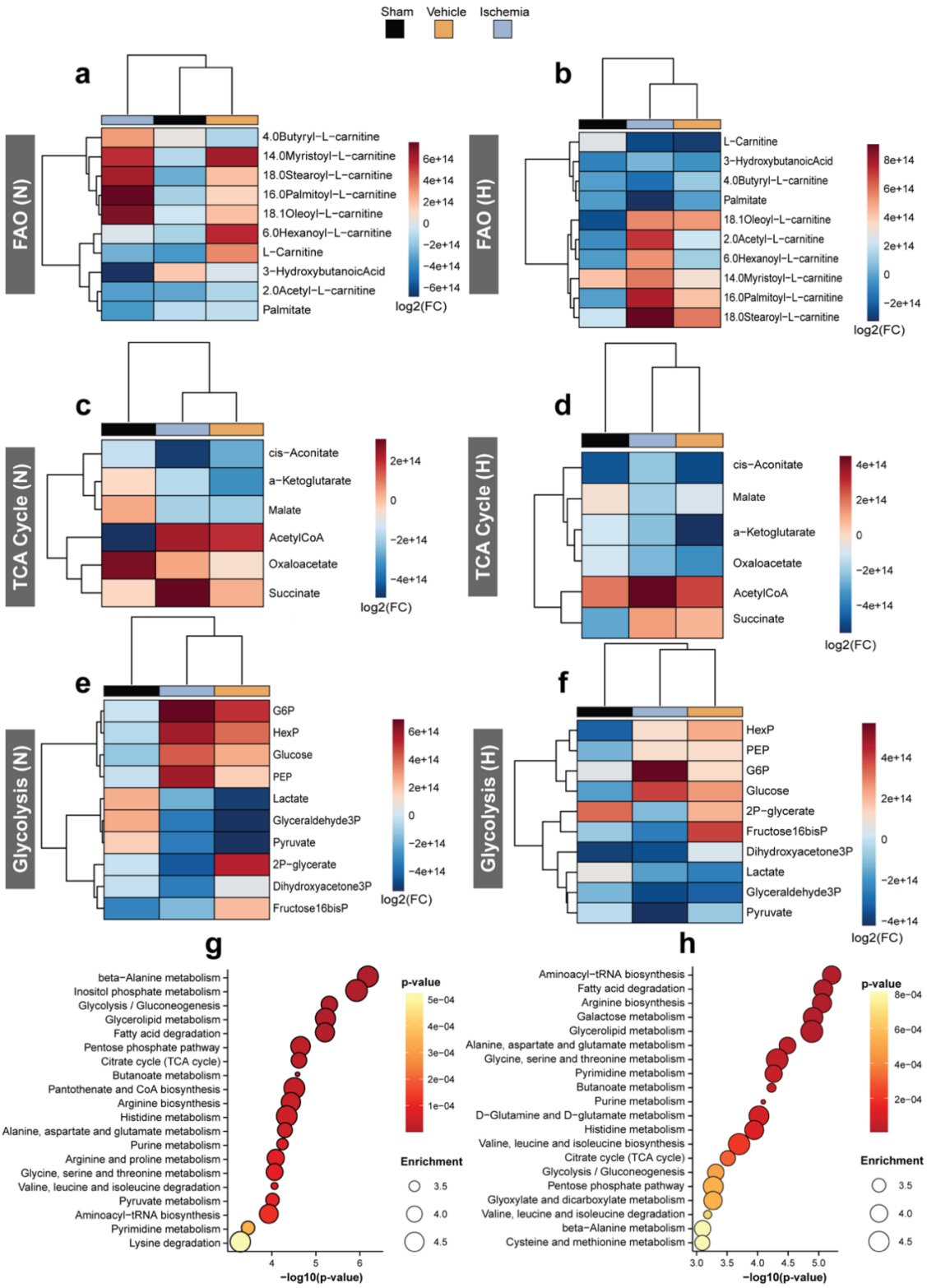

Figure 7. Metabolomics profile of ischemic ciPTECs in normoxia and hypoxia. Heatmaps of the key metabolites involved in fatty acid oxidation (FAO) (**a-b**), tricarboxylic acid (TCA) cycle (**c-d**), and glycolysis (**e-f**). Metabolite sets enrichment overview of ischemic N- ciPTECs (**g**) and H-ciPTECs (**h**), compared to sham, representing their physiological relevance. Heatmap results are shown as log_2(FC) compared to the sham group. Red colors indicate increased values, while blue colors indicate decreased values. **N**, normoxia; **H**, hypoxia.

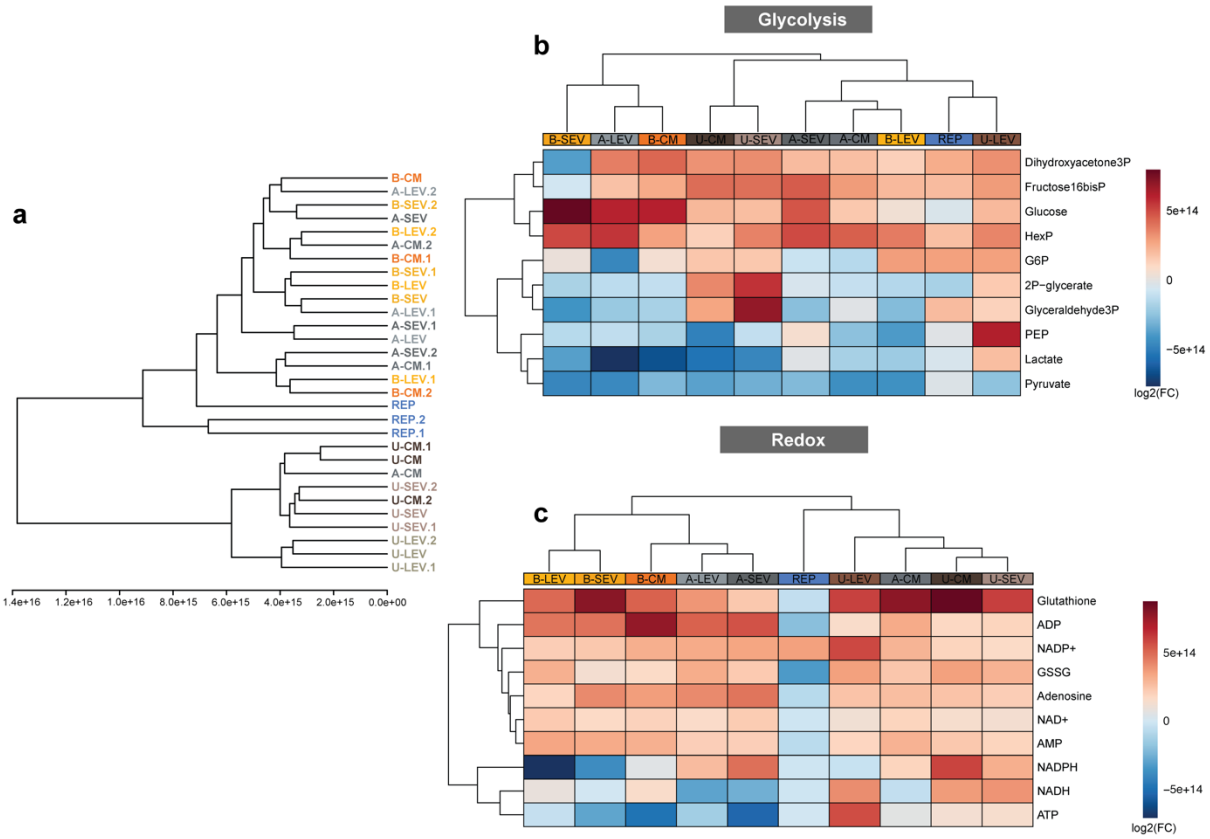

Figure 8. Metabolomics profile of normoxia-treated ischemic ciPTECs (N-ciPTECs). (**a**) Hierarquical cluster analysis of the different conditions tested. (**b**) Heatmaps of the key metabolites involved in glycolysis (**c**) and redox. **A**, adipose tissue; **B**, bone marrow; **U**, umbilical cord; **CM**, conditioned medium; **LEV**, large EVs; **SEV**, small EVs. Data are shown as log2 fold-change of the reperfusion group; Red colors indicate increased values, while blue colors indicate decreased values.

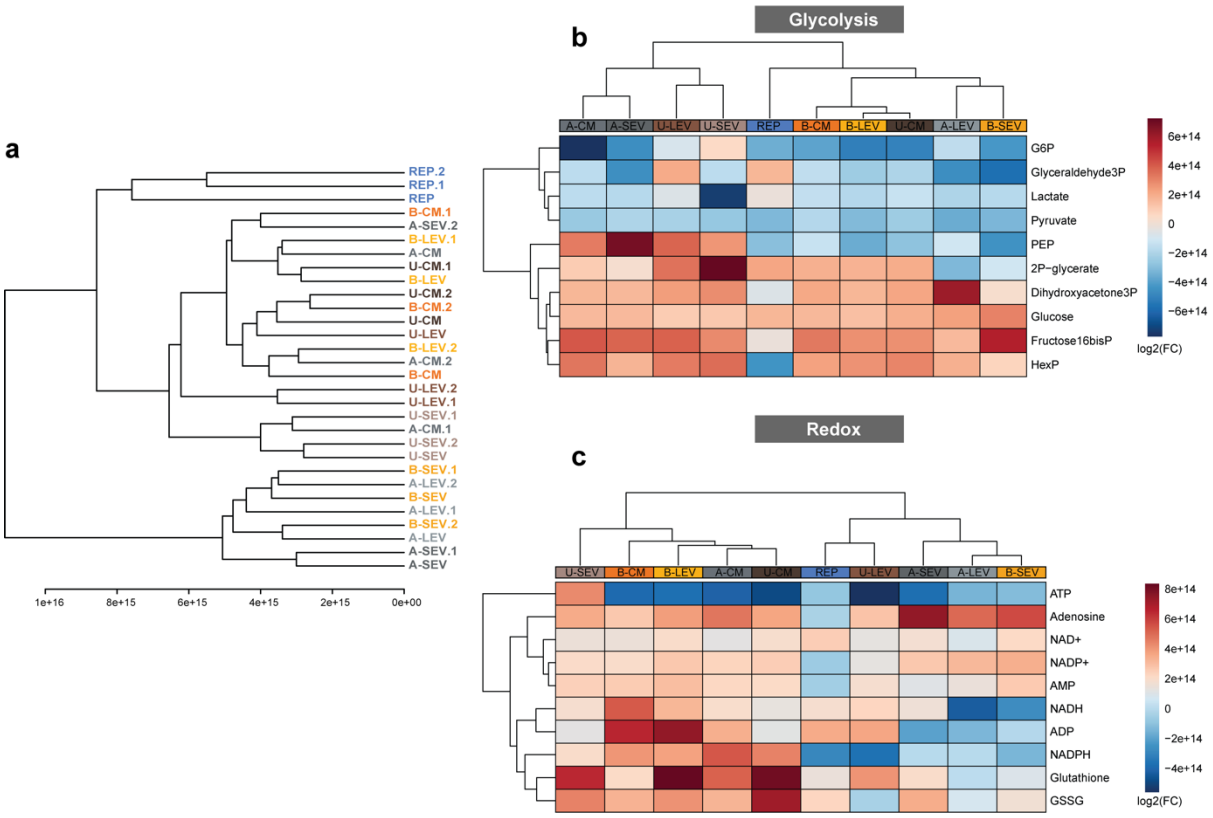

Figure 9. **Metabolomics profile of hypoxia-treated ischemic ciPTECs (H-ciPTECs).** (**a**) Hierarquical cluster analysis of the different conditions tested. (**b**) Heatmaps of the key metabolites involved in glycolysis (**c**) and redox. **A**, adipose tissue; **B**, bone marrow; **U**, umbilical cord; **CM**, conditioned medium; **LEV**, large EVs; **SEV**, small EVs. Data are shown as log2 fold-change of the reperfusion group; Red colors indicate increased values, while blue colors indicate decreased values.

4. DISCUSSION

Using an optimized *in vitro* model, we here demonstrate that the MSC secretome reduces oxidative stress and improves energy production following ischemic injury. We evaluated three different sources of MSC secretome and demonstrated that critical hallmarks of the acute ischemic phase, including cytoskeletal rearrangements, energetic imbalance, increased oxidative stress, mitochondrial dysfunction, and altered antioxidant defenses and redox homeostasis, were achieved at 24 hours following ischemic induction and were enhanced further under hypoxia. During the reperfusion phase, *viz.* treatment with MSC secretome, particularly U-MSC restored cell morphology and metabolic derangements, partially reversing ischemia-induced damage. The described improvements in cell morphology could be derived from changes in the activation of cell death programs that typically convey during severe ischemic damage [45], as presented by others [46-48], and should be explored further in follow-up studies. To our knowledge, this is the first *in vitro* study to compare the therapeutic efficacy of three sources of MSC secretome in this setting.

Proximal tubule cells are highly susceptible to ischemic injury, and their metabolic and mitochondrial function are critical to maintaining renal homeostasis [49]. A decline in mitochondrial activity leads to a reduction in ATP production and an increase in the release of harmful products, such as ROS as seen in injured cells. Following ischemia, a loss of mitochondrial content and impaired mitochondrial activity were reflected in the bioenergetic profile, with decreased oxygen consumption. Morphological and functional alterations in the mitochondrial pool following an ischemic insult may also impact the recovery phase [50]. The improved bioenergetic status, despite reduced mitochondrial mass, following MSC treatment may reflect the clearance of damaged mitochondria and the initiation of biogenesis and regeneration. In agreement, U-MSC EVs were found to alleviate mitochondrial fragmentation [51] and B-MSCs and their SEVs promoted mitophagy through microRNA-dependent mechanisms [52], supporting their renoprotective potential in favor of tissue regeneration.

The metabolomic profile of ischemic cells demonstrated imbalanced fatty acid metabolism and a general defect in mitochondria's catabolic activity as seen by the accumulation of metabolic byproducts, such as acylcarnitines that contribute to cellular damage and apoptosis [53, 54]. The TCA cycle activity is dependent on the availability of oxygen and nutrients, thus imbalanced FAO may alter the TCA cycle activity. The accumulation of acetyl-coA, an intermediate in both pathways, is a hallmark of this dysfunction due to its effects on inhibiting enzymes involved in the TCA cycle, exacerbating energy deficit [55, 56]. The metabolic rewiring that takes place during acute injury aimed to sustain cell viability is characterized by an increase in glycolytic rates [57-60], an effect widely described in the literature that supports

the increase seen in key upstream glycolytic metabolites. Other downstream effects, such as glucose 6-phosphate or PEP, were found decreased following ischemia. PEP has been shown to exert cytoprotective and anti-oxidative properties that prevent a decrease in ATP content [61, 62], which could explain the moderate decrease in ATP under normoxic culture. While an increase in ATP production was observed across all treatments following ischemia, the metabolic profile of treated ischemic cells varied. In N-ciPTECs, larger changes in bioenergetics and redox homeostasis were mainly exerted by U-MSC therapy. Similar results were seen in H-ciPTECs, despite their metabolic profiles being more heterogeneous and higher oxidative imbalance. The changes found are in line with previous findings that suggest U-MSCs mediate the recovery process following IRI through various mechanisms that lead to reduced oxidative stress [8, 63] and increased energy balance [64], critical to ensure cell viability following ischemic insults.

All U-MSC secretome, and in particular U-LEV, showed an enrichment in PPP and beta-alanine, with N-ciPTECs exhibiting a greater enrichment compared to H-ciPTECs. Increased NAD metabolism has been identified as a protection mechanism by restoring oxidative metabolism [65], stimulating mitochondrial biogenesis and increasing oxygen consumption [66, 67]. In addition, PPP not only generates NADPH but also ribulose-5-phosphate, which is essential for nucleotide synthesis as well as ATP synthesis. Additionally, beta-alanine might indirectly support ATP production by supporting the function of enzymes involved in ATP synthesis [68]. This increase in bioenergetics and redox homeostasis is further supported by previous studies that have shown the presence of mitochondrial components and antioxidant miRNAs in EVs, providing metabolic support to damaged cells [69-71].

We found that for each MSC source, the respective LEVs and SEVs showed similar metabolic profiles in the treated cells. However, the mechanism behind their therapeutic efficacy was not clear because they had similar basal respiration, ATP production, SRC and nonmitochondrial respiration levels. We found that A- and B-EV treated N-ciPTECs resulted in a significant increase in SRC compared to the reperfusion group, which has been shown to be regulated by AMPK [72, 73]. This increase in SRC has been demonstrated in cases of metabolic stress, in which cells show increased cell survival by adapting to oxidative stress. The extrapolated metabolite enrichment pathway analysis of U-MSC treated N- and H-ciPTECs showed a difference in pathways. One possible explanation for these results is that the metabolic response to ischemia differs depending on the severity of the injury, with H-ciPTECs being subjected to a more energy deficient microenvironment, hence the enrichment in the TCA cycle and glycerolipid metabolism. We suggest that the superior therapeutic effect of U-MSC may be due to their embryonic origin, which is thought to confer higher survival rate,

and most importantly, a richer secretome [74, 75]. In addition to increasing ATP content, MSC therapy partially reverted the disruption of the actin cytoskeleton observed in ischemic ciPTECs. While this effect was attributed to an increase in ATP, a key player in the polymerization of actin filaments [76], heat shock proteins (HSPs) have also been shown to improve the repair of structural proteins after ischemia-induced cytoskeleton damage [77]. In an earlier study, HSPs have been identified in a proteomic analysis of MSCs, suggesting that they may contribute to the therapeutic effect of MSC secretome [78].

While our *in vitro* model effectively reproduces molecular and morphological changes seen *in vivo* during renal IRI and offers valuable insights into the therapeutic effect of the MSC secretome, it has inherent limitations. These include the use of a single cell type in a two-dimensional monolayer, which incompletely represents the adult kidney. The incorporation of additional cell types will improve the physiological relevance of our model and give an in-depth understanding of the therapeutic effect of MSC secretome. For instance, T-cells, particularly $CD3^+$ T-cells, have been shown to play a significant role in mediating post-ischemic damage by increasing the release of pro-inflammatory cytokines [79], whereas regulatory T-cells have an anti-inflammatory role in IRI [80]. Furthermore, microvascular leakage is another hallmark of IRI, exacerbating ischemic damage by inducing, among others, the release of inflammatory cytokines by leukocytes (*e.g.*, lymphocytes) [81, 82]. To address this, integrating models like organ-on-chip systems would provide a more accurate representation of the complex cellular interplay between the various cell types. An example of such a model was developed in which PTECs and endothelial cells were exposed to hypoxia and normoxia to recreate the IRI microenvironment, and the therapeutic efficacy of vitamin therapy in ameliorating the damage could be demonstrated [83]. Traditionally, IRI and therapies for ischemic damage are mainly studied and tested in rodent models, but the variability of the injury and response to therapy between individual animals makes it difficult to obtain consistent results. Additionally, *in vivo* models may not fully replicate the complex cellular and molecular interactions that occur during IRI in humans as well, which limits their translational value. Therefore, human-based *in vitro* models, such as organ-on-chip, could potentially be valuable for studying the cellular and molecular mechanisms underlying biological processes in health and disease, and for developing and testing new therapeutic strategies.

5. CONCLUSIONS

Altogether, we showcase the advantage of using a chemically-induced ischemia model in combination with hypoxia to more accurately mimic the physiological cellular response to ischemia and to evaluate the benefits of MSC-derived therapies during experimental reperfusion. Further research is needed to determine the exact mechanism of action of MSCs, in particular the effects seen by U-MSC secretome. Additionally, dose-response studies should be taken along to evaluate optimal therapeutic delivery. Nonetheless, our data expands the current understanding that the PT is highly susceptible to ischemic damage and showcases the therapeutic effect of MSC secretome in improving the bioenergetic profile of ischemic PT cells.

ACKNOWLEDGMENTS

Not applicable.

FUNDING

This study has received funding from the European Union's Horizon 2020 research and innovation programme under the Marie Skłodowska-Curie grant agreement No 813839. The funding body played no role in the design of the study and collection, analysis, and interpretation of data and in writing the manuscript.

AUTHOR CONTRIBUTIONS

J.F., **S.CiC.**, **R.S.**, **B.B.**, **T.O'B.**, **S.M.M.**, and **R.M.** conceived the study and designed the experiments. **J.F.**, **S.CiC.**, and **R.S.** performed the main experiments and analyzed data. **B.C.B.**, **A.J.B.**, and **E.A.Z.** supported the main experiments. **J.F.**, **S.CiC.**, and **R.S.** wrote the manuscript. **B.B.**, **T.O'B.**, **S.M.M.**, and **R.M.** revised the manuscript and approved the manuscript for publication.

ETHICS DECLARATIONS

ETHICS APPROVAL

A-MSCs from lipoaspirates (healthy donors of both gender in a range of age 47–25 years) were processed in Heidelberg after obtaining informed consent (title of approved project: isolation and characterization of MSCs from human adipose tissue; institutional approval committee: Mannheim Ethics Commission II; approval number: 2006-192N-MA; date of approval: 18.04.2005, re-confirmed 26.02.2009 with subsequent approvals). BM-MSCs provided by Galway were isolated from bone marrow aspirates (healthy young male donors)

purchased from Lonza (Basel, Switzerland) (title of approved project: Isolation of Human Marrow Stem Cells from Healthy Donors; Bone Marrow Research Study", institutional approval committee: Galway University Hospital Clinical Research Ethics Committee; approval number: 02/08; date of approval: November 2008 with subsequent approvals for amendments). UC-MSCs with informed consent obtained in accordance with the Declaration of Helsinki were sourced from the NHS Blood and Transplant and transferred to the University of Liverpool (project title: the provision of mesenchymal stromal cells to the University of Liverpool for use in the RenalToolBox project; institutional approval unit: NHS Blood and Transplant, Cellular and Molecular Therapies; approval number: RTB21112019; date of approval: 21 November 2019).

CONSENT FOR PUBLICATION

Not applicable.

COMPETING INTERESTS

The authors declare no conflicts of interest with the contents of this article. Rosalinde Masereeuw is co-inventor of the cell line ciPTEC-OAT1, for which the patent is held by Radboud University Nijmegen, the Netherlands. Timothy O'Brien, co-author of this manuscript and Editor-in-Chief of Stem Cell Research & Therapy, declares that he was not involved in the peer review or decision making of this article.

DATA AVAILABILITY

Data from the current study are available from the corresponding author on reasonable request. Metabolomics data are deposited at MetaboLights (MetaboLights) with identifier MTBLS6279.

SUPPLEMENTARY MATERIALS

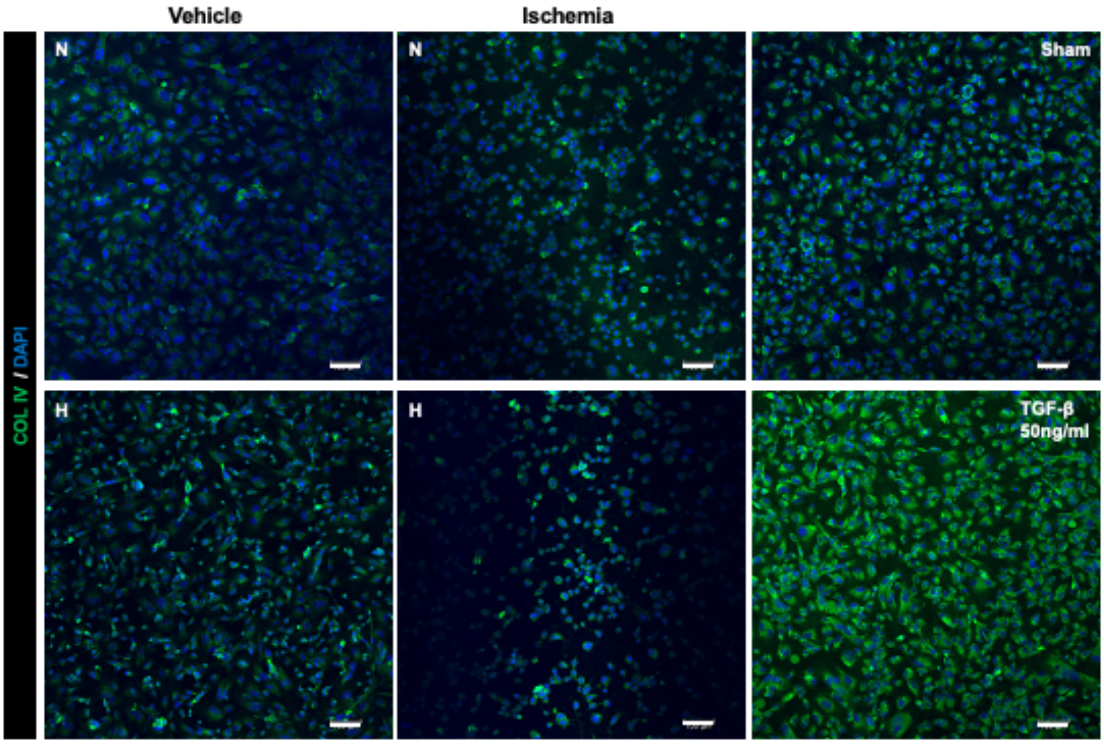

Supplementary Figure S1. Immunofluorescence of the cellular organization of ciPTECs cultured under normoxia (N) and hypoxia (H) conditions. TGF-β (pro-fibrotic mediator) was used as positive control. In blue: DAPI (nuclei staining), in green: collagen IV. Scale bar: 100 μm.

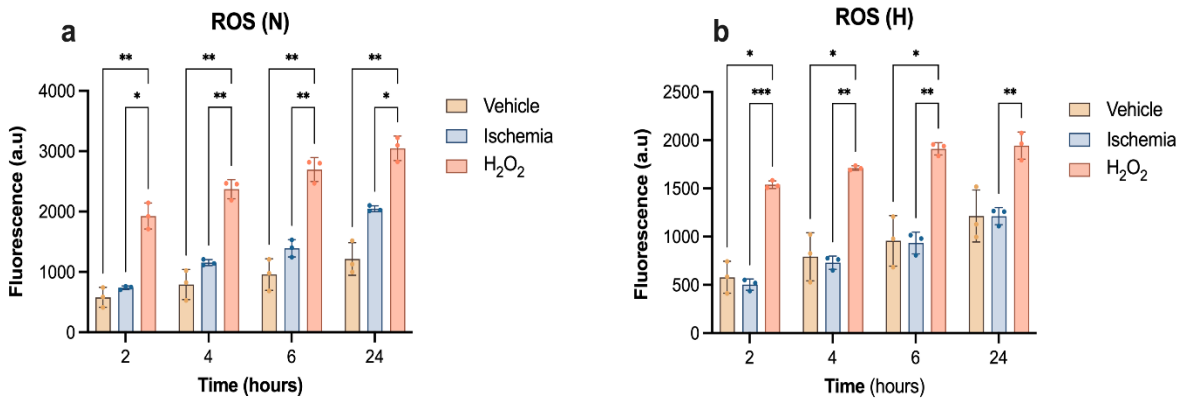

Supplementary Figure S2. (**a-b**) **Intracellular reactive oxygen species (ROS).** Data are shown as mean ± SD of four replicates of three independent experiments. H_2O_2 was used as a positive control. Two-way ANOVA statistical analysis performed with Tukey's multiple comparisons test (*p-value < 0.05; **p-value < 0.01; *** p-value <0.001; **** p-value < 0.0001). **N**, normoxia; **H**, hypoxia.

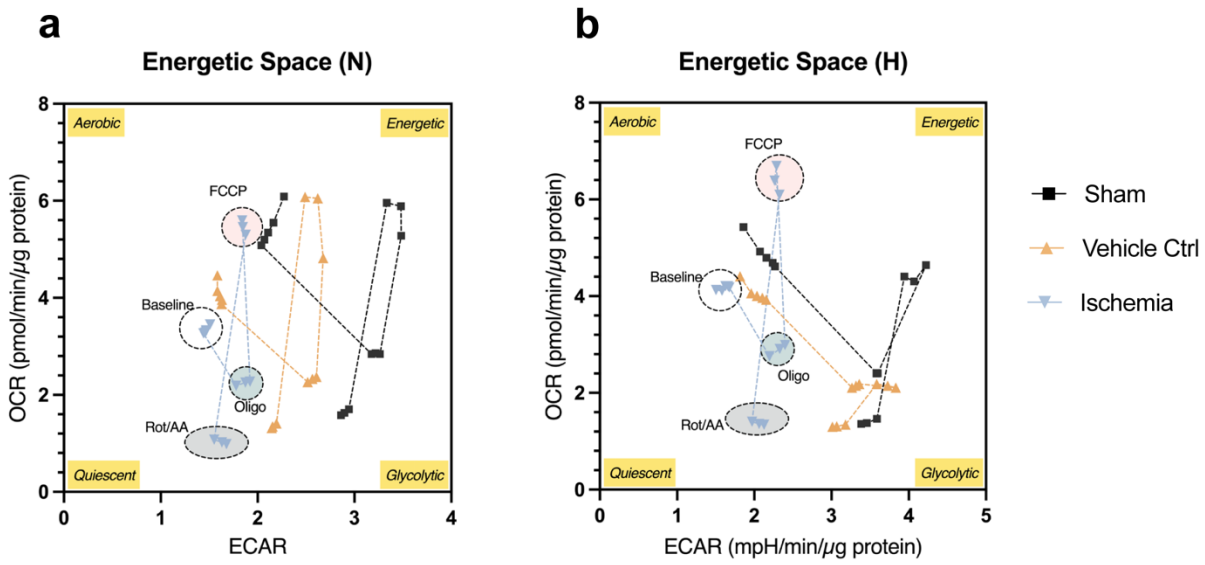

Supplementary Figure S3. Bioenergetic alterations following ischemic conditioning in kidney proximal tubule cells. (**a**, **b**) Energetic space generated by plotting OCR vs ECAR levels before and after injections of oligomycin, FCCP, and rotenone/antimycin A. Data are shown as mean ± SD of ten replicates of three independent experiments. One-way ANOVA statistical analysis performed (*p-value < 0.05; **p-value < 0.01; *** p-value <0.001; **** p-value < 0.0001). **N**, normoxia; **H**, Hypoxia.

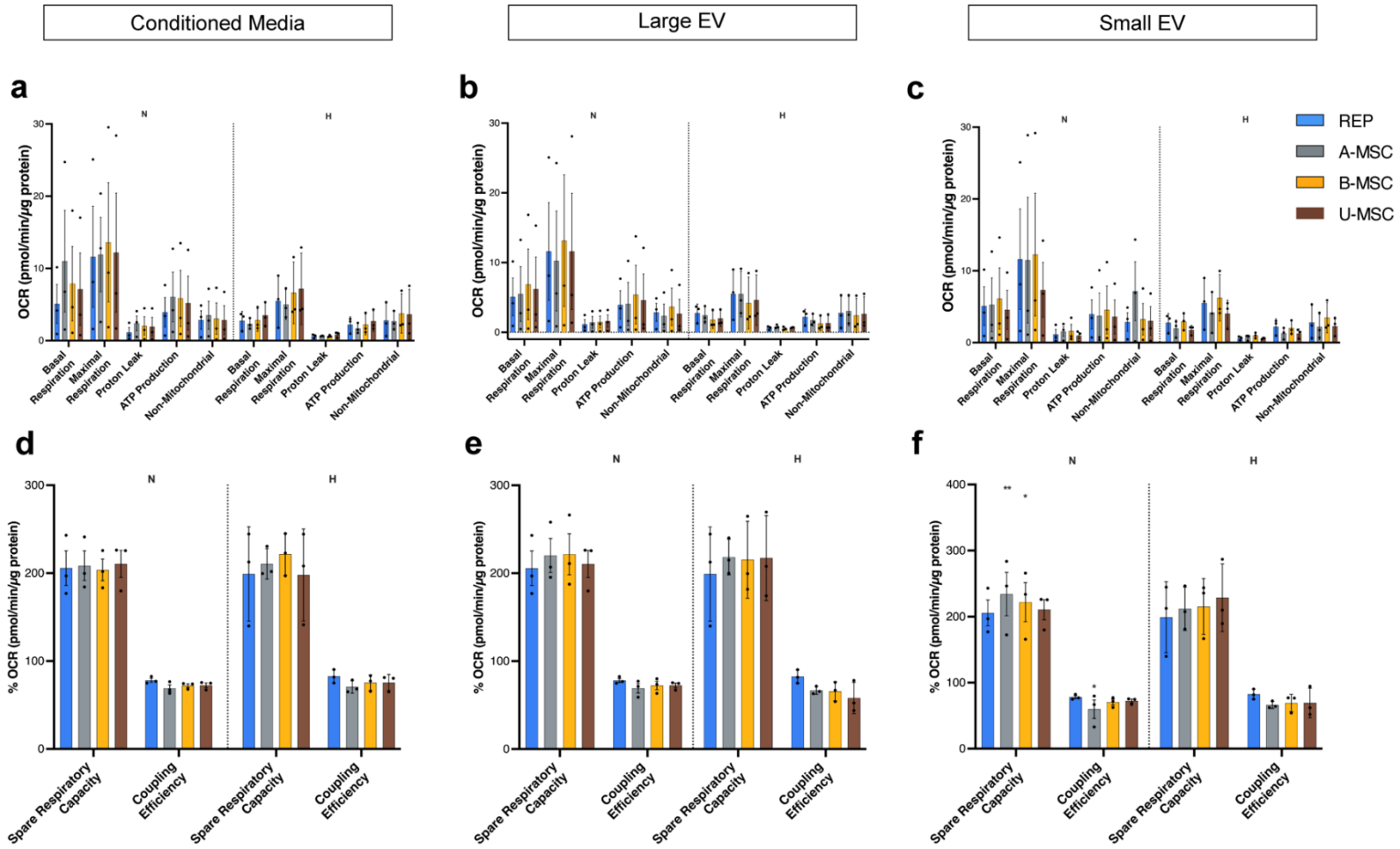

Supplementary Figure S4. Supplementary Figure S5. Breakdown of OCR-related parameters of MSC-treated N-ciPTECs and H-ciPTECs of CM (a,d), Large EVs (b,e), and Small EVs (c,f). Data are shown as mean ± SD of 6 replicates of three independent experiments. Statistical analysis performed using Two-Way ANOVA with Dunnett's post-hoc test. *p-value < 0.05; **p-value < 0.01; *** p-value <0.001; **** p-value <0.0001). **N**, normoxia; **H**, hypoxia.

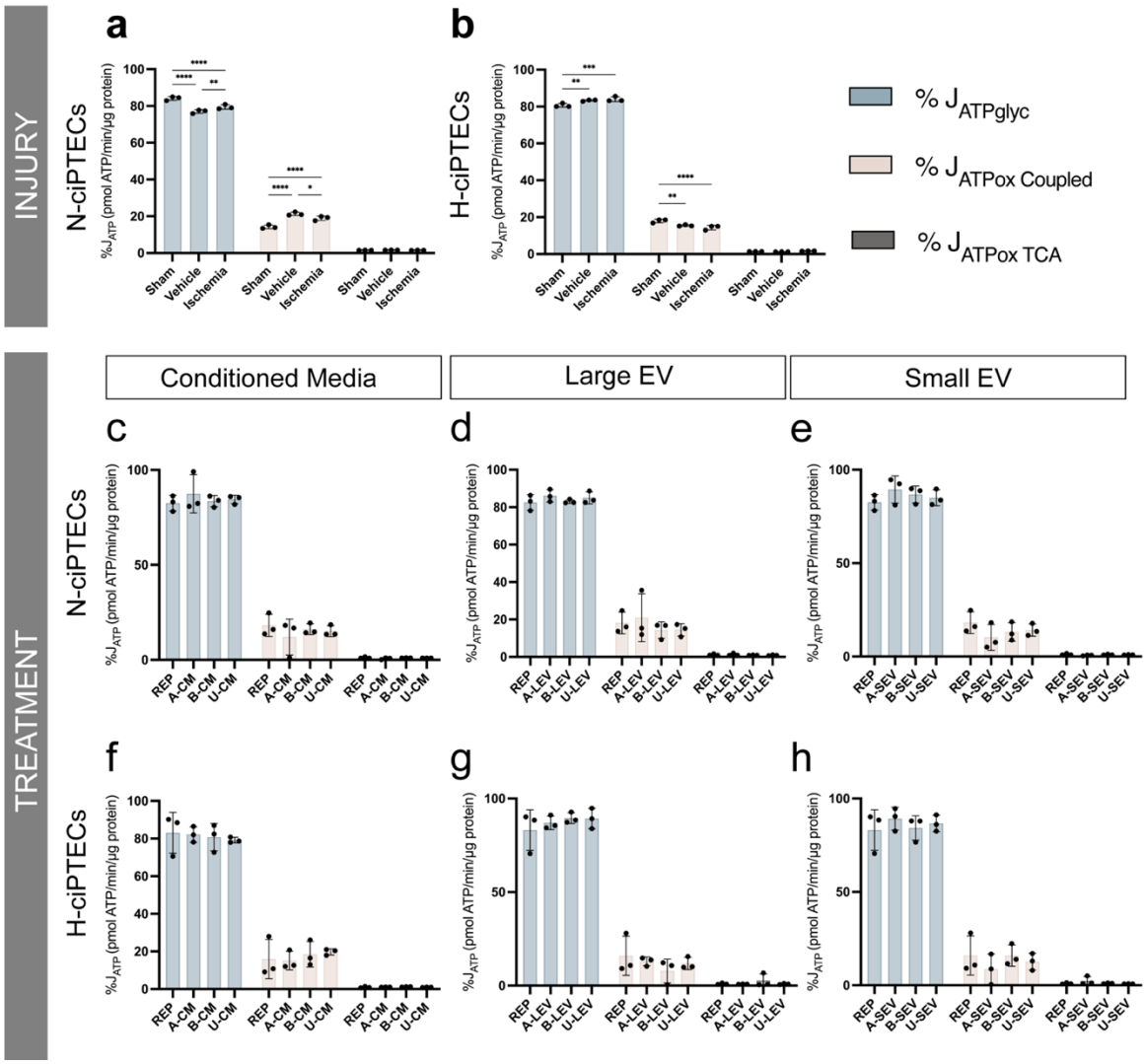

Supplementary Figure S5. **Net rate of ATP production (JATP) of ischemic ciPTECs (a,b), and ischemic ciPTECs treated with MSC secretome (c-h).** The JATP divided in its three main components ($J_{ATPglyc}$, J_{ATPox} coupled, $J_{ATPox\ TCA}$). Statistical analysis performed using Two-way ANOVA and Dunnet's post-hoc test (*p-value < 0.05). Data are shown as mean ± SD of 6 replicates of three independent experiments.

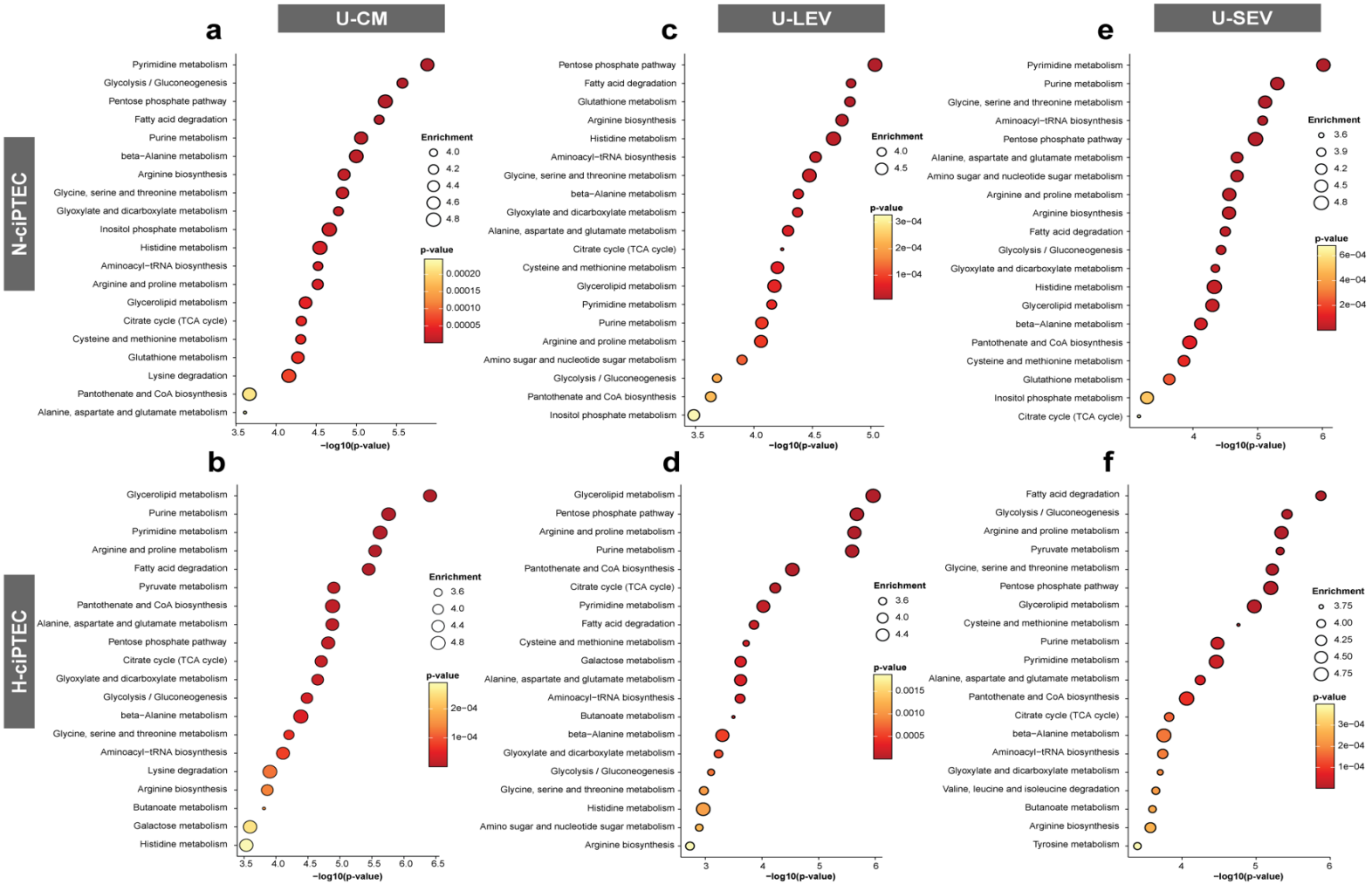

Supplementary Figure S6. Metabolite sets enrichment overview showing the most altered metabolites revealed in ischemic ciPTECs treated with U-CM (a,b), U-LEV (c,d), or U-SEV (e-f), representing their physiological relevance. The top 25 metabolites for each treatment were compared to the reperfusion group (positive control). **N**, normoxia; **H**, hypoxia.

Supplementary Table S1. Immunofluorescence analysis antibodies.

Antibody	Species	Dilution	Catalog #	Company
Phalloidin		1:1000		Invitrogen
Col IV	Goat	1:50	134001	SouthernBiotech
Alexa-488 goat anti-mouse	Goat	1:500	Ab150113	Abcam
DAPI		1:1000	D3571	ThermoFischer

REFERENCES

1. R. Munshi, C. Hsu and J. Himmelfarb. Advances in understanding ischemic acute kidney injury. BMC Med 2011;9:11

2. P. Devarajan. The Current State of the Art in Acute Kidney Injury. Front Pediatr 2020;8:70

3. Y. Li, M. Hepokoski, W. Gu*, et al.* Targeting Mitochondria and Metabolism in Acute Kidney Injury. J Clin Med 2021;10(17)

4. M. Malek and M. Nematbakhsh. Renal ischemia/reperfusion injury; from pathophysiology to treatment. J Renal Inj Prev 2015;4(2):20-27

5. J. A. Schaub, M. A. Venkatachalam and J. M. Weinberg. Proximal Tubular Oxidative Metabolism in Acute Kidney Injury and the Transition to CKD. Kidney360 2021;2(2):355-364

6. M. El Sabbahy and V. S. Vaidya. Ischemic kidney injury and mechanisms of tissue repair. Wiley Interdiscip Rev Syst Biol Med 2011;3(5):606-618

7. N. Perico, F. Casiraghi and G. Remuzzi. Clinical Translation of Mesenchymal Stromal Cell Therapies in Nephrology. J Am Soc Nephrol 2018;29(2):362-375

8. W. Zhuo, L. Liao, T. Xu*, et al.* Mesenchymal stem cells ameliorate ischemia-reperfusion-induced renal dysfunction by improving the antioxidant/oxidant balance in the ischemic kidney. Urol Int 2011;86(2):191-196

9. G. Zhang, X. Zou, Y. Huang*, et al.* Mesenchymal Stromal Cell-Derived Extracellular Vesicles Protect Against Acute Kidney Injury Through Anti-Oxidation by Enhancing Nrf2/ARE Activation in Rats. Kidney Blood Press Res 2016;41(2):119-128

10. M. E. Reinders, J. R. Bank, G. J. Dreyer*, et al.* Autologous bone marrow derived mesenchymal stromal cell therapy in combination with everolimus to preserve renal structure and function in renal transplant recipients. J Transl Med 2014;12:331

11. I. C. S. Calcat, C. Sanz-Nogues and T. O'Brien. When Origin Matters: Properties of Mesenchymal Stromal Cells From Different Sources for Clinical Translation in Kidney Disease. Front Med (Lausanne) 2021;8:728496

12. L. Perico, M. Morigi, C. Rota*, et al.* Human mesenchymal stromal cells transplanted into mice stimulate renal tubular cells and enhance mitochondrial function. Nat Commun 2017;8(1):983

13. R. Stavely and K. Nurgali. The emerging antioxidant paradigm of mesenchymal stem cell therapy. Stem Cells Transl Med 2020;9(9):985-1006

14. X. Liang, Y. Ding, Y. Zhang*, et al.* Paracrine mechanisms of mesenchymal stem cell-based therapy: current status and perspectives. Cell Transplant 2014;23(9):1045-1059

15. M. Jafarinia, F. Alsahebfosoul, H. Salehi*, et al.* Mesenchymal Stem Cell-Derived Extracellular Vesicles: A Novel Cell-Free Therapy. Immunol Invest 2020;49(7):758-780

16. L. Birtwistle, X. M. Chen and C. Pollock. Mesenchymal Stem Cell-Derived Extracellular Vesicles to the Rescue of Renal Injury. Int J Mol Sci 2021;22(12)

17. B. Bi, R. Schmitt, M. Israilova*, et al.* Stromal cells protect against acute tubular injury via an endocrine effect. J Am Soc Nephrol 2007;18(9):2486-2496

18. F. Togel, Z. Hu, K. Weiss*, et al.* Administered mesenchymal stem cells protect against ischemic acute renal failure through differentiation-independent mechanisms. Am J Physiol Renal Physiol 2005;289(1):F31-42

19. M. Shariatzadeh, J. Song and S. L. Wilson. The efficacy of different sources of mesenchymal stem cells for the treatment of knee osteoarthritis. Cell Tissue Res 2019;378(3):399-410

20. D. Byrnes, C. Masterson, J. Brady*, et al.* Delayed MSC therapy enhances resolution of organized pneumonia induced by antibiotic resistant Klebsiella pneumoniae infection. Front Med (Lausanne) 2023;10:1132749

21. S. C. M. Wu, M. Zhu, S. C. C. Chik*, et al.* Adipose tissue-derived human mesenchymal stromal cells can better suppress complement lysis, engraft and inhibit acute graft-versus-host disease in mice. Stem Cell Res Ther 2023;14(1):167

22. C. Gregoire, C. Ritacco, M. Hannon*, et al.* Comparison of Mesenchymal Stromal Cells From Different Origins for the Treatment of Graft-vs.-Host-Disease in a Humanized Mouse Model. Front Immunol 2019;10:619

23. M. J. Wilmer, M. A. Saleem, R. Masereeuw*, et al.* Novel conditionally immortalized human proximal tubule cell line expressing functional influx and efflux transporters. Cell Tissue Res 2010;339(2):449-457

24. J. Vriend, C. A. Hoogstraten, K. R. Venrooij*, et al.* Organic anion transporters 1 and 3 influence cellular energy metabolism in renal proximal tubule cells. Biol Chem 2019;400(10):1347-1358

25. J. Vriend, J. G. P. Peters, T. T. G. Nieskens*, et al.* Flow stimulates drug transport in a human kidney proximal tubule-on-a-chip independent of primary cilia. Biochim Biophys Acta Gen Subj 2020;1864(1):129433

26. M. Mihajlovic, S. Hariri, K. C. G. Westphal*, et al.* Safety evaluation of conditionally immortalized cells for renal replacement therapy. Oncotarget 2019;10(51):5332-5348

27. I. C. S. Calcat, E. Rendra, E. Scaccia*, et al.* Harmonised culture procedures minimise but do not eliminate mesenchymal stromal cell donor and tissue variability in a decentralised multicentre manufacturing approach. Stem Cell Res Ther 2023;14(1):120

28. R. Skovronova, C. Grange, V. Dimuccio*, et al.* Surface Marker Expression in Small and Medium/Large Mesenchymal Stromal Cell-Derived Extracellular Vesicles in Naive or Apoptotic Condition Using Orthogonal Techniques. Cells 2021;10(11)

29. L. T. Wang, B. L. Chen, C. T. Wu*, et al.* Protective role of AMP-activated protein kinase-evoked autophagy on an in vitro model of ischemia/reperfusion-induced renal tubular cell injury. PLoS One 2013;8(11):e79814

30. P. M. Holloway and F. N. Gavins. Modeling Ischemic Stroke In Vitro: Status Quo and Future Perspectives. Stroke 2016;47(2):561-569

31. P. F. Shanley, M. Brezis, K. Spokes*, et al.* Differential responsiveness of proximal tubule segments to metabolic inhibitors in the isolated perfused rat kidney. Am J Kidney Dis 1986;7(1):76-83

32. E. Peters, T. Schirris, A. H. van Asbeck*, et al.* Effects of a human recombinant alkaline phosphatase during impaired mitochondrial function in human renal proximal tubule epithelial cells. Eur J Pharmacol 2017;796:149-157

33. R. S. Lindoso, F. Collino and G. Camussi. Extracellular vesicles derived from renal cancer stem cells induce a pro-tumorigenic phenotype in mesenchymal stromal cells. Oncotarget 2015;6(10):7959-7969

34. R. Moghadasali, H. A. Mutsaers, M. Azarnia*, et al.* Mesenchymal stem cell-conditioned medium accelerates regeneration of human renal proximal tubule epithelial cells after gentamicin toxicity. Exp Toxicol Pathol 2013;65(5):595-600

35. J. Faria, S. Ahmed, D. Stamatialis*, et al.* Bioengineered Kidney Tubules Efficiently Clear Uremic Toxins in Experimental Dialysis Conditions. Int J Mol Sci 2023;24(15)

36. E. Nowak, S. Kammerer and J. H. Kupper. ATP-based cell viability assay is superior to trypan blue exclusion and XTT assay in measuring cytotoxicity of anticancer drugs Taxol and Imatinib, and

proteasome inhibitor MG-132 on human hepatoma cell line HepG2. Clin Hemorheol Microcirc 2018;69(1-2):327-336
37. M. Mihajlovic, M. M. Krebber, Y. Yang, *et al.* Protein-Bound Uremic Toxins Induce Reactive Oxygen Species-Dependent and Inflammasome-Mediated IL-1beta Production in Kidney Proximal Tubule Cells. Biomedicines 2021;9(10)
38. R. Lamb, B. Ozsvari, G. Bonuccelli, *et al.* Dissecting tumor metabolic heterogeneity: Telomerase and large cell size metabolically define a sub-population of stem-like, mitochondrial-rich, cancer cells. Oncotarget 2015;6(26):21892-21905
39. S. S. Santos, M. K. C. Brunialti, L. Rodrigues, *et al.* Effects of the PARP Inhibitor Olaparib on the Response of Human Peripheral Blood Leukocytes to Bacterial Challenge or Oxidative Stress. Biomolecules 2022;12(6)
40. X. Gu, Y. Ma, Y. Liu, *et al.* Measurement of mitochondrial respiration in adherent cells by Seahorse XF96 Cell Mito Stress Test. STAR Protoc 2021;2(1):100245
41. S. A. Mookerjee, A. A. Gerencser, D. G. Nicholls, *et al.* Quantifying intracellular rates of glycolytic and oxidative ATP production and consumption using extracellular flux measurements. J Biol Chem 2017;292(17):7189-7207
42. S. A. Mookerjee and M. D. Brand. Measurement and Analysis of Extracellular Acid Production to Determine Glycolytic Rate. J Vis Exp 2015(106):e53464
43. E. A. Zaal, W. Wu, G. Jansen, *et al.* Bortezomib resistance in multiple myeloma is associated with increased serine synthesis. Cancer Metab 2017;5:7
44. D. Kula-Alwar, H. A. Prag and T. Krieg. Targeting Succinate Metabolism in Ischemia/Reperfusion Injury. Circulation 2019;140(24):1968-1970
45. J. V. Bonventre and L. Yang. Cellular pathophysiology of ischemic acute kidney injury. J Clin Invest 2011;121(11):4210-4221
46. D. K. de Vries, A. F. Schaapherder and M. E. Reinders. Mesenchymal stromal cells in renal ischemia/reperfusion injury. Front Immunol 2012;3:162
47. V. Miceli, M. Bulati, A. Gallo, *et al.* Role of Mesenchymal Stem/Stromal Cells in Modulating Ischemia/Reperfusion Injury: Current State of the Art and Future Perspectives. Biomedicines 2023;11(3)
48. X. Yuan, D. Li, X. Chen, *et al.* Extracellular vesicles from human-induced pluripotent stem cell-derived mesenchymal stromal cells (hiPSC-MSCs) protect against renal ischemia/reperfusion injury via delivering specificity protein (SP1) and transcriptional activating of sphingosine kinase 1 and inhibiting necroptosis. Cell Death Dis 2017;8(12):3200
49. R. L. Chevalier. The proximal tubule is the primary target of injury and progression of kidney disease: role of the glomerulotubular junction. Am J Physiol Renal Physiol 2016;311(1):F145-161
50. W. Jassem and N. D. Heaton. The role of mitochondria in ischemia/reperfusion injury in organ transplantation. Kidney Int 2004;66(2):514-517
51. D. Gu, X. Zou, G. Ju, *et al.* Mesenchymal Stromal Cells Derived Extracellular Vesicles Ameliorate Acute Renal Ischemia Reperfusion Injury by Inhibition of Mitochondrial Fission through miR-30. Stem Cells Int 2016;2016:2093940
52. Z. Sun, Z. Gao, J. Wu, *et al.* MSC-Derived Extracellular Vesicles Activate Mitophagy to Alleviate Renal Ischemia/Reperfusion Injury via the miR-223-3p/NLRP3 Axis. Stem Cells Int 2022;2022:6852661
53. A. K. Aranda-Rivera, A. Cruz-Gregorio, O. E. Aparicio-Trejo, *et al.* Mitochondrial Redox Signaling and Oxidative Stress in Kidney Diseases. Biomolecules 2021;11(8)

54. C. Quijano, M. Trujillo, L. Castro*, et al.* Interplay between oxidant species and energy metabolism. Redox Biol 2016;8:28-42

55. I. Martinez-Reyes and N. S. Chandel. Mitochondrial TCA cycle metabolites control physiology and disease. Nat Commun 2020;11(1):102

56. Z. Zhu, J. Hu, Z. Chen*, et al.* Transition of acute kidney injury to chronic kidney disease: role of metabolic reprogramming. Metabolism 2022;131:155194

57. K. Cargill and S. Sims-Lucas. Metabolic requirements of the nephron. Pediatr Nephrol 2020;35(1):1-8

58. A. Faivre, T. Verissimo, H. Auwerx*, et al.* Tubular Cell Glucose Metabolism Shift During Acute and Chronic Injuries. Front Med (Lausanne) 2021;8:742072

59. R. Lan, H. Geng, P. K. Singha*, et al.* Mitochondrial Pathology and Glycolytic Shift during Proximal Tubule Atrophy after Ischemic AKI. J Am Soc Nephrol 2016;27(11):3356-3367

60. V. Miguel and R. Kramann. Metabolic reprogramming heterogeneity in chronic kidney disease. FEBS Open Bio 2023;13(7):1154-1163

61. Y. Kondo, Y. Ishitsuka, D. Kadowaki*, et al.* Phosphoenolpyruvic acid, an intermediary metabolite of glycolysis, as a potential cytoprotectant and anti-oxidant in HeLa cells. Biol Pharm Bull 2012;35(4):606-611

62. Y. Ishitsuka, Y. Fukumoto, Y. Kondo*, et al.* Comparative Effects of Phosphoenolpyruvate, a Glycolytic Intermediate, as an Organ Preservation Agent with Glucose and N-Acetylcysteine against Organ Damage during Cold Storage of Mouse Liver and Kidney. ISRN Pharmacol 2013;2013:375825

63. Y. Zhou, H. Xu, W. Xu*, et al.* Exosomes released by human umbilical cord mesenchymal stem cells protect against cisplatin-induced renal oxidative stress and apoptosis in vivo and in vitro. Stem Cell Res Ther 2013;4(2):34

64. R. S. Lindoso, F. Collino, S. Bruno*, et al.* Extracellular vesicles released from mesenchymal stromal cells modulate miRNA in renal tubular cells and inhibit ATP depletion injury. Stem Cells Dev 2014;23(15):1809-1819

65. M. T. Tran, Z. K. Zsengeller, A. H. Berg*, et al.* PGC1alpha drives NAD biosynthesis linking oxidative metabolism to renal protection. Nature 2016;531(7595):528-532

66. S. Y. Li and K. Susztak. The Role of Peroxisome Proliferator-Activated Receptor gamma Coactivator 1alpha (PGC-1alpha) in Kidney Disease. Semin Nephrol 2018;38(2):121-126

67. M. Tran, D. Tam, A. Bardia*, et al.* PGC-1alpha promotes recovery after acute kidney injury during systemic inflammation in mice. J Clin Invest 2011;121(10):4003-4014

68. J. Caruso, J. Charles, K. Unruh*, et al.* Ergogenic effects of beta-alanine and carnosine: proposed future research to quantify their efficacy. Nutrients 2012;4(7):585-601

69. L. D. Zorova, S. I. Kovalchuk, V. A. Popkov*, et al.* Do Extracellular Vesicles Derived from Mesenchymal Stem Cells Contain Functional Mitochondria? Int J Mol Sci 2022;23(13)

70. Q. Luo, P. Xian, T. Wang*, et al.* Antioxidant activity of mesenchymal stem cell-derived extracellular vesicles restores hippocampal neurons following seizure damage. Theranostics 2021;11(12):5986-6005

71. J. Mao, C. Li, F. Wu*, et al.* MSC-EVs transferring mitochondria and related components: A new hope for the treatment of kidney disease. Front Immunol 2022;13:978571

72. J. Pfleger, M. He and M. Abdellatif. Mitochondrial complex II is a source of the reserve respiratory capacity that is regulated by metabolic sensors and promotes cell survival. Cell Death Dis 2015;6(7):e1835

73. P. Marchetti, Q. Fovez, N. Germain*, et al.* Mitochondrial spare respiratory capacity: Mechanisms, regulation, and significance in non-transformed and cancer cells. FASEB J 2020;34(10):13106-13124
74. M. Yousefifard, F. Nasirinezhad, H. Shardi Manaheji*, et al.* Human bone marrow-derived and umbilical cord-derived mesenchymal stem cells for alleviating neuropathic pain in a spinal cord injury model. Stem Cell Res Ther 2016;7:36
75. S. Shin, J. Lee, Y. Kwon*, et al.* Comparative Proteomic Analysis of the Mesenchymal Stem Cells Secretome from Adipose, Bone Marrow, Placenta and Wharton's Jelly. Int J Mol Sci 2021;22(2)
76. B. A. Molitoris, J. Leiser and M. C. Wagner. Role of the actin cytoskeleton in ischemia-induced cell injury and repair. Pediatr Nephrol 1997;11(6):761-767
77. C. Aufricht, B. Bidmon, D. Ruffingshofer*, et al.* Ischemic conditioning prevents Na,K-ATPase dissociation from the cytoskeletal cellular fraction after repeat renal ischemia in rats. Pediatr Res 2002;51(6):722-727
78. A. O. Pires, B. Mendes-Pinheiro, F. G. Teixeira*, et al.* Unveiling the Differences of Secretome of Human Bone Marrow Mesenchymal Stem Cells, Adipose Tissue-Derived Stem Cells, and Human Umbilical Cord Perivascular Cells: A Proteomic Analysis. Stem Cells Dev 2016;25(14):1073-1083
79. D. B. Ascon, S. Lopez-Briones, M. Liu*, et al.* Phenotypic and functional characterization of kidney-infiltrating lymphocytes in renal ischemia reperfusion injury. J Immunol 2006;177(5):3380-3387
80. G. R. Kinsey, L. Huang, A. L. Vergis*, et al.* Regulatory T cells contribute to the protective effect of ischemic preconditioning in the kidney. Kidney Int 2010;77(9):771-780
81. T. A. Sutton. Alteration of microvascular permeability in acute kidney injury. Microvasc Res 2009;77(1):4-7
82. J. A. Kloka, B. Friedrichson, P. Wulfroth*, et al.* Microvascular Leakage as Therapeutic Target for Ischemia and Reperfusion Injury. Cells 2023;12(10)
83. A. R. Chethikkattuveli Salih, A. Asif, A. Samantasinghar*, et al.* Renal Hypoxic Reperfusion Injury-on-Chip Model for Studying Combinational Vitamin Therapy. ACS Biomater Sci Eng 2022;8(9):3733-3740

CHAPTER 6

Diabetic Proximal Tubulopathy: Can We Mimic the Disease for *In Vitro* Screening of SGLT Inhibitors?

João Faria[1], Karin G.F. Gerritsen[2], Tri Q. Nguyen[2], Silvia M. Mihăilă[1], Rosalinde Masereeuw[1]

[1] Div. Pharmacology, Utrecht Institute for Pharmaceutical Sciences, Utrecht University, the Netherlands

[2] Dept. Nephrology and Hypertension, University Medical Center Utrecht, the Netherlands

[3] Dept. Pathology, University Medical Center Utrecht, the Netherlands

Published in Eur J Pharmacol. 2021; 908:174378

ABSTRACT

Diabetic kidney disease (DKD) is the foremost cause of renal failure. While the glomeruli are severely affected in the course of the disease, the main determinant for disease progression is the tubulointerstitial compartment. DKD does not develop in the absence of hyperglycemia. Since the proximal tubule is the major player in glucose reabsorption, it has been widely studied as a therapeutic target for the development of new therapies. Currently, there are several proximal tubule cell lines available, being the HK-2 and HKC-8 cell lines the ones widely used for studying mechanisms of DKD. Studies in these models have pushed forward the understanding on how DKD unravels, however, these cell culture models possess limitations that hamper research, including lack of transporters and dedifferentiation. The sodium-glucose cotransporters (SGLT) are identified as key players in glucose reabsorption and pharmacological inhibitors have shown to be beneficial for the long-term clinical outcome in DKD. However, their mechanism of action has, as of yet, not been fully elucidated. To comprehend the protective effects of SGLT inhibitors, it is essential to understand the complete functional, structural, and molecular features of the disease, which until now have been difficult to recapitulate. This review addresses the molecular events of diabetic proximal tubulopathy. In addition, we evaluate the protective role of SGLT inhibitors in cardiovascular and renal outcomes, and provide an overview of various *in vitro* models mimicking diabetic proximal tubulopathy used so far. Finally, new insights on advanced *in vitro* systems to surpass past limitations are postulated.

KEYWORDS: diabetic kidney disease, hyperglycemia, proximal tubule, SGLT inhibitors, *in vitro* models.

1. INTRODUCTION

Diabetic kidney disease (DKD) is the foremost cause of kidney failure worldwide [1]. The rising numbers in DKD parallel the increasing prevalence of diabetes mellitus (DM) worldwide. Globally, diabetic patients are expected to reach 642 million cases by the year of 2040, of which people with Type 2 DM account for 90% of the cases [2]. DKD is characterized by albuminuria and accompanied by decreased glomerular filtration rate (GFR) and often causes an array of serious complications as a result of disturbances in hemodynamic and metabolic homeostasis [3].

The kidney contributes to glucose homeostasis through different processes, including gluconeogenesis and glucose reabsorption. [4]. Glucose is filtered in the glomerulus, and under normal conditions, glucose is completely reabsorbed by the proximal tubule epithelial cells (PTECs) followed by diffusion into the peritubular capillaries. This transepithelial reabsorption process is accomplished by glucose transporters, of which the sodium-glucose co-transporter 1 (SGLT1) and SGLT2 are responsible for the uptake of glucose through a Na^+ gradient across the apical membrane, while the glucose transporter 1 (GLUT1) and GLUT2 facilitate the transport across the basolateral membrane into the systemic circulation (**Figure 1**) [5].

Owing to the fact that SGLT2 is responsible for the majority of glucose reabsorption, it has been widely studied as a therapeutic target to treat patients with Type 2 Diabetes Mellitus (T2DM). In case of hyperglycemia an excess of glucose is filtered by the glomerulus which leads to an increased expression of SGLTs mediating its reabsorption [6]. With this in mind, a class of drugs was developed inhibiting SGLTs, also known as gliflozins, that decrease the risk of hyperglycemia by reducing the renal tubular reabsorption of glucose [7]. **Table 1** summarizes the SGLT inhibitors currently prescribed to DKD patients, while providing an overview of the therapeutic benefits and the risks associated with this therapy.

DKD does not develop in the absence of hyperglycemia. Hyperglycemia induces activation of several pathways, including the polyol pathway and the protein kinase C pathway that contribute to oxidative stress [8, 9]. Hyperglycemia also causes tubulointerstitial fibrosis and inflammation, and accumulation of extracellular matrix proteins, such as collagen IV, fibronectin, and laminin [10]. Identification of the mediators implicated in the above-mentioned processes will provide more information on the underlying molecular mechanisms of DKD, aiding in the development of new targeted therapies.

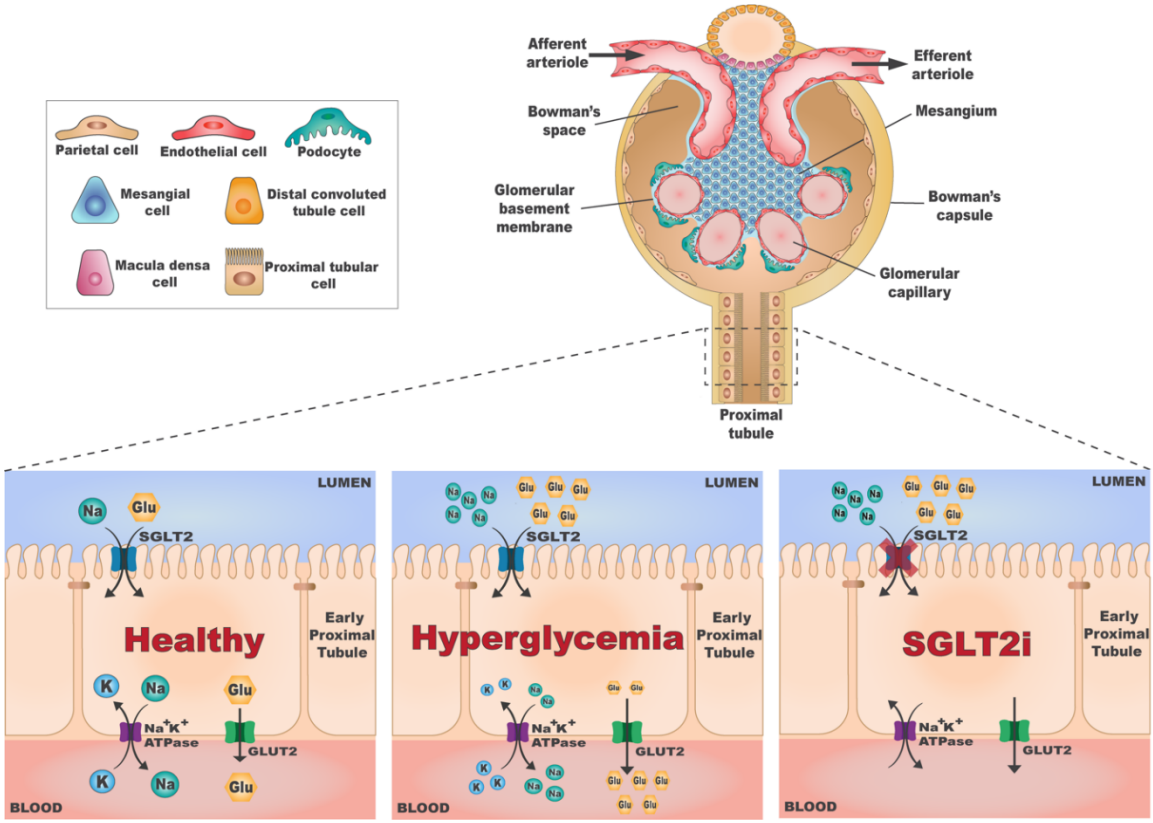

Figure 1. Glucose handling in the kidney proximal tubule. The glomerulus filters glucose after which the proximal tubule is responsible for its reabsorption. In healthy conditions, SGLT2 reabsorbs roughly 90 % of glucose in co-transport with sodium. SGLT1 reabsorbs the residual 10 % in the late segments of the proximal tubule (not shown). In a hyperglycemic environment, elevated glucose filtration results in high glucose and sodium reabsorption. Increased tubular sodium reabsorption causes a decrease in sodium levels at the macula densa. This activates the tubuloglomerular feedback (TGF) mechanism, causing vasodilation of the afferent arteriole to elevate the glomerular pressure state. SGLT2 inhibitors reduce hyperfiltration via TGF, therefore minimizing the risks observed in DKD. Excessive glucose filtered, yet not reabsorbed, will cause glycosuria.

To investigate the mechanisms behind DKD both animal models and cell culture systems can be used. The use of animal models allows researchers to study the physiological aspects of the disease, however, these models fail to control biological changes of renal cells in real-time, while conveying expensive costs and being time consuming [11]. *In vivo* studies also pose ethical issues, but most importantly, these models do not accurately correlate to human systems as they are either resistant to develop DKD or do not recapitulate all the different stages of the disease [12]. For example, it is known that most diabetic rodent models can mimic key features of advanced human DKD in glomeruli, but they usually do not develop the characteristic widespread tubular atrophy and interstitial fibrosis. Even in models in which the renin-angiotensin-aldosterone system (RAAS) is strongly activated, the severity of tubular

atrophy and interstitial fibrosis is still less than seen in human DKD [13].

Table 1. Summary of the different SGLT inhibitors either commercially available or currently on clinical trials.

SGLT2 inhibitor	Mechanism of action	Indication	Benefits	Side effects	References
Canagliflozin[a] (INVOKANA)	Selective SGLT2 inhibitor Mild intestinal and renal SGLT1 inhibition	T2DM	HbA1c reduction Reduced glomerular hyperfiltration via TGF	Hypoglycemia Dehydration Urinary tract infections Ketoacidosis	[14]
Dapagliflozin[a] (FARXIGA)	Selective SGLT2 inhibitor	T2DM	Reduced albuminuria		[15]
Empagliflozin[a] (JARDIANCE)	Selective SGLT2 inhibitor	T2DM	Reduction in plasma levels of uric acid		[16]
Tofogliflozin[b] (DEBERZA)	Selective SGLT2 inhibitor	T2DM	Anti-inflammatory and anti-fibrotic properties		[17]
Luseogliflozin[b] (LUSEFI)	Selective SGLT2 inhibitor	T2DM			[18]
Remogliflozin etabonate[c] (Remo™, Remozen™)	Selective SGLT2 inhibitor (prodrug)	T2DM	Reduction in natriuretic peptides Possible synergetic effect with anti-hypertensive drugs		[19]
Ertugliflozin[a] (STEGLATRO)	Selective SGLT2 inhibitor	T2DM			[20]
Sotagliflozin[d] (ZYNQUISTA)	Dual SGLT1/2 inhibition	T1DM	Diuretic effect		[21]

[a] FDA and EMA approved; [b] Japan approved; [c] India approved, [d]EMA approved; T1/2DM Type 1/2 Diabetes Mellitus; Data retrieved from https://clinicaltrials.gov

To overcome this problem, 2D culture systems can provide some answers concerning the cellular effects of glucose. However, these models lack the complex 3D tissue architecture that is important for the correct understanding of the different disease states found *in vivo* [22]. Recent advances in the stem cell field [23-25] and microphysiological systems [26, 27] have shown promising clues on how to prevent DKD from progressing to kidney failure, however, as of yet a perfect *in vitro* model capable of replicating the disease does not exist.

With regard to treatment options, the pharmacological inhibition of SGLT2, the major player in glucose reabsorption, has shown renoprotective benefits [28]. The SGLT2 inhibitors have been extensively studied both alone or in combination with other diabetic medication, however it is still yet to know whether these benefits are primarily due to SGLT2 inhibition or

if off-target effects also play a role. To understand the protective effects of current therapies, such as SGLT2 inhibitors, as well as other pharmacological treatments currently on market or possible future therapeutic candidates, a comprehensive study of the aetiopathogenesis of DKD is required.

In this review, we aim at providing readers an overview of what is known about the cellular and molecular pathophysiological mechanisms of diabetic proximal tubulopathy and the potential role of SGLT inhibitors. Using a literature search on the most relevant human proximal tubule *in vitro* models used to study the disease, we provide some recommendations for the requirements of a physiologically relevant *in vitro* model that allows studying DKD.

2. Pathophysiology of Diabetic Proximal Tubulopathy

As mentioned before, the proximal tubule is a prime mover in DKD pathogenic cascade. In diabetes, there is an excessive glucose flux which leads to an increased proximal tubular reabsorption of glucose via the sodium-glucose cotransporter 2 (SGLT2). This increased glucose reabsorption is dependent on the level of SGLT2 protein expression, as once a glucose transport maximum (T_m) is reached, there is a saturation of the transporter resulting in glycosuria [29].

In case of hyperglycemia there is an increase in the formation of advanced glycation end products (AGEs) [30]. Low molecular weight AGEs are filtered by the glomeruli and reabsorbed by the PTECs contributing to diabetic tubulointerstitial injury [31]. The proximal tubule requires substantial amounts of energy to perform its role in waste removal and nutrient reabsorption. The active hyperreabsorption of sodium and glucose observed in the diabetic milieu is coupled with high levels of oxygen consumption, which may be accompanied by release of reactive oxygen species (ROS) by the mitochondrial electron transport chain [32]. Other major sources for ROS production include the accumulated AGEs [33], NADPH oxidase (NOX) and uncoupled nitric oxide synthase (NOS) [34].

Hyperglycemia has also been known to induce extracellular fluid volume depletion via glucose-induced osmotic diuresis. The volume depletion strongly stimulates the sympathetic nervous system that further promotes the activation of the RAAS, contributing to proteinuria and kidney disease progression [3].

The understanding of how tubular (or tubulointerstitial) injury unravels will help researchers identify new targets for therapy along the way. A brief overview of the pathophysiological events of diabetic proximal tubulopathy is discussed below, whereas its underlying molecular events are shown in **Figure 2**.

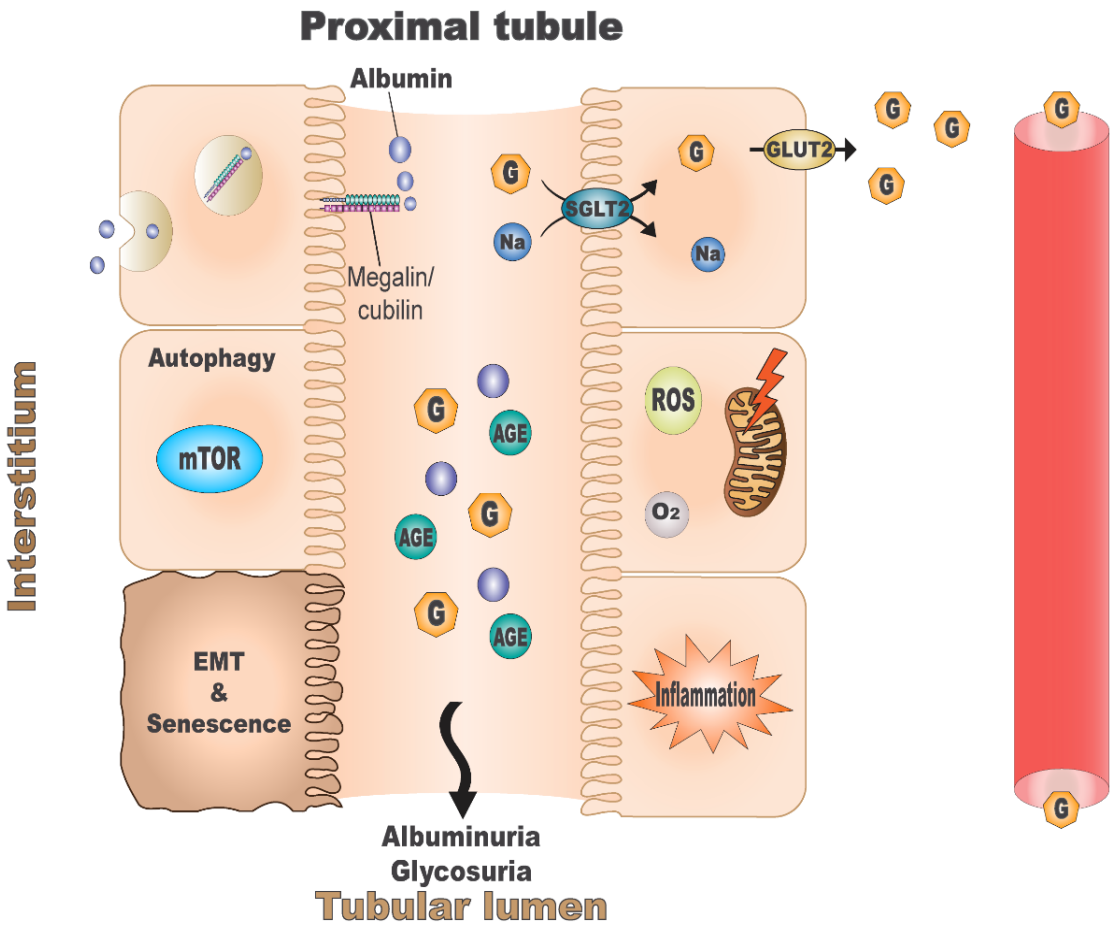

Figure 2. Cellular and pathophysiological events in diabetic proximal tubulopathy. Damage to the glomerulus as a result of diabetes leads to impaired glomerular filtration barrier (GFB). Subsequently, excessive glucose (G), albumin, and advanced glycated end-products (AGEs) levels in the proximal tubule stimulate a process of inflammation, epithelial-mesenchymal transition (EMT) and senescence in the tubule cells. As a result of excessive tubular hyperreabsoprtion of glucose, elevated levels of reactive oxygen species (ROS) are produced together with an increase in oxygen (O2) consumption causing intrarenal hypoxia. Excessive albumin excretion due to damaged GFB cannot be fully reabsorbed by the apical megalin/cubilin complex, resulting in the secretion of pro-inflammatory cytokines by the proximal tubule epithelial cells (PTECs). The accumulation of glucose, albumin and AGEs contributes to secretion of pro-fibrotic mediators that in turn lead to fibrosis. Damaged PTECs lose their original phenotype, eventually start expressing α-SMA and transition into myofibroblasts. Autophagy is also disrupted by the accumulation of AGE, caused by the upregulation of mTOR in PTECs. Ultimately, these hyperglycemia-induced processes cause significant damage to the proximal tubule resulting in glycosuria and albuminuria, key markers of DKD.

2.1. Oxidative Stress and Hypoxia

The balance between oxygen delivery and oxygen consumption (QO_2) is compromised in diabetic patients [35] as the excessive reabsorption capability of the kidney involves a great demand for ATP production. However, the kidneys are not able to compensate for this inflation. The reduction in oxygen availability affects the cellular metabolism as it moves it towards a more glycolytic pathway that is less energy efficient, resulting in a lower ATP yield [36]. During ATP generation, some electrons may escape from the respiratory chain and bind to oxygen to form ROS, such as superoxide radicals. ROS production occurs naturally via several cellular pathways; however, the elevated levels of ROS being generated in DKD surpass the local antioxidant capacity, causing an inflammatory cascade that ultimately leads to tubulointerstitial fibrosis [37].

Besides oxidative stress, both tubular overload and increased QO_2 may cause intrarenal hypoxia [38]. To counteract the effects of hypoxia, the hypoxia-inducible transcription factor (HIF) family promotes vasculogenesis via production of vascular endothelial growth factor (VEGF), causing an increase in oxygen delivery and alterations in cellular metabolism [39]. HIFs are composed of two subunits: an α-subunit that is degraded in the presence of oxygen and a constitutive β-subunit. Due to a lack of oxygen, there is an accumulation of the α-subunit that, in turn, binds to the β-subunit, resulting in the transcription of hypoxia- responsive genes involved in cell regulatory mechanisms (*i.e.*, angiogenesis, cell proliferation, etc.) [40]. The persistent hypoxia observed in DKD has been linked to low levels of HIF-1α expression, therefore inhibiting the activation of compensatory mechanisms to revert the state of hypoxia [41]. The use of HIF stabilizers, such as prolyl hydroxylase inhibitors, have shown a renoprotective effect by altering diabetic renal metabolism in early stages of DKD [42]. For this reason, further investigation should be done throughout the different stages of the disease to really understand the renoprotective effect of these drugs.

2.2. Albuminuria

DKD is characterized by albuminuria due to a damaged glomerular filtration barrier and reduced tubular reabsorption [43]. Albuminuria is a predictor of DKD progression [44], therefore understanding its mechanism to prevent urinary protein leakage is of great interest. Filtered albumin is reabsorbed by PTECs via the apical megalin-cubilin complex, whereas the neonatal Fc receptor (FcRn) also plays a role in albumin transcytosis [45]. The increased tubular protein reabsorption is followed by an inflammatory cascade as PTECs start secreting an array of pro-inflammatory cytokines and chemokines, such as interleukin 8 (IL-8), IL-18, RANTES and monocyte chemotactic protein 1 (MCP1) [46, 47]. An increase in expression of

adhesion molecules also occur in the proximal tubule, including intercellular adhesion molecule 1 (ICAM1) and vascular adhesion molecule 1 (VCAM1). These adhesion molecules play a role in the initiation of renal inflammation [48]. In addition, the NF-κB pathway has been associated as a regulator of the inflammatory pathomecanisms involved in protein tubular overload [49]. The proinflammatory response of PTECs also leads to the recruitment of macrophages and lymphocytes, sources of pro-fibrotic proteins such as TGF-β, stimulating tubulointerstitial fibrosis progression [50]. It is still to be fully understood if albuminuria is either a cause or consequence of DKD progression as there is some debate on whether it is the albumin alone or the combination with other compounds, such as fatty acids, that actually lead to cytotoxic effects [51].

With regard to treatments, patients diagnosed with albuminuria receive anti-hypertensive treatment, such as angiotensin-converting enzyme inhibitors (ACEi) and angiotensin II receptor blockers (ARBs), with the goal to block RAS, thus reducing hyperfiltration and consequently lowering urinary albumin levels [52].

2.3. Inflammation

The inflammatory response in the tubular compartment plays a role in disease progression [53]. The role of toll-like receptors (TLRs), mediators in the production of inflammatory cytokines and chemokines, have been linked to metabolic syndrome, such as hyperglycemia, with an emphasis for TLR2 and TLR4. Under diabetic conditions, cultured PTECs have shown to increase TLR4 expression via a PKC-dependent pathway, resulting in the upregulation of pro-inflammatory mediators [54]. Inflammasomes, together with TLRs, are key components of the innate immune system. In particular the NLRP3 inflammasome has been shown to play a role in DKD progression, a complex involved in mitochondrial disfunction [55], albuminuria [56], and renal fibrosis [57].

Another important mediator in the inflammatory cascade is the activation of the NF-κB pathway, activated upon different stimuli, including oxidative stress, hyperglycemia, AGEs, and albuminuria [48, 58]. Among cytokines, TNF-α is a major driver of inflammation, therefore making it an ideal target for therapeutic intervention [59]. Studies have shown that pentoxifylline (PTF), inhibitor of TNF-α, has anti-inflammatory and antiproteinuric effects [60, 61]. In addition, the combination of PTF and RAAS blockers led to a significant reduction in protein excretion [62, 63]. *In vitro*, hyperglycemia has also shown to increase the expression of tubular kallikrein 1 (KLK1) and bradykinin, mediators of the kallikrein-kinin system, resulting in tubular inflammation [64].

2.4. EMT and Cellular Senescence

Tubulointerstitial fibrosis is predominantly found in the diabetic kidney. PTECs' response to high glucose and albuminuria includes the secretion of TGF-β and extracellular matrix components [65, 66]. TGF-β is the primary mediator of fibrogenesis as it activates the Smad pathway, specifically TGF-β1 activates Smad3 leading to fibrosis [67]. Epithelial-to-mesenchymal transition (EMT) is considered an initiating factor that triggers the development and progression of tubulointerstitial fibrosis. In DKD, EMT is mainly stimulated through the accumulation of AGEs [68], hyperlipidemia [69], and proteinuria [70]. During this process, PTECs start losing their original phenotype as (1) cell polarity disappears, (2) cell-cell interaction is broken due to the disruption of tight junctions, (3) the basement membrane is slowly destroyed leading to the migration of these cells into the interstitium, and (4) PTECs start expressing α-smooth muscle actin (α-SMA), resulting in their transition into myofibroblasts [71]. The same stimuli that trigger EMT also promote the activation of several pathways, such as the JAK/STAT pathway [72], PKC pathway [73], MAPK pathway [74], Notch [75] and Wnt/β-Catenin [76] pathways, resulting in structural and functional changes in PTECs that aggravate the progression of renal fibrosis. Several microRNAs have also been identified as promoters of TGF-β1/Smad3 activation, of which miR-21 [77] and miR-192 [78] show the most aberrant effects on fibrogenesis progression, serving as potential targets in anti-fibrotic therapies. Hyperglycemia has also been linked to an increase in cellular senescence in PTECs, a process concerning the loss of regenerative capacity of cells in response to stress. This process is involved in ageing and metabolic diseases, such as diabetes [79]. The secretion of pro-fibrotic mediators during the course of DKD due to cellular senescence can lead to persistent fibrosis, which, when combined with other pathological processes, can lead to disease progression [80]. For this reason, targeting senescent PTECs can provide new opportunities for the treatment of DKD.

2.5. Nutrient-Sensing Pathways

In DKD, the autophagy machinery is disrupted leading to abnormalities of several nutrient-sensing pathways, such as the mammalian target of rapamycin (mTOR), AMP-activated protein kinase (AMPK), and sirtuins (SIRT) [81]. Type 2 diabetes is characterized by suppression of both AMPK and SIRT1, whereas mTOR is upregulated which causes autophagy flux to decrease in PTECs [82].

Autophagy upregulates lysosomal activity in PTECs upon AGE exposure leading to its degradation. However, the accumulation of AGEs observed in the diabetic kidney reduces lysosomal function due to the stagnation of autophagy [83]. In addition, the transcription factor

EB (TFEB), known mediator of the mTOR pathway, is downregulated upon AGEs overload leading to impaired autophagic activity in PTECs [84]. Similarly to rapamycin-mediated inhibition of mTOR, which can reverse the impaired autophagy, targeting TFEB can present a therapeutic strategy to activate autophagy.

3. SGLT Inhibitors

The proximal tubule is accountable for the reabsorption of filtered glucose via SGLT1 and SGLT2, the latter being responsible for the majority of glucose reabsorption [5]. SGLTs are therefore perfect targets for anti-hyperglycemic therapies. With the goal to inhibit this hyperreabsorption of glucose, inhibitors of SGLT1 and SGLT2 have been developed (**Table 1**). At first, the O-glucoside phlorizin, a nonselective SGLT1/2 inhibitor, showed promising results as its normalized plasma glucose levels in diabetic rat models. These studies showed that phlorizin not only leads to glycosuria but also blocks intestinal glucose absorption, resulting in intestinal malabsorption complications [85] This major drawback led to the development of a new class of glucose-lowering drugs, C-glucosides, that proved to be selective for SGLT2 with longer half-lives compared to phlorizin [86]. The advantages of SGLT2 inhibition go beyond lowering glucose plasma levels, such as reduction in urinary albumin excretion [87], blood pressure control [88], and diuretic effect [89]. The main disadvantage of this therapy is that it leads to glycosuria, therewith increasing the risk of urinary tract infections (**Table 1**) [90]. Although very uncommon, SGLT2-induced glycosuria can cause euglycemic ketoacidosis due to reduced glucose availability and reduced insulin-to-glucagon ratio, enhancing lipolysis and lipid oxidation [91].

In terms of beneficial effects, SGLT2 inhibition also leads to improved cardiovascular outcomes. The protective effects of SGLT2 inhibition extends to different patient groups, whether diabetes is present or not. The DAPA-CKD trial [92] with dapagliflozin has shown that chronic kidney disease patients were associated with lower risk for cardiovascular death and heart failure, independently of the presence or absence of type 2 diabetes. In the EMPEROR-Reduced trial [93] with empagliflozin, the same therapeutic profile was confirmed. Further studies in the clinical trials EMPA-TROPISM [94] and EMBRACE-HF [95], have shown evidence that empagliflozin may lead to reverse left ventricular remodeling, which could explain the cardiovascular benefits of empagliflozin seen in both diabetic and nondiabetic patients. Overall, these results demonstrate a broader therapeutic effect of SGLT2 inhibition, that not only proves to be beneficial in terms of cardiovascular outcomes but also to the therapeutic management of chronic kidney disease.

From a physiological point of view, SGLT2 inhibition causes an increase in the delivery

of sodium to the macula densa, in turn, restoring the tubuloglomerular feedback and reducing hyperfiltration [96]. By reducing hyperfiltration, the processes of oxidative stress, albuminuria, inflammation, EMT, cellular senescence, and eventually fibrosis are also minimized. On the molecular side, the protective effects of SGLT2 inhibition include increased antioxidant capacity via reduction of ROS production [97], anti-inflammatory and anti-fibrotic response due to a decreased expression of TLR2/4 and TGF-β, respectively [98]. A possible role in RAAS activation is still under debate [99]. In the heart, SGLT2 inhibition has been reported inhibit the Na^+/H^+ exchanger 1 (NHE1), a transporter involved in regulation of $[Na^+]$ and $[Ca2^+]$ intracellular levels, thus explaining a reduced risk in heart failure [100]. However, this hypothesis has been proven wrong in a new study [101] suggesting that the therapeutic effects of SGLT2 inhibitors are, as of yet, not fully understood.

Due to immense research done over the past years on SGLT2 inhibition, and having in mind that inhibition of SGLT2 leads to an upregulation of SGLT1 to limit glycosuria, new insights have been gained on the role of SGLT1 in the control of the tubuloglomerular feedback and glomerular filtration rate [102, 103]. In addition, a dual SGLT inhibition, sotagliflozin (**Table 1**), currently under phase 3 studies has shown similar advantages as, already available, SGLT2 inhibitors while providing delayed glucose absorption in the intestine [104]. The SOLOIST-WHF trial [105] with sotagliflozin has concluded that this therapy is also associated with cardiorenal protective effects, including a decreased incidence in cardiovascular mortality and hospitalization for heart failure.

4. Can We Replicate the Disease *In Vitro*?

To date, several *in vitro* models have been used to study the underlying mechanisms of proximal tubulopathy, both in 2D and in 3D. While 2D models have enabled great advances on the understanding of this pathology based on the cellular effects of high glucose, they fail to represent the *in vivo* state as single cell lines or primary cells are used, and therefore do not show the interplay between the proximal tubule and the peritubular capillaries. The interaction between these two compartments is key to understand such a complex disorder, as peritubular capillary rare fraction is also correlated with DKD and decline in kidney function [106]. Different PTEC lines are presently available due to the importance of this nephron's segment for multiple studies. **Table 2** summarizes the characteristics of relevant PTEC *in vitro* models, while providing an overview of DKD-related pathways studied over time in these models.

Adopting the most suitable model is vital as some models are not ideal for studying DKD. In addition, a combination rather than single exposures of diabetic mediators such as high

glucose, TGF-β, AGE-albumin, hypoxia and angiotensin II will provide a better understanding of the disease [107].

Based on what it was described earlier in this review regarding the pathophysiology of diabetic proximal tubulopathy, an ideal PTEC *in vitro* model should include 1) glucose transporters (SGLTs and GLUTs), 2) a functional megalin-cubilin protein reabsorption complex, 3) interaction between AGEs and its receptor RAGE, 4) angiotensin II receptor, 5) capability to undergo EMT and cellular senescence, and 6) susceptibility to hypoxia. The HK-2 cell line (**Table 2**) has been widely used as it expresses the glucose transporters, however, to investigate albumin reabsorption, specific culture conditions need to be met, as the endocytosis receptors, megalin and cubilin, appear not present [108]. When trying to recreate the hypoxic environment found *in vivo*, researchers found that the combination of high glucose and hypoxia (1% O_2) led to an impaired HIF-1α stabilization as seen in the diabetic kidney [109]. This model, however, also lacks several relevant PTEC transporters involved in toxin removal [110], and due to its oncogene-mediated immortalization, the cell line may be more resistant to PTEC toxicants than other more relevant cell lines. Although not as widely used, the HKC-8 cell line (**Table 2**) is another PTEC model possessing comparable biochemical properties as the HK-2 cell line, such as glucose transport, abrogated by phlorizin [111]. HKC-8 cells have also shown impairment of autophagy and mitochondrial dysfunction upon exposure to high glucose, both reverted by treatment with SGLT2 inhibitors and an activator of the AMPK pathway, respectively [112, 113]. A recent study by Khundmiri *et al.*, in which several human and non-human cell lines' transcriptomes were compared to native tissue, demonstrated a higher similarity of HK-2 cells to human kidney than HKC8 cells [114]. As this study was based on cells cultured in their standard media, it is still possible that upon exposure to different conditions, such as hyperglycemia, the transcriptomic profile of these cell lines differ. Although possessing key features of the native proximal tubule, the previously mentioned cell lines were immortalized using methods that can alter their characteristics over time. Immortalization using the human telomerase reverse transcriptase has since been employed as the resulting cell lines do not undergo senescence and still retain features of primary cells even at high passages [115]. Examples of such cell lines include the RPTEC/TERT1 [116]and the conditionally immortalized PTEC (ciPTEC) [117], both closely resembling the native proximal tubule. The latter does not express the glucose transporters (**Table 2**) important for studying DKD, however, similar to RPTEC/TERT1, the remaining DKD pathways can still be extensively studied.

To highlight that for recreating the disease *in vitro*, researchers should be aware that media composition can influence the outcome of the study. Immortalized cell lines tend to

have a higher metabolic rate when compared to primary cells, which reflects the high glucose concentration found in most commercially available cell culture media. Thus, lowering glucose levels in the media before exposure to DKD mediators is imperative to obtain clinically relevant results. The same issue arises from using fetal bovine/calf serum as it alters cell growth and functional behavior [118].

Table 2. Overview of the most prominent in vitro models capable of replicating features of diabetic proximal tubulopathy.

Model	Transporters/Receptors	Pathways	Cons	Reference
HK-2	SGLT2 Na^+K^+-ATPase AT1R, AT2R TGF-βR CTGF RAGE Megalin/cubilin complex HIF-1α LC3-I, LC3-II TLR2/4 β-galactosidase activity	AGE-RAGE EMT AMPK/mTOR p38 MAPK HIF-1α-HRE TLR/NF-κB Polyol pathway PKC pathway	Absence of drug transporters (SLC22 family) Immortalization process	[108, 109, 119-128]
HKC8	SGLT2 Na^+K^+-ATPase Megalin/cubilin complex LC3-II TGF-β CTGF AGER1 RAGE RANTES	AGE-RAGE EMT AMPK/mTOR NF-κB/RANTES PKC pathway	Absence of drug transporters (SLC22 family) Immortalization process	[65, 111-113, 126, 129-132]
RPTEC/TERT1	SGLT2 Na^+K^+-ATPase Megalin/cubilin complex TGF-β SMAD3 HIF-1α	TGF-β/SMAD3 EMT AMPK/mTOR NF-κB LPS/TLR4	Absence of AT1R	[116, 133-138]
ciPTEC	Na^+K^+-ATPase Megalin/Cubilin complex SLC22 family HIF-1α TLR4 NLRP3	LPS/TLR4 AMPK/mTOR EMT	Absence of SGLT2	[117, 139-144]

AGER1, advanced glycation end product receptor-1; **AMPK**, AMP-activated kinase; **AT1R**, angiotensin II receptor type 1; **ciPTEC,** conditionally immortalized proximal tubular epithelial cell line; **CTGF**, connective tissue growth factor; **EMT**, epithelial-mesenchymal transition; **HIF-1a**, hypoxia-inducible factor 1-alpha; **HK-2**, human kidney 2; **HKC8,** human kidney proximal tubular epithelial cell line (clone-8); **HRE**, hypoxia response element; **LC3**, microtubule-associated proteins 1A/1B light chain 3; **mTOR**, mammalian target of rapamycin; **NF-kB**, nuclear factor-kB; **NLRP3**, NLR family pyrin domain containing 3; **PKC,** protein kinase C; **RAGE**, receptor for advanced

glycation end products; **RANTES**, regulated on activation, normal T cell expressed and secreted; **RPTEC/TERT1**, renal proximal tubule epithelial cell/TERT1 immortalized ; **SGLT2**, sodium/glucose cotransporter 2; **SLC22**, organic solute carrier 22 family; **SMAD3**, SMAD family member 3; **TGF-b**, transforming growth factor beta; **TLR,** toll-like receptor.

Not only chemical methods, such as exposure to DKD mediators, but genetic methods can also be employed to study the pathophysiology of the disease. To this end, induced pluripotent stem cells (iPSCs) can be genetically modified via CRISPR-Cas9 technology to be more susceptible to developing the disease [145]. With respect to 3D models, kidney organoids and iPSC-derived organoids have recently been highlighted for their potential use in diabetes research, however these models still resemble both genetically and structurally kidneys in fetal stages of development which hampers their use. Another disadvantage of organoids includes their heterogenous population that can detract from toxic effects, and due to their encapsulation in hydrogels, longer incubation times to DKD mediators may be required when compared to 2D culture systems [25].

Moving towards more advanced *in vitro* models where multiple cell types and the 3D architecture are included can definitely improve the knowledge acquired so far. Organ-on-chip (OoC) is the perfect example of such desirable model in which different cell types can be combined in a 3D microenvironment that most likely resembles the *in vivo* state [146]. Different OoC models have been designed to study the reabsorption and secretion capacities of the proximal tubule [147-151]. Overall, these models successfully showed the possibility to recapitulate both function and structure of the proximal tubule *in vitro* while demonstrating epithelium-endothelium crosstalk via exposure to high glucose, however no efforts to mimic more complex molecular mechanisms involved in diabetic proximal tubulopathy were made. While OoC models are paving the way towards deeper understanding of such complex diseases, they face several challenges including standardization, technical problems (*e.g.*, leak tight seals and robust connectors) as well as finding the appropriate culture medium to grow the different cell types [152].

The development of *in vitro* models to study DKD has improved in recent years. A variety of *in vitro* models, each with its own advantages and disadvantages is currently available (**Table 2**). Whereas culture models, such as the HK-2 cell line, have provided valuable data on the effects of diabetic mediators, this model lacks important transporters that are required to understand the therapeutic effects of certain drugs. Empagliflozin, an SGLT2 inhibitor, is excreted into urine via the organic anion transporter 3 (OAT3) [153]. The study of the glucosuric effect of Empagliflozin in the HK-2 cell line is not possible due to the lack of OAT transporters [154], therefore limiting the use of this model for drug screening. Replacing this

model with others better equipped with drug transporters, such as RPTEC/TERT1, can improve the quality and reliability of the results. Note that a full characterization of transporter expression in human-derived proximal tubule cell lines is of great need to understand the full potential of these *in vitro* models for the study of DKD [114].

Not only replacing with better *in vitro* models, but also improving their functionality by increasing complexity with bioengineering approaches, such as co-cultures and pulsatile flow on-chip systems can lead to greater progress in research. With regard to co-culture models, the RPTEC/TERT1 cell line has been used to study the therapeutic effects of mesenchymal stromal cells as a treatment option for DKD [137], however with regard to vascularization and cell to cell interactions to study the different outcomes of the disease, such as inflammation, oxidative stress, and EMT, no co-culture systems have been applied so far. A kidney-on-chip model comprised of the proximal tubule (RPTEC/TERT1) and a vascular compartment has been designed and proved to show a functional tubular-vascular exchange, including glucose transport abolished by a SGLT2 inhibitor [150]. This shows great promise for studying DKD, in which a model that closely resembles the *in vivo* situation can be tuned to respond to external stimuli, and possibly connected to microsensors that will allow a close look at the cellular changes in the environment [155]. Given the growing list of candidate genes for DKD [156], engineered *in vitro* disease models may also help boost the knowledge on disease progression and treatment.

5. CONCLUSION AND FUTURE PERSPECTIVE

The impact of DKD in global health is a burden that weighs great responsibility on researchers into trying to find new approaches to prevent and treat the disease. Even though the complex clinical picture of DKD cannot be replicated by the use of a single nephron segment, attempts have been made to study the individual parts involved in the progression of the disease. Early changes in the diabetic kidney are mainly observed in the glomerulus and the proximal tubule, however, due to the important role of the latter in glucose reabsorption, more attention should be directed towards this nephron segment. Anti-diabetic drugs, such as the recently emerged SGLT2 inhibitors, have provided great benefits to diabetic patients, nevertheless the protective effects of these drugs are not fully understood due to very complex pathology of DKD.

To aid the understanding of how changes in the kidney proximal tubule lead to DKD progression, an *in vitro* model is crucial. High glucose exposure is key to mimic DKD; however, a cocktail of relevant disease-related mediators is crucial to properly understand its pathophysiology. A robust *in vitro model* not only has to show a consistent response to stimuli but it is also expected to respond to currently available treatments in a clinically relevant manner. The response to different exposure times should be further studied since acquisition of specific DKD markers may be transient in the early stages. Whereas studying glucose transport is important, further studies on the functionality of PTEC transporters should not be overlooked. The development of engineered *in vitro* disease models can also provide deeper insights on how the disease is unraveled. With regard to kidney organoids and iPSC-derived organoids, efforts to improve the maturity and relevance of these models is essential.

Overall, no reliable *in vitro* model to study DKD is currently available due to the complexity of the organ and its multiple structures and cell types, all playing a role in the development of diabetic complications. Choosing the ‘right’ model depends on the specific research question, however that model should consist of different cell types equipped with appropriate transporters and receptors to study specific mechanisms while being in a dynamically controlled microenvironment that closely resembles the *in vivo* state. All together, these features will provide a cheaper and more biologically alternative to animals to investigate the underlying molecular mechanisms of the disease and to identify potential drug candidates relieving DKD symptoms.

AUTHOR CONTRIBUTION

JF, **KGFG**, **SMM** and **RM** devised the main conceptual ideas, **JF** wrote the initial draft of the manuscript and prepared the figures. **KGFG**, **TN**, **SMM** and **RM** reviewed and edited the manuscript. **KGFG**, **SMM** and **RM** supervised the study.

DECLARATION OF COMPETING INTEREST

The authors declare that there are no conflicts of interest.

ACKNOWLEDGEMENTS

This study has received funding from the European Union's Horizon 2020 research and innovation programme under the Marie Skłodowska-Curie Grant agreement no. 813839.

REFERENCES

1. R. Z. Alicic, M. T. Rooney and K. R. Tuttle. Diabetic Kidney Disease: Challenges, Progress, and Possibilities. Clin J Am Soc Nephrol 2017;12(12):2032-2045

2. Y. Zheng, S. H. Ley and F. B. Hu. Global aetiology and epidemiology of type 2 diabetes mellitus and its complications. Nat Rev Endocrinol 2018;14(2):88-98

3. M. C. Thomas, M. Brownlee, K. Susztak*, et al.* Diabetic kidney disease. Nat Rev Dis Primers 2015;1:15018

4. A. Mather and C. Pollock. Glucose handling by the kidney. Kidney Int Suppl 2011(120):S1-6

5. C. Ghezzi, D. D. F. Loo and E. M. Wright. Physiology of renal glucose handling via SGLT1, SGLT2 and GLUT2. Diabetologia 2018;61(10):2087-2097

6. V. Vallon and K. Sharma. Sodium-glucose transport: role in diabetes mellitus and potential clinical implications. Curr Opin Nephrol Hypertens 2010;19(5):425-431

7. D. S. Hsia, O. Grove and W. T. Cefalu. An update on sodium-glucose co-transporter-2 inhibitors for the treatment of diabetes mellitus. Curr Opin Endocrinol Diabetes Obes 2017;24(1):73-79

8. M. Dunlop. Aldose reductase and the role of the polyol pathway in diabetic nephropathy. Kidney Int Suppl 2000;77:S3-12

9. H. Noh and G. L. King. The role of protein kinase C activation in diabetic nephropathy. Kidney Int Suppl 2007(106):S49-53

10. K. Reidy, H. M. Kang, T. Hostetter*, et al.* Molecular mechanisms of diabetic kidney disease. J Clin Invest 2014;124(6):2333-2340

11. A. J. King. The use of animal models in diabetes research. Br J Pharmacol 2012;166(3):877-894

12. A. Giralt-Lopez, M. Molina-Van den Bosch, A. Vergara*, et al.* Revisiting Experimental Models of Diabetic Nephropathy. Int J Mol Sci 2020;21(10)

13. X. He, T. Zhang, M. Tolosa*, et al.* A new, easily generated mouse model of diabetic kidney fibrosis. Sci Rep 2019;9(1):12549

14. Y. Liang, K. Arakawa, K. Ueta*, et al.* Effect of canagliflozin on renal threshold for glucose, glycemia, and body weight in normal and diabetic animal models. PLoS One 2012;7(2):e30555

15. S. Han, D. L. Hagan, J. R. Taylor*, et al.* Dapagliflozin, a selective SGLT2 inhibitor, improves glucose homeostasis in normal and diabetic rats. Diabetes 2008;57(6):1723-1729

16. R. Grempler, L. Thomas, M. Eckhardt*, et al.* Empagliflozin, a novel selective sodium glucose cotransporter-2 (SGLT-2) inhibitor: characterisation and comparison with other SGLT-2 inhibitors. Diabetes Obes Metab 2012;14(1):83-90

17. Y. Ohtake, T. Sato, T. Kobayashi*, et al.* Discovery of tofogliflozin, a novel C-arylglucoside with an O-spiroketal ring system, as a highly selective sodium glucose cotransporter 2 (SGLT2) inhibitor for the treatment of type 2 diabetes. J Med Chem 2012;55(17):7828-7840

18. H. Kakinuma, T. Oi, Y. Hashimoto-Tsuchiya*, et al.* (1S)-1,5-anhydro-1-[5-(4-ethoxybenzyl)-2-methoxy-4-methylphenyl]-1-thio-D-glucitol (TS-071) is a potent, selective sodium-dependent glucose cotransporter 2 (SGLT2) inhibitor for type 2 diabetes treatment. J Med Chem 2010;53(8):3247-3261

19. A. Markham. Remogliflozin Etabonate: First Global Approval. Drugs 2019;79(10):1157-1161

20. V. Mascitti, T. S. Maurer, R. P. Robinson*, et al.* Discovery of a clinical candidate from the structurally unique dioxa-bicyclo[3.2.1]octane class of sodium-dependent glucose cotransporter 2 inhibitors. J Med Chem 2011;54(8):2952-2960

21. B. Zambrowicz, J. Freiman, P. M. Brown*, et al.* LX4211, a dual SGLT1/SGLT2 inhibitor, improved glycemic control in patients with type 2 diabetes in a randomized, placebo-controlled trial. Clin Pharmacol Ther 2012;92(2):158-169

22. S. Caddeo, M. Boffito and S. Sartori. Tissue Engineering Approaches in the Design of Healthy and Pathological In Vitro Tissue Models. Front Bioeng Biotechnol 2017;5:40

23. Y. Bai, J. Wang, Z. He*, et al.* Mesenchymal Stem Cells Reverse Diabetic Nephropathy Disease via Lipoxin A4 by Targeting Transforming Growth Factor beta (TGF-beta)/smad Pathway and Pro-Inflammatory Cytokines. Med Sci Monit 2019;25:3069-3076
24. J. Rogal, A. Zbinden, K. Schenke-Layland*, et al.* Stem-cell based organ-on-a-chip models for diabetes research. Adv Drug Deliv Rev 2019;140:101-128
25. A. Tsakmaki, P. Fonseca Pedro and G. A. Bewick. Diabetes through a 3D lens: organoid models. Diabetologia 2020;63(6):1093-1102
26. A. Petrosyan, P. Cravedi, V. Villani*, et al.* A glomerulus-on-a-chip to recapitulate the human glomerular filtration barrier. Nat Commun 2019;10(1):3656
27. L. Wang, T. Tao, W. Su*, et al.* A disease model of diabetic nephropathy in a glomerulus-on-a-chip microdevice. Lab Chip 2017;17(10):1749-1760
28. D. Kawanami, K. Matoba, Y. Takeda*, et al.* SGLT2 Inhibitors as a Therapeutic Option for Diabetic Nephropathy. Int J Mol Sci 2017;18(5)
29. R. R. Poudel. Renal glucose handling in diabetes and sodium glucose cotransporter 2 inhibition. Indian J Endocrinol Metab 2013;17(4):588-593
30. M. Brownlee. Advanced protein glycosylation in diabetes and aging. Annu Rev Med 1995;46:223-234
31. A. Saito, T. Takeda, K. Sato*, et al.* Significance of proximal tubular metabolism of advanced glycation end products in kidney diseases. Ann N Y Acad Sci 2005;1043:637-643
32. J. M. Forbes and D. R. Thorburn. Mitochondrial dysfunction in diabetic kidney disease. Nat Rev Nephrol 2018;14(5):291-312
33. S. Yamagishi and T. Matsui. Advanced glycation end products, oxidative stress and diabetic nephropathy. Oxid Med Cell Longev 2010;3(2):101-108
34. M. Sedeek, R. Nasrallah, R. M. Touyz*, et al.* NADPH oxidases, reactive oxygen species, and the kidney: friend and foe. J Am Soc Nephrol 2013;24(10):1512-1518
35. P. Hansell, W. J. Welch, R. C. Blantz*, et al.* Determinants of kidney oxygen consumption and their relationship to tissue oxygen tension in diabetes and hypertension. Clin Exp Pharmacol Physiol 2013;40(2):123-137
36. C. Laustsen, S. Lycke, F. Palm*, et al.* High altitude may alter oxygen availability and renal metabolism in diabetics as measured by hyperpolarized [1-(13)C]pyruvate magnetic resonance imaging. Kidney Int 2014;86(1):67-74
37. J. M. Forbes, M. T. Coughlan and M. E. Cooper. Oxidative stress as a major culprit in kidney disease in diabetes. Diabetes 2008;57(6):1446-1454
38. J. O'Neill, A. Fasching, L. Pihl*, et al.* Acute SGLT inhibition normalizes O2 tension in the renal cortex but causes hypoxia in the renal medulla in anaesthetized control and diabetic rats. Am J Physiol Renal Physiol 2015;309(3):F227-234
39. R. Cerychova and G. Pavlinkova. HIF-1, Metabolism, and Diabetes in the Embryonic and Adult Heart. Front Endocrinol (Lausanne) 2018;9:460
40. S. B. Catrina, K. Okamoto, T. Pereira*, et al.* Hyperglycemia regulates hypoxia-inducible factor-1alpha protein stability and function. Diabetes 2004;53(12):3226-3232
41. L. Nordquist, M. Friederich-Persson, A. Fasching*, et al.* Activation of hypoxia-inducible factors prevents diabetic nephropathy. J Am Soc Nephrol 2015;26(2):328-338
42. S. Hasegawa, T. Tanaka, T. Saito*, et al.* The oral hypoxia-inducible factor prolyl hydroxylase inhibitor enarodustat counteracts alterations in renal energy metabolism in the early stages of diabetic kidney disease. Kidney Int 2020;97(5):934-950
43. P. K. Dabla. Renal function in diabetic nephropathy. World J Diabetes 2010;1(2):48-56
44. S. S. Kim, S. H. Song, I. J. Kim*, et al.* Urinary cystatin C and tubular proteinuria predict progression of diabetic nephropathy. Diabetes Care 2013;36(3):656-661
45. L. E. Dickson, M. C. Wagner, R. M. Sandoval*, et al.* The proximal tubule and albuminuria: really! J Am Soc Nephrol 2014;25(3):443-453

46. V. Vallon. The proximal tubule in the pathophysiology of the diabetic kidney. Am J Physiol Regul Integr Comp Physiol 2011;300(5):R1009-1022
47. C. Zoja, R. Donadelli, S. Colleoni*, et al.* Protein overload stimulates RANTES production by proximal tubular cells depending on NF-kappa B activation. Kidney Int 1998;53(6):1608-1615
48. J. F. Navarro-Gonzalez, C. Mora-Fernandez, M. Muros de Fuentes*, et al.* Inflammatory molecules and pathways in the pathogenesis of diabetic nephropathy. Nat Rev Nephrol 2011;7(6):327-340
49. C. Zoja, M. Morigi and G. Remuzzi. Proteinuria and phenotypic change of proximal tubular cells. J Am Soc Nephrol 2003;14 Suppl 1:S36-41
50. A. Eddy. Role of cellular infiltrates in response to proteinuria. Am J Kidney Dis 2001;37(1 Suppl 2):S25-29
51. K. R. Long, Y. Rbaibi, M. L. Gliozzi*, et al.* Differential kidney proximal tubule cell responses to protein overload by albumin and its ligands. Am J Physiol Renal Physiol 2020;318(3):F851-F859
52. S. Basi, P. Fesler, A. Mimran*, et al.* Microalbuminuria in type 2 diabetes and hypertension: a marker, treatment target, or innocent bystander? Diabetes Care 2008;31 Suppl 2:S194-201
53. K. Matoba, Y. Takeda, Y. Nagai*, et al.* Unraveling the Role of Inflammation in the Pathogenesis of Diabetic Kidney Disease. Int J Mol Sci 2019;20(14)
54. M. R. Dasu, S. Devaraj, S. Park*, et al.* Increased toll-like receptor (TLR) activation and TLR ligands in recently diagnosed type 2 diabetic subjects. Diabetes Care 2010;33(4):861-868
55. Y. Han, X. Xu, C. Tang*, et al.* Reactive oxygen species promote tubular injury in diabetic nephropathy: The role of the mitochondrial ros-txnip-nlrp3 biological axis. Redox Biol 2018;16:32-46
56. L. Fang, D. Xie, X. Wu*, et al.* Involvement of endoplasmic reticulum stress in albuminuria induced inflammasome activation in renal proximal tubular cells. PLoS One 2013;8(8):e72344
57. S. Song, D. Qiu, F. Luo*, et al.* Knockdown of NLRP3 alleviates high glucose or TGFB1-induced EMT in human renal tubular cells. J Mol Endocrinol 2018;61(3):101-113
58. R. E. Perez-Morales, M. D. Del Pino, J. M. Valdivielso*, et al.* Inflammation in Diabetic Kidney Disease. Nephron 2019;143(1):12-16
59. J. F. Navarro and C. Mora-Fernandez. The role of TNF-alpha in diabetic nephropathy: pathogenic and therapeutic implications. Cytokine Growth Factor Rev 2006;17(6):441-450
60. J. F. Navarro, F. J. Milena, C. Mora*, et al.* Renal pro-inflammatory cytokine gene expression in diabetic nephropathy: effect of angiotensin-converting enzyme inhibition and pentoxifylline administration. Am J Nephrol 2006;26(6):562-570
61. F. A. Garcia, J. F. Reboucas, T. Q. Balbino*, et al.* Pentoxifylline reduces the inflammatory process in diabetic rats: relationship with decreases of pro-inflammatory cytokines and inducible nitric oxide synthase. J Inflamm (Lond) 2015;12:33
62. O. Harmankaya, S. Seber and M. Yilmaz. Combination of pentoxifylline with angiotensin converting enzyme inhibitors produces an additional reduction in microalbuminuria in hypertensive type 2 diabetic patients. Ren Fail 2003;25(3):465-470
63. J. F. Navarro, C. Mora, M. Muros*, et al.* Additive antiproteinuric effect of pentoxifylline in patients with type 2 diabetes under angiotensin II receptor blockade: a short-term, randomized, controlled trial. J Am Soc Nephrol 2005;16(7):2119-2126
64. S. C. Tang, L. Y. Chan, J. C. Leung*, et al.* Bradykinin and high glucose promote renal tubular inflammation. Nephrol Dial Transplant 2010;25(3):698-710
65. R. Diwakar, A. L. Pearson, P. Colville-Nash*, et al.* The role played by endocytosis in albumin-induced secretion of TGF-beta1 by proximal tubular epithelial cells. Am J Physiol Renal Physiol 2007;292(5):F1464-1470
66. J. P. Stephan, W. Mao, E. Filvaroff*, et al.* Albumin stimulates the accumulation of extracellular matrix in renal tubular epithelial cells. Am J Nephrol 2004;24(1):14-19
67. L. Zhao, Y. Zou and F. Liu. Transforming Growth Factor-Beta1 in Diabetic Kidney Disease. Front Cell Dev Biol 2020;8:187

68. J. Zhao, R. Randive and J. A. Stewart. Molecular mechanisms of AGE/RAGE-mediated fibrosis in the diabetic heart. World J Diabetes 2014;5(6):860-867
69. T. Toyama, M. Shimizu, K. Furuichi*, et al.* Treatment and impact of dyslipidemia in diabetic nephropathy. Clin Exp Nephrol 2014;18(2):201-205
70. Y. Wang, G. K. Rangan, Y. C. Tay*, et al.* Induction of monocyte chemoattractant protein-1 by albumin is mediated by nuclear factor kappaB in proximal tubule cells. J Am Soc Nephrol 1999;10(6):1204-1213
71. I. Loeffler and G. Wolf. Epithelial-to-Mesenchymal Transition in Diabetic Nephropathy: Fact or Fiction? Cells 2015;4(4):631-652
72. Q. Liu, L. Xing, L. Wang*, et al.* Therapeutic effects of suppressors of cytokine signaling in diabetic nephropathy. J Histochem Cytochem 2014;62(2):119-128
73. M. Meier, J. Menne, J. K. Park*, et al.* Deletion of protein kinase C-epsilon signaling pathway induces glomerulosclerosis and tubulointerstitial fibrosis in vivo. J Am Soc Nephrol 2007;18(4):1190-1198
74. M. J. Rane, Y. Song, S. Jin*, et al.* Interplay between Akt and p38 MAPK pathways in the regulation of renal tubular cell apoptosis associated with diabetic nephropathy. Am J Physiol Renal Physiol 2010;298(1):F49-61
75. Y. Sirin and K. Susztak. Notch in the kidney: development and disease. J Pathol 2012;226(2):394-403
76. J. Mu, Q. Pang, Y. H. Guo*, et al.* Functional implications of microRNA-215 in TGF-beta1-induced phenotypic transition of mesangial cells by targeting CTNNBIP1. PLoS One 2013;8(3):e58622
77. B. N. Chau, C. Xin, J. Hartner*, et al.* MicroRNA-21 promotes fibrosis of the kidney by silencing metabolic pathways. Sci Transl Med 2012;4(121):121ra118
78. A. Krupa, R. Jenkins, D. D. Luo*, et al.* Loss of MicroRNA-192 promotes fibrogenesis in diabetic nephropathy. J Am Soc Nephrol 2010;21(3):438-447
79. A. K. Palmer, T. Tchkonia, N. K. LeBrasseur*, et al.* Cellular Senescence in Type 2 Diabetes: A Therapeutic Opportunity. Diabetes 2015;64(7):2289-2298
80. Y. Xiong and L. Zhou. The Signaling of Cellular Senescence in Diabetic Nephropathy. Oxid Med Cell Longev 2019;2019:7495629
81. S. Cetrullo, S. D'Adamo, B. Tantini*, et al.* mTOR, AMPK, and Sirt1: Key Players in Metabolic Stress Management. Crit Rev Eukaryot Gene Expr 2015;25(1):59-75
82. D. Yang, M. J. Livingston, Z. Liu*, et al.* Autophagy in diabetic kidney disease: regulation, pathological role and therapeutic potential. Cell Mol Life Sci 2018;75(4):669-688
83. W. J. Liu, T. T. Shen, R. H. Chen*, et al.* Autophagy-Lysosome Pathway in Renal Tubular Epithelial Cells Is Disrupted by Advanced Glycation End Products in Diabetic Nephropathy. J Biol Chem 2015;290(33):20499-20510
84. W. Zhang, X. Li, S. Wang*, et al.* Regulation of TFEB activity and its potential as a therapeutic target against kidney diseases. Cell Death Discov 2020;6:32
85. J. R. Ehrenkranz, N. G. Lewis, C. R. Kahn*, et al.* Phlorizin: a review. Diabetes Metab Res Rev 2005;21(1):31-38
86. M. Isaji. SGLT2 inhibitors: molecular design and potential differences in effect. Kidney Int Suppl 2011(120):S14-19
87. D. Z. I. Cherney, B. Zinman, S. E. Inzucchi*, et al.* Effects of empagliflozin on the urinary albumin-to-creatinine ratio in patients with type 2 diabetes and established cardiovascular disease: an exploratory analysis from the EMPA-REG OUTCOME randomised, placebo-controlled trial. Lancet Diabetes Endocrinol 2017;5(8):610-621
88. M. Mazidi, P. Rezaie, H. K. Gao*, et al.* Effect of Sodium-Glucose Cotransport-2 Inhibitors on Blood Pressure in People With Type 2 Diabetes Mellitus: A Systematic Review and Meta-Analysis of 43 Randomized Control Trials With 22 528 Patients. J Am Heart Assoc 2017;6(6)

89. T. M. Ansary, D. Nakano and A. Nishiyama. Diuretic Effects of Sodium Glucose Cotransporter 2 Inhibitors and Their Influence on the Renin-Angiotensin System. Int J Mol Sci 2019;20(3)
90. J. Liu, L. Li, S. Li*, et al.* Effects of SGLT2 inhibitors on UTIs and genital infections in type 2 diabetes mellitus: a systematic review and meta-analysis. Sci Rep 2017;7(1):2824
91. J. Rosenstock and E. Ferrannini. Euglycemic Diabetic Ketoacidosis: A Predictable, Detectable, and Preventable Safety Concern With SGLT2 Inhibitors. Diabetes Care 2015;38(9):1638-1642
92. H. J. L. Heerspink, B. V. Stefansson, R. Correa-Rotter*, et al.* Dapagliflozin in Patients with Chronic Kidney Disease. N Engl J Med 2020;383(15):1436-1446
93. M. Packer, S. D. Anker, J. Butler*, et al.* Cardiovascular and Renal Outcomes with Empagliflozin in Heart Failure. N Engl J Med 2020;383(15):1413-1424
94. C. G. Santos-Gallego, A. P. Vargas-Delgado, J. A. Requena-Ibanez*, et al.* Randomized Trial of Empagliflozin in Nondiabetic Patients With Heart Failure and Reduced Ejection Fraction. J Am Coll Cardiol 2021;77(3):243-255
95. M. E. Nassif, M. Qintar, S. L. Windsor*, et al.* Empagliflozin Effects on Pulmonary Artery Pressure in Patients With Heart Failure: Results From the EMBRACE-HF Trial. Circulation 2021;143(17):1673-1686
96. P. Fioretto, A. Zambon, M. Rossato*, et al.* SGLT2 Inhibitors and the Diabetic Kidney. Diabetes Care 2016;39 Suppl 2:S165-171
97. H. Yaribeygi, A. E. Butler, S. L. Atkin*, et al.* Sodium-glucose cotransporter 2 inhibitors and inflammation in chronic kidney disease: Possible molecular pathways. J Cell Physiol 2018;234(1):223-230
98. H. J. L. Heerspink, P. Perco, S. Mulder*, et al.* Canagliflozin reduces inflammation and fibrosis biomarkers: a potential mechanism of action for beneficial effects of SGLT2 inhibitors in diabetic kidney disease. Diabetologia 2019;62(7):1154-1166
99. H. Yaribeygi, L. E. Simental-Mendía, M. Banach*, et al.* The major molecular mechanisms mediating the renoprotective effects of SGLT2 inhibitors: An update. Biomedicine & Pharmacotherapy 2019;120:109526
100. L. Uthman, A. Baartscheer, B. Bleijlevens*, et al.* Class effects of SGLT2 inhibitors in mouse cardiomyocytes and hearts: inhibition of Na(+)/H(+) exchanger, lowering of cytosolic Na(+) and vasodilation. Diabetologia 2018;61(3):722-726
101. Y. J. Chung, K. C. Park, S. Tokar*, et al.* Off-target effects of SGLT2 blockers: empagliflozin does not inhibit Na+/H+ exchanger-1 or lower [Na+]i in the heart. Cardiovasc Res 2020
102. P. Song, W. Huang, A. Onishi*, et al.* Knockout of Na(+)-glucose cotransporter SGLT1 mitigates diabetes-induced upregulation of nitric oxide synthase NOS1 in the macula densa and glomerular hyperfiltration. Am J Physiol Renal Physiol 2019;317(1):F207-F217
103. J. Zhang, J. Wei, S. Jiang*, et al.* Macula Densa SGLT1-NOS1-Tubuloglomerular Feedback Pathway, a New Mechanism for Glomerular Hyperfiltration during Hyperglycemia. J Am Soc Nephrol 2019;30(4):578-593
104. C. M. A. Cefalo, F. Cinti, S. Moffa*, et al.* Sotagliflozin, the first dual SGLT inhibitor: current outlook and perspectives. Cardiovasc Diabetol 2019;18(1):20
105. D. L. Bhatt, M. Szarek, P. G. Steg*, et al.* Sotagliflozin in Patients with Diabetes and Recent Worsening Heart Failure. N Engl J Med 2021;384(2):117-128
106. B. Afsar, R. E. Afsar, T. Dagel*, et al.* Capillary rarefaction from the kidney point of view. Clin Kidney J 2018;11(3):295-301
107. J. Slyne, C. Slattery, T. McMorrow*, et al.* New developments concerning the proximal tubule in diabetic nephropathy: in vitro models and mechanisms. Nephrol Dial Transplant 2015;30 Suppl 4:iv60-67
108. C. Slattery, Y. Jang, W. A. Kruger*, et al.* gamma-Secretase inhibition promotes fibrotic effects of albumin in proximal tubular epithelial cells. Br J Pharmacol 2013;169(6):1239-1251

109. A. Valdes, M. Castro-Puyana, C. Garcia-Pastor*, et al.* Time-series proteomic study of the response of HK-2 cells to hyperglycemic, hypoxic diabetic-like milieu. PLoS One 2020;15(6):e0235118
110. H. A. Mutsaers, M. J. Wilmer, L. P. van den Heuvel*, et al.* Basolateral transport of the uraemic toxin p-cresyl sulfate: role for organic anion transporters? Nephrol Dial Transplant 2011;26(12):4149
111. L. C. Racusen, C. Monteil, A. Sgrignoli*, et al.* Cell lines with extended in vitro growth potential from human renal proximal tubule: characterization, response to inducers, and comparison with established cell lines. J Lab Clin Med 1997;129(3):318-329
112. S. Y. Lee, J. M. Kang, D. J. Kim*, et al.* PGC1alpha Activators Mitigate Diabetic Tubulopathy by Improving Mitochondrial Dynamics and Quality Control. J Diabetes Res 2017;2017:6483572
113. Y. H. Lee, S. H. Kim, J. M. Kang*, et al.* Empagliflozin attenuates diabetic tubulopathy by improving mitochondrial fragmentation and autophagy. Am J Physiol Renal Physiol 2019;317(4):F767-F780
114. S. J. Khundmiri, L. Chen, E. D. Lederer*, et al.* Transcriptomes of Major Proximal Tubule Cell Culture Models. J Am Soc Nephrol 2021;32(1):86-97
115. Y. Wang, S. Chen, Z. Yan*, et al.* A prospect of cell immortalization combined with matrix microenvironmental optimization strategy for tissue engineering and regeneration. Cell Biosci 2019;9:7
116. M. Wieser, G. Stadler, P. Jennings*, et al.* hTERT alone immortalizes epithelial cells of renal proximal tubules without changing their functional characteristics. Am J Physiol Renal Physiol 2008;295(5):F1365-1375
117. M. J. Wilmer, M. A. Saleem, R. Masereeuw*, et al.* Novel conditionally immortalized human proximal tubule cell line expressing functional influx and efflux transporters. Cell Tissue Res 2010;339(2):449-457
118. G. Gstraunthaler. Alternatives to the use of fetal bovine serum: serum-free cell culture. ALTEX 2003;20(4):275-281
119. Y. Zhu, H. Cui, J. Lv*, et al.* AT1 and AT2 receptors modulate renal tubular cell necroptosis in angiotensin II-infused renal injury mice. Sci Rep 2019;9(1):19450
120. N. P. Visavadiya, Y. Li and S. Wang. High glucose upregulates upstream stimulatory factor 2 in human renal proximal tubular cells through angiotensin II-dependent activation of CREB. Nephron Exp Nephrol 2011;117(3):e62-70
121. H. L. Guo, X. H. Liao, Q. Liu*, et al.* Angiotensin II Type 2 Receptor Decreases Transforming Growth Factor-beta Type II Receptor Expression and Function in Human Renal Proximal Tubule Cells. PLoS One 2016;11(2):e0148696
122. F. Huang, Q. Wang, F. Guo*, et al.* FoxO1-mediated inhibition of STAT1 alleviates tubulointerstitial fibrosis and tubule apoptosis in diabetic kidney disease. EBioMedicine 2019;48:491-504
123. S. Sakai, T. Yamamoto, Y. Takabatake*, et al.* Proximal Tubule Autophagy Differs in Type 1 and 2 Diabetes. J Am Soc Nephrol 2019;30(6):929-945
124. P. Chen, Y. Yuan, T. Zhang*, et al.* Pentosan polysulfate ameliorates apoptosis and inflammation by suppressing activation of the p38 MAPK pathway in high glucosetreated HK2 cells. Int J Mol Med 2018;41(2):908-914
125. C. Garcia-Pastor, S. Benito-Martinez, V. Moreno-Manzano*, et al.* Mechanism and Consequences of The Impaired Hif-1alpha Response to Hypoxia in Human Proximal Tubular HK-2 Cells Exposed to High Glucose. Sci Rep 2019;9(1):15868
126. S. Kroening, E. Neubauer, J. Wessel*, et al.* Hypoxia interferes with connective tissue growth factor (CTGF) gene expression in human proximal tubular cell lines. Nephrol Dial Transplant 2009;24(11):3319-3325

127. M. Morigi, D. Macconi, C. Zoja*, et al.* Protein overload-induced NF-kappaB activation in proximal tubular cells requires H(2)O(2) through a PKC-dependent pathway. J Am Soc Nephrol 2002;13(5):1179-1189

128. X. Jiang, X. L. Ruan, Y. X. Xue*, et al.* Metformin Reduces the Senescence of Renal Tubular Epithelial Cells in Diabetic Nephropathy via the MBNL1/miR-130a-3p/STAT3 Pathway. Oxid Med Cell Longev 2020;2020:8708236

129. Y. Li, X. Wen and Y. Liu. Tubular cell dedifferentiation and peritubular inflammation are coupled by the transcription regulator Id1 in renal fibrogenesis. Kidney Int 2012;81(9):880-891

130. S. Coffey, T. Costacou, T. Orchard*, et al.* Akt Links Insulin Signaling to Albumin Endocytosis in Proximal Tubule Epithelial Cells. PLoS One 2015;10(10):e0140417

131. H. Feng, H. Hu, P. Zheng*, et al.* AGE receptor 1 silencing enhances advanced oxidative protein product-induced epithelial-to-mesenchymal transition of human kidney proximal tubular epithelial cells via RAGE activation. Biochem Biophys Res Commun 2020;529(4):1201-1208

132. U. Storch, A. L. Forst, F. Pardatscher*, et al.* Dynamic NHERF interaction with TRPC4/5 proteins is required for channel gating by diacylglycerol. Proc Natl Acad Sci U S A 2017;114(1):E37-E46

133. T. Zhou, M. Luo, W. Cai*, et al.* Runt-Related Transcription Factor 1 (RUNX1) Promotes TGF-beta-Induced Renal Tubular Epithelial-to-Mesenchymal Transition (EMT) and Renal Fibrosis through the PI3K Subunit p110delta. EBioMedicine 2018;31:217-225

134. L. Aschauer, L. N. Gruber, W. Pfaller*, et al.* Delineation of the key aspects in the regulation of epithelial monolayer formation. Mol Cell Biol 2013;33(13):2535-2550

135. H. Kim, J. Sung, H. Kim*, et al.* Expression and secretion of CXCL12 are enhanced in autosomal dominant polycystic kidney disease. BMB Rep 2019;52(7):463-468

136. A. Wilmes, C. Bielow, C. Ranninger*, et al.* Mechanism of cisplatin proximal tubule toxicity revealed by integrating transcriptomics, proteomics, metabolomics and biokinetics. Toxicol In Vitro 2015;30(1 Pt A):117-127

137. M. N. Islam, T. P. Griffin, E. Sander*, et al.* Human mesenchymal stromal cells broadly modulate high glucose-induced inflammatory responses of renal proximal tubular cell monolayers. Stem Cell Res Ther 2019;10(1):329

138. F. Sallustio, A. Stasi, C. Curci*, et al.* Renal progenitor cells revert LPS-induced endothelial-to-mesenchymal transition by secreting CXCL6, SAA4, and BPIFA2 antiseptic peptides. FASEB J 2019;33(10):10753-10766

139. J. Jansen, M. Fedecostante, M. J. Wilmer*, et al.* Bioengineered kidney tubules efficiently excrete uremic toxins. Sci Rep 2016;6:26715

140. Y. Sun, A. Goes Martini, M. J. Janssen*, et al.* Megalin: A Novel Endocytic Receptor for Prorenin and Renin. Hypertension 2020;75(5):1242-1250

141. E. Peters, S. Geraci, S. Heemskerk*, et al.* Alkaline phosphatase protects against renal inflammation through dephosphorylation of lipopolysaccharide and adenosine triphosphate. Br J Pharmacol 2015;172(20):4932-4945

142. A. Di Mise, G. Tamma, M. Ranieri*, et al.* Activation of Calcium-Sensing Receptor increases intracellular calcium and decreases cAMP and mTOR in PKD1 deficient cells. Sci Rep 2018;8(1):5704

143. J. Vriend, J. G. P. Peters, T. T. G. Nieskens*, et al.* Flow stimulates drug transport in a human kidney proximal tubule-on-a-chip independent of primary cilia. Biochim Biophys Acta Gen Subj 2020;1864(1):129433

144. H. A. Mutsaers, P. Caetano-Pinto, A. E. Seegers*, et al.* Proximal tubular efflux transporters involved in renal excretion of p-cresyl sulfate and p-cresyl glucuronide: Implications for chronic kidney disease pathophysiology. Toxicol In Vitro 2015;29(7):1868-1877

145. C. Hurtado Del Pozo, E. Garreta, J. C. Izpisua Belmonte*, et al.* Modeling epigenetic modifications in renal development and disease with organoids and genome editing. Dis Model Mech 2018;11(11)

146. Q. Wu, J. Liu, X. Wang*, et al.* Organ-on-a-chip: recent breakthroughs and future prospects. Biomed Eng Online 2020;19(1):9
147. K. A. Homan, D. B. Kolesky, M. A. Skylar-Scott*, et al.* Bioprinting of 3D Convoluted Renal Proximal Tubules on Perfusable Chips. Sci Rep 2016;6:34845
148. K. J. Jang, A. P. Mehr, G. A. Hamilton*, et al.* Human kidney proximal tubule-on-a-chip for drug transport and nephrotoxicity assessment. Integr Biol (Camb) 2013;5(9):1119-1129
149. K. J. Jang and K. Y. Suh. A multi-layer microfluidic device for efficient culture and analysis of renal tubular cells. Lab Chip 2010;10(1):36-42
150. N. Y. C. Lin, K. A. Homan, S. S. Robinson*, et al.* Renal reabsorption in 3D vascularized proximal tubule models. Proc Natl Acad Sci U S A 2019;116(12):5399-5404
151. E. M. Vedula, J. L. Alonso, M. A. Arnaout*, et al.* A microfluidic renal proximal tubule with active reabsorptive function. PLoS One 2017;12(10):e0184330
152. J. Rogal, C. Probst and P. Loskill. Integration concepts for multi-organ chips: how to maintain flexibility?! Future Sci OA 2017;3(2):FSO180
153. Y. Fu, D. Breljak, A. Onishi*, et al.* Organic anion transporter OAT3 enhances the glucosuric effect of the SGLT2 inhibitor empagliflozin. Am J Physiol Renal Physiol 2018;315(2):F386-F394
154. S. E. Jenkinson, G. W. Chung, E. van Loon*, et al.* The limitations of renal epithelial cell line HK-2 as a model of drug transporter expression and function in the proximal tubule. Pflugers Arch 2012;464(6):601-611
155. J. Kieninger, A. Weltin, H. Flamm*, et al.* Microsensor systems for cell metabolism - from 2D culture to organ-on-chip. Lab Chip 2018;18(9):1274-1291
156. M. Tziastoudi, I. Stefanidis and E. Zintzaras. The genetic map of diabetic nephropathy: evidence from a systematic review and meta-analysis of genetic association studies. Clin Kidney J 2020;13(5):768-781

CHAPTER 7

The Impact of Palmitic Acid and Glycated Albumin on Proximal Tubule Cells in Diabetic Kidney Disease: Insights and Interventions

João Faria[1], Isa Tummers[1], Bonnie C. Broeksma[2], Rosalinde Masereeuw[1], Silvia M. Mihăilă[1]

[1] Division of Pharmacology, Department of Pharmaceutical Sciences, Utrecht Institute for Pharmaceutical Sciences, Utrecht University, Utrecht, The Netherlands

[2] Danone Nutricia Research, Utrecht, The Netherlands

ABSTRACT

Diabetic kidney disease (DKD) is a prevalent complication affecting a significant proportion of individuals with type 2 diabetes mellitus (T2DM), and it remains a leading cause of end-stage kidney failure globally. The proximal tubule (PT) is central to glucose reabsorption and is strongly implicated in the pathogenesis of DKD. While hyperglycemia and metabolic alterations have been associated with DKD, emerging evidence implicates free fatty acids, particularly palmitic acid (PA,) and glycated albumin (GA) in disease progression. This study aimed to provide a comprehensive assessment of how PA or GA affect metabolic and mitochondrial activity, as well as structural integrity in PT cells. Furthermore, we evaluated the potential protective effect of empagliflozin, a selective sodium-glucose co-transporter 2 (SGLT2) inhibitor, on PT cells in the context of diabetic injury, as assessed by injury markers, namely kidney injury molecule-1 (KIM-1) and neutrophil gelatinase-associated lipocalin (NGAL). Our findings reveal that both PA and GA induce morphological derangements in PT cells, as evidenced by the disruption of F-actin filaments, while not significantly affecting metabolic activity or ATP production. Interestingly, PA and GA modestly enhance mitochondrial dynamics, including processes related to mitophagy, fusion and fission processes, while preserving mitochondrial mass levels. Moreover, exposure to PA or GA leads to increased NGAL excretion, which was ameliorated by empagliflozin treatment. Overall, our study underscores the exacerbating effects of PA and GA on diabetic PT cells *in vitro*, with empagliflozin mitigating PT injury. These findings offer valuable insights into the complex pathogenesis of DKD and highlight the potential of SGLT2 inhibitors as interventions in mitigating its progression.

KEYWORDS: Diabetic kidney disease, hypoxia, hyperglycemia, palmitic acid, glycated albumin, empagliflozin

1. INTRODUCTION

Diabetic kidney disease (DKD) is a prevalent complication affecting approximately 40% of individuals with type 2 diabetes mellitus (T2DM) and remains the primary cause of end-stage kidney failure worldwide [1]. The involvement of the kidney proximal tubule (PT) in the development of DKD has been extensively investigated, with a particular focus on the critical therapeutic targeting of glucose levels and metabolic alterations.

The PT assumes a pivotal role in the reabsorption of filtered glucose alongside sodium from the glomerular filtrate, a two-step process orchestrated by the coordinated activity of the sodium glucose co-transporter 2 (SGLT2) at the apical membrane and glucose transporter 2 (GLUT2) at the basolateral side [2]. This mechanism ensures the highly efficient reabsorption (99%) of filtered glucose, preventing its loss in urine. In DKD, several factors contribute to the disruption of glucose reabsorption and sodium uptake. Hyperglycemia, a hallmark of T2DM, causes an excess glucose load entering the PT that surpasses its normal reabsorption capacity. This overload demands an increase in ATP and, consequently, an increase in oxygen consumption, culminating in cellular hypoxia [3, 4]. These two pivotal factors, hyperglycemia and hypoxia, play a central role in DKD progression, resulting in extensive modifications in glucose metabolism, mitochondrial dysfunction, oxidative stress, inflammation, and cytoskeletal damage [3-6]. A comprehensive understanding in these changes is imperative for elucidating the pathophysiology of DKD and identifying potential therapeutic targets, particularly because the combined effects of hyperglycemia and hypoxia are not fully understood.

Animal models of DKD have provided invaluable insights into disease mechanisms and potential treatments, yet their inherent differences from humans in disease progression and physiological responses impose limitations. While valuable, endpoints might not fully reflect human outcomes, and responses to treatment may diverge [7-9]. To holistically address the complexity of DKD, researchers often complement animal studies with *in vitro* models and human data. To faithfully replicate the biochemical milieu of diabetes *in vitro*, many studies have adopted a combination of high glucose levels and low oxygen concentrations [10-15]. Nevertheless, it is essential to recognize that while the pathology of DKD is multifaceted, these conditions in isolation might not capture all relevant aspects of the disease. In addition to elevated glucose and reduced oxygen, other factors may contribute to disease progression, such as free fatty acids (FFAs), with a particular emphasis on palmitic acid (PA), highly prevalent in human urine [16], and glycated albumin (GA), which have, as of yet, not been fully validated *in vitro*.

In DKD, an imbalance in FFAs metabolism can lead to elevated circulating FFAs levels,

resulting in their accumulation within PT cells and consequent lipotoxicity [17]. In addition, impaired intracellular fatty acid metabolism disrupts mitochondrial function in the PT, characterized by the accumulation of damaged mitochondria and decreased ATP pro duction [18]. As the disease advances, GA emerges as a significant indicator of chronic hyperglycemia [19, 20]. GA is formed through non-enzymatic reactions between glucose and albumin and is known to lead to oxidative stress. Additionally, GA can promote inflammation and directly impair kidney function, exacerbating renal damage in DKD [21].

The primary objective of this study was to comprehensively investigate the impact of PA and GA on PT cells, under conditions resembling diabetes, specifically focusing on their roles in causing structural damage and mitochondrial dysfunction, as observed in DKD. We cultured PT cells in a diabetic-like environment with high glucose and low oxygen levels to investigate how these compounds affected cellular responses. Additionally, we evaluated the efficacy of empagliflozin, a SGLT2 inhibitor, in reducing PT cell injury and providing valuable insights into the intricate pathology of DKD, potentially opening up new avenues for therapeutic interventions.

2. MATERIALS AND METHODS

2.1. Cell Culture

Human kidney proximal tubular epithelial cells (HK-2; ATCC, CRL-2190TM) were maintained in Keratinocyte Growth Medium 2 (Sigma-Aldrich, C-20011) supplemented with 4 μL/mL bovine pituitary extract (BPE), 0.125 ng/mL human recombinant epidermal growth factor (EGF), 5 μg/mL human recombinant insulin, 0.33 μg/mL hydrocortisone, 0.39 μg/mL epinephrine, 10 μg/mL human recombinant transferrin, 0.06 mM $CaCl_2$, 1% fetal calf serum (FCS; Gibco, ThermoFisher Scientific, 16000044), and 1% Penicillin-Streptomycin (PenStrep; Gibco, ThermoFisher Scientific, 15276355) at 37 °C in a 5% (*v*/*v*) CO_2 atmosphere. The medium was refreshed every other day.

2.1.1. HK-2 Diabetic Model

Prior to experiments, cells were seeded at 42,000 cells/cm^2 in 96-well plates (Corning®) unless otherwise specified, and grown for 2 days in low glucose (LG; 5.6 mM) Dulbecco's modified Eagle's medium (DMEM; Sigma-Aldrich, D4947) supplemented with 15 mM HEPES (Gibco, ThermoFisher Scientific, 15630080), 5 ng/mL EGF, 1% insulin-transferrin-selenium (ITS; Roche, 11074547001), 1% FCS, and 1% PenStrep at 37 °C in a 5% (*v*/*v*) CO_2, under normoxic conditions (20% O_2), to achieve a quiescent state before exposures. Subsequently, HK-2 cells were exposed to LG (control medium), and diabetic conditions that included high glucose (HG; 25 mM glucose; Gibco, ThermoFisher Scientific, A2494001) alone and supplemented with 100 nM palmitic acid (HG+PA; HY-N0830, MCE) [22], or HG supplemented with 100 μg/mL GA (HG+GA; A8301, Sigma- Aldrich) [23]. All conditions were applied under hypoxic conditions (1% O_2) for 24 and 48h. Osmolarity balance was achieved by supplementing the control medium with 19.4 mM mannitol (MAN, M4125, Sigma-Aldrich).

For the treatment with empagliflozin, HK-2 cells were cultured as described above. After 48 h of exposure, the cells were incubated with 500 nM empagliflozin [24] in control medium for an additional 24h under normoxic conditions (20% O_2).

2.2. Injury and Treatment Readouts

Upon exposure to the diabetic mediators, a comprehensive panel of mitochondrial-related parameters were assessed as described below. Similarly, diabetic cells treated with empagliflozin were also evaluated, but focusing on metabolic activity, ATP production, and release of kidney injury markers.

2.2.1. Metabolic Activity

HK-2 metabolic activity was measured using PrestoBlue® reagent (A13262, Invitrogen, ThermoFischer Scientific). HK-2 cells were rinsed once with Hank's Balanced Salt Solution (HBSS; Gibco, Life Technologies) incubated with PrestoBlue® (diluted 1:10 in control medium) for 1 hour at 37°C after which fluorescence was measured using the GloMax® Discover microplate reader (excitation wavelength: 520 nm; emission wavelength range: 580-640 nm).

2.2.2. ATP Production

Intracellular ATP production was measured using the CellTiter-Glo® 2.0 Assay (G9241, Promega) following manufacturers' instructions. Briefly, 100 μL of ATP solution was added to each well and mixed on an orbital shaker for 2 min. Plates were then incubated for 10min at room temperature, after which luminescence was measured using a GloMax® Discover microplate reader.

2.2.3. Mitochondrial Mass

To assess active mitochondria with an intact mitochondrial membrane potential, treated HK-2 cells were stained with MitoTracker™ Orange CMTMRos (M7510, Invitrogen, ThermoFischer Scientific). After exposure, cells were incubated with the reagent (500 nM) and Hoechst 33342 (1 µM) in control medium for 30 minutes at 37°C in the dark. Cells were then washed with HBSS and fluorescence was measured using a GloMax® microplate reader (excitation wavelength: 520 nm; emission range: 580-640 nm; Hoechst, excitation wavelength: 365 nm; emission range: 500-550 nm).

2.2.4. Bioenergetic Profile

The bioenergetic profile of the cells was determined by the Seahorse XF assay. HK-2 cells were seeded in a XF96 cell culture microplate (Seahorse Bioscience) at 8.000 cells/well and cultured and exposed as described above for up to 48 hours. Bioenergetic profiles were measured by serial injections of oligomycin (2 μM), carbonyl cyanide-4 (trifluoromethoxy) phenylhydrazone (FCCP, 1 μM) and rotenone/antimycin A (Rot/AA, both 0.5 μM) with the Seahorse XF Cell Mito Stress Test [25]. The oxygen consumption rate (OCR) and the extracellular acidification rate (ECAR) were measured by the Seahorse Bioscience Extracellular Flux Analyzer (Agilent Technologies) following manufacturers protocol. OCR and ECAR values were used to determine the following mitochondrial related factors: basal

respiration, maximal respiration, ATP-linked respiration, and spare respiratory capacity.

2.2.5. Lipid Accumulation

Lipid accumulation was detected using the BODIPY™ (D3922, Invitrogen, ThermoFischer Scientific) fluorescent probe. First, the cells were washed with HBSS, stained with BODIPY (2 μM), and incubated for 15min at 37°C. The cells were then washed twice with HBSS and fixed in 4% PFA for 10 minutes at room temperature (RT). Afterwards, the cells were again washed two times with HBSS and fluorescence was measured using a GloMax® microplate Reader (excitation wavelength: 475 nm; emission range: 500-550 nm).

2.2.6. RNA Extraction, cDNA Synthesis, and Real Time qPCR

HK-2 cells were cultured in 12-well plates (Corning®) and exposed as described above. Cells were lysed and RNA was isolated with the PureLink™ RNA Mini Kit (12183018A, Invitrogen, Life technologies) following manufactures protocol. The RNA concentration of the samples was measured using NanoDrop One, and the samples were stored at -80°C until further analysis. cDNA synthesis was performed with the iScript™ cDNA synthesis kit (1708890, Bio-Rad) following manufacturer's instructions. RT-qPCR was used to determine relative gene expression. Primers and their temperatures are listed in **Supplementary Table S1**. The housekeeping gene hypoxanthine phosphoribosyltransferase 1 (HRPT1) was used to normalize gene expression.

2.2.7. Immunofluorescence Analysis

For immunofluorescence analysis, HK-2 cells were cultured in a 96-well black/*clear* bottom plates (ThermoFischer, 165305). Upon exposure, cells were washed twice with HBSS and fixed with 4% paraformaldehyde (PFA; VWR Chemicals, 9713.1000) for 10 min at RT. After fixation, cells were washed three times with PBS containing 0.1% Tween20 for 5 min. Afterwards, cells were permeabilized with 0.3% Triton X-100 in PBS for 10 min at RT, and blocked in blocking buffer (2% FCS, 2% bovine serum albumin and 0.1% Tween20 in PBS) for 30min at RT. To stain F-actin filaments, phalloidin 594 (ThermoFischer, A12381). The cells were then washed three times with PBS containing 0.1% Tween20 for 2 min. Nuclei were stained using 4',6-diamidino-2-fenylindool (DAPI), followed by three washing steps in PBS for 3min. Images were taken with a confocal microscope (Leica TCS SP8X) and software Leica Application Suite X.

2.2.8. Enzyme-Linked Immunosorbent Assay (ELISA)

To assess the effect of empagliflozin (500 nM), a SGLT2 inhibitor, cell culture supernatants were collected after 24h of treatment, centrifuged for 10 min, 240x g and 4°C, and then stored at -20°C until further use. The levels of kidney injury markers were measured using the DuoSet ELISA kits kidney injury marker-1 (KIM-1; DY1750; R&D Systems) and neutrophil gelatinase-associated lipocalin (NGAL; DY1757; R&D Systems), following the manufacturer's instructions. The optical density of each well was measured at 450 nm using a GloMax® microplate reader. Each sample was measured in duplicates and quantified using Microplate Manager software (version 6.0, Bio-Rad Laboratories, Hercules, CA, USA), generating a four-parameter logistic (4-PL) curve-fit.

2.2.9. Protein Content

To quantify protein content and use it for data normalization where applicable, we employed the Pierce™ BCA Protein Assay Kit (23225, ThermoScientific) in accordance to the manufacturer's protocol.

2.3. Statistical Analysis

The results are shown as mean ± standard deviation (SD), n indicates the number of independent experiments replicates and N the number of technical replicates. In fluorescence and luminescence-based assays, data were corrected for background, normalized to untreated cells, and presented as fold-change to control group (LG). Statistical analyses were performed in GraphPad version 10.0.2. The statistical test is indicated in the figure legends. A p-value < 0.05 was considered statistically significant.

3. RESULTS

3.1. A Diabetic Microenvironment Leads to Cytoskeletal Deterioration Without Significant Changes in Mitochondrial Health

To evaluate a more complex microenvironment of DKD *in vitro*, HK-2 cells were treated with high glucose (HG) alone or combined with either palmitic acid (PA) or glycated albumin (GA) under hypoxia (**Figure 1A**). For all conditions tested, we did not observe changes in protein content (**Supplementary Figure S1**), however a progressive deterioration in the integrity of the cell monolayer was observed over time (**Figure 1B**). This deterioration in cytoskeleton organization, evident by the presence of holes in the cell monolayer, was particularly evident in both HG+PA and HG+GA groups, with the most pronounced effect at 48h post exposure (**Figure 1B**). Next, metabolic activity, ATP production and mitochondrial mass were evaluated. We observed a modest decrease in metabolic activity in the diabetic groups compared to the control (LG) during the first 24 h of exposure (**Figure 1C**), whereas at 48 h there was an observable increase metabolic activity within the diabetic groups, surpassing that of the LG control group (**Figure 1D**). Despite this, differences in ATP production were not detected across the different conditions and time points (**Figure 1E, F**). Furthermore, a minor increase in mitochondrial mass was found in the HG and HG+GA groups compared to control at 24h (**Figure 1G**). Moreover, at 48h, the HG and HG+PA groups showed a minor decrease in mitochondrial mass compared to control (**Figure 1F**). These data suggest that metabolic activity and mitochondrial mass in the diabetes groups undergo dynamic changes over the 48h of exposure, whereas ATP production remained constant across conditions.

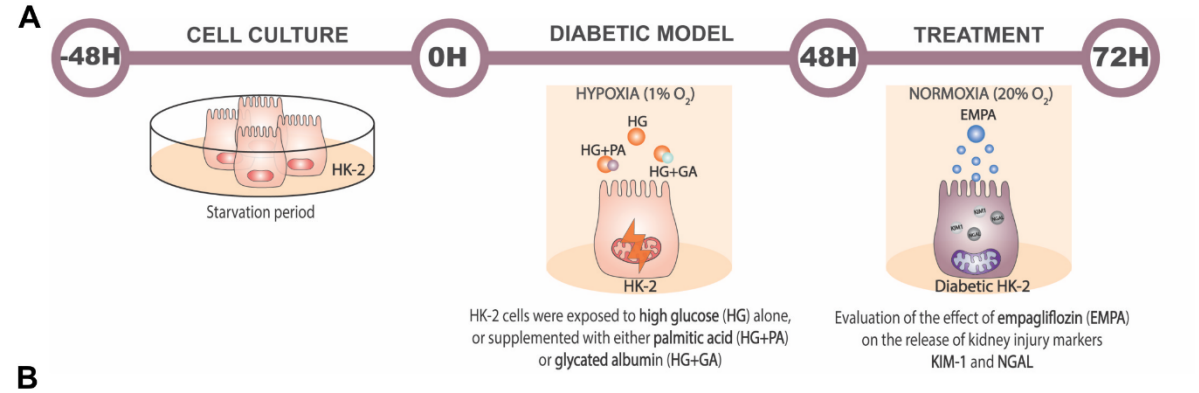
A
-48H
CELL CULTURE
0H
DIABETIC MODEL
48H
TREATMENT
72H
HK-2
Starvation period
HYPOXIA (1% O2)
HG
HG+PA
HG+GA
HK-2
NORMOXIA (20% O2)
EMPA
Diabetic HK-2
HK-2 cells were exposed to high glucose (HG) alone, or supplemented with either palmitic acid (HG+PA) or glycated albumin (HG+GA)
Evaluation of the effect of empagliflozin (EMPA) on the release of kidney injury markers KIM-1 and NGAL

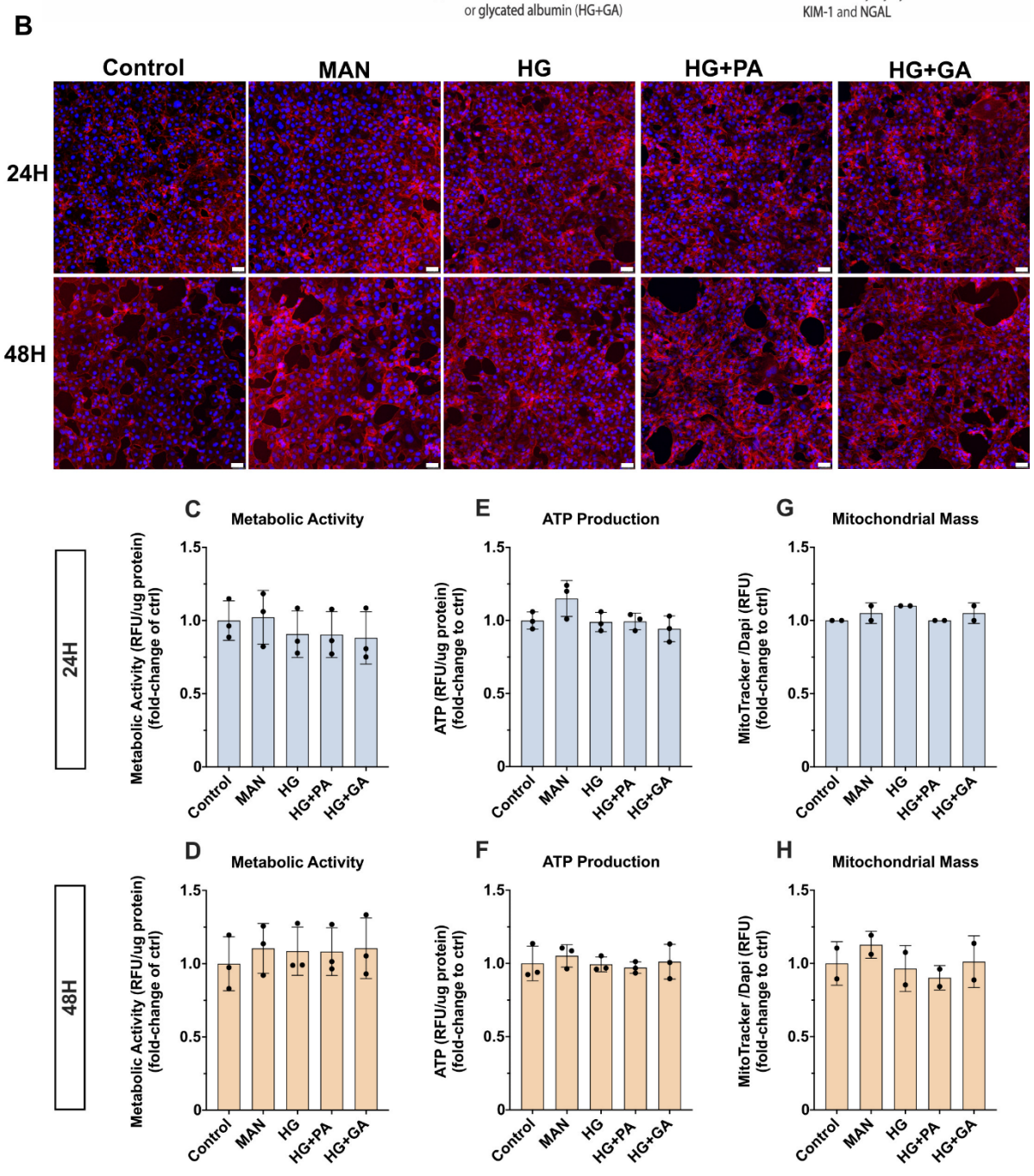
B
Control
MAN
HG
HG+PA
HG+GA
24H
48H
C
Metabolic Activity
Metabolic Activity (RFU/ug protein) (fold-change of ctrl)
E
ATP Production
ATP (RFU/ug protein) (fold-change to ctrl)
G
Mitochondrial Mass
MitoTracker /Dapi (RFU) (fold-change to ctrl)
D
F
H
1.5
1.0
0.5
0

Figure 1. Morphological and mitochondrial changes of HK-2 cells following exposure to diabetic conditions. (A) Schematic overview of the protocol for inducing diabetic-like effects in HK-2 cells, followed by treatment with empagliflozin. **(B)** Immunofluorescence of HK-2 cells exposed to diabetic conditions for 24h or 48h. In blue: DAPI (nuclei staining), in red: Phalloidin (F-actin filaments). Scale bar: 50 μm. To evaluate the mitochondrial dysfunction upon exposure to diabetic conditions compared to control (low glucose), we looked into **(C, D)** metabolic activity (n=3 in triplicate), **(E, F)** ATP production (n=3 in triplicate), and **(G, H)** mitochondrial mass (n=2 in triplicate). Data are shown as mean ± SD (n=3 in triplicate). **Abbreviations**: **MAN** – mannitol; **HG** – high glucose; **HG+PA** – high glucose supplemented with palmitic acid; **HG+GA** – high glucose supplemented with glycated albumin.

3.2. The Diabetic Microenvironment Increases SGLT2 Expression

During DKD, PT cells respond to increased glucose reabsorption by upregulating *SGLT2* expression to handle the excess glucose load [5]. In agreement, *SGLT2* expression increased at 24 h for all diabetic conditions compared to control which was significant for the HG group (**Figure 2A**). Interestingly, HG+PA and HG+GA groups showed a significant decrease in SGLT2 expression compared to HG group. At 48h, the increase in *SGLT2* expression was significantly increased for the HG+PA and HG+GA groups (**Figure 2B**), in line with the increase in glucose concentration in the culture medium. Subsequently, we investigated the expression of *Na^+K^+-ATPase*, which plays a role in regulating the expression and function of SGLT2 [26]. Interestingly, in contrast to SGLT2, the levels of Na+K+-ATPase remained consistent across all groups at 24 hours (**Figure 2C**), with only a minor increase observed at 48 hours for the HG and HG+PA groups (**Figure 2D**). These results hint at a possible correlation between the unchanged ATP levels (**Figure 1E-F**), and *Na^+K^+-ATPase* (**Figure 2C-D**), however assessment of *Na^+K^+-ATPase* activity is required to validate this hypothesis.

Furthermore, we investigated the impact of diabetic conditions in DKD on the expression of HIF-1α, a key regulator of cellular responses to hypoxia [27], which expression exhibited a minor decrease at 24 h for all diabetic conditions compared to the control (**Figure 2E**). In contrast, at 48 h, there was a minor increase in HIF-1α expression in the HG and HG+PA groups compared to the control (**Figure 2F**). These findings suggest that exposure to diabetic conditions, in particular HG+PA, influenced HIF-1α expression in a time-dependent manner.

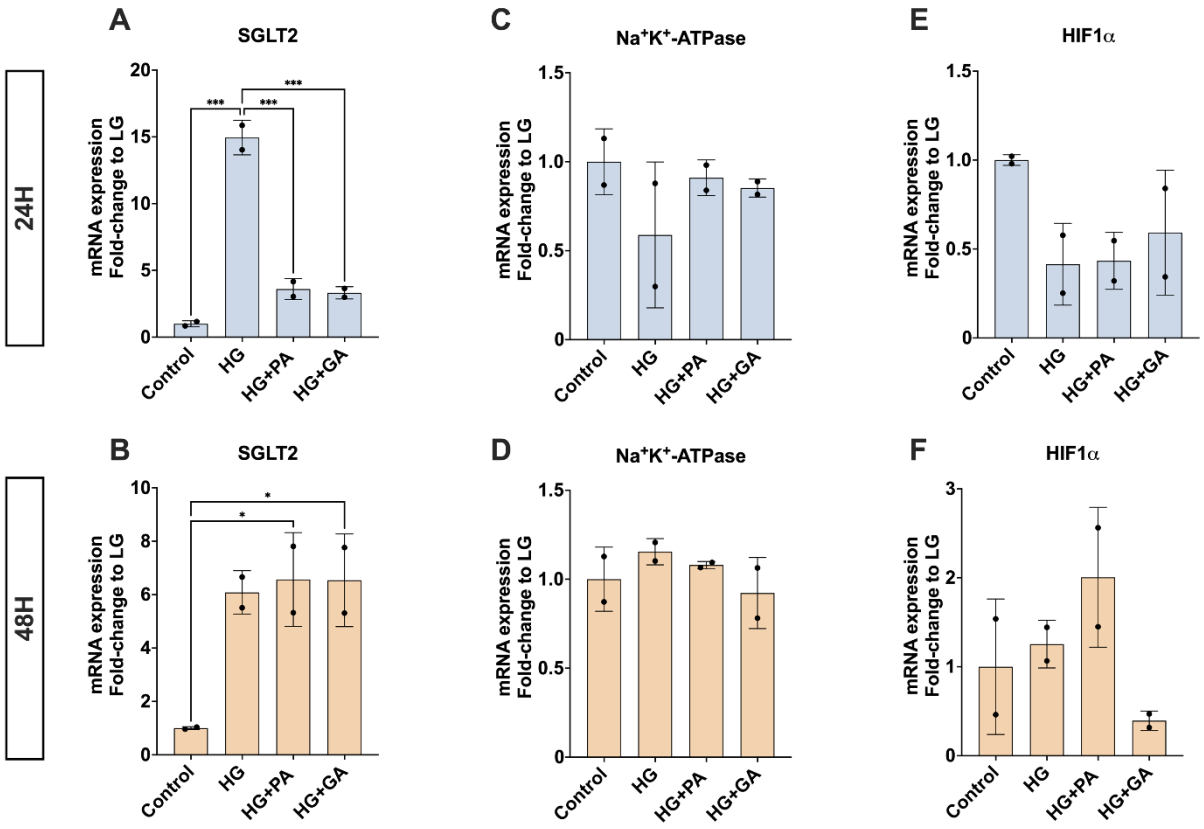

Figure 2. Gene expression analysis of (A-B) SGLT2, (C-D) Na^+K^+-ATPase, and (E-F) HIF1a upon exposure to diabetes conditions compared to control (low glucose), for 24h or 48 h. Data are shown as mean ± SD (n=2 in triplicate). Ordinary one-way ANOVA with Tukey's multiple comparisons test analysis performed (*p-value < 0.05). **Abbreviations**: **HG** – high glucose; **HG+PA** – high glucose supplemented with palmitic acid; **HG+GA** – high glucose supplemented with glycated albumin.

3.3. A Diabetic Microenvironment Influences Mitochondrial Dynamics by Increasing Mitochondrial Fusion and Fission

Alterations in mitochondrial dynamics are usually reflected by an imbalance in the fusion and fission processes along with suppressed mitophagy [18]. To understand these dynamics, we investigated the potential impact of PA and GA on mitochondrial dynamics. Initially, we assessed mitophagy, a selective form of autophagy targeting damaged/dysfunctional mitochondria [28]. The expression of the mitophagy marker PINK1 slightly increased in the diabetic groups, particularly in the HG+PA group, compared to control. This increase in mitophagy was evident at 24h (**Figure 3A**) and persisted at 48h (**Figure 3B**), indicating a higher level of mitophagy in these groups. Additionally, we delved into the impact of the diabetic microenvironment on mitochondrial fission and fusion processes. Mitochondrial fission is the process of segregating damaged mitochondria for removal, whereas

mitochondrial fusion maintains mitochondrial health [28]. We observed elevated gene expression levels of DRP1, a key player in mitochondrial fission. These increased levels were evident at both 24h **(Figure 3C**) and 48h (**Figure 3D**) for all diabetic conditions when compared to control. Notably, the HG+PA group exhibited the most pronounced increase in DRP1 expression, suggesting an increased degree of mitochondrial damage compared to HG alone. Interestingly, OPA1, a marker associated with mitochondrial fusion, also showed a non-significant increase in the diabetic groups at 24h **(Figure 3E**), with a significant increase at 48h (**Figure 3F**), with HG+PA again showing the highest expression. These observations suggest that within the diabetic microenvironment, cells respond to damage by regulating mitochondrial turnover, as evidenced by a slight increase in mitophagy and fission processes, particularly in the HG+PA group. This adaptive response might mitigate further damage, which aligns with the increase in mitochondrial fusion and the consistent levels of mitochondrial mass (**Figure 1G-H**).

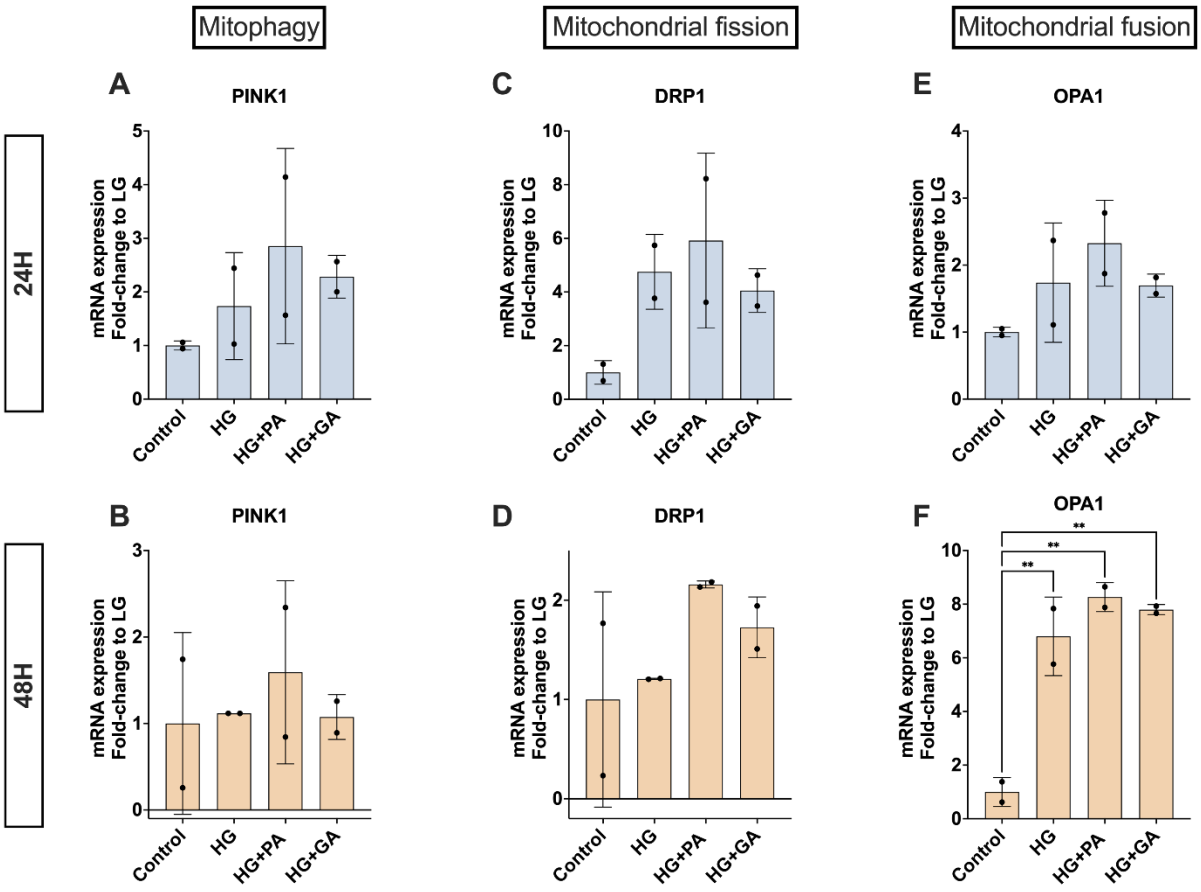

Figure 3. Gene expression analysis of (A-B) PINK1, a mitophagy marker, (C-D) DRP1, involved in mitochondrial fission, and (E-F) OPA1 a regulator of mitochondrial fusion, upon exposure to diabetes conditions compared to control (low glucose), for 24h or 48 h. Data are shown as mean ± SD (n=2, in triplicate). Ordinary one-way ANOVA with Tukey's multiple comparisons test analysis

performed (**p-value < 0.01). **Abbreviations**: **HG** – high glucose; **HG+PA** – high glucose supplemented with palmitic acid; **HG+GA** – high glucose supplemented with glycated albumin; **PINK**1, phosphatase and tensin homolog (PTEN)-induced kinase 1; **DRP1**, dynamin-related protein 1; **OPA1**, optic atrophy protein 1.

3.4. A Diabetic Microenvironment Decreases Oxygen Consumption and Extracellular Acidification Rates

Next, we conducted real-time measurements of OCR and ECAR. Our findings revealed a slight decrease in OCR levels in the diabetes conditions compared to control (**Figure 4A**), with HG+GA displaying the lowest OCR level amongst all conditions (**Figure 4A**). ECAR is an indicator of glycolysis, for which the levels showed a minor reduction in the diabetes conditions compared to control (**Figure 4B**). Subsequently, we examined various parameters of cellular respiration. Basal respiration, ATP-linked respiration, and maximal respiration were similar amongst all groups (**Figure 4C-F**). These data suggest that the diabetic groups did not compromise overall mitochondrial bioenergetics.

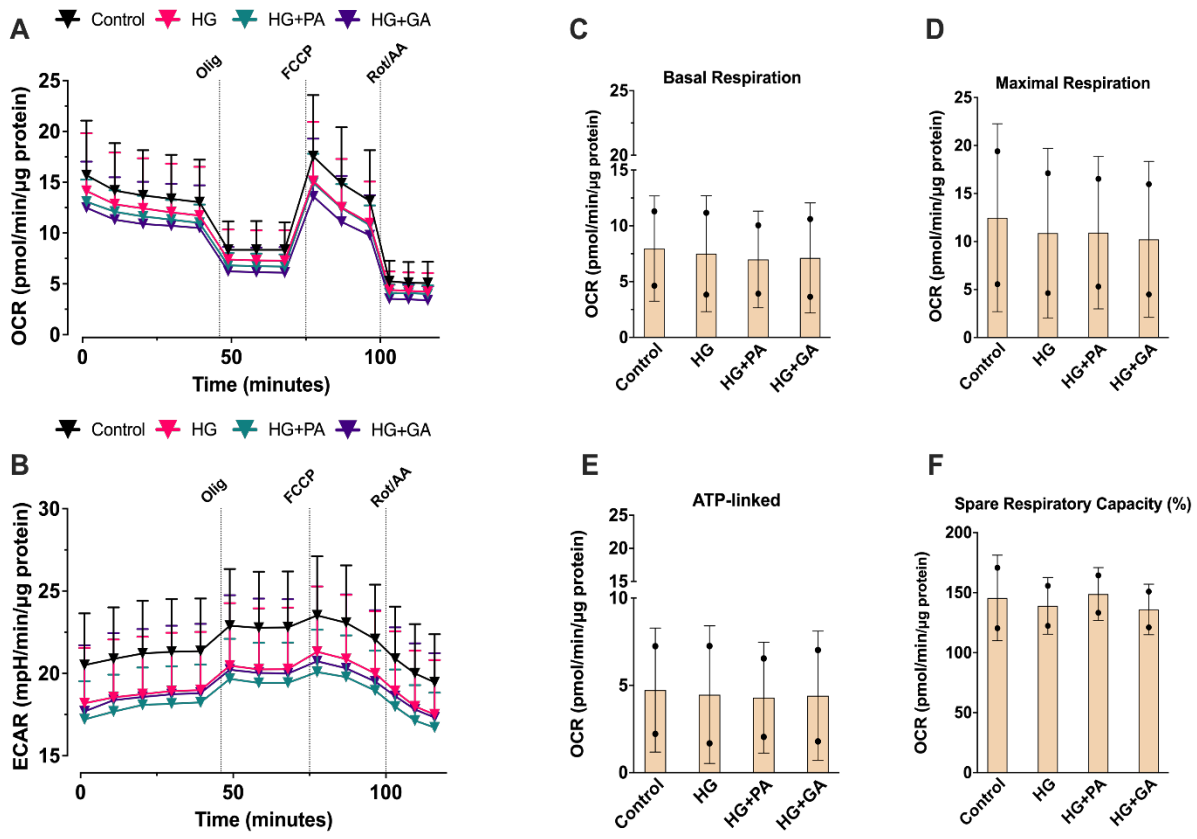

Figure 4. Bioenergetic profile of HK-2 cells exposed to diabetic conditions compared to control (low glucose), for 48h under hypoxia. (**A)** OCR and (**B**) ECAR levels measured before and after injections of oligomycin, FCCP, and rotenone/antimycin A. Specific parameters derived from OCR

levels, including (**C**) basal respiration**, (D**) maximal respiration, (**E**) ATP-linked respiration, and (**F**) spare respiratory capacity was plotted in bar graphs. Data are shown as mean ± SD (n=2, in quintuplicate). **Abbreviations**: **HG** – high glucose; **HG+PA** – high glucose supplemented with palmitic acid; **HG+GA** – high glucose supplemented with glycated albumin; **FCCP** – carbonyl cyanide-p-trifluoromethoxyphenylhydrazone; **olig** – oligomycin; **rot/AA** –rotenone/antimycin A.

3.5. The Diabetic Microenvironment Increases Intracellular Lipid Accumulation

Mitochondrial bioenergetics is tightly linked to lipid metabolism, and dyslipidemia is another hallmark of DKD [29]. Interestingly, we observed a time-dependent increase in the fluorescence intensity of BODIPY, a marker of neutral lipids, across all groups (**Figure 5A**). Notably, a non-significant increase in fluorescence intensity was seen in the diabetic conditions compared to control (**Figure 5A**). Importantly, quantification of the intensity also showed the same response (**Figure 5B-C**), however the effects were not to statistically significant, hence no conclusions could be drawn regarding lipid accumulation. Furthermore, we investigated the expression of the carnitine palmitoyltransferase 1A gene (*CPT1A*), a key player in fatty acid β-oxidation and export. At 24h, the diabetic conditions exhibited a slight decrease in *CPT1A* expression compared to the LG group (**Figure 5D**), whereas the opposite was found at 48h, with HG and HG+PA groups showing the highest *CPT1A* expression (**Figure 5E**). These findings suggest that this lipid accumulation can also be translated into an enhanced fatty acid oxidation to meet/counteract energy requirements.

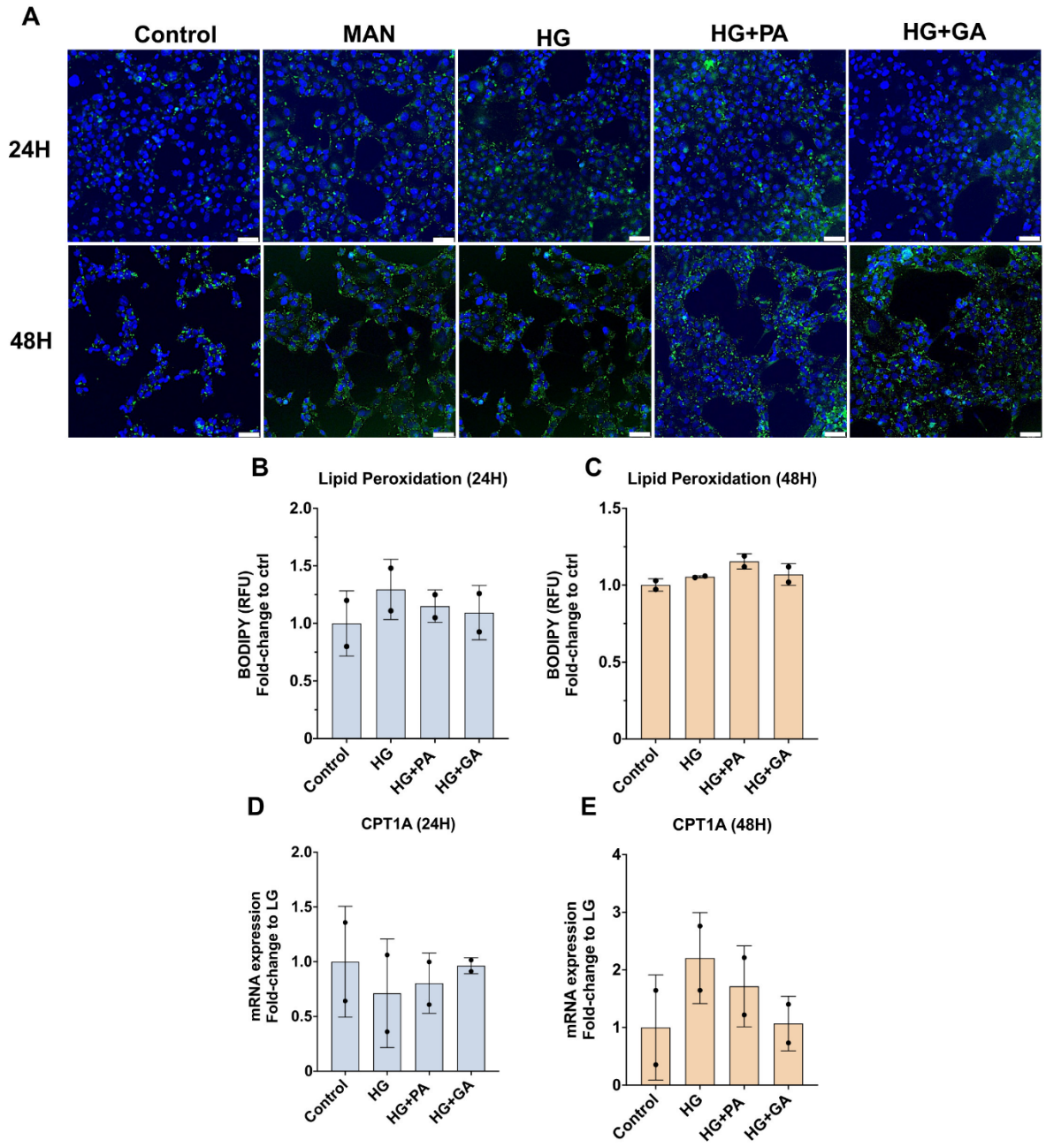

Figure 5. Assessment of lipid accumulation in HK-2 cells exposed to diabetic conditions under hypoxia. (**A**) Representative images of uptake of BODIPY by HK-2 cells exposed to diabetic conditions, compared to control (low glucose), under hypoxia for 24 h and 48 h. Scale bar: 50 μm. (**B-C**) Quantification of BODIPY uptake as a measure of lipid peroxidation. (**D-E**) qRT-PCR analysis of CPT1C, a marker involved in fatty acid β-oxidation and export. Data are shown as mean ± SD (n=2, in triplicate). **Abbreviations**: **MAN** – mannitol; **HG** – high glucose; **HG+PA** – high glucose supplemented with palmitic acid; **HG+GA** – high glucose supplemented with glycated albumin; **CPT1A**, carnitine palmitoyltransferase 1A.

3.6. Empagliflozin Reduces NGAL Secretion in Diabetic Conditions

To assess the potential role of SGLT2 inhibition in mitigating PT injury, we evaluated the effects of empagliflozin on mitochondrial health and release of kidney epithelial injury markers. HK-2 cells maintained in diabetic conditions for 48h were treated for an additional 24h with empagliflozin. Our results revealed that upon treatment, in all diabetes conditions, no differences in metabolic activity were observed (**Figure 6A**), and ATP production was unchanged (**Figure 6B**). We then assessed the effect of empagliflozin on ameliorating PT damage by assessing the levels of the injury markers KIM-1 and NGAL. Our findings showed a decrease in KIM-1 release in the HG group upon treatment with empagliflozin, but not in the other treated groups (**Figure 6C**). Similarly, empagliflozin treatment led to a significant decrease in NGAL secretion in the HG-GA group, and approaching statistical significance (p-value = 0.0597) in the HG group (**Figure 6D**). These findings suggest a recovering effect of empagliflozin, and a potential role of NGAL as an indicator to assess empagliflozin efficacy.

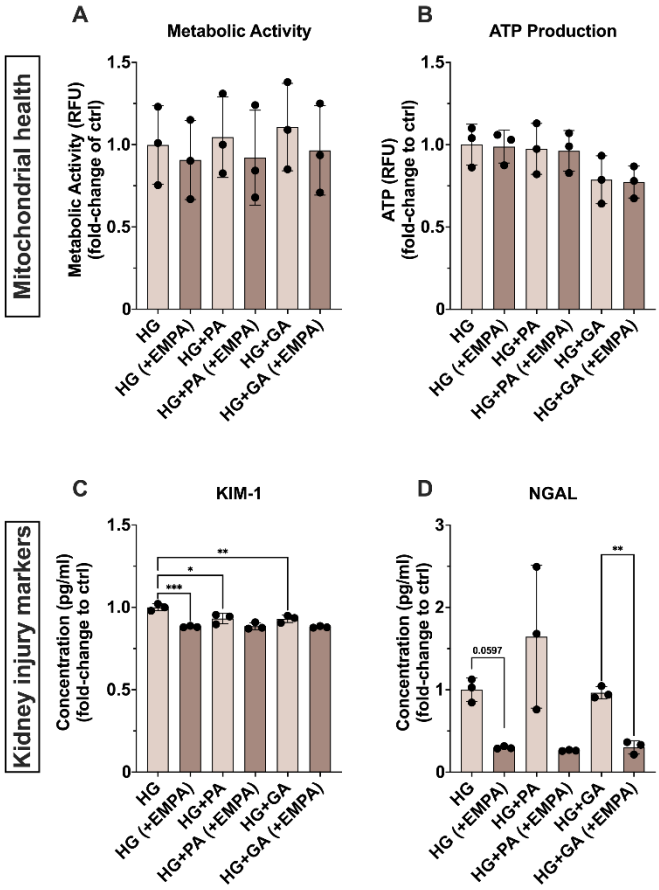

Figure 6. Evaluation of the impact of empagliflozin on diabetic PT cells. Upon exposure to diabetic conditions, HK-2 cells were treated with empagliflozin, and subsequently evaluated for mitochondrial dysfunction by measuring (**A**) metabolic activity, and (**B**) ATP production. Additionally, the release kidney epithelial injury markers, (**C**) KIM1 and (**D**) NGAL were quantified. Data are shown as mean ±

SD (n=3, in triplicate). Ordinary one-way ANOVA with (**C**) Tukey's and (**D**) Dunnet's multiple comparison's test analysis performed (*p-value < 0.05; **p-value < 0.01, *** p-value <0.001). **Abbreviations: HG** – high glucose; **HG+PA** – high glucose supplemented with palmitic acid; **HG+GA** – high glucose supplemented with glycated albumin; **EMPA**, empagliflozin; **KIM-1**, kidney injury molecule-1; **NGAL**, neutrophil gelatinase-associated lipocalin.

4. DISCUSSION

This study aimed to investigate the effects of fatty acids, specifically PA, and GA on PT injury under conditions of hypoxic hyperglycemia. Our findings revealed that addition of PA or GA led to an increase in morphological derangements compared to HG alone, with effects being most pronounced after 48h. However, while mitochondrial homeostasis and lipid accumulation were not significantly affected in this diabetic microenvironment, the addition of PA or GA resulted in alterations in mitochondrial dynamics. Furthermore, the diabetic conditions, particularly HG+PA, led to increase in NGAL secretion, an injury marker, which was reversed by SGLT2 inhibitor, empagliflozin, indicating its potential protective effect in mitigating kidney injury.

The detrimental effects of HG on cellular function, such as oxidative stress and impaired energy metabolism, can contribute to the disruption of the cell monolayer integrity [30, 31]. In our study, we observed similar disruptions in cell monolayer under all diabetic conditions, which were evident predominantly after 48h of exposure in the HG+PA and HG+GA groups. The addition of PA, associated with cellular dysfunction [32], and GA, known to potentiate cellular stress [19], most likely led to disruption of the cell monolayer as observed. Furthermore, apoptosis has been associated with changes in cell morphology [33-36], hence assessing the effects of PA and GA on apoptosis should be addressed in future studies.

Mitochondria are prone to degradation through mitophagy due to increased fragmentation, a result of excessive mitochondrial fission, and disrupted bioenergetics [37]. While mitophagy aids in maintaining mitochondrial quality, it also contributes to mitochondrial mass reduction [38]. In the kidney, the PT has the highest mitophagy rate in the nephron, an indication of high mitochondrial turnover [39]. This partly explains why the PT is highly susceptible to injury. Our findings show that diabetic conditions, in particular exposure to HG+PA, led to a slight increase in mitophagy and fission processes, an indication of mitochondrial turnover, as well as an increase in mitochondrial fusion. These results suggest an adaptive response aimed at maintaining mitochondrial quality and cellular homeostasis during injury. However, for a more comprehensive assessment of these processes, the analysis with electron microscopy images to examine mitochondrial morphology should be taken along. Furthermore, evaluating mitochondrial membrane potential, assessing the enzyme activity of the mitochondrial respiratory complexes, and quantifying mitochondrial DNA should also be included as important indicators of mitochondrial health. Mitophagy is highly dependent on mitochondrial membrane potential [40], an interplay shown in HK-2 cells exposed HG in which both membrane potential and mitophagy levels were reduced [41]. In the current study, despite the changes observed in mitochondrial dynamics, variations in

mitochondrial mass and ATP production were not found. Another study also demonstrated that there were no differences in ATP production between the LG and HG groups [42]. This suggests a compensatory mechanism aimed at maintaining ATP levels. Several possibilities can account for this: 1) The increase in mitochondrial fusion, through exchanging functional components, can potentially allow preservation of ATP synthesis; 2) other metabolic pathways, such as glycolysis, may be upregulated to compensate for the reduced OXPHOS capacity. An increase in lactate/pyruvate ratio is often used as direct association with a shift towards anaerobic glycolysis [43]. Moreover, lactate production is tightly connected to NADH/NAD+ homeostasis [43], hence these measurements will help to properly assess cellular redox state. Aiding to the possibility of a metabolic switch in our diabetic conditions, thorough metabolomics [10] and transcriptomic [11] studies were performed with HK-2 cells exposed to HG and hypoxia. These studies concluded that several proteins and intracellular metabolites involved in glycolysis were upregulated [10, 11]; 3) Impaired mitochondrial biogenesis, as this process is essential for maintaining mitochondrial mass and bioenergetic output [37]. Mitochondrial biogenesis is tightly regulated by peroxisome proliferator-activated receptor γ (PPARγ)-coactivator 1α (PGC1α), whose decreased expression has been associated with DKD progression. Sharma, *et al*., using urine metabolomics, demonstrated that DKD patients showed a decrease in both mitochondrial protein and mitochondrial DNA content [44], which could indicate a decrease in mitochondrial biogenesis. Moreover, another study using HK-2 cells showed that reduced PGC-1α expression led to mitochondrial fragmentation [45], whereas Kang, *et al*. demonstrated that *in vitro* overexpression of PGC-1α protected PT cells from tubulointerstitial fibrosis by reducing ATP consumption and restoring FA oxidation [46]. These findings suggest that for future studies, the process of mitochondrial biogenesis should be investigated by evaluating PGC1α expression in our diabetic conditions.

The accumulation of lipid intermediates, known to potentially contribute to mitochondrial dysfunction, was found similar across diabetic conditions, and even in the control (LG) group. The latter could be explained by the hypoxic microenvironment used in our experimental conditions which has been associated with lipid accumulation [47, 48]. Nevertheless, further investigation is required to elucidate the role of lipid accumulation within the diabetic microenvironment. In support of this, a lipidomic study demonstrated a decrease in cardiolipin levels, located in the inner mitochondrial membrane, in HK-2 cells exposed to high glucose [49]. Cardiolipin plays a role in maintaining mitochondrial structure, hence its reduced levels were associated with mitochondrial dysfunction [49]. Furthermore, Zhang *et al*. showed that cardiolipin is crucial for maintaining mitochondrial function in mice with type I diabetes [50].

For future studies, a comprehensive assessment of the lipid profile of diabetic HK-2 cells should be assessed to gain insights into the influence of lipids on overall mitochondrial dysfunction.

In response to hypoxia, HIF-1α expression is known to increase [51, 52], however, our results revealed a first decrease at 24h in all diabetic conditions which was reversed at 48h. The initial decrease of HIF-1α at 24h can be explained by (1) increased prolyl hydrolylases (PHD) activity, enzymes responsible for HIF-1α degradation, (2) activation of protein kinase C pathway, or (3) impaired oxygen utilization due a disrupted metabolic state and OXPHOS activity. While we did not directly investigate the first two explanations, the increased mitochondrial dynamics found in our conditions has been linked to the increased HIF-1α expression [53-55]. The other possible conclusions have been validated in *in vitro* studies of HK-2 cells exposed to HG and hypoxia [51, 56, 57], suggesting that supplementation of the hypoxic hyperglycemic state further triggers changes in the cell that affect the downstream signaling cascade associated with HIF-1α stabilization and transcriptional activity. However, the increase found at 48h could be an indication of disease progression. Several studies have shown that increased levels of HIF-1α are associated with kidney structural and morphological damage [58-60], which correlates with our morphological findings. For this reason, further analysis is required to fully understand the results obtained, including the quantification of the protein levels of HIF-1α, and the analysis of HIF-1α regulators (*e.g.*, PHD activity).

Upon assessing the effects of our diabetic conditions in overall mitochondrial dysfunction, as a proof of concept, we investigated the effect of empagliflozin, a SGLT2 inhibitor, on cell metabolism and secretion of kidney epithelial injury markers. Notably, no changes in KIM-1, predominantly found in PTCs, were found following empagliflozin treatment. These findings suggest that HK-2 cells may not be sensitive enough to detect KIM-1 changes as opposed to primary cells or other PT cell lines [61, 62]. Interestingly, a consistent decrease in NGAL secretion was observed in all treated groups, indicating the restoring effect of empagliflozin in ameliorating PT damage.

Nonetheless, this study has certain limitations that should be addressed. First, HK-2 cells have phenotypic differences compared to native PTCs. HK-2 cells exhibit high glycolytic and gluconeogenic activities even at basal level [63-66], whereas native PTCs predominantly rely on oxidative metabolism [2, 67, 68]. Despite this disparity, in DKD the glycolytic flux is found to play a role in disease progression [69], hence the results found in this study might still be pathologically relevant. Another limitation is the lack of expression of several drug transporters and metabolizing enzymes which limits the capacity of this cell line for nephrotoxicity testing [61, 62]. However, HK-2 cells do express glucose transporters, which are important for

studying DKD and account for the majority of published studies in this field. On the other hand, the conventional 2D cell culture model for HK-2 cells restricts the accurate representation of the diabetic microenvironment [70, 71]. To address this, enhancing the complexity of the model by incorporating extracellular matrix components, fluid flow, and other cell types (*e.g.*, endothelial and immune cells) will complement the obtained results [72-74]. Wang *et al.* have developed a 3D microfluidic model utilizing an organ-on-chip platform with glomerular endothelial cells and podocytes that were cultured under flow conditions, and successfully replicating the high-glucose induced injury phenotype found in humans [75]. Integrating PTCs in such models could yield valuable insights into the development of DKD and serve as a drug testing platform.

In summary, our *in vitro* model addresses the impact of PA and GA in context of DKD pathophysiology. Importantly, our findings draw attention to PA as a notable contributor to injury. Specifically, we observed that PA increased mitochondrial turnover and NGAL secretion, with the latter prevented by selective SGLT2 inhibition. These findings underscore the importance of considering PA as a key player in driving DKD progression.

SUPPLEMENTARY MATERIALS

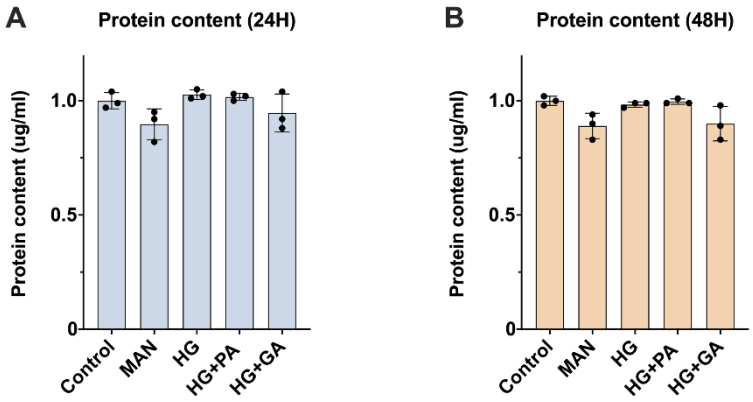

Supplementary Figure S1. Protein content of HK-2 cells exposed to diabetic conditions compared to control (low glucose) for (A) 24h and (B) 48h.

Supplementary Table S1. Primer list.

Gene	Primer sequence (5'-3')	Annealing Temperature (°C)
PINK1	Forward: GCCTCATCGAGGAAAAACAGG Reverse: GTCTCGTGTCCAACGGGTC	60
DRP1	Forward: TTTGACACTTGTGGATTTGCCA Reverse: AGTGACAGCGAGGATAATGGA	60
OPA1	Forward: AGCCTCGCAGGAATTTTTGG Reverse: AGCCGATCCTAGTATGAGATAGC	60
CPT1A	Forward: CGGGAGGAAATCAAACCAATT Reverse: GGGATCCGGGAAGTATTAAACAT	60
HPRT1	Forward: ACATCTGGAGTCCTATTGACATCG Reverse: CCGCCCAAAGGGAACTGATAG	60

REFERENCES

1. S. Hussain, M. Chand Jamali, A. Habib*, et al.* Diabetic kidney disease: An overview of prevalence, risk factors, and biomarkers. Clinical Epidemiology and Global Health 2021;9:2-6
2. V. Vallon. The proximal tubule in the pathophysiology of the diabetic kidney. Am J Physiol Regul Integr Comp Physiol 2011;300(5):R1009-1022
3. A. C. Hesp, J. A. Schaub, P. V. Prasad*, et al.* The role of renal hypoxia in the pathogenesis of diabetic kidney disease: a promising target for newer renoprotective agents including SGLT2 inhibitors? Kidney Int 2020;98(3):579-589
4. D. K. Singh, P. Winocour and K. Farrington. Mechanisms of disease: the hypoxic tubular hypothesis of diabetic nephropathy. Nat Clin Pract Nephrol 2008;4(4):216-226
5. R. G. Amorim, G. D. S. Guedes, S. M. L. Vasconcelos*, et al.* Kidney Disease in Diabetes Mellitus: Cross-Linking between Hyperglycemia, Redox Imbalance and Inflammation. Arq Bras Cardiol 2019;112(5):577-587
6. C. Vinovskis, L. P. Li, P. Prasad*, et al.* Relative Hypoxia and Early Diabetic Kidney Disease in Type 1 Diabetes. Diabetes 2020;69(12):2700-2708
7. W. Luo, S. Tang, X. Xiao*, et al.* Translation Animal Models of Diabetic Kidney Disease: Biochemical and Histological Phenotypes, Advantages and Limitations. Diabetes Metab Syndr Obes 2023;16:1297-1321
8. F. E. Sembach, M. V. Ostergaard, N. Vrang*, et al.* Rodent models of diabetic kidney disease: human translatability and preclinical validity. Drug Discov Today 2021;26(1):200-217
9. A. Giralt-Lopez, M. Molina-Van den Bosch, A. Vergara*, et al.* Revisiting Experimental Models of Diabetic Nephropathy. Int J Mol Sci 2020;21(10)
10. A. Valdes, F. J. Lucio-Cazana, M. Castro-Puyana*, et al.* Comprehensive metabolomic study of the response of HK-2 cells to hyperglycemic hypoxic diabetic-like milieu. Sci Rep 2021;11(1):5058
11. A. Valdes, M. Castro-Puyana, C. Garcia-Pastor*, et al.* Time-series proteomic study of the response of HK-2 cells to hyperglycemic, hypoxic diabetic-like milieu. PLoS One 2020;15(6):e0235118
12. S. Sumual, S. Saad, O. Tang*, et al.* Differential regulation of Snail by hypoxia and hyperglycemia in human proximal tubule cells. Int J Biochem Cell Biol 2010;42(10):1689-1697
13. A. Owczarek, K. B. Gieczewska, R. Jarzyna*, et al.* Transcription Factor ChREBP Mediates High Glucose-Evoked Increase in HIF-1alpha Content in Epithelial Cells of Renal Proximal Tubules. Int J Mol Sci 2021;22(24)
14. N. Jiang, H. Zhao, Y. Han*, et al.* HIF-1alpha ameliorates tubular injury in diabetic nephropathy via HO-1-mediated control of mitochondrial dynamics. Cell Prolif 2020;53(11):e12909
15. X. Liang, D. M. Potenza, A. Brenna*, et al.* Hypoxia Induces Renal Epithelial Injury and Activates Fibrotic Signaling Through Up-Regulation of Arginase-II. Front Physiol 2021;12:773719
16. S. Bouatra, F. Aziat, R. Mandal*, et al.* The human urine metabolome. PLoS One 2013;8(9):e73076
17. L. Opazo-Rios, S. Mas, G. Marin-Royo*, et al.* Lipotoxicity and Diabetic Nephropathy: Novel Mechanistic Insights and Therapeutic Opportunities. Int J Mol Sci 2020;21(7)
18. P. Narongkiatikhun, S. C. Chattipakorn and N. Chattipakorn. Mitochondrial dynamics and diabetic kidney disease: Missing pieces for the puzzle of therapeutic approaches. J Cell Mol Med 2022;26(2):249-273
19. C. M. Zheng, W. Y. Ma, C. C. Wu*, et al.* Glycated albumin in diabetic patients with chronic kidney disease. Clin Chim Acta 2012;413(19-20):1555-1561

20. R. V. Giglio, B. Lo Sasso, L. Agnello*, et al.* Recent Updates and Advances in the Use of Glycated Albumin for the Diagnosis and Monitoring of Diabetes and Renal, Cerebro- and Cardio-Metabolic Diseases. J Clin Med 2020;9(11)
21. M. P. Cohen, E. Shea, S. Chen*, et al.* Glycated albumin increases oxidative stress, activates NF-kappa B and extracellular signal-regulated kinase (ERK), and stimulates ERK-dependent transforming growth factor-beta 1 production in macrophage RAW cells. J Lab Clin Med 2003;141(4):242-249
22. Y. Hou, Q. Wang, B. Han*, et al.* CD36 promotes NLRP3 inflammasome activation via the mtROS pathway in renal tubular epithelial cells of diabetic kidneys. Cell Death Dis 2021;12(6):523
23. Y. Sun, X. Ge, X. Li*, et al.* High-fat diet promotes renal injury by inducing oxidative stress and mitochondrial dysfunction. Cell Death Dis 2020;11(10):914
24. W. C. Lee, Y. Y. Chau, H. Y. Ng*, et al.* Empagliflozin Protects HK-2 Cells from High Glucose-Mediated Injuries via a Mitochondrial Mechanism. Cells 2019;8(9)
25. X. Gu, Y. Ma, Y. Liu*, et al.* Measurement of mitochondrial respiration in adherent cells by Seahorse XF96 Cell Mito Stress Test. STAR Protoc 2021;2(1):100245
26. J. Liu, J. Tian, K. Sodhi*, et al.* The Na/K-ATPase Signaling and SGLT2 Inhibitor-Mediated Cardiorenal Protection: A Crossed Road? J Membr Biol 2021;254(5-6):513-529
27. G. L. Semenza. HIF-1: mediator of physiological and pathophysiological responses to hypoxia. J Appl Physiol (1985) 2000;88(4):1474-1480
28. B. Westermann. Mitochondrial fusion and fission in cell life and death. Nat Rev Mol Cell Biol 2010;11(12):872-884
29. P. H. Lin and P. Duann. Dyslipidemia in Kidney Disorders: Perspectives on Mitochondria Homeostasis and Therapeutic Opportunities. Front Physiol 2020;11:1050
30. S. H. Park, H. J. Choi, J. H. Lee*, et al.* High glucose inhibits renal proximal tubule cell proliferation and involves PKC, oxidative stress, and TGF-beta 1. Kidney Int 2001;59(5):1695-1705
31. M. N. Islam, T. P. Griffin, E. Sander*, et al.* Human mesenchymal stromal cells broadly modulate high glucose-induced inflammatory responses of renal proximal tubular cell monolayers. Stem Cell Res Ther 2019;10(1):329
32. A. Mitrofanova, G. Burke, S. Merscher*, et al.* New insights into renal lipid dysmetabolism in diabetic kidney disease. World J Diabetes 2021;12(5):524-540
33. B. J. Padanilam. Cell death induced by acute renal injury: a perspective on the contributions of apoptosis and necrosis. Am J Physiol Renal Physiol 2003;284(4):F608-627
34. A. Ortiz, C. Lorz, P. Justo*, et al.* Contribution of apoptotic cell death to renal injury. J Cell Mol Med 2001;5(1):18-32
35. S. Bamri-Ezzine, Z. J. Ao, I. Londono*, et al.* Apoptosis of tubular epithelial cells in glycogen nephrosis during diabetes. Lab Invest 2003;83(7):1069-1080
36. G. Priante, L. Gianesello, M. Ceol*, et al.* Cell Death in the Kidney. Int J Mol Sci 2019;20(14)
37. P. Bhargava and R. G. Schnellmann. Mitochondrial energetics in the kidney. Nat Rev Nephrol 2017;13(10):629-646
38. M. J. Livingston, J. Wang, J. Zhou*, et al.* Clearance of damaged mitochondria via mitophagy is important to the protective effect of ischemic preconditioning in kidneys. Autophagy 2019;15(12):2142-2162
39. D. Bhatia and M. E. Choi. The Emerging Role of Mitophagy in Kidney Diseases. J Life Sci (Westlake Village) 2019;1(3):13-22
40. A. Hamacher-Brady and N. R. Brady. Mitophagy programs: mechanisms and physiological implications of mitochondrial targeting by autophagy. Cell Mol Life Sci 2016;73(4):775-795

41. Y. Y. Yang, D. J. Gong, J. J. Zhang*, et al.* Diabetes aggravates renal ischemia-reperfusion injury by repressing mitochondrial function and PINK1/Parkin-mediated mitophagy. Am J Physiol Renal Physiol 2019;317(4):F852-F864
42. W.-C. Lee, Y.-Y. Chau, H.-Y. Ng*, et al.* Empagliflozin Protects HK-2 Cells from High Glucose-Mediated Injuries via a Mitochondrial Mechanism. Cells 2019;8(9):1085
43. X. Li, Y. Yang, B. Zhang*, et al.* Lactate metabolism in human health and disease. Signal Transduct Target Ther 2022;7(1):305
44. K. Sharma, B. Karl, A. V. Mathew*, et al.* Metabolomics reveals signature of mitochondrial dysfunction in diabetic kidney disease. J Am Soc Nephrol 2013;24(11):1901-1912
45. H. Y. Jeong, J. M. Kang, H. H. Jun*, et al.* Chloroquine and amodiaquine enhance AMPK phosphorylation and improve mitochondrial fragmentation in diabetic tubulopathy. Sci Rep 2018;8(1):8774
46. H. M. Kang, S. H. Ahn, P. Choi*, et al.* Defective fatty acid oxidation in renal tubular epithelial cells has a key role in kidney fibrosis development. Nat Med 2015;21(1):37-46
47. I. Mylonis, H. Sembongi, C. Befani*, et al.* Hypoxia causes triglyceride accumulation by HIF-1-mediated stimulation of lipin 1 expression. J Cell Sci 2012;125(Pt 14):3485-3493
48. G. Schley, S. Grampp and M. Goppelt-Struebe. Inhibition of oxygen-sensing prolyl hydroxylases increases lipid accumulation in human primary tubular epithelial cells without inducing ER stress. Cell Tissue Res 2020;381(1):125-140
49. C. Garcia-Pastor, S. Benito-Martinez, V. Moreno-Manzano*, et al.* Mechanism and Consequences of The Impaired Hif-1alpha Response to Hypoxia in Human Proximal Tubular HK-2 Cells Exposed to High Glucose. Sci Rep 2019;9(1):15868
50. S. Koyasu, M. Kobayashi, Y. Goto*, et al.* Regulatory mechanisms of hypoxia-inducible factor 1 activity: Two decades of knowledge. Cancer Sci 2018;109(3):560-571
51. X. Huang, L. Zhao and R. Peng. Hypoxia-Inducible Factor 1 and Mitochondria: An Intimate Connection. Biomolecules 2022;13(1)
52. M. W. van Gisbergen, K. Offermans, A. M. Voets*, et al.* Mitochondrial Dysfunction Inhibits Hypoxia-Induced HIF-1alpha Stabilization and Expression of Its Downstream Targets. Front Oncol 2020;10:770
53. X. Zheng, S. Narayanan, C. Xu*, et al.* Repression of hypoxia-inducible factor-1 contributes to increased mitochondrial reactive oxygen species production in diabetes. Elife 2022;11
54. H. Noh and G. L. King. The role of protein kinase C activation in diabetic nephropathy. Kidney Int Suppl 2007(106):S49-53
55. E. Temes, S. Martin-Puig, J. Aragones*, et al.* Role of diacylglycerol induced by hypoxia in the regulation of HIF-1alpha activity. Biochem Biophys Res Commun 2004;315(1):44-50
56. D. F. Higgins, K. Kimura, W. M. Bernhardt*, et al.* Hypoxia promotes fibrogenesis in vivo via HIF-1 stimulation of epithelial-to-mesenchymal transition. J Clin Invest 2007;117(12):3810-3820
57. T. W. Hung, J. H. Liou, K. T. Yeh*, et al.* Renal expression of hypoxia inducible factor-1alpha in patients with chronic kidney disease: a clinicopathologic study from nephrectomized kidneys. Indian J Med Res 2013;137(1):102-110
58. M. K. Dallatu, M. Choi and A. O. Oyekan. Inhibition of prolyl hydroxylase domain-containing protein on hypertension/renal injury induced by high salt diet and nitric oxide withdrawal. J Hypertens 2013;31(10):2043-2049
59. S. E. Jenkinson, G. W. Chung, E. van Loon*, et al.* The limitations of renal epithelial cell line HK-2 as a model of drug transporter expression and function in the proximal tubule. Pflugers Arch 2012;464(6):601-611

60. J. Faria, S. Ahmed, K. G. F. Gerritsen*, et al.* Kidney-based in vitro models for drug-induced toxicity testing. Arch Toxicol 2019;93(12):3397-3418
61. A. Czajka and A. N. Malik. Hyperglycemia induced damage to mitochondrial respiration in renal mesangial and tubular cells: Implications for diabetic nephropathy. Redox Biol 2016;10:100-107
62. R. A. Zager, A. C. Johnson and S. Y. Hanson. Proximal tubular cholesterol loading after mitochondrial, but not glycolytic, blockade. Am J Physiol Renal Physiol 2003;285(6):F1092-1099
63. L. Li, H. Zhao, B. Chen*, et al.* FXR activation alleviates tacrolimus-induced post-transplant diabetes mellitus by regulating renal gluconeogenesis and glucose uptake. J Transl Med 2019;17(1):418
64. M. Sasaki, T. Sasako, N. Kubota*, et al.* Dual Regulation of Gluconeogenesis by Insulin and Glucose in the Proximal Tubules of the Kidney. Diabetes 2017;66(9):2339-2350
65. W. G. Guder, S. Wagner and G. Wirthensohn. Metabolic fuels along the nephron: pathways and intracellular mechanisms of interaction. Kidney Int 1986;29(1):41-45
66. J. A. Schaub, M. A. Venkatachalam and J. M. Weinberg. Proximal Tubular Oxidative Metabolism in Acute Kidney Injury and the Transition to CKD. Kidney360 2021;2(2):355-364
67. K. M. Sas, P. Kayampilly, J. Byun*, et al.* Tissue-specific metabolic reprogramming drives nutrient flux in diabetic complications. JCI Insight 2016;1(15):e86976
68. J. Faria, K. G. F. Gerritsen, T. Q. Nguyen*, et al.* Diabetic proximal tubulopathy: Can we mimic the disease for in vitro screening of SGLT inhibitors? Eur J Pharmacol 2021;908:174378
69. J. Slyne, C. Slattery, T. McMorrow*, et al.* New developments concerning the proximal tubule in diabetic nephropathy: in vitro models and mechanisms. Nephrol Dial Transplant 2015;30 Suppl 4:iv60-67
70. A. Tsakmaki, P. Fonseca Pedro and G. A. Bewick. Diabetes through a 3D lens: organoid models. Diabetologia 2020;63(6):1093-1102
71. H. Wang, T. Zhang, A. Cardilla*, et al.* WCN23-0535 HUMAN STEM CELL-DERIVED KIDNEY ORGANOID TO MODEL DIABETIC NEPHROPATHY. Kidney International Reports 2023;8(3, Supplement):S215
72. V. Palau, B. Nugraha, M. Emmert*, et al.* SO026HUMAN KIDNEY PROXIMAL TUBULAR 3D SPHEROIDS TO STUDY THE ROLE OF ADAM17 IN DIABETIC NEPHROPATHY. Nephrology Dialysis Transplantation 2020;35(Supplement_3)
73. L. Wang, T. Tao, W. Su*, et al.* A disease model of diabetic nephropathy in a glomerulus-on-a-chip microdevice. Lab Chip 2017;17(10):1749-1760

CHAPTER 8

Summary and General discussion

The proximal tubule (PT), a vital component of the renal system, plays a crucial role in CKD progression as it actively participates in both the secretion and reabsorption of many exogenous and endogenous compounds, making it highly susceptible to injury.

This thesis research focused on the factors that render the PT vulnerable to injury, with a particular focus on uremic toxins, ischemia and hyperglycemia. It is important to note that animal models, while valuable, do not always faithfully replicate clinical findings. To address this, *in vitro* models could offer a simpler and faster means of screening disease mediators involved in CKD progression, thus allowing for the development of targeted therapies. The goal of this thesis was to **uncover the intricate interactions between the PT and disease mediators through the development and application of *in vitro* models**. For this, we extensively reviewed the currently available PT *in vitro* models, followed by the application of a series of *in vitro* PT models designed to address the factors contributing to injury. Our initial focus was on understanding the interactions between uremic toxins (UTs), particularly those bound to albumin (PBUTs), and drugs prescribed for treatment of CKD complications. Notably, our findings revealed that certain drugs, including angiotensin receptor blockers and the diuretic, furosemide, may inadvertently compromise PBUTs uptake, thus leading to their accumulation and kidney function deterioration. Additionally, this finding has implications in the efficacy of the bioartificial kidney (BAK), designed to complement conventional dialysis by removing PBUTs. To advance its clinical application, we investigated the performance of a BAK functional unit in conditions that mimic dialysis. Our results showed that dialysis fluid, a solution used in dialysis to aid waste product removal and maintain patients' electrolyte levels, is cytocompatible with the BAK-containing cells and does not interfere with PBUTs clearance.

Furthermore, given the high mitochondrial density found in PT required for ATP production needed for transport and metabolism functions, we explored the implications of impaired mitochondrial function, as a result of ischemia and hyperglycemia. In response to this damage, we employed therapeutic strategies, including stem cell therapy and diabetes medication. Our findings showcase that stem cell therapy successfully restored the bioenergetic profile of ischemic PT cells, while a diabetes drug effectively reduced the secretion of kidney injury markers. This chapter delves into the implications of these findings and places them in the perspective of future research.

1. REFINING PROXIMAL TUBULE CELL MODELS FOR KIDNEY RESEARCH

The PT is primarily involved in the reabsorption of the majority of solutes from the glomerular filtrate, including glucose, albumin, amino acids, and various electrolytes. Secondly, the PT is a major site for the metabolism and excretion of xenobiotics. Despite their importance in homeostasis, these functions can equally trigger defects in the PT due to their role in the accumulation of solutes and/or their metabolites [1]. Consequently, interest in developing models that can effectively unravel how disease factors impact PT function has arisen. Notably, *in vitro* models offer a valuable tool for gaining a comprehensive mechanistic insight of how disease factors impact PT function, surpassing the inherent complexity and challenges associated with *in vivo* models. Such insights are instrumental in evaluating mediators of disease progression, thereby facilitating the development of therapeutic interventions for CKD.

Within this context, **Chapter 2** and **Chapter 6** provide a comprehensive overview of various PT *in vitro* models, spanning from primary cell cultures to organoids and organ-on-chip systems. These chapters highlight that a suitable PT model for either drug toxicity testing (**Chapter 2**) or diabetic kidney disease research (DKD) (**Chapter 6**) should have the following characteristics: 1) intricate structural and functional resemblance to the native PT, entailing a comprehensive array of transporters, incorporating extracellular matrix (ECM) components, and the presence of different cell types (*e.g.,* endothelial and immune cells); 2) dynamic traits, facilitated by the incorporation of fluid flow, solute transport dynamics, and the cellular responses to insults; 3) reproducibility, and 4) translatability, important for the development of new drugs and therapies for kidney disease. **Table 1** shows a comparison between different *in vitro* PT models used in research. For further details on the distinctive characteristics of each PT model, we refer readers to **Table 3** in **Chapter 2** [2].

Table 1. Different levels of complexity in which PT *in vitro* models are used in research in comparison to animal models (*in vivo*).

	2D culture	Organoids	Organ-on-chip	*In vivo*
Ease of use	+++	++	++	+
Throughput	+++	+++	++	+
Human relevance	Basic	Intermediate	Advanced	Translational
Stromal cues	x	+	++	+++
Fluid flow	x	x	++	+++
Drug toxicity	+	++	+++	+++
Time to result	Minutes-Hours	Hours-Days	Days	Weeks-Months
Cost	$	$$	$$	$$$$
Data content	Low	Medium	HIgh	High

***+**: possible; **++**: suitable; **+++**: best; **$** - cheap-to-moderate; **$$** - expensive; **$$$** - very expensive; **x**: not suitable*

Human primary cells, while retaining native PT morphology and function, are difficult to obtain and isolate and demonstrate a gradual loss of functionality in culture with limited proliferative potential. To address these issues, researchers pursued to immortalize primary cells, facilitating indefinite culture while retaining (some) functional and morphological (*e.g.*, cobblestone morphology) characteristics. Additionally, albeit lack of important transporters, genetic manipulations can enrich the cells' functional profile with (multiple) transporters of interest, thus expanding their utility in kidney research. Of note, conditionally immortalized proximal tubule epithelial cell (ciPTEC) and renal PTEC immortalized using human telomerase (RPTEC/TERT1) are two immortalized cell lines that have been modified to overexpress organic anion transporter 1 and 3 (OAT1/3; in ciPTECs [3] and RPTEC/TERT1 [4]) and organic cation transporter 2 (OCT2; in RPTEC/TERT1 [4]). The expression of these important drug transporters allows for their study in drug disposition and their interaction with inhibitors, important for predicting renal drug clearance and drug-drug interactions (explored in **Chapter 3 and 4**). However, the overexpression of uptake transporters may lead to false positive results in drug toxicity studies when efflux transporters are expressed at a reduced level than that reported in humans, thus leading to higher drug accumulation than seen *in vivo*. An alternative approach for generating PTECs is to derive them from stem cells, such as induced pluripotent stem cells (iPSCs) or adult stem cells (ASCs), leading to the generation of 3D structures containing multiple kidney-specific cell types, among which PTECs, that better replicate organ organization, cellular distribution and function, named organoids [5]. While iPSC-derived organoids comprise different parts of the nephron, ASC-derived organoids, termed tubuloids, mainly represent the tubular compartment [6]. Using patient-derived cells or genome-editing technologies, such as CRISPR/Cas9, researchers can delve into the pathophysiological mechanisms of diseases and develop effective therapies. IPSC-derived organoids have been successfully modified to model diseases, such as cystinosis [7], nephrotic syndrome [8-10], nephronophthisis [11], and diabetes [12]. Despite this, iPSC-derived organoids remain primitive in their feature, as they resemble the embryonic state of kidney development, while tubuloids exhibit a more mature phenotype, though not comparable to the native PT. However, tubuloids have, as of yet, not successfully been employed for gene editing, but proven successful in modeling several diseases, including BK virus infection, Wilms tumor, cystic fibrosis and cystinosis [6, 13]. Notably, tubuloids derived from cystinosis patients, a metabolic disorder leading to lysosomal cystine accumulation, were also used to test a novel therapy by combining cysteamine, the only effective cystinosis treatment, with the anti-androgen bicalutamide, targeting the metabolic phenotype in cystinotic cells. The dual therapy showed improvement in PT function when compared to cysteamine treatment alone

[13].

Central to the maturation of these organoid models is the incorporation of ECM components in their culture conditions, whether through direct coating of cell culture dishes [14, 15], biofunctionalized synthetic scaffolds through coating with ECM components to improve cellular adhesion and tissue integration [16, 17], or as hydrogels [18]. The ECM plays a pivotal role in recapitulating native tissue characteristics essential for supporting cell maturation and function. It provides a structural scaffold based on the biomechanical properties of the tissue, allowing cells to adhere, proliferate, and different into a more mature and functional phenotype [19]. Coating strategies using combinations between collagen IV, laminin, and l-3,4-dihydroxyphenylalanine (L-DOPA) were shown to increase culture time, improve monolayer formation, and increase expression of PT transporters [17, 20-23]. Additionally, culturing PTECs within an ECM matrix, mainly collagen I and/or Matrigel, resulted in the formation of tube-like structures and increased PT transporters expression [24-27]. Nevertheless, organoids embedded in an ECM matrix pose some limitations, including difficulty in 'real time' live imaging, accessing the apical side for transport studies and lack of vascularization, which hinders maturation [28]. To overcome this, ECM-coated polymer hollow fiber membranes (HFMs), particularly suitable for tube-like tissues, offer a more accessible 3D system as cells can be seeded onto HFMs allowing live cell imaging and transepithelial transport (as employed in **Chapter 4**). Additionally, surface features, such as topographical patterns and porosities may affect cell behavior [29]. For example, PTECs cultured on curved surfaces showed increased cell height, as well as increased polarity when compared to flat 2D cultures [30]. Van Genderen *et al.* compared scaffold surfaces with square-, random-, and rhombus-shaped pores to assess which would benefit cell growth and functionality (drug transporter activity). The authors concluded that rhombus-shaped pores outperformed the others by supporting cell orientation, increasing ECM deposition by the cells and a higher expression of transporters of the organic cation system, namely organic cation transporter 2 (OCT2; *SLC22A2*) and P-glycoprotein (P-gp; *ABCB1*) [31]. Moreover, the incorporation of fluid flow, absent in 2D and 3D static cultures, has also shown to improve cell maturation and transport activity [32-36]. Fluid flow has been employed in microfluid devices, called organ-on-chip, in which single or dual channel models have cells grown in/against a coated/uncoated ECM surface, and in case of dual channel devices, separated by a semipermeable membrane or matrix to allow solute transport. Of note, the OrganoPlate® (Mimetas, Leiden, The Netherlands), is a microfluidic device in which cells are grown on a membrane-free, collagen containing, surface, and allows the free movement of compounds between their 2- or 3-channel configurations [37-40]. While ECM components and fluid flow can indeed increase

the complexity of the *in vitro* model, the choice of the cell source is of great importance. For example, primary PTECs and HK-2 cells were cultured in a microfluidic device in order to assess whether such model could improve their use in nephrotoxicity testing. In here, flow increased overall cell morphology and transporter function; however, when testing the toxicity of chemotherapeutic drugs (cisplatin, doxorubicin and sunitinib) or antibiotics (polymyxin B) the authors found HK-2 to be less sensitive than primary PTECs, and polymyxin B was not toxic to HK-2 cells [41]. In another study, organoid-derived PTECs showed increased expression and polarization of drug transporters upon fluid flow stimulation, which was further assessed and validated by drug uptake and inhibition assays [42]. Additionally, Yin *et al.* demonstrated in a kidney-on-chip comprised of both PTECs and endothelial cells the possibility of using this system for drug screening by testing the effects of known nephrotoxicants and respective transporter inhibition [43]. These findings suggest that kidney-on-chip models can be used for drug toxicity testing, however the choice of cell source and device will determine the outcome. Furthermore, numerous kidney-on-chip models have been used to study a variety of genetic kidney diseases, as reviewed elsewhere [44]. For studying DKD, up to date only a glomerulus-on-chip [45] and a proof-of-concept PT-vasculature model showing the effects of SGLT2 inhibition in glucotoxicity [46] have been reported.

Lastly, to predict disease prognosis and treatment response, a panel of suitable cell-based assays, as well as identification of biomarkers are critical. While drug toxicity studies have predominantly focused on assessing cell death, cytoskeleton derangements and/or mitochondrial dysfunction, these effects are valid solely within a homogenous cell population, but fail in heterogenous populations. This discrepancy arises from the fact that a nephrotoxicant, while directly targeting a specific cell type, might not necessarily affect the whole cell population. The identification of novel disease- and cell-specific biomarkers, as explored in **Chapter 2**, will offer higher specificity over potency assays, which can be relatively complex and present variability across different laboratories [47]. Of interest, kidney injury molecule-1 (KIM-1) and neutrophil gelatinase-associated lipocalin (NGAL) have been associated with the transition between acute to CKD, and show better accuracy than traditional glomerular filtration rate (GFR)-related biomarkers (*e.g.*, creatinine and urea) [48]. Another approach to assess kidney injury involves the use of fluorescent probes targeting specific kidney functions. Within the framework of the RenalToolBox, a project funded by the European Union [https://www.renaltoolbox.org], a transcutaneous device, intended for clinical use, was tested on rodent models to evaluate kidney function using fluorescent dyes. These dyes were designed to measure glomerular filtration rate, and tubular reabsorption and secretion functions [49], building upon previous work [50, 51]. Such approach offers a rapid,

and non-invasive alternative to those established in the clinic.

In conclusion, the pursuit to enhance our understanding of kidney function and to unravel the pathophysiological mechanisms of kidney diseases has led to remarkable progress in refining current *in vitro* PT models. These models have increased in complexity, highlighting ECM components and fluid flow as key factors driving PT maturation and function, thus rendering them suitable for addressing specific research questions. These refinements not only enhance their potential for drug screening and disease modeling, but also underscore their "fit-for-purpose" approach in elucidating the intricacies of kidney biology. Additionally, the identification of new diagnostic biomarkers and development of fluorescent probes targeting specific kidney functions will aid this process.

2. IMPLICATIONS FOR BAK APPLICATIONS

Dialysis, as an option for patients who are not eligible for organ transplantation or those waiting for an organ donor, is hampered by its inability to remove PBUTs. UTs have been classified based on their physicochemical properties and dialytic removal patterns [52], and their accumulation in the blood, particularly PBUTs, is associated with kidney dysfunction [53]. The albumin binding capacities can be altered by plasma albumin concentration or by altering albumin conformation due to environmental cues, such as high glucose [54], heat [55], as well as oxidative stress, which is enhanced in CKD patients [56]. These factors can alter albumin binding properties, thus increasing or decreasing ligand affinity. For instance, PBUTs buildup, including indoxyl sulfate (IS) were reported to bind strongly to albumin and increase its thermal stability, however this binding changed the secondary structure of albumin and inhibited its hydrolase activity, which is required for the breakdown of drugs (*e.g.*, antibiotics) [57]. Additionally, albumin glycation and oxidation, processes known to co-occur with each other [58], lead to a decrease in its drug binding capacity [59]. This effect can impair drug disposition and efficacy, contributing to disease progression, similar to the effects found for PBUTs [57].

To address the previous challenges, several strategies have been developed to enhance the removal of drugs and PBUTs, beyond conventional dialysis methods. One promising approach involves the development of bioartificial kidneys (BAK), designed to complement traditional dialysis by actively secreting PBUTs. Furthermore, a complementary strategy involves the use of competitive binders that are meant to displace PBUTs from albumin, aiding the removal of the free fraction via dialysis [55]. In the PT, organic anion transporters 1 (OAT1; *SLC22A6*) and 3 (OAT3; *SLC22A8*) facilitate the secretion of PBUTs, while also mediating the uptake of many drugs prescribed to treat CKD [60-64]. In **Chapter 3**, the potential competition between PBUTs and drugs for OAT1-mediated uptake was studies using fluorescein as a

probe for OAT1 uptake capacity. From a panel of antihypertensive drugs, *viz.* angiotensin-converting enzyme inhibitors (ACEIs: captopril, enalaprilate, lisinopril), angiotensin receptor blockers (ARBs: losartan and valsartan), diuretics (furosemide) and cholesterol-lowering drugs (statins: pravastatin and simvastatin), we concluded that solely ARBs and furosemide significantly reduced fluorescein uptake, and this was further exacerbated in the presence of PBUTs, particularly indoxyl sulfate (IS), kynurenic acid (KA), and p-cresyl sulfate (PCS), thus indicating a potential competition of fluorescein, PBUTs and drugs for the transport [65]. Furthermore, a study by André *et al.* reported in kidney transplant patients that a higher blood concentration of tacrolimus, an immunosuppressant drug, was correlated with increased plasma levels of IS and PCS found in these patients. This association was attributed to the higher affinity of these UTs to albumin binding sites, thereby competing with tacrolimus for binding, and increasing their free fraction [66]. Despite tacrolimus not being an OAT1 substrate, the tested UTs in this study are, and align with our previous findings that OAT1-mediated IS uptake is enhanced in the presence of albumin [67, 68].

Many attempts at developing BAK devices have been made over the last 25 years. **Table 2** provides an overview of the BAK devices developed so far. The first BAK device, named renal tubule assist device (RAD), was developed by Humes *et al*. The RAD consisted of PTECs seeded intraluminally in a HFM system, and then connected in series with a conventional hemofilter. Preclinical studies demonstrated that the RAD effectively replicated the native PT functions, including vectorial transport, along with metabolic and endocrine functions [69-73]. Notably, the RAD is the only BAK-like device successfully tested in humans, and showing promising results in improving renal function of AKI patients [74]. However, despite its potential, the RAD was discontinued due to the lack of a commercially viable manufacturing process, which included the challenge of expanding large amounts of cells for clinical use. To overcome this issue, the same group developed the bioartificial renal epithelial cell system (BRECS), in which PTECs are expanded in large scale within a perfusion bioreactor. Upon expansion, the BRECS can be cryopreserved for future use, enabling a superior alternative to RAD, with a long-term storage and off-the shelf features [75]. Similar to RAD, BRECS was tested in large animal to determine its safety and efficacy. While promising results were obtained, including improvements in cardiovascular performance, immunomodulatory function, and assessment of metabolic and endocrine functions, BRECS was not tested for PBUTs removal [76, 77]. This important feature of the kidney was only effectively demonstrated in the so-called BAK living membranes [17, 78-81]. Like other HFM-based BAK devices [82-86], these living membranes are composed of ECM-coated HFM, and seeded extraluminally with PTECs. This BAK system demonstrated active PBUTs secretion

[17, 78, 81], thus showing to be a promising alternative to previous attempts. However, it needs *in vivo* validation to advance its potential clinical use.

Altogether, the intended application of the BAK consists of an extracorporeal device connected in series with a hemofilter. Blood is first pumped through the hemofilter to allow the diffusive transport of non-PBUTs, and subsequently, it flows into the BAK. In both setups, dialysis fluid (DF) is applied, however, it is only in the BAK that it comes into direct contact with cells. Consequently, it becomes imperative to assess its effect on cell behavior, particularly on PBUT secretion (**Figure 1**). Addressing this concern, **Chapter 4** employed a series of *in vitro* models aiming at evaluating DF's effect on cell viability markers, monolayer integrity, and cell function. Our results indicated that, over the course of a dialysis session (4h), DF does not disrupt cell functionality, namely the basolateral-to-apical secretion of PBUTs. Additionally, utilizing a bioengineered kidney tubule microfluidic device, simulating the BAK's functional unit, we showed that DF did not interfere with the clearance of multiple PBUTs, and that addition of albumin enhanced their clearance [81]. These findings corroborate the above-mentioned conclusions that albumin facilitates OAT1-mediated UTs uptake [67, 68]. Furthermore, our study evaluated the model's effectiveness in eliminating PBUTs from uremic plasma, mirroring a clinical BAK setting. While successful in PBUTs removal, the efficacy was slightly lower compared to our controlled uremic conditions (PBUTs alone or in combination with albumin) [81]. We associated this drawback to the uremic plasma's unknown composition and contains many more UTs and drugs prescribed to CKD patients, as mentioned in **Chapter 4**. Another limitation of our study was the absence of an apical flow (**Figure 1**) and the exploration of different flow rates to evaluate their impact on PBUTs clearance. A clinical study has demonstrated that increasing DF flow rate (from 300 to 800 ml/min) resulted in almost doubled clearance rates of IS and PCS [87]. Moreover, Maheshwari *et al*. developed a mathematical model in which they evaluated the effects of DF and blood flow rates on PBUTs removal. The authors demonstrated that increasing DF flow rate (from 500 to 800 ml/min) results in the removal of only strongly albumin-bound UTs (namely IS and PCS), whereas for moderate-to-weakly albumin-bound toxins (indole-3-acetic acid and p-cresyl glucuronide) it is advised to increase blood flow rate instead (from 300 to 500 ml/min) [88]. While promising, enhancing DF flow rates will require more DF which will incur additional costs. In **Chapter 4**, we also contemplated on strategies to enhance PBUTs removal. We have previously demonstrated that short exposures to IS resulted in stimulation of OAT1 expression and function [89]. This observation was attributed to the binding of IS to the epidermal growth factor receptor, subsequently activating the aryl hydrocarbon receptor signaling pathway and induction of OAT1 [89]. Such response can be harvested to enhance

the clearance capacity of the BAK. Additionally, the use of adsorbents, particularly the charcoal absorbent AST-120, have proven to be effective in decreasing serum/urine levels of IS and PCS in dialysis patients [90, 91]. Furthermore, as observed in **Chapter 3**, PBUTs might compete with CKD drugs for uptake. Tao *et al*. demonstrated this effect in an *ex vivo* approach in which human blood was spiked with UTs, including IS, and dialyzed with a combination of ibuprofen and furosemide, resulting in increased IS removal [92]. Other studies included the use of salvianolic acids [93] and free fatty acids (oleic or linoleic acids) [94] for evaluation of their PBUT-removal effects. Moreover, by increasing plasma ionic strength, achieved through an increase in Na^+ concentration, UTs can be separated from albumin and more efficiently removed [95, 96].

In conclusion, the challenges posed by PBUTs in dialysis have led to the development of approaches aimed at their removal. Among these, BAK applications have emerged as the most promising solution. Nevertheless, despite advances in improving BAK design and function, its implementation in the clinics remains a challenge.

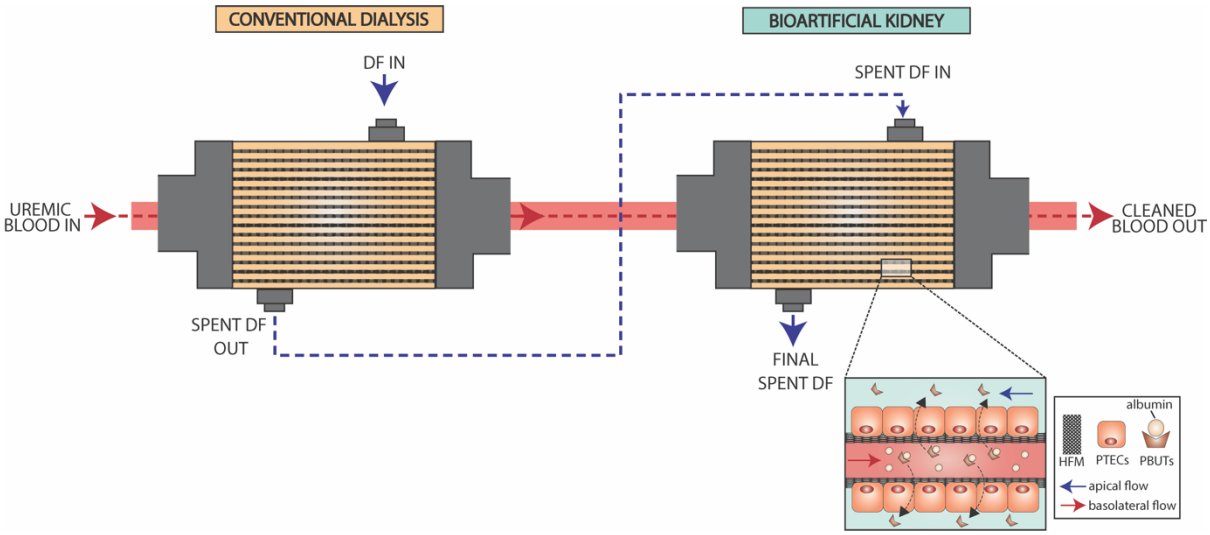

Figure 1. Schematic representation of a bioartificial kidney connected in series with a hemofilter, a conventional dialysis component. The process begins with the patient's blood flowing through the hemofilter, where small and medium-sized molecules, along with excess fluid, are effectively removed. Subsequently, the blood proceeds into the bioartificial kidney, which is comprised of extraluminally seeded proximal tubule epithelial cells (PTECs) on polyethersulfone hollow fiber membranes (HFMs). Within the bioartificial kidney, PTECs are responsible for the removal of protein-bound uremic toxins (PBUTs) by basolateral organic and cation organic transporters from the blood to the dialysis fluid (DF) via apical efflux transporters. Finally, the purified blood, now devoid of uremic toxins, returns to the patient.

Table 2. Overview of currently available cell-based BAK prototypes.

System	Material, MWCO, and configuration	Cells and coating	Features	References
RAD	Polysulphone hollow fibers Surface area (0.4 m^2 or 0.7 m^2) 50 kDA Connected to a hemofilter in series	Porcine and human PTECs Seeded intraluminally Pronectin-L coating	***In vitro*:** Active vectorial transport Ammoniagenesis and gluthathione metabolism Vitamin D_3 synthesis **In vivo** (bilateral nephrectomy and endotoxin shock dogs): Increased ammonia excretion Immunoprotection Active glutathione metabolism Vitamin D_3 production **Clinical studies:** Phase I/II trial (AKI and MOF): Glutathione degradation Vitamin D_3 production Reduced IL-6, IL-10 production Increased survival at day 180 Rapid renal recovery No information on PBUT clearance	[1-6]
BRECs	Porous, niobium-coated carbon disks within a polycarbonate bioreactor **Size**: *In vitro* and sheep models (9 cm×7.5 cm×3 cm) Pig model (8.5 cm×8.5 cm×1.5 cm) **Internal fill volume:** *In vitro* and sheep models (30 ml) Pig model (10ml) <65 kDA	Human PTECs derived from adult progenitor cells Collagen IV coating	Wearable Cryopreservable system Perfusable ***In vitro*:** Consistent metabolic profile Vitamin D_3 synthesis ***In vivo*** (porcine model of septic shock): Cardiovascular improvement Systemic immunomodulation Prolonged survival ***In vivo*** (anephric sheep): Confirmed immunoprotection Vitamin D_3 synthesis Reduced oxidative stress No information on PBUT clearance Awaiting clinical trials	[7-9]

System	Material, MWCO, and configuration	Cells and coating	Features	References
BTD	EVAL hollow fiber modules (0.8 m^2) Mini modules (65 cm^2) <65 kDa	Human PTECs Seeded intraluminally Attachin coating	***In vitro*:** Reabsorption of water, sodium and glucose Metabolic decrease of β2-microglobulin and pentosidine (mini modules) ***In vivo*** (bilateral nephrectomy and LPS): Extended lifespan Reduced expression of inflammatory cytokines and plasma IL-6 levels Culture in serum-free medium No information on PBUT clearance	[10-12]
BAK	Hollow fiber membranes (Highflux PAES and PSU, and PES/PVP) <65 kDa	Human PTECs Seeded extraluminally L-DOPA and collagen IV coating	***In vitro***: Organic anion transport Prevention of leakage of urea and creatinine Release of IL-6 and IL-8 No follow-up	[13, 14]
BAK living membranes	PES and microPES hollow fibers 150 kDa	ciPTECs Seeded extraluminally L-DOPA and collagen IV coating	***In vitro***: Maintenance of barrier function Absence of immunogenic effect of ciPTECs Albumin reabsorption Confirmed PBUTs clearance Upscaling to multiple fiber module Safe to use with dialysis fluid	[15-19]

AKI, acute kidney injury; **BAK**, bioartificial kidney; **BRECS**, bioartificial renal epithelial cell system; **BTD**, bioartificial renal tubule device; **ciPTECs**, conditionally immortalized proximal tubule epithelial cell; **EVAL**, ethylene vinyl alcohol; **IL**, interleukin, **L-DOPA**, L-3,4-dihydroxyphenylalanine; **LPS**, lipopolysaccharide; **MOF**, multiorgan failure; **MWCO**, molecular weigth cut-off; **PAES**, polyarylethersulfone; **PBUT**, protein -bound uremic toxin; **PES/PVP**, polyethersulfone/polyvinylpyrrolidone; **PSU**, polysulfone; **PTECs**, proximal tubule epithelial cells; **RAD**, renal tubule assist device.

3. MITOCHONDRIAL HEALTH IN DISEASE PROGRESSION AND THERAPEUTIC INTERVENTIONS

Mitochondria, often referred to as the cellular powerhouses, play a vital role in ATP production, cell differentiation and death, as well as regulating reactive oxygen species (ROS) and calcium homeostasis. Given these essential functions, it is not a surprise that mitochondria are implicated in the pathogenesis of numerous diseases [1, 2]. The kidneys, after the heart, have the highest oxygen consumption rate (OCR) and mitochondrial abundance, with the PT showing the highest mitochondrial density [3, 4]. Consequently, the PT is the primary site for ATP generation which is consumed predominantly by Na^+K^+-ATPase to maintain all reabsorption and secretion processes. For ATP production, PTECs rely solely on oxidative phosphorylation (OXPHOS) through fatty acid β-oxidation (**Figure 2**) [5, 6]. Unlike other nephron segments, the PT exhibits minimal to no glycolytic capacity. This unique trait leaves it particularly vulnerable to oxygen changes, which are required for effective β-oxidation. Additionally, it has been proposed that glycolytic ATP production in PTECs might have harmful effects, given the high glucose concentration resulting from glucose reabsorption, especially in disease conditions, like diabetes [6]. Mitochondria-associated tubulopathies can arise from either genetic mutations (leading to OXPHOS imbalance) or cellular insults (*e.g.,* ischemia, sepsis, hyperglycemia, and nephrotoxicants) [7-9]. In this thesis, we focused on mitochondrial dysfunction as a result of cellular insults, namely ischemia and hyperglycemia. In **Chapter 5**, we developed an ischemic PT *in vitro* model by subjecting ciPTECs to a combination of antimycin A, a mitochondrial respiration inhibitor, and 2-deoxy-D-glucose, a glycolysis inhibitor, reported to mimic ischemic damage [10-13]. Additionally, to enhance the simulation of blood supply disruption which deprives cells from nutrients, we exposed these chemically-treated ciPTECs to a hypoxic environment (1% O_2). Our findings indicated that combined exposure of physical- and chemically-induced ischemia resulted in a pronounced cell monolayer degradation and increased mitochondrial dysfunction, as evidenced by a decrease in mitochondrial membrane potential and mass, and reduced ATP production, features that were reported *in vivo* as well [14-18]. Additionally, cell bioenergetics confirmed mitochondrial dysfunction as both OCR and extracellular acidification rate (ECAR) were found decreased, along with several OCR-related parameters associated with OXPHOS impairment, such as maximal and ATP-linked respiration, and coupling efficiency. Furthermore, metabolites essential to the TCA cycle, crucial for ATP production via OXPHOS, were reduced, further corroborating the decline in mitochondrial bioenergetics. Collectively, our *in vitro* model demonstrates the need to carefully select the metabolic stressors to better mimic ischemia *in vivo*. This model also serves as a platform to develop effective mitochondrial-targeted

therapies that are currently still lacking [19-21]. With this in mind, we pursued to assess the effect of mesenchymal stromal cells' (MSCs) therapy on ameliorating the ischemic damage observed in our model. MSCs therapy has emerged as a very promising, regenerative tool in treating many diseases due to 1) their easy collection from different sources (*e.g*, adipose tissue, bone marrow, dental pulp, and umbilical cord) and culture expansion [22]; 2) their homing ability, demonstrated by their capacity to migrate to injured sites upon transplantation [23]; 3) their ability to differentiate into various cell types, potentially replacing damaged cells [24], and 4) their paracrine functions through the secretion of soluble factors and extracellular vesicles, exerting anti-inflammatory and cytoprotective properties [25-29]. Within **Chapter 5**, we observed that upon MSC treatment, with either conditioned medium, containing the entire fraction of soluble factors, or extracellular vesicles, ischemic ciPTECs showed a significant increase in ATP production, glycolysis intermediates and antioxidant metabolites. These findings align with the growing evidence that MSCs therapy exerts antioxidant properties by increasing mitochondrial bioenergetics [30-33]. Furthermore, these antioxidant properties have been associated with the transfer of healthy mitochondria to injured cells, facilitated by tunneling nanotubes, tubular protrusions connecting the plasma membranes of donor and recipient cells, or extracellular vesicles [34]. This transfer has been shown to restore cellular respiratory function, increase ATP production, and to suppress apoptosis in lung epithelial cells [35, 36], cardiomyocytes [37, 38], and astrocytes [39], a mechanism that could also underly our findings. Furthermore, Doulamis *et al*. demonstrated in a porcine IRI model that mitochondria transplantation yielded improved kidney function and reduced histological damage [40]. Moreover, Konari *et al*. showed successful MSCs mitochondrial transfer to diabetic-impaired PT cells both *in vivo* and *in vitro*. *In vivo*, the transferred mitochondria improved cellular morphological and structural phenotypes, while *in vitro* it suppressed apoptosis and ROS production [41]. Notably, these *in vitro* findings demonstrated that in hyperglycemia conditions, the peroxisome proliferator–activated receptor gamma coactivator-1α (PGC-1α), a master regulator of mitochondrial biogenesis (**Figure 2**), underwent nuclear translocation [41]. PGC-1α, typically found in the cytoplasm in healthy states, can shift to the nucleus as a response to changes in energy demand and metabolic stresses [42]. Likewise, the authors associated this process with a compensatory mechanism in response to impaired mitochondria [41]. When activated, PGC-1α leads to an increase in mitochondria's number and mass, thus enhancing ATP production to meet the energy demands [43]. Decreased PGC-1α expression and activity have been shown in several diabetes studies [44-46], with PT cells and podocytes showing a decrease in mitochondrial biogenesis and ATP production [47-49]. Due to the important role of PGC-1α in regulating mitochondrial biogenesis and

bioenergetics, many therapeutic strategies have been employed aiming at increasing its expression and attenuating kidney damage, thus mitigating disease progression [50-52]. Additionally, PGC-1α can regulate mitochondrial dynamics, which include the coordinated processes of mitochondrial fission and fusion of mitochondria (**Figure 2**) [42].

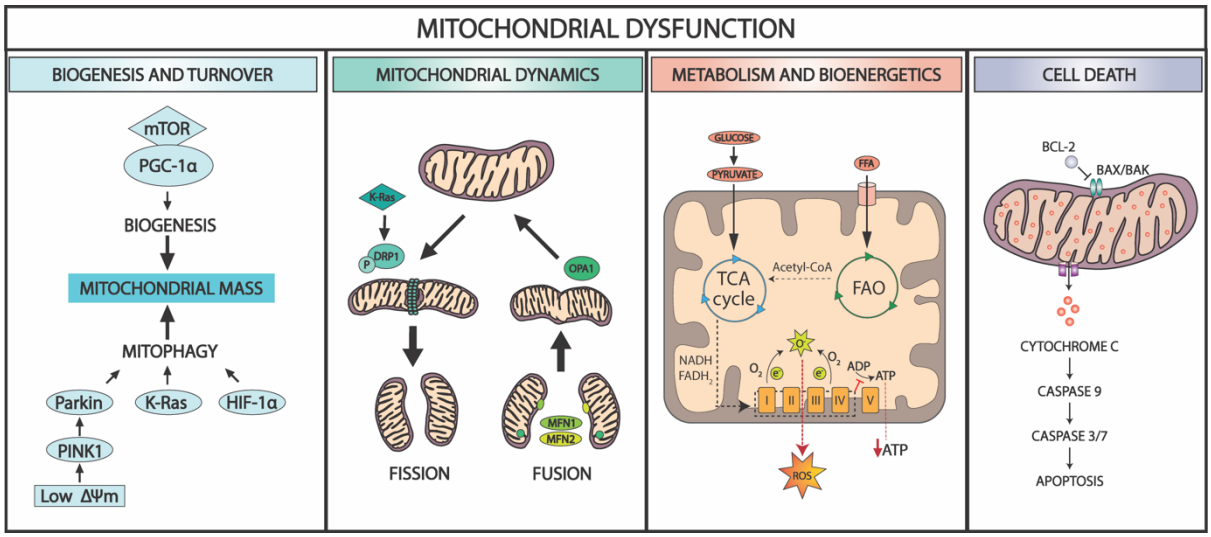

Figure 2. Schematic representation of different mechanisms of mitochondria biology that contribute to dysfunction, including biogenesis and turnover, mitochondrial dynamics, metabolism and bioenergetics, and cell death. The different mechanisms also serve as potential targets for pharmacological intervention. **BAK**, BCL-2 homologous antagonist/killer; **BAX**, BCL-2 associated X; **BCL-2**, B-cell lymphoma 2; **DRP1**, dynamin-related protein 1; **FAO**, fatty acid β-oxidation; **FFA**, free fatty acid; **HIF-1α**, hypoxia inducible factor 1 subunit alpha; **K-Ras**, Kirsten rat sarcoma viral oncogene homolog; **MFN**, mitofusin; **mTOR**, mammalian target of rapamycin; **OPA1**, optic atrophy 1; **PGC-1α**, peroxisome proliferator–activated receptor gamma coactivator-1α; **PINK1**, phosphatase and tensin homolog-induced kinase 1; **ROS**, reactive oxygen species; **TCA**, tricarboxylic acid.

In the context of DKD, numerous *in vitro* studies demonstrated that upon exposure to hyperglycemia, kidney cells experienced an increase in mitochondrial fission, a process that segregates damaged mitochondria for removal. Conversely, the fusion process, which maintains mitochondrial health, decreased [53-59]. Moreover, mitochondrial biogenesis was suppressed in these cells [55, 59], and mitophagy, a selective form of autophagy targeting damaged/dysfunctional mitochondria, was impaired [53, 56]. As a consequence, these cellular events led to mitochondrial dysfunction and decreased ATP production [53-59]. Taking these observations into account, in **Chapter 7**, we employed a diabetic PT model *in vitro* using HK-2 cells. Here, cells were exposed to a combination of hyperglycemia and hypoxia to better resemble the diabetic milleu [60-62]. To further enhance the relevance of the model, these cells were simultaneously exposed to high glucose, low oxygen concentrations and either

palmitic acid (PA), the most abundant free fatty acid in human urine [63], or glycated albumin (GA), formed when glucose reacts non-enzymatically with albumin [64]. In DKD, the accumulation of these two factors have been associated with disease progression [64-68]. Our findings diverged from the previously noted balance between mitochondrial fission and fusion, as well as the impaired mitophagy evident in hyperglycemia-induced injury. Instead, the addition of PA or GA resulted in an increase of these processes. While the loss of mitochondrial quality control in our study, observed by the imbalanced fission and fusion processes, has been associated to DKD progression [69], we concluded that the increase found was most likely related to an adaptive response to impaired mitochondria. This observation is in line with unchanged levels of mitochondrial mass and ATP production found in our study, which are normally found decreased in DKD [8, 70]. Additionally, mitophagy and fission are interconnected processes, and mitophagy is tightly controlled by mitochondrial membrane potential. Depolarized mitochondria, due to a decrease in $\Delta\Psi$, are not efficiently removed by mitophagy, as the latter is impaired (**Figure 2**) [69]. While we did not assess membrane potential, the increased levels of mitophagy imply that, in our model, mitochondria were not depolarized. Additionally, the fusion processes can happen in the outer membrane, which is regulated by mitofusins [71], or in the inner membrane, where optic atrophy-1 (OPA1) mediates the fusion (**Figure 2**) [72]. Inner membrane fusion requires a high membrane potential for it to happen [73], suggesting that only active mitochondria can properly fuse. The increased levels of OPA1 found in our model again argue that mitochondrial membrane potential was not compromised. Of great interest, we found an increase in the release of the injury marker NGAL in our diabetic conditions, which was reversed upon treatment with empagliflozin, a SGLT2 inhibitor. These findings highlight the potential benefit of empagliflozin in mitigating NGAL release, which was not found for other SGLT2 inhibitors, such as ertugliflozin [74] and dapagliflozin [75]. Moreover, in a study by Lee *et al*., it was demonstrated that exposing HK-2 cells to high glucose led to an increase in mitochondrial ROS, and decreased ATP and MMP, which was reversed upon treatment with empagliflozin [76]. Additionally, this treatment was also found to decrease the levels of fission proteins, associated with mitochondrial damage, and increase mitochondrial fusion proteins [76]. These results suggest an additional role of empagliflozin in improving mitochondria dynamics and bioenergetics. Furthermore, SGLT2 inhibitors have shown antioxidant properties in PT cells *in vitro* [77-79]. These benefits make this therapy appealing not only for diabetic conditions, but also for non-diabetic kidney failure characterized by mitochondrial dysfunction, such as IRI, as discussed in **Chapter 5**. While promising, SGLT2 inhibitors can increase the risk of urinary tract infections due to its glycosuric effect [80]. Additionally, concerns arose from the

possible overlap between SGLT2 inhibitors with OAT1 and/or OAT3, which might compromise their transport function and, subsequently the treatments efficacy through influencing the drug plasma levels [81]. For instance, empagliflozin is a substrate of OAT3, but not OAT1. In a mouse model, it was demonstrated that OAT3 enhanced the glucosuric effect of empagliflozin by increasing its plasma levels [82]. Understanding the interplay between these transporters and to assess whether SGLT2 inhibition could influence the clearance of commonly prescribed CKD drugs but also the removal of anionic PBUTs, as assessed in **Chapter 3**, would be of great interest. For such study, a cell model expressing both glucose transporters (SGLT2 and GLUT2) and OATs is essential, for which HK-2 cells are not of added value as these cells do not express OATs [83].

With this goal in mind, CRISPR/Cas9 technology was employed to genetically modify ciPTECs, enabling the expression of both glucose transporters. Briefly, we used a peptide-mediated delivery method (LAH5) to introduce two plasmids, containing the SGLT2 and GLUT2 transporters. Each plasmid contained a fluorescent gene, mCherry and GFP, respectively, and flanking homology-independent targeted insertion (HITI) sequences at both insert ends, which allowed for the selection and sorting of the cells that introduced the two genes simultaneously. Preliminary data showed efficient transfection of both SGLT2 and GLUT2, evidenced by their gene expression levels, surpassing those observed in HK-2 cells (**Figure 3A-B**). Additionally, we conducted a glucose transport by using a fluorescent D-glucose analog, 2-[N-(7-nitrobenz-2-oxa-1,3-diazol-4-yl)amino]-2-deoxy-D-glucose (2-NBDG) [84]. Our results demonstrated active glucose transport in our modified cells, which was inhibited upon exposure to canagliflozin (**Figure 3C-D**). The expression of the glucose transporters along with OAT1 and OCT2, responsible for the uptake of other diabetic drugs (*e.g.,* metformin), expressions will allow us to evaluate the interplay between these transporters in DKD and CKD. Among applications, the use of this new cell line will aid in a more in-depth characterization of pharmacokinetic properties and efficacy of drugs, important features in drug development. Additionally, given the presence of glucose transporters, it will enable us to re-evaluate PBUTs clearance within our BAK device (described in **Chapter 4**) under the influence of diabetic drugs.

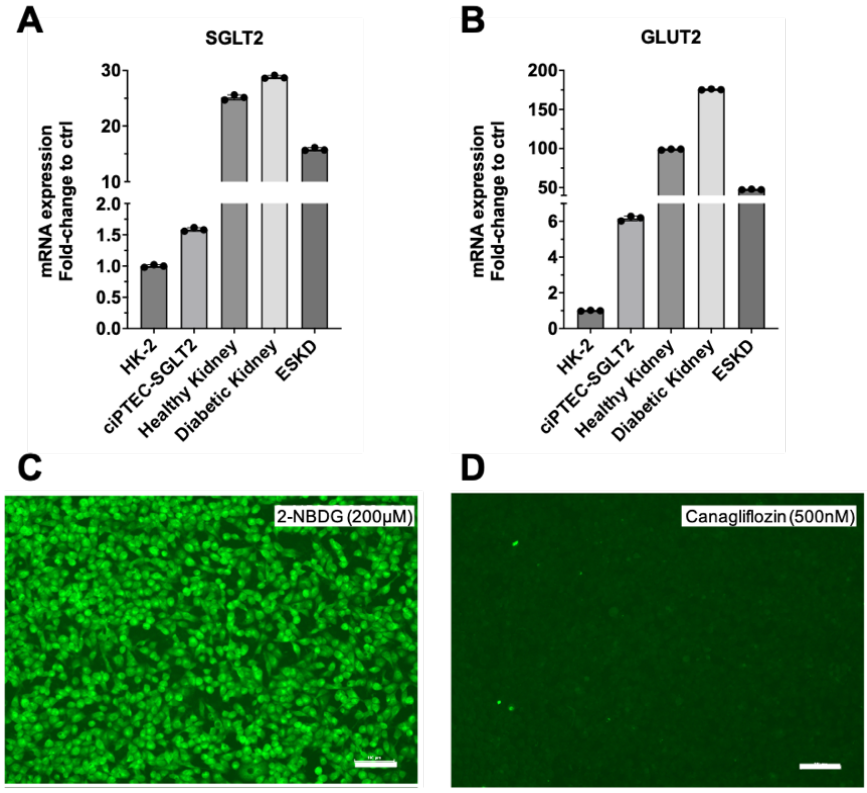

Figure 3. Preliminary data of genetically modified ciPTEC expressing glucose transporters. Gene expression levels of (**A**) SGLT2 and (**B**) GLUT2 (n=1, in triplicate). (**C**-**D**) Glucose transport was assessed by assessing the fluorescence accumulation of the glucose analog 2-NBDG (200 μM), which was blocked using canagliflozin (500 nM).

CONCLUSIONS

This thesis demonstrated the importance of redirecting the focus of renal translational research to the PT, given its important role in the progression from AKI to CKD. We also emphasized the pressing need for more complex *in vitro* models to better mimic the (patho)physiological events seen *in vivo*. Our work sheds light on the impact of mitochondria dysfunction in driving disease progression. The PT, rich in mitochondria, generates ATP via oxidative phosphorylation which relies on a consistent oxygen consumption and supply of nutrients, thus being particularly vulnerable when there is a shortage of these factors. Given the critical role of PT in overall kidney function, any malfunction of this nephron segment has been associated with disease progression. Although considerable efforts have been made into targeting mitochondrial dysfunction, contributing factor in reduced transport activity in PT, the complex mitochondrial responses to injury and its subsequent signaling pathways require further studies, allowing for the development of better targeted therapies. Among promising therapeutic approaches, we highlighted MSCs secretome which contributed to a restoration of tubular cell bioenergetics upon ischemic damage, a pivotal step towards functional recovery. While promising, further studies are required to understand its mechanism of action.

For this, multi-cellular *in vitro* models, such as organoids, will be required as the intricate renal microenvironment is comprised of multiple cell types, all playing an important role in disease progression and in regeneration processes. While kidney organoids have shown promise, their limited maturation phenotype remains a challenge for which improvements in their culture conditions and addition of vasculature have been investigated. Nevertheless, organ-on-chip models stand as the frontrunners in this regard by combining multiple cell types in a dynamic microenvironment that resemble the one found *in vivo*, but require further optimization in terms of biomaterial used and cell source. Despite this, their official approval by the Food and Drug Administration for use in drug development (along with animal models) highlights their great potential. While these models alone can provide mechanistic insights into kidney physiology, advances in multi-omics approaches will offer a holistic view, enabling the identification of multiple drug target-disease mediators.

Furthermore, our findings extend to kidney replacement therapies, as demonstrated by the development of a BAK in which PT cells showed active PBUTs clearance, unaffected by DF. This remarkable feature of our model surpasses prior attempts, although further *in vivo* validation is a requisite step. In addition, we demonstrated another critical clinical insight. The prescription of multiple medications to CKD patients can inadvertently impact tubular transport function as some of these drugs compete with PBUTs for OAT1 uptake, bearing significant implications for the management of CKD. Collectively, our findings enhance the understanding

that PT is a prime target for disease modeling and for the development of targeted therapies.

REFERENCES

1. S. Javadov, A. V. Kozlov and A. K. S. Camara. Mitochondria in Health and Diseases. Cells 2020;9(5)

2. R. J. Tinker, A. Z. Lim, R. J. Stefanetti*, et al.* Current and Emerging Clinical Treatment in Mitochondrial Disease. Mol Diagn Ther 2021;25(2):181-206

3. D. J. Pagliarini, S. E. Calvo, B. Chang*, et al.* A mitochondrial protein compendium elucidates complex I disease biology. Cell 2008;134(1):112-123

4. P. M. O'Connor. Renal oxygen delivery: matching delivery to metabolic demand. Clin Exp Pharmacol Physiol 2006;33(10):961-967

5. R. L. Chevalier. The proximal tubule is the primary target of injury and progression of kidney disease: role of the glomerulotubular junction. Am J Physiol Renal Physiol 2016;311(1):F145-161

6. J. M. Forbes. Mitochondria-Power Players in Kidney Function? Trends Endocrinol Metab 2016;27(7):441-442

7. L. P. Govers, H. R. Toka, A. Hariri*, et al.* Mitochondrial DNA mutations in renal disease: an overview. Pediatr Nephrol 2021;36(1):9-17

8. L. Yao, X. Liang, Y. Qiao*, et al.* Mitochondrial dysfunction in diabetic tubulopathy. Metabolism 2022;131:155195

9. A. J. Clark and S. M. Parikh. Mitochondrial Metabolism in Acute Kidney Injury. Semin Nephrol 2020;40(2):101-113

10. P. C. Dagher. Modeling ischemia in vitro: selective depletion of adenine and guanine nucleotide pools. Am J Physiol Cell Physiol 2000;279(4):C1270-1277

11. L. T. Wang, B. L. Chen, C. T. Wu*, et al.* Protective role of AMP-activated protein kinase-evoked autophagy on an in vitro model of ischemia/reperfusion-induced renal tubular cell injury. PLoS One 2013;8(11):e79814

12. P. M. Holloway and F. N. Gavins. Modeling Ischemic Stroke In Vitro: Status Quo and Future Perspectives. Stroke 2016;47(2):561-569

13. P. F. Shanley, M. Brezis, K. Spokes*, et al.* Differential responsiveness of proximal tubule segments to metabolic inhibitors in the isolated perfused rat kidney. Am J Kidney Dis 1986;7(1):76-83

14. R. Lan, H. Geng, P. K. Singha*, et al.* Mitochondrial Pathology and Glycolytic Shift during Proximal Tubule Atrophy after Ischemic AKI. J Am Soc Nephrol 2016;27(11):3356-3367

15. S. Liu, Y. Soong, S. V. Seshan*, et al.* Novel cardiolipin therapeutic protects endothelial mitochondria during renal ischemia and mitigates microvascular rarefaction, inflammation, and fibrosis. Am J Physiol Renal Physiol 2014;306(9):F970-980

16. C. Brooks, Q. Wei, S. G. Cho*, et al.* Regulation of mitochondrial dynamics in acute kidney injury in cell culture and rodent models. J Clin Invest 2009;119(5):1275-1285

17. L. J. S. Lerink, M. J. C. de Kok, J. F. Mulvey*, et al.* Preclinical models versus clinical renal ischemia reperfusion injury: A systematic review based on metabolic signatures. Am J Transplant 2022;22(2):344-370

18. A. M. Hall, G. J. Rhodes, R. M. Sandoval*, et al.* In vivo multiphoton imaging of mitochondrial structure and function during acute kidney injury. Kidney Int 2013;83(1):72-83

19. M. P. Murphy and R. C. Hartley. Mitochondria as a therapeutic target for common pathologies. Nat Rev Drug Discov 2018;17(12):865-886

20. A. Singh, D. Faccenda and M. Campanella. Pharmacological advances in mitochondrial therapy. EBioMedicine 2021;65:103244

21. C. Ma, F. Xia and S. O. Kelley. Mitochondrial Targeting of Probes and Therapeutics to the Powerhouse of the Cell. Bioconjug Chem 2020;31(12):2650-2667

22. A. Markov, L. Thangavelu, S. Aravindhan*, et al.* Mesenchymal stem/stromal cells as a valuable source for the treatment of immune-mediated disorders. Stem Cell Res Ther 2021;12(1):192

23. J. Zheng, H. Li, L. He, et al. Preconditioning of umbilical cord-derived mesenchymal stem cells by rapamycin increases cell migration and ameliorates liver ischaemia/reperfusion injury in mice via the CXCR4/CXCL12 axis. Cell Prolif 2019;52(2):e12546

24. Y. Han, X. Li, Y. Zhang*, et al.* Mesenchymal Stem Cells for Regenerative Medicine. Cells 2019;8(8)

25. S. Keshtkar, N. Azarpira and M. H. Ghahremani. Mesenchymal stem cell-derived extracellular vesicles: novel frontiers in regenerative medicine. Stem Cell Res Ther 2018;9(1):63

26. Q. H. Jin, H. K. Kim, J. Y. Na*, et al.* Anti-inflammatory effects of mesenchymal stem cell-conditioned media inhibited macrophages activation in vitro. Sci Rep 2022;12(1):4754

27. J. Wang, J. Xia, R. Huang*, et al.* Mesenchymal stem cell-derived extracellular vesicles alter disease outcomes via endorsement of macrophage polarization. Stem Cell Res Ther 2020;11(1):424

28. L. Chen, E. E. Tredget, P. Y. Wu*, et al.* Paracrine factors of mesenchymal stem cells recruit macrophages and endothelial lineage cells and enhance wound healing. PLoS One 2008;3(4):e1886

29. H. R. Hofer and R. S. Tuan. Secreted trophic factors of mesenchymal stem cells support neurovascular and musculoskeletal therapies. Stem Cell Res Ther 2016;7(1):131

30. R. Stavely and K. Nurgali. The emerging antioxidant paradigm of mesenchymal stem cell therapy. Stem Cells Transl Med 2020;9(9):985-1006

31. G. S. Chiu, N. Boukelmoune, A. C. A. Chiang*, et al.* Nasal administration of mesenchymal stem cells restores cisplatin-induced cognitive impairment and brain damage in mice. Oncotarget 2018;9(85):35581-35597

32. W. Nie, X. Ma, C. Yang*, et al.* Human mesenchymal-stem-cells-derived exosomes are important in enhancing porcine islet resistance to hypoxia. Xenotransplantation 2018;25(5):e12405

33. Y. Yuan, M. Shi, L. Li*, et al.* Mesenchymal stem cell-conditioned media ameliorate diabetic endothelial dysfunction by improving mitochondrial bioenergetics via the Sirt1/AMPK/PGC-1alpha pathway. Clin Sci (Lond) 2016;130(23):2181-2198

34. A. M. Rodriguez, J. Nakhle, E. Griessinger*, et al.* Intercellular mitochondria trafficking highlighting the dual role of mesenchymal stem cells as both sensors and rescuers of tissue injury. Cell Cycle 2018;17(6):712-721

35. M. N. Islam, S. R. Das, M. T. Emin*, et al.* Mitochondrial transfer from bone-marrow-derived stromal cells to pulmonary alveoli protects against acute lung injury. Nat Med 2012;18(5):759-765

36. N. Fergie, N. Todd, L. McClements*, et al.* Hypercapnic acidosis induces mitochondrial dysfunction and impairs the ability of mesenchymal stem cells to promote distal lung epithelial repair. FASEB J 2019;33(4):5585-5598

37. J. Zhang, J. Zhang, L. Zhao*, et al.* Differential roles of microtubules in the two formation stages of membrane nanotubes between human mesenchymal stem cells and neonatal mouse cardiomyocytes. Biochem Biophys Res Commun 2019;512(3):441-447

38. H. Han, J. Hu, Q. Yan*, et al.* Bone marrow-derived mesenchymal stem cells rescue injured H9c2 cells via transferring intact mitochondria through tunneling nanotubes in an in vitro simulated ischemia/reperfusion model. Mol Med Rep 2016;13(2):1517-1524

39. V. A. Babenko, D. N. Silachev, V. A. Popkov*, et al.* Miro1 Enhances Mitochondria Transfer from Multipotent Mesenchymal Stem Cells (MMSC) to Neural Cells and Improves the Efficacy of Cell Recovery. Molecules 2018;23(3)
40. I. P. Doulamis, A. Guariento, T. Duignan*, et al.* Mitochondrial transplantation by intra-arterial injection for acute kidney injury. Am J Physiol Renal Physiol 2020;319(3):F403-F413
41. N. Konari, K. Nagaishi, S. Kikuchi*, et al.* Mitochondria transfer from mesenchymal stem cells structurally and functionally repairs renal proximal tubular epithelial cells in diabetic nephropathy in vivo. Sci Rep 2019;9(1):5184
42. L. Chen, Y. Qin, B. Liu*, et al.* PGC-1alpha-Mediated Mitochondrial Quality Control: Molecular Mechanisms and Implications for Heart Failure. Front Cell Dev Biol 2022;10:871357
43. A. Dabrowska, J. L. Venero, R. Iwasawa*, et al.* PGC-1alpha controls mitochondrial biogenesis and dynamics in lead-induced neurotoxicity. Aging (Albany NY) 2015;7(9):629-647
44. M. Fontecha-Barriuso, D. Martin-Sanchez, J. M. Martinez-Moreno*, et al.* The Role of PGC-1alpha and Mitochondrial Biogenesis in Kidney Diseases. Biomolecules 2020;10(2)
45. Q. Wang, B. Zhao, J. Zhang*, et al.* Faster lipid beta-oxidation rate by acetyl-CoA carboxylase 2 inhibition alleviates high-glucose-induced insulin resistance via SIRT1/PGC-1alpha in human podocytes. J Biochem Mol Toxicol 2021;35(7):e22797
46. Y. Yuan, L. Yuan, L. Li*, et al.* Mitochondrial transfer from mesenchymal stem cells to macrophages restricts inflammation and alleviates kidney injury in diabetic nephropathy mice via PGC-1alpha activation. Stem Cells 2021;39(7):913-928
47. H. Xue, P. Li, Y. Luo*, et al.* Salidroside stimulates the Sirt1/PGC-1alpha axis and ameliorates diabetic nephropathy in mice. Phytomedicine 2019;54:240-247
48. X. Xu, N. Zheng, Z. Chen*, et al.* Puerarin, isolated from Pueraria lobata (Willd.), protects against diabetic nephropathy by attenuating oxidative stress. Gene 2016;591(2):411-416
49. T. Imasawa, E. Obre, N. Bellance*, et al.* High glucose repatterns human podocyte energy metabolism during differentiation and diabetic nephropathy. FASEB J 2017;31(1):294-307
50. G. Lee, M. J. Uddin, Y. Kim*, et al.* PGC-1alpha, a potential therapeutic target against kidney aging. Aging Cell 2019;18(5):e12994
51. J. M. Chambers and R. A. Wingert. PGC-1alpha in Disease: Recent Renal Insights into a Versatile Metabolic Regulator. Cells 2020;9(10)
52. M. Zhao, Y. Yuan, M. Bai*, et al.* PGC-1alpha overexpression protects against aldosterone-induced podocyte depletion: role of mitochondria. Oncotarget 2016;7(11):12150-12162
53. M. Zhan, I. M. Usman, L. Sun*, et al.* Disruption of renal tubular mitochondrial quality control by Myo-inositol oxygenase in diabetic kidney disease. J Am Soc Nephrol 2015;26(6):1304-1321
54. W. Wang, Y. Wang, J. Long*, et al.* Mitochondrial fission triggered by hyperglycemia is mediated by ROCK1 activation in podocytes and endothelial cells. Cell Metab 2012;15(2):186-200
55. L. Xiao, X. Zhu, S. Yang*, et al.* Rap1 ameliorates renal tubular injury in diabetic nephropathy. Diabetes 2014;63(4):1366-1380
56. P. Gao, M. Yang, X. Chen*, et al.* DsbA-L deficiency exacerbates mitochondrial dysfunction of tubular cells in diabetic kidney disease. Clin Sci (Lond) 2020;134(7):677-694
57. J. Sheng, H. Li, Q. Dai*, et al.* DUSP1 recuses diabetic nephropathy via repressing JNK-Mff-mitochondrial fission pathways. J Cell Physiol 2019;234(3):3043-3057
58. K. Guo, J. Lu, Y. Huang*, et al.* Protective role of PGC-1alpha in diabetic nephropathy is associated with the inhibition of ROS through mitochondrial dynamic remodeling. PLoS One 2015;10(4):e0125176

59. J. Sheng, H. Li, Q. Dai*, et al.* NR4A1 Promotes Diabetic Nephropathy by Activating Mff-Mediated Mitochondrial Fission and Suppressing Parkin-Mediated Mitophagy. Cell Physiol Biochem 2018;48(4):1675-1693

60. A. C. Hesp, J. A. Schaub, P. V. Prasad*, et al.* The role of renal hypoxia in the pathogenesis of diabetic kidney disease: a promising target for newer renoprotective agents including SGLT2 inhibitors? Kidney Int 2020;98(3):579-589

61. H. L. Barrett, K. C. Donaghue and J. M. Forbes. Going in Early: Hypoxia as a Target for Kidney Disease Prevention in Diabetes? Diabetes 2020;69(12):2578-2580

62. A. M. Stanigut, C. Pana, M. Enciu*, et al.* Hypoxia-Inducible Factors and Diabetic Kidney Disease-How Deep Can We Go? Int J Mol Sci 2022;23(18)

63. S. Bouatra, F. Aziat, R. Mandal*, et al.* The human urine metabolome. PLoS One 2013;8(9):e73076

64. C. M. Zheng, W. Y. Ma, C. C. Wu*, et al.* Glycated albumin in diabetic patients with chronic kidney disease. Clin Chim Acta 2012;413(19-20):1555-1561

65. A. Mitrofanova, G. Burke, S. Merscher*, et al.* New insights into renal lipid dysmetabolism in diabetic kidney disease. World J Diabetes 2021;12(5):524-540

66. Y. Hou, Q. Wang, B. Han*, et al.* CD36 promotes NLRP3 inflammasome activation via the mtROS pathway in renal tubular epithelial cells of diabetic kidneys. Cell Death Dis 2021;12(6):523

67. Y. Sun, X. Ge, X. Li*, et al.* High-fat diet promotes renal injury by inducing oxidative stress and mitochondrial dysfunction. Cell Death Dis 2020;11(10):914

68. A. Ortega, A. Fernandez, M. I. Arenas*, et al.* Outcome of acute renal injury in diabetic mice with experimental endotoxemia: role of hypoxia-inducible factor-1 alpha. J Diabetes Res 2013;2013:254529

69. W. Dai, H. Lu, Y. Chen*, et al.* The Loss of Mitochondrial Quality Control in Diabetic Kidney Disease. Front Cell Dev Biol 2021;9:706832

70. D. L. Galvan, K. Mise and F. R. Danesh. Mitochondrial Regulation of Diabetic Kidney Disease. Front Med (Lausanne) 2021;8:745279

71. H. Chen, S. A. Detmer, A. J. Ewald*, et al.* Mitofusins Mfn1 and Mfn2 coordinately regulate mitochondrial fusion and are essential for embryonic development. J Cell Biol 2003;160(2):189-200

72. A. Olichon, L. Baricault, N. Gas*, et al.* Loss of OPA1 perturbates the mitochondrial inner membrane structure and integrity, leading to cytochrome c release and apoptosis. J Biol Chem 2003;278(10):7743-7746

73. P. Mishra, V. Carelli, G. Manfredi*, et al.* Proteolytic cleavage of Opa1 stimulates mitochondrial inner membrane fusion and couples fusion to oxidative phosphorylation. Cell Metab 2014;19(4):630-641

74. H. Liu, V. S. Sridhar, L. E. Lovblom*, et al.* Markers of Kidney Injury, Inflammation, and Fibrosis Associated With Ertugliflozin in Patients With CKD and Diabetes. Kidney Int Rep 2021;6(8):2095-2104

75. C. C. J. Dekkers, S. Petrykiv, G. D. Laverman*, et al.* Effects of the SGLT-2 inhibitor dapagliflozin on glomerular and tubular injury markers. Diabetes Obes Metab 2018;20(8):1988-1993

76. W. C. Lee, Y. Y. Chau, H. Y. Ng*, et al.* Empagliflozin Protects HK-2 Cells from High Glucose-Mediated Injuries via a Mitochondrial Mechanism. Cells 2019;8(9)

77. N. Zaibi, P. Li and S. Z. Xu. Protective effects of dapagliflozin against oxidative stress-induced cell injury in human proximal tubular cells. PLoS One 2021;16(2):e0247234

78. K. Shirakawa and M. Sano. Sodium-Glucose Co-Transporter 2 Inhibitors Correct Metabolic Maladaptation of Proximal Tubular Epithelial Cells in High-Glucose Conditions. Int J Mol Sci 2020;21(20)
79. S. Maeda, T. Matsui, M. Takeuchi*, et al.* Sodium-glucose cotransporter 2-mediated oxidative stress augments advanced glycation end products-induced tubular cell apoptosis. Diabetes Metab Res Rev 2013;29(5):406-412
80. J. Liu, L. Li, S. Li*, et al.* Effects of SGLT2 inhibitors on UTIs and genital infections in type 2 diabetes mellitus: a systematic review and meta-analysis. Sci Rep 2017;7(1):2824
81. P. Evenepoel, B. Meijers, R. Masereeuw*, et al.* Effects of an SGLT Inhibitor on the Production, Toxicity, and Elimination of Gut-Derived Uremic Toxins: A Call for Additional Evidence. Toxins (Basel) 2022;14(3)
82. Y. Fu, D. Breljak, A. Onishi*, et al.* Organic anion transporter OAT3 enhances the glucosuric effect of the SGLT2 inhibitor empagliflozin. Am J Physiol Renal Physiol 2018;315(2):F386-F394
83. S. E. Jenkinson, G. W. Chung, E. van Loon*, et al.* The limitations of renal epithelial cell line HK-2 as a model of drug transporter expression and function in the proximal tubule. Pflugers Arch 2012;464(6):601-611
84. C. Zou, Y. Wang and Z. Shen. 2-NBDG as a fluorescent indicator for direct glucose uptake measurement. J Biochem Biophys Methods 2005;64(3):207-215

CHAPTER 9

Nederlandse Samenvatting

List of Abbreviations

About the Author

List of Publications

Acknowledgements

Het potentieel van proximale niertubulus cellen voor ziektemodellering en therapeutische interventies

Chronische nierziekte is een progressieve ziekte die meer dan 10% van de wereldbevolking treft, waarbij diabetes mellitus en hypertensie tot de belangrijkste risicofactoren behoren. Tot op heden bestaat er geen geneesmiddel voor chronische nierziekte en de diagnose ervan is afhankelijk van het beoordelen van de filtratie snelheid, wat niet altijd accuraat hoeft te zijn. Naarmate chronische nierziekte vordert bereiken patiënten uiteindelijk het eindstadium nierfalen waarvoor nierfunctie vervangende therapieën nodig zijn, zoals orgaantransplantatie. Het tekort aan beschikbare organen vormt echter een aanzienlijke uitdaging voor de overleving van patiënten. Wanneer een geschikt orgaan niet beschikbaar is, wordt een andere nierfunctie vervangende therapie, nl. dialyse, een optie, vooral voor patiënten die niet in aanmerking komen voor transplantatie. Gezien de beperkingen in zowel de diagnose als de behandeling van chronische nierziekte, is de primaire klinische uitdaging het identificeren van potentiële biomarkers voor vroege ziektedetectie en het ontwikkelen van effectieve therapieën voor chronische nierziekte. In de nier speelt de proximale tubulus (PT) een cruciale rol bij de progressie van chronische nierziekte, omdat dit weefsel actief deelneemt aan zowel de uitscheiding als de reabsorptie van veel endogene en exogene stoffen. Dit maakt de PT ook extra gevoelig voor schade.

Het onderzoek beschreven in dit proefschrift richtte zich op de ontwikkeling van een reeks *in vitro* modellen die de belangrijkste fenotypische en moleculaire kenmerken van de native PT kunnen nabootsen en op het toepassen ervan bij het bestuderen van de progressie van chronische nierziekte. Daarnaast zijn de modellen gebruikt voor het bestuderen van interventies en het identificeren van mogelijke therapeutische aangrijpingspunten.

Hoofdstuk 2 biedt een uitgebreid overzicht van geneesmiddelen die niertoxiciteit induceren en modellen waarmee dit onderzocht is, variërend van traditionele 2D-modellen tot geavanceerde (3-dimensionale; 3D) *in vitro*-modellen. Bovendien werden de verschillende *in vitro* modellen vergeleken voor wat betreft hun complexiteitsniveau en fysiologische relevantie. Zo konden sleutelkenmerken worden geïdentificeerd die belangrijk zijn in de ontwikkeling van nieuwe en meer fysiologisch relevante *in vitro* modellen. Daarnaast is een overzicht gemaakt van de beschikbare biomarkers voor toxiciteit en/of schade welke vergeleken zijn met de klinische gouden standaard. Ten slotte is de noodzaak van het valideren van deze biomarkers voor het beoordelen van ziekteprogressie en weefselherstel onderzocht.

Hoofdstuk 3 concentreerde zich op het evalueren van de rol van de organische aniontransporter 1 (OAT1) bij de uitscheiding van medicijnen die vaak worden voorgeschreven bij de behandeling van chronische nierziekte en van eiwitgebonden uremische toxines (PBUTS; ofwel endogene metabolieten die zich ophopen bij nierfalen). Aangezien PBUT's en geneesmiddelen beide substraten zijn voor OAT1 werd de hypothese getoetst dat hun combinatie mogelijk de resterende nierfunctie kunnen belemmeren door met elkaar te concurreren. Om dit te onderzoeken, is de OAT1-activiteit bestudeerd aan de hand van de opname 'an fluoresceïne, een fluorescerend OAT1-substraat, in aanwezigheid van medicijnen en/of PBUT's. De resultaten toonden aan dat angiotensine-receptorblokkers en het diureticum furosemide de opname van fluoresceïne significant verminderden. Dit effect werd versterkt in aanwezigheid van PBUT's, wat erop wijst dat PBUT's inderdaad kunnen concurreren met geneesmiddelen voor de opname en uitscheiding door OAT1, waardoor de resterende nierfunctie bij patiënten met nierfalen mogelijk in gevaar komt.

In **hoofdstuk 4** hebben we ons verdiept in de beoordeling van de cytocompatibiliteit van dialysevloeistof (DF) bij de toepassing van een biologische kunstnier. Hierbij werd de levensvatbaarheid van de cellen en de integriteit van de celmonolagen in 3D-kweken beoordeeld. Verder hebben we transepitheliale transportstudies uitgevoerd met behulp van biologische nierbuisjes die de functionele eenheden van een biologische kunstnier representeren. We concludeerden dat blootstelling aan DF geen nadelige effecten had op de levensvatbaarheid van de cellen, de membraanintegriteit of de PT functie. Bovendien kon worden vastgesteld dat DF de verwijdering van PBUTs door de nierbuisjes niet in gevaar brengt. Deze resultaten demonstreren dat het biologische kunstniermodel in staat is om PBUT's uit te scheiden en hierdoor een potentiële klinische behandelingsmethode voor nierfalen kan worden.

In **hoofdstuk 5** hebben we een nieuw *in vitro* model ontwikkeld om ischemie-reperfusieschade te kunnen bestuderen. Dit treedt vaak op bij niertransplantatie en kan worden nagebootst door het onderdrukken van de mitochondriale ademhaling en glycolyse onder hypoxie. De schadelijke effecten van ischemie werden beoordeeld aan de hand van verschillende parameters van de mitochondriale gezondheid. Vervolgens werden de ischemische cellen behandeld met blaasjes van mesenchymale stromacellen (MSC), waarvoor verschillende bronnen naast elkaar werden getest (vetweefsel, beenmerg en navelstreng). De resultaten toonden aan dat ischemische schade leidt tot verslechtering van het cytoskelet, een verlaagd zuurstofverbruik, verhoogde oxidatieve stress, mitochondriale

disfunctie en een verminderd celmetabolisme. Na behandeling met de MSC-blaasjes, met name die van de navelstreng, werden de morfologische verstoringen gedeeltelijk ongedaan gemaakt, nam de ATP-productie toe, samen met de mitochondriële functie van de cellen en de ophoping van antioxidantmetabolieten. Deze bevindingen geven aan dat behandeling met MSC-blaasjes een potentiële therapie kan zijn voor ischemische schade.

In **hoofdstuk 6** hebben we ons verdiept in de pathofysiologie van diabetische proximale tubulopathie, waarbij de belangrijkste processen die de ziekteprogressie aansturen zijn beschreven. Verder zijn de vereiste kenmerken onderzocht die nodig zijn voor een ideaal PT *in vitro* model, terwijl we ook de voor- en nadelen van de meest gebruikte PT *in vitro* modellen bespreken. Daarnaast is een uitgebreid overzicht gegeven van het therapeutische potentieel van de natrium-glucose-cotransporter 2 (SGLT2) -remmers voor de behandeling van diabetische proximale tubulopathie.

In **hoofdstuk 7** hebben we Human Kidney-2 (HK-2) cellen blootgesteld aan een combinatie van hoog glucose (hyperglykemie) en een laag zuurstofgehalte, waarvan bekend is dat deze het diabetische milieu nabootsen, samen met twee andere diabetische mediatoren, namelijk palmitinezuur (PA) of geglyceerd albumine (GA). De bevindingen toonden aan dat zowel PA als GA morfologische verstoringen van de cellen gaven, maar dat ze de metabolische activiteit en ATP-productie niet beïnvloedden. Bovendien leidden zowel PA als GA tot een toename van de mitochondriële dynamiek terwijl de mitochondriële massa's gelijk bleven. Een SGLT2-remmer, empagliflozine, kon de nierschade deels voorkomen. Deze resultaten bieden waardevolle inzichten in de complexe pathofysiologie van diabetische nierziekten en benadrukken het beschermende effect van empagliflozine.

Ten slotte biedt **hoofdstuk 8** een uitgebreide samenvatting en discussie van de bevindingen van het proefschrift, waarin het belang van translationeel onderzoek naar de PT wordt benadrukt en de behoefte aan geavanceerde *in vitro* modellen om (patho)fysiologische gebeurtenissen die *in vivo* worden waargenomen nauwkeurig te kunnen repliceren. De bevindingen van dit proefschrift geven aan dat nierfunctie-vervangende therapieën zoals de biologische kunstnier een effectief alternatief voor bestaande therapieën kan worden. Bovendien werpt dit proefschrift licht op de impact van het gebruik van meerdere medicijnen op de PT-transportfunctie bij nierpatiënten, waaruit blijkt dat bepaalde medicijnen kunnen concurreren met PBUT's voor uitscheiding. Bovendien benadrukt het gepresenteerde onderzoek de cruciale rol van mitochondriale dysfunctie bij ziekteprogressie en onderstreept

het potentieel van MSC-blaasjes bij het herstellen van de mitochondriële functie na ischemische schade. Over het geheel genomen onderstreept dit proefschrift de cruciale rol van de PT bij het modelleren van ziekten en de ontwikkeling van gerichte therapieën.

LIST OF ABBREVIATIONS

2-nbdg 2-(*N*-(7-Nitrobenz-2-oxa-1,3-diazol-4-yl)Amino)-2-Deoxyglucose

2D Two-dimensional

3D Three-dimensional

A Adipose tissue

AA Antimycin A

ABC ATP-binding cassette

ACEI Angiotensin-converting enzyme inhibitors

ADME Absorption, distribution, metabolism, and excretion

ADPKD Autosomal dominant polycystic kidney disease

AGE Advanced glycation end products

AGER Advanced glycation end products receptor

AIN Acute interstitial nephritis

AKI: Acute kidney injury

ALP Alkaline phosphatase

AMPK 5' adenosine monophosphate-activated protein kinase

ARB Angiotensin receptor blocker

ASC Adult stem cell

AT1R Angiotensin II receptor type 1

ATN Acute tubular necrosis

ATP Adenosine triphosphate

B Bone marrow

B2M Beta-2 microglobulin

BAK BCL-2 homologous antagonist/killer

BAK Bioartificial kidney

BAX BCL-2 associated X

BCL-2 B-cell lymphoma 2

BCRP Breast cancer resistance protein

BPE Bovine pituitary extract

BRECS Bioartificial renal epithelial cell system

BSA Bovine serum albumin

BTD Bioartificial renal tubule device

BUN Blood urea nitrogen

CIHP Conditionally immortalized human podocyte

ciPTEC Conditionally immortalized proximal tubule epithelial cell

CKD Chronic kidney disease

CLU Clusterin

CM: Conditioned medium

CPT1A Carnitine palmitoyltransferase 1a

CRISPR/CAS9 Clustered regularly interspaced short palindromic repeats-associated protein 9

CRS Cardiorenal syndrome

CTGF *Connective tissue growth factor*

CYP Cytochrome P450

CysC Cystatin C

DAPI 4′,6-diamidino-2-phenylindole

DDI Drug-drug interaction

DF Dialysis fluid

DKD Diabetic kidney disease

DME Drug-metabolizing enzymes

DMEM *Dulbecco's Modified Eagle Medium*

DRP1 Dynamin-related protein 1

ECAR Extracellular acidification rate

ECM Extracellular matrix

ELISA Enzyme-Linked Immunosorbent Assay

EMA European Medicines Agency

EMPA Empagliflozin

EMT Epithelial–mesenchymal transition

ESC Embryonic stem cell

ESKD End-stage kidney disease

ETC Electron transport chain

EVAL Ethylene vinyl alcohol;

Evs Extracellular vesicles

FAO Fatty acid oxidation

FBS Fetal bovine serum

FCCP Carbonyl cyanide-p-trifluoromethoxyphenylhydrazone

FcRn Neonatal Fc receptor

FCS Fetal calf serum

FDA Food and Drug Administration

FFA Free fatty acid

FITC Fluorescein isothiocyanate

GA Glycated albumin

GFR Glomerular filtration rate

GGT γ-Glutamyl Transpeptidase

GLUT Glucose transporter

GMEC Glomerular microvascular endothelial cell

GST Glutathione S-Transferase

Gγ-GT γ-Glutamyl Transpeptidase Transferase

H Hypoxia

H2DCFDA 2′,7′-dichlorodihydrofluorescein diacetate

H2RA Histamine H2-Receptor Antagonists

HA Hippuric acid

HBSS Hanks' Balanced Salt Solution

HEPES 4-(2-hydroxyethyl)-1-piperazineethanesulfonic acid

HFM Hollow fiber membrane

HG High glucose

HIF Hypoxia-inducible factor

HK-2 Human kidney-2

HKC-8 Human kidney proximal tubular epithelial cell line (clone-8)

HO Heme oxygenase

HP Human plasma

HPRT1 Hypoxanthine Phosphoribosyltransferase 1

HRE Hypoxia response element

HRS Hepatorenal syndrome

HSA Human serum albumin

hTERT Human telomerase reverse transcriptase

HUS Hemolytic-uremic syndrome

IAA Indole-3-acetic acid

ICAM1 Intercellular Adhesion Molecule 1

IGFBP Insulin-like growth factor-binding protein

IL Interleukin

IMM: Inner mitochondrial membrane

IPSC Induced pluripotent stem cell

IRI Ischemia/reperfusion injury

IS Indoxyl sulfate

IVIG Intravenous immunoglobulin

IVIVE *In vitro* to *in vivo* extrapolation

K-RAS Kirsten rat sarcoma virus

KA Kynurenic acid

KIM Kidney injury molecule

KLK Kallikrein

KYN Kynurenine

L-DOPA 3,4-dihydroxyl-L-phenylalanine

L-FABP Liver type-fatty acid binding protein

LC3 Microtubule-associated proteins 1A/1B light chain 3

LDH L*actate dehydrogenase*

LEVs: Large extracellular vesicles

LG *Low glucose*

LPS Lipopolysaccharide

MAN Mannitol

MATE Multidrug and toxin extrusion protein

MCP Monocyte chemotactic protein

MEM Microelectromechanical systems

miRNA MicroRNA

MMP Matrix metalloproteinase

MOF Multiorgan failure

MPS Microphysiological systems

MRP Multidrug resistance protein

MSC Mesenchymal stromal cell

mTOR Mammalian target of rapamycin

MTX Methotrexate

MWCO Molecular weigth cut-off

N Normoxia

NAG N-acetyl-β-glucosaminidase

NF-kB, Nuclear factor-kB

NGAL Neutrophil gelatinase-associated lipocalin

NHE1 Sodium/hydrogen exchanger-1

NLRP3 NLR family pyrin domain containing 3

NSAIDs Nonsteroidal anti-inflammatory drugs

OAT Organic anion transporters

OCR: Oxygen consumption rate

OCT Organic cation transporter

OLIG Oligomycin

OoC Organ-on-chip

OPA1 Optic atrophy 1

OPN Osteopontin

OXPHOS Oxidative phosphorylation

P-gp P-glycoprotein

PA Palmitic acid

PAES Polyarylethersulfone

PBPK Physiologically-based pharmacokinetic

PBS *Phosphate-buffered saline*

PBUT Protein-bound uremic toxin

PCG p-cresyl glucuronide

PCS p-cresyl sulfate

PES/PVP Polyethersulfone/ polyvinylpyrrolidone

PGC1α Peroxisome proliferator–activated receptor gamma coactivator-1α

PHD Prolyl hydroxylase

PINK1 Phosphatase and tensin homolog-induced kinase 1

PKC Protein kinase c

PSTC Predictive Safety Testing Consortium

PSU Polysulfone

PT Proximal tubule

PTEC Proximal tubule epithelial cell

PTF Pentoxifyline

RAAS *Renin–angiotensin–aldosterone system*

RAD Renal tubule assist device

RANTES Regulated on activation, normal T cell expressed and secreted

RBP Retinol binding protein

ROS Reactive oxygen species

ROT/AA rotenone/antimycin a

RPA Renal papillary antigen

RPTEC Renal proximal tubule epithelial cell

RT Room temperature

sCr Serum creatinine

SD Standard deviation

SDS Sodium dodecyl sulfate

SEVs Small extracellular vesicles

SGLT Sodium-glucose cotransporter

SIRT Sirtuin

SLC Solute carrier family

SRC Spare respiratory capacity

SV40T Simian virus 40 large T antigen

T2DM Type 2 Diabetes Mellitus

TCA Tricarboxylic acid

TEER Transepithelial electrical resistance

TFEB Transcription factor EB

TFF Trefoil factor

TGF Tubuloglomerular feedback

TGF-B Transforming growth factor beta

TIMP Tissue inhibitor of metalloproteinase

TLR Toll-like receptor

U Umbilical cord

uALB Urinary albumin

UP Uremic plasma

UT Uremic toxin

UTOX Uremic toxin mix

uTP Urinary total

VCAM1 Vascular cell adhesion molecule 1

VEGF *Vascular endothelial growth factor*

α-SMA Alpha smooth muscle actin

ΔΨ Mitochondrial membrane potential

ABOUT THE AUTHOR

João Faria, born on 11th January 1994, in Vizela, Portugal. After completing his high school education in 2012, João moved to Porto, where he enrolled at the Faculty of Engineering of the University of Porto. There, he pursued an Integrated Masters in Bioengineering, specializing in Molecular Biotechnology. During his masters, João engaged in two trainee internships. In 2017, he embarked on his first internship at the VIB-KU Leuven Center for Cancer Biology (Leuven, Belgium), working under the guidance of Prof. dr. Massimiliano Mazzone and Pawel Bieniasz-Krzywiec. His project there focused on investigating the role of podoplanin in lymphangiogenesis using a murine model of breast cancer. In 2018, João pursued his second internship, this time at the Faculty of Veterinary Medicine in Utrecht (The Netherlands), under the guidance of Dr. Bart Spee. During this period, he developed a protocol for the *in vitro* differentiation of human liver organoids into cholangiocytes.

Upon completing his master's degree, João moved to Utrecht (The Netherlands) on January 2019 to start his PhD research at the Division of Pharmacology within the Utrecht Institute for Pharmaceutical Sciences at Utrecht University. He was enrolled as an early-stage researcher within the RenalToolBox Training Network (EU-FP7, Marie Skłodowska-Curie actions), under the supervision of Prof. dr. Roos Masereeuw and Dr. Silvia M. Mihăilă. Additionally, João enrolled in the Regenerative Medicine PhD program. The results of his PhD research are described and discussed in this thesis. His innovative work and significant contributions have been presented at various international conferences, including the Termis 6th World Congress in 2021, and ASK Kidney Week 2022.

LIST OF PUBLICATIONS

Faria J*, Calcat-i-Cervera S*, Skovronova R*, Broeksma BC, Berends AJ1, Zaal EA, Bussolati B, O'Brien T, Mihăilă SM, Masereeuw R. **Mesenchymal Stromal Cells Secretome Restores Bioenergetic and Redox Homeostasis in Human Proximal Tubule Cells after Ischemic Injury.** *Published at Stem Cell Res Ther*, **2023**; 14, 353

Garví ES, **Faria J**, Casellas CP, Thijssen S, Wubbolts EJ, Jamalpoor A, Harrison P, Masereeuw R, Janssen MJ **Gene surgery as a potential treatment option for Nephropathic Cystinosis in vitro**. *BioRxiv **2023**.11.01.565117*

Faria J; Ahmed S; Stamatialis D; Verhaar MC; Masereeuw R; Gerritsen KGF; Mihăilă SM **Bioengineered Kidney Tubules Efficiently Clear Uremic Toxins in Experimental Dialysis Conditions**. *Int J Mol Sci* **2023**;24(15):12435

Wang Z, **Faria J**, van der Laan LJW, Penning LC, Masereeuw R, Spee B **Human Cholangiocytes Form a Polarized and Functional Bile Duct on Hollow Fiber Membranes.** *Front Bioeng Biotechnol* **2022**:10:868857

Valverde MG*, **Faria J***, Garví ES, Janssen MJ, Masereeuw R, Mihăilă SM. **Organs-on-chip technology: a tool to tackle genetic kidney diseases.** *Pediatr Nephrol* **2022**;37(12):2985-2996

Faria J, Gerritsen KGF, Nguyen TQ, Mihăilă SM, Masereeuw R. **Diabetic proximal tubulopathy: Can we mimic the disease for in vitro screening of SGLT inhibitors?** *J Pharmacol* **2021**; 908:174378

Wang Z, **Faria J**, Penning LC, Masereeuw R, Spee B. **Tissue-Engineered Bile Ducts for Disease Modeling and Therapy.** *Tissue Eng Part C Methods* **2021**;27(2):59-76

Mihăilă SM, **Faria J**, Stefens MFJ, Stamatialis D, Verhaar MC, Gerritsen KGF, Masereeuw R. **Drugs Commonly Applied to Kidney Patients May Compromise Renal Tubular Uremic Toxins Excretion.** *Toxins (Basel)* **2020**;12(6):391

Faria J*, Ahmed S*, Gerritsen KGF, Mihăilă SM, Masereeuw R. **Kidney-based in vitro models for drug-induced toxicity testing.** *Arch Toxicol* **2019**;93(12):3397-3418

*These authors contributed equally

ACKNOWLEDGEMENTS